

Vol. 24, no. 1, 2024

eISSN 2687-1653

PEER-REVIEWED SCIENTIFIC AND PRACTICAL JOURNAL

Advanced Engineering Research (Rostov-on-Don)

Mechanics

Machine Building
and Machine Science

Information Technology,
Computer Science
and Management



www.vestnik-donstu.ru
DOI 10.23947/2687-1653



Advanced Engineering Research (Rostov-on-Don)

Peer-reviewed scientific and practical journal (published since 2000)

eISSN 2687–1653

DOI: 10.23947/2687–1653

Vol. 24, no. 1, 2024

The journal is aimed at informing the readership about the latest achievements and prospects in the field of mechanics, mechanical engineering, computer science and computer technology. The publication is a forum for cooperation between Russian and foreign scientists, it contributes to the convergence of the Russian and world scientific and information space.

The journal is included in the List of the leading peer-reviewed scientific publications (Higher Attestation Commission under the Ministry of Science and Higher Education of the Russian Federation), where basic scientific results of dissertations for the degrees of Doctor and Candidate of Science in scientific specialties and their respective branches of science should be published.

The journal publishes articles in the following fields of science:

- Theoretical Mechanics, Dynamics of Machines (Engineering Sciences)
- Deformable Solid Mechanics (Engineering, Physical and Mathematical Sciences)
- Mechanics of Liquid, Gas and Plasma (Engineering Sciences)
- Mathematical Simulation, Numerical Methods and Program Systems (Engineering Sciences)
- System Analysis, Information Management and Processing, Statistics (Engineering Sciences)
- Automation and Control of Technological Processes and Productions (Engineering Sciences)
- Software and Mathematical Support of Machines, Complexes and Computer Networks (Engineering Sciences)
- Computer Modeling and Design Automation (Engineering, Physical and Mathematical Sciences)
- Computer Science and Information Processes (Engineering Sciences)
- Machine Science (Engineering Sciences)
- Machine Friction and Wear (Engineering Sciences)
- Technology and Equipment of Mechanical and Physicotechnical Processing (Engineering Sciences)
- Engineering Technology (Engineering Sciences)
- Welding, Allied Processes and Technologies (Engineering Sciences)
- Methods and Devices for Monitoring and Diagnostics of Materials, Products, Substances and the Natural Environment (Engineering Sciences)
- Hydraulic Machines, Vacuum, Compressor Equipment, Hydraulic and Pneumatic Systems (Engineering Sciences)

<i>Indexing and Archiving</i>	RSCI, CyberLeninka, EBSCO, Dimensions, DOAJ, Index Copernicus, Internet Archive, Google Scholar
<i>Name of the Body that Registered the Publication</i>	Extract from the Register of Registered Mass Media ЭЛ № ФС 77 – 78854 dated August 07, 2020, issued by the Federal Service for Supervision of Communications, Information Technology and Mass Media
<i>Founder and Publisher</i>	Federal State Budgetary Educational Institution of Higher Education Don State Technical University (DSTU)
<i>Periodicity</i>	4 issues per year
<i>Address of the Founder and Publisher</i>	1, Gagarin sq., Rostov-on-Don, 344003, Russian Federation
<i>E-mail</i>	vestnik@donstu.ru
<i>Telephone</i>	+7 (863) 2–738–372
<i>Website</i>	http://vestnik-donstu.ru
<i>Date of Publication</i>	30.03.2024





Advanced Engineering Research (Rostov-on-Don)

Рецензируемый научно-практический журнал (издается с 2000 года)

eISSN 2687–1653

DOI: 10.23947/2687–1653

Том 24, № 1, 2024

Создан в целях информирования читательской аудитории о новейших достижениях и перспективах в области механики, машиностроения, информатики и вычислительной техники. Издание является форумом для сотрудничества российских и иностранных ученых, способствует сближению российского и мирового научно-информационного пространства.

Журнал включен в перечень рецензируемых научных изданий, в котором должны быть опубликованы основные научные результаты диссертаций на соискание ученой степени кандидата наук, на соискание ученой степени доктора наук (Перечень ВАК) по следующим научным специальностям:

- 1.1.7 – Теоретическая механика, динамика машин (технические науки)
- 1.1.8 – Механика деформируемого твердого тела (технические, физико-математические науки)
- 1.1.9 – Механика жидкости, газа и плазмы (технические науки)
- 1.2.2 – Математическое моделирование, численные методы и комплексы программ (технические науки)
- 2.3.1 – Системный анализ, управление и обработка информации, статистика (технические науки)
- 2.3.3 – Автоматизация и управление технологическими процессами и производствами (технические науки)
- 2.3.5 – Математическое и программное обеспечение вычислительных систем, комплексов и компьютерных сетей (технические науки)
- 2.3.7 – Компьютерное моделирование и автоматизация проектирования (технические, физико-математические науки)
- 2.3.8 – Информатика и информационные процессы (технические науки)
- 2.5.2 – Машиноведение (технические науки)
- 2.5.3 – Трение и износ в машинах (технические науки)
- 2.5.5 – Технология и оборудование механической и физико-технической обработки (технические науки)
- 2.5.6 – Технология машиностроения (технические науки)
- 2.5.8 – Сварка, родственные процессы и технологии (технические науки)
- 2.5.9 – Методы и приборы контроля и диагностики материалов, изделий, веществ и природной среды (технические науки)
- 2.5.10 – Гидравлические машины, вакуумная, компрессорная техника, гидро- и пневмосистемы (технические науки)

Индексация и архивация:	РИНЦ, CyberLeninka, CrossRef, Dimensions, DOAJ, EBSCO, Index Copernicus, Internet Archive, Google Scholar
Наименование органа, зарегистрировавшего издание	Выписка из реестра зарегистрированных средств массовой информации ЭЛ № ФС 77 – 78854 от 07 августа 2020 г., выдано Федеральной службой по надзору в сфере связи, информационных технологий и массовых коммуникаций
Учредитель и издатель	Федеральное государственное бюджетное образовательное учреждение высшего образования «Донской государственный технический университет» (ДГТУ)
Периодичность	4 выпуска в год
Адрес учредителя и издателя	344003, Российская Федерация, г. Ростов-на-Дону, пл. Гагарина, 1
E-mail	vestnik@donstu.ru
Телефон	+7 (863) 2–738–372
Сайт	http://vestnik-donstu.ru
Дата выхода в свет	30.03.2024



Editorial Board

Editor-in-Chief, Alexey N. Beskopylny, Dr.Sci. (Eng.), Professor, Don State Technical University (Rostov-on-Don, Russian Federation);

Deputy Chief Editor, Alexandr I. Sukhinov, Corresponding Member, Russian Academy of Sciences, Dr.Sci. (Phys.-Math.), Professor, Don State Technical University (Rostov-on-Don, Russian Federation);

Executive Editor, Manana G. Komakhidze, Cand.Sci. (Chemistry), Don State Technical University (Rostov-on-Don, Russian Federation);

Executive Secretary, Nadezhda A. Shevchenko, Don State Technical University (Rostov-on-Don, Russian Federation);

Sergey M. Aizikovitch, Dr.Sci. (Phys.-Math.), Professor, Don State Technical University (Rostov-on-Don, Russian Federation);

Kamil S. Akhverdiev, Dr.Sci. (Eng.), Professor, Rostov State Transport University (Rostov-on-Don, Russian Federation);

Imad R. Antipas, Cand.Sci. (Eng.), Don State Technical University (Rostov-on-Don, Russian Federation);

Hubert Anysz, PhD (Eng.), Assistant Professor, Warsaw University of Technology (Republic of Poland);

Ahilan Appathurai, National Junior Research Fellow, Anna University Chennai (India);

Gultekin Basmaci, PhD (Eng.), Professor, Burdur Mehmet Akif Ersoy University (Turkey);

Yuri O. Chernyshev, Dr.Sci. (Eng.), Professor, Don State Technical University (Rostov-on-Don, Russian Federation);

Evgenii A. Demekhin, Dr.Sci. (Phys.-Math.), Professor, Financial University under the RF Government, Krasnodar branch (Krasnodar, Russian Federation);

Oleg V. Dvornikov, Dr.Sci. (Eng.), Professor, Belarusian State University (Belarus);

Karen O. Egiazaryan, Dr.Sci. (Eng.), Professor, Tampere University of Technology (Finland);

Victor A. Ereemeev, Dr.Sci. (Phys.-Math.), Professor, Southern Scientific Center of RAS (Rostov-on-Don, Russian Federation);

Nikolay E. Galushkin, Dr.Sci. (Eng.), Professor, Institute of Service and Business, DSTU branch (Shakhty, Russian Federation);

LaRoux K. Gillespie, Dr.Sci. (Eng.), Professor, President-Elect of the Society of Manufacturing Engineers (USA);

Ali M. Hasan, PhD (Computer Engineering), Al Nahrain University (Baghdad, Iraq);

Huchang Liao, Professor, IAAM Fellow, IEEE Business School Senior Fellow, Sichuan University (China);

Hamid A. Jalab, PhD (Computer Science & IT), University of Malaya (Malaysia);

Revaz Z. Kavtaradze, Dr.Sci. (Eng.), Professor, Raphiel Dvali Institute of Machine Mechanics (Georgia);

Janusz Witalis Kozubal, Dr.Sci. (Eng.), Wrocław Polytechnic University (Republic of Poland);

Ilya I. Kudish, PhD (Phys.-Math.), Kettering University (USA);

Victor M. Kureychik, Dr.Sci. (Eng.), Professor, Southern Federal University (Rostov-on-Don, Russian Federation);

Geny V. Kuznetsov, Dr.Sci. (Phys.-Math.), Professor, Tomsk Polytechnic University (Tomsk, Russian Federation);

Vladimir I. Lysak, Dr.Sci. (Eng.), Professor, Volgograd State Technical University (Volgograd, Russian Federation);

Vladimir I. Marchuk, Dr.Sci. (Eng.), Professor, Institute of Service and Business, DSTU branch (Shakhty, Russian Federation);

Vladimir M. Mladenovic, Dr.Sci. (Eng.), Professor, University of Kragujevac (Serbia);

Murman A. Mukutadze, Dr.Sci. (Eng.), Professor, Rostov State Transport University (Rostov-on-Don, Russian Federation);

Andrey V. Nasedkin, Dr.Sci. (Phys.-Math.), Professor, Southern Federal University (Rostov-on-Don, Russian Federation);

Tamaz M. Natriashvili, Academician, Raphiel Dvali Institute of Machine Mechanics (Georgia);

Nguyen Dong Ahn, Dr.Sci. (Phys.-Math.), Professor, Academy of Sciences and Technologies of Vietnam (Vietnam);

Nguyen Xuan Chiem, Dr.Sci. (Eng.), Le Quy Don Technical University (Vietnam);

Sergey G. Parshin, Dr.Sci. (Eng.), Associate Professor, St. Petersburg Polytechnic University (St. Petersburg, Russian Federation);

Konstantin V. Podmaster'ev, Dr.Sci. (Eng.), Professor, Orel State University named after I.S. Turgenev (Orel, Russian Federation);

Roman N. Polyakov, Dr.Sci. (Eng.), Associate Professor, Orel State University named after I.S. Turgenev (Orel, Russian Federation);

Valentin L. Popov, Dr.Sci. (Phys.-Math.), Professor, Berlin University of Technology (Germany);

Nikolay N. Prokopenko, Dr.Sci. (Eng.), Professor, Don State Technical University (Rostov-on-Don, Russian Federation);

José Carlos Quadrado, PhD (Electrical Engineering and Computers), DSc Habil, Polytechnic Institute of Porto (Portugal);

Alexander T. Rybak, Dr.Sci. (Eng.), Professor, Don State Technical University (Rostov-on-Don, Russian Federation);

Muzafer H. Saračević, Full Professor, Novi Pazar International University (Serbia);

Arestak A. Sarukhanyan, Dr.Sci. (Eng.), Professor, National University of Architecture and Construction of Armenia (Armenia);

Vladimir N. Sidorov, Dr.Sci. (Eng.), Russian University of Transport (Moscow, Russian Federation);

Arkady N. Solovyev, Dr.Sci. (Phys.-Math.), Professor, Crimean Engineering and Pedagogical University the name of Fevzi Yakubov (Simferopol, Russian Federation);

Mezhlum A. Sumbatyan, Dr.Sci. (Phys.-Math.), Professor, Southern Federal University (Rostov-on-Don, Russian Federation);

Mikhail A. Tamarkin, Dr.Sci. (Eng.), Professor, Don State Technical University (Rostov-on-Don, Russian Federation);

Murat Tezer, Professor, Near East University (Turkey);

Bertram Torsten, Dr.Sci. (Eng.), Professor, TU Dortmund University (Germany);

Vyacheslav G. Tsybulin, Dr.Sci. (Phys.-Math.), Associate Professor, Southern Federal University (Rostov-on-Don, Russian Federation);

Umid M. Turdaliev, Dr.Sci. (Eng.), Professor, Andijan Machine-Building Institute (Uzbekistan);

Ahmet Uyumaz, PhD (Eng.), Professor, Burdur Mehmet Akif Ersoy University (Turkey);

Valery N. Varavka, Dr.Sci. (Eng.), Professor, Don State Technical University (Rostov-on-Don, Russian Federation);

Igor M. Verner, PhD (Eng.), Professor, Technion — Israel Institute of Technology (Israel);

Sergei A. Voronov, Dr.Sci. (Eng.), Associate Professor, Russian Foundation of Fundamental Research (Moscow, Russian Federation);

Batyr M. Yazyev, Dr.Sci. (Eng.), Professor, Don State Technical University (Rostov-on-Don, Russian Federation);

Vilor L. Zakovorotny, Dr.Sci. (Eng.), Professor, Don State Technical University (Rostov-on-Don, Russian Federation).

Редакционная коллегия

Главный редактор, Бескопыйный Алексей Николаевич, доктор технических наук, профессор, Донской государственный технический университет (Ростов-на-Дону, Российская Федерация);

заместитель главного редактора, Сухинов Александр Иванович, член-корреспондент РАН, доктор физико-математических наук, профессор, Донской государственный технический университет (Ростов-на-Дону, Российская Федерация);

ответственный редактор, Комахидзе Манана Гивиевна, кандидат химических наук, Донской государственный технический университет (Ростов-на-Дону, Российская Федерация);

ответственный секретарь, Шевченко Надежда Анатольевна, Донской государственный технический университет (Ростов-на-Дону, Российская Федерация);

Айзикович Сергей Михайлович, доктор физико-математических наук, профессор, Донской государственный технический университет (Ростов-на-Дону, Российская Федерация);

Антибас Имад Ризакалла, кандидат технических наук, Донской государственный технический университет (Ростов-на-Дону, Российская Федерация);

Ахилан Аппатурай, младший научный сотрудник, Инженерно-технологический колледж PSN, Университет Анны Ченнаи (Индия);

Ахвердиев Камил Самед Оглы, доктор технических наук, профессор, Ростовский государственный университет путей сообщения (Ростов-на-Дону, Российская Федерация);

Варавка Валерий Николаевич, доктор технических наук, профессор, Донской государственный технический университет (Ростов-на-Дону, Российская Федерация);

Вернер Игорь Михайлович, доктор технических наук, профессор, Технологический институт в Израиле (Израиль);

Воронов Сергей Александрович, доктор технических наук, доцент, Российский фонд фундаментальных исследований (Москва, Российская Федерация);

Галушкин Николай Ефимович, доктор технических наук, профессор, Институт сферы обслуживания и предпринимательства, филиал ДГТУ (Шахты, Российская Федерация);

Лару Гиллеспи, доктор технических наук, профессор, Президент Общества машиностроителей (США);

Аныш Губерт, доктор наук, доцент, Варшавский технологический университет (Польша);

Басмачи Гюльтекин, доктор наук, профессор, Университет Бурдура Мехмета Акифа Эрсоя (Турция);

Дворников Олег Владимирович, доктор технических наук, профессор, Белорусский государственный университет (Беларусь);

Демехин Евгений Афанасьевич, доктор физико-математических наук, профессор, Краснодарский филиал Финансового университета при Правительстве РФ (Краснодар, Российская Федерация);

Хамид Абдулла Джалаб, доктор наук (информатика и ИТ), университет Малайя (Малайзия);

Егназарян Карен Оникович, доктор технических наук, профессор, Технологический университет Тампере (Финляндия);

Еремеев Виктор Анатольевич, доктор физико-математических наук, профессор, Южный научный центр РАН (Ростов-на-Дону, Российская Федерация);

Заковоротный Вилор Лаврентьевич, доктор технических наук, профессор, Донской государственный технический университет (Ростов-на-Дону, Российская Федерация);

Кавтарадзе Реваз Зурабович, доктор технических наук, профессор, Институт механики машин им. Р. Двали (Грузия);

Козубал Януш Виталис, доктор технических наук, профессор, Вроцлавский технический университет (Польша);

Хосе Карлос Куадрадо, доктор наук (электротехника и компьютеры), Политехнический институт Порту (Португалия);

Кудин Илья Исидорович, доктор физико-математических наук, Университет Кеттеринга (США);

Кузнецов Генний Владимирович, доктор физико-математических наук, профессор, Томский политехнический университет (Томск, Российская Федерация);

Курейчик Виктор Михайлович, доктор технических наук, профессор, Южный федеральный университет (Ростов-на-Дону, Российская Федерация);

Лысак Владимир Ильич, доктор технических наук, профессор, Волгоградский государственный технический университет (Волгоград, Российская Федерация);

Марчук Владимир Иванович, доктор технических наук, профессор, Институт сферы обслуживания и предпринимательства, филиал ДГТУ (Шахты, Российская Федерация);

Владимир Младенович, доктор технических наук, профессор, Крагуевацкий университет (Сербия);

Мукутадзе Мурман Александрович, доктор технических наук, доцент, Ростовский государственный университет путей сообщения (Ростов-на-Дону, Российская Федерация);

Наседкин Андрей Викторович, доктор физико-математических наук, профессор, Южный федеральный университет (Ростов-на-Дону, Российская Федерация);

Натришвили Тамаз Мамиевич, академик, Институт механики машин им. Р. Двали (Грузия);

Нгуен Донг Ань, доктор физико-математических наук, профессор, Институт механики Академии наук и технологий Вьетнама (Вьетнам);

Нгуен Суан Тьем, доктор технических наук, Вьетнамский государственный технический университет им. Ле Куй Дона (Вьетнам);

Паршин Сергей Георгиевич, доктор технических наук, доцент, Санкт-Петербургский политехнический университет (Санкт-Петербург, Российская Федерация);

Подмастерьев Константин Валентинович, доктор технических наук, профессор, Орловский государственный университет им. И. С. Тургенева (Орел, Российская Федерация);

Поляков Роман Николаевич, доктор технических наук, доцент, Орловский государственный университет им. И. С. Тургенева (Орел, Российская Федерация);

Попов Валентин Леонидович, доктор физико-математических наук, профессор, Институт механики Берлинского технического университета (Германия);

Прокопенко Николай Николаевич, доктор технических наук, профессор, Донской государственный технический университет (Ростов-на-Дону, Российская Федерация);

Рыбак Александр Тимофеевич, доктор технических наук, профессор, Донской государственный технический университет (Ростов-на-Дону, Российская Федерация);

Музафер Сарачевич, доктор наук, профессор, Университет Нови-Пазара (Сербия);

Саруханиян Арестак Араманович, доктор технических наук, профессор, Национальный университет архитектуры и строительства Армении (Армения);

Сидоров Владимир Николаевич, доктор технических наук, Российский университет транспорта (Москва, Российская Федерация);

Соловьёв Аркадий Николаевич, доктор физико-математических наук, профессор, Крымский инженерно-педагогический университет имени Февзи Якубова (Симферополь, Российская Федерация);

Сумбатян Междум Альбертович, доктор физико-математических наук, профессор, Южный федеральный университет (Ростов-на-Дону, Российская Федерация);

Тамаркин Михаил Аркадьевич, доктор технических наук, профессор, Донской государственный технический университет (Ростов-на-Дону, Российская Федерация);

Мурат Тезер, профессор, Ближневосточный университет (Турция);

Бертрам Торстен, доктор технических наук, профессор, Технический университет Дортмунда (Германия);

Турдиалиев Умид Мухтаралиевич, доктор технических наук, профессор, Андижанский машиностроительный институт (Узбекистан);

Ахмет Уюмаз, доктор технических наук, профессор, университет Бурдура Мехмета Акифа Эрсоя (Турция);

Али Маджид Хасан Алваэли, доктор наук (компьютерная инженерия), доцент, Университет Аль-Нахрейн (Ирак);

Цибулин Вячеслав Георгиевич, доктор физико-математических наук, доцент, Южный федеральный университет (Ростов-на-Дону, Российская Федерация);

Чернышев Юрий Олегович, доктор технических наук, профессор, Донской государственный технический университет (Ростов-на-Дону, Российская Федерация);

Хуан Ляо, профессор, научный сотрудник ИААМ; Старший член Школы бизнеса IEEE, Университет Сычуань (Китай);

Языев Батыр Меретович, доктор технических наук, профессор, Донской государственный технический университет (Ростов-на-Дону, Российская Федерация).

Contents

MECHANICS

Optimal Vibration Fields in Problems of Modeling Dynamic States of Technical Objects	7
<i>AV Eliseev, NK Kuznetsov</i>	
Coupled Axisymmetric Thermoelastoelectricity Problem for a Round Rigidly Fixed Plate.....	23
<i>DA Shlyakhin, EV Savinova</i>	
Prediction of Rheological Parameters of Polymers by Machine Learning Methods.....	36
<i>TN Kondratieva, AS Chepurnenko</i>	

MACHINE BUILDING AND MACHINE SCIENCE

Application of Special Calculation Techniques in the Design of All-Welded Gastight Structures of Boiler Units.....	48
<i>MP Kurepin, MYu Serbinovskiy</i>	
Stress Martensite Nucleation in a State of Premartensitic Lattice Instability	58
<i>YV Dolgachev, VN Pustovoi, YM Vernigorov</i>	
Improving the Principles of Identifying Critical Requirements for the Assembly of High-Precision Products	66
<i>AV Nazaryev, PYu Bochkarev</i>	

INFORMATION TECHNOLOGY, COMPUTER SCIENCE AND MANAGEMENT

Approximation of the Profile of Gas Turbine Engine Blades.....	78
<i>ME Soloviev, YN Shuleva, SL Baldaev, LKh Baldaev</i>	
Design of Instrumentation and Control Components of Power Distribution Systems	88
<i>YA Klimenko, YE Lvovich, AP Preobrazhensky</i>	
Computer Program for Primer Design for Loop-Mediated Isothermal Amplification (LAMP)	98
<i>LU Akhmetzianova</i>	
Optimal Temperature Calculation for Multicriteria Optimization of the Hydrogenation of Polycyclic Aromatic Hydrocarbons by NSGA-II Method	109
<i>AA Alexandrova, SN Koledin</i>	

Содержание

МЕХАНИКА

Оптимальные вибрационные поля в задачах моделирования динамических состояний технических объектов	7
<i>А.В. Елисеев, Н.К. Кузнецов</i>	
Связанная осесимметричная задача термоэлектроупругости для круглой жестко закрепленной пластины.....	23
<i>Д.А. Шляхин, Е.В. Савинова</i>	
Прогнозирование реологических параметров полимеров методами машинного обучения.....	36
<i>Т.Н. Кондратьева, А.С. Чепурненко</i>	

МАШИНОСТРОЕНИЕ И МАШИНОВЕДЕНИЕ

Применение специальных расчётных методик при проектировании цельносварных газоплотных конструкций котлоагрегатов	48
<i>М.П. Курепин, М.Ю. Сербиновский</i>	
Зарождение мартенсита напряжения в состоянии предмартенситной неустойчивости решетки	58
<i>Ю.В. Долгачев, В.Н. Пустовойт, Ю.М. Вернигор</i>	
Технологическое обеспечение сборки на основе принципов выявления критичных требований к высокоточным изделиям	66
<i>А.В. Назарьев, П.Ю. Бочкарев</i>	

ИНФОРМАТИКА, ВЫЧИСЛИТЕЛЬНАЯ ТЕХНИКА И УПРАВЛЕНИЕ

Аппроксимация профиля лопаток газотурбинных двигателей	78
<i>М.Е. Соловьев, Ю.Н. Шулева, С.Л. Балдаев, Л.Х. Балдаев</i>	
Проектирование контрольно-измерительных компонент распределительных энергетических систем	88
<i>Ю.А. Клименко, Я.Е. Львович, А.П. Преображенский</i>	
Компьютерная программа подбора праймеров для LAMP-амплификации.....	98
<i>Л.У. Ахметзянова</i>	
Расчет оптимальной температуры при многокритериальной оптимизации процесса гидрирования полициклических ароматических углеводородов методом NSGA-II.....	109
<i>А.А. Александрова, С.Н. Коледин</i>	

MECHANICS МЕХАНИКА



UDC 629.4.015, 62-752, 621.01, 62-932.4, 51-74, 534.014, 531.4

Research article

<https://doi.org/10.23947/2687-1653-2024-24-1-7-22>

Optimal Vibration Fields in Problems of Modeling Dynamic States of Technical Objects

 Andrey V. Eliseev^{1,2} , Nikolai K. Kuznetsov² 
¹ Irkutsk State Railway Transport Engineering University, Irkutsk, Russian Federation² Irkutsk National Research Technical University, Irkutsk, Russian Federation✉ eavsh@ya.ru

EDN: FAKNHP

Abstract

Introduction. Vibration interaction control is timely in production processes related to liquid and bulk media, systems of solids experiencing kinematic or force disturbances. At the same time, there is no single methodological basis for the formation of vibrational interactions. The issues of constructing optimal vibration fields of technical objects have not been addressed. The objective of the study is to develop a structural approach to the development of mathematical models in the problems of formation, evaluation, and correction of vibration fields of technical objects under conditions of intense force and kinematic loads. The task is to build vibration fields that are optimal in terms of the set of requirements, with the possibility of selecting the criterion of optimality of the vibration field of a technical object.

Materials and Methods. A structural approach was used as the basic methodology. It was based on a comparison of mechanical vibratory systems used as computational schemes of technical objects, and structural schemes of automatic control systems, which are equivalent in dynamic terms. Lagrange formalism, elements of operational calculus based on Laplace integral transformations, sections of vibration theories, algebraic methods, and the theory of spline functions were used for structural mathematical modeling.

Results. An approach to the selection of criteria for the optimality of vibration fields based on minimizing the residual of vibration fields for various required conditions was proposed. The problem was considered within the framework of a mechanical vibratory system formed by solids. It was shown that the optimal vibration field was determined by an external disturbance and was to satisfy condition $A\bar{y} = b$. There, A — matrix mapping the operator of conditions to the shape of the vibration field at control points; b — vector of values of vibration field characteristics; “—” above y meant the vibration amplitude of the steady-state component of the coordinate. To evaluate the field with account for noisy or unreliable requirements for dynamic characteristics, the smoothing parameter was used, indicating the priority of the criterion of optimality of the vibration field shape. The construction of a field for a mechanical vibratory system showed that the value of the vibration amplitudes of generalized coordinates remained constant when the frequency of external kinematic disturbances changed. Two approaches to the correction of the field optimality criteria were considered: equalization of the vibration amplitudes of the coordinates of a technical object and the selection of an energy operator.

Discussion and Conclusion. The development of the applied theory of optimal vibration fields involved, firstly, the correlation of the energy operator and the operator of the requirements for the shape of the vibration field in the theory of abstract splines. The second pair of comparable elements was the criterion of optimality of the vibration field and a system of requirements for the characteristics of the field at control points. The structural theory of optimal vibration fields improved in this way will find application in various industries. Accurate calculations in the formation, assessment, and correction of the states of systems under vibration loading are required in the tasks of increasing the durability of structures, improving measurements in complex vibratory systems, and developing new technologies and materials.

Keywords: structural mathematical modeling, mechanical vibratory systems, optimal vibration field, minimizing the residual of vibration fields

Acknowledgments. The authors would like to thank the Editorial board and the reviewers for their attentive attitude to the article and for the specified comments that improved the quality of the article.

For citation. Eliseev AV, Kuznetsov NK. Optimal Vibration Fields in Problems of Modeling Dynamic States of Technical Objects. *Advanced Engineering Research (Rostov-on-Don)*. 2024;24(1):7–22. <https://doi.org/10.23947/2687-1653-2024-24-1-7-22>

Научная статья

Оптимальные вибрационные поля в задачах моделирования динамических состояний технических объектов

А.В. Елисеев^{1,2}  , Н.К. Кузнецов² 

¹ Иркутский государственный университет путей сообщения, г. Иркутск, Российская Федерация

² Иркутский национальный исследовательский технический университет, г. Иркутск, Российская Федерация

 eavsh@ya.ru

Аннотация

Введение. Управление вибрационными взаимодействиями актуально в производственных процессах, связанных с жидкими и сыпучими средами, системами твердых тел, испытывающих кинематические или силовые возмущения. При этом нет единой методологической основы для формирования вибрационных взаимодействий. Не решены вопросы построения оптимальных вибрационных полей технических объектов. Цель исследования — развитие структурного подхода к разработке математических моделей в задачах формирования, оценки и коррекции вибрационных полей технических объектов в условиях интенсивных силовых и кинематических нагружений. Ставится задача построения вибрационных полей, оптимальных по совокупности требований, с возможностью выбора критерия оптимальности вибрационного поля технического объекта.

Материалы и методы. В качестве базовой методологии применяется структурный подход. Он основан на сопоставлении механических колебательных систем, используемых как расчетные схемы технических объектов, и структурных схем систем автоматического управления, эквивалентных в динамическом отношении. Для структурного математического моделирования использовали формализм Лагранжа, элементы операционного исчисления на основе интегральных преобразований Лапласа, разделы теорий колебаний, алгебраические методы, теорию сплайн-функций.

Результаты исследования. Предложен подход к выбору критериев оптимальности вибрационных полей на основе минимизации невязки вибрационных полей для различных необходимых условий. Проблема рассматривается в рамках механической колебательной системы, образованной твердыми телами. Показано, что оптимальное вибрационное поле определяется внешним возмущением и должно удовлетворять условию $A\bar{u} = b$. Здесь A — матрица, отображающая оператор условий на форму вибрационного поля в контрольных точках; b — вектор значений характеристик вибрационного поля; « \bar{u} » над u означает амплитуду колебания установившейся компоненты координаты. Для оценки поля с учетом зашумленных или недостоверных требований к динамическим характеристикам используется параметр сглаживания, обозначающий приоритет критерия оптимальности формы вибрационного поля. Построение поля для механической колебательной системы показало, что значение амплитуд колебания обобщенных координат сохраняется постоянным при изменении частоты внешних кинематических возмущений. Рассмотрены два подхода к коррекции критериев оптимальности поля: уравнивание амплитуд колебаний координат технического объекта и выбор энергетического оператора.

Обсуждение и заключение. Развитие прикладной теории оптимальных вибрационных полей предполагает, во-первых, сопоставление оператора энергии и оператора требований к форме вибрационного поля в теории абстрактных сплайнов. Вторая пара сопоставляемых элементов — критерий оптимальности вибрационного поля и система требований к характеристикам поля в контрольных точках. Усовершенствованная таким образом структурная теория оптимальных вибрационных полей найдет применение в разных отраслях. Точные расчеты в формировании, оценке и коррекции состояний систем при вибрационном нагружении необходимы в задачах повышения долговечности конструкций, улучшения измерений в сложных колебательных системах, разработке новых технологий и материалов.

Ключевые слова: структурное математическое моделирование, механические колебательные системы, оптимальное вибрационное поле, минимизация невязки вибрационных полей

Благодарности. Авторы выражают благодарность редакции и рецензентам за внимательное отношение к статье и указанные замечания, которые позволили повысить ее качество.

Для цитирования. Елисеев А.В., Кузнецов Н.К. Оптимальные вибрационные поля в задачах моделирования динамических состояний технических объектов. *Advanced Engineering Research (Rostov-on-Don)*. 2024;24(1):7–22. <https://doi.org/10.23947/2687-1653-2024-24-1-7-22>

Introduction. Features of vibration interactions are taken into account when creating production technologies [1]. The use of vibration methods for the intensification of production processes requires the development of mathematical modeling of the dynamic states of technical objects under conditions of vibration loading. The scientific and applied literature studies issues of the theory of vibrations and automatic control, theoretical mechanics, and dynamics of machines [2]. In particular, in the dynamics of machines, features of vibration interactions are taken into account in two types of tasks. The first one is the tasks of vibration isolation and vibroprotection [3]. The second includes tasks related to the assessment, formation, and correction of the states of technical objects under conditions of intense force or kinematic loads [4]. In the latter case, attention is drawn to the effects of vibrational interactions, which are used in the following production processes:

- transportation of rocks;
- fractionation of bulk materials;
- hardening of surfaces of long elements of aircraft structures;
- spatial orientation of parts during assembly.

Tasks of vibroprotection are related to solving the problems of railway transport safety. It is referred, specifically, to the issues of the dynamic state of the suspension elements [5], noise and vibration [6]. The problems of estimating dynamic states caused by significant loads arise when evaluating the vibration characteristics of a rail track with composite sleepers [7]. Harmful vibrations propagating in the urban environment from a moving train require control, and in this case, an assessment of complex dynamic states is also needed [8]. Similar examples are related to tracking the interactions of a wagon trolley with rails [9]. The dynamic state is formed when the sliding contact of the pantograph head and the contact wire is violated [10]. In this context, it is worth mentioning the tasks of analyzing the reaction of the rail to vertical impacts from a moving vehicle [11].

Another extensive group of tasks requiring an assessment of the dynamic states of elements is the vibration processes of production machines [12]. Thus, the dynamic state of vibration screening machines depends on the formation of dynamic states of several housings, which can be considered as solids, taking into account the nature of elastic linkage between them [13]. An essential factor determining the dynamic states of production facilities is the vibration frequency [14]. Separately, it is necessary to mention vibrating transport machines, whose dynamic state determines characteristics of movements [15].

It is worth noting the result of generalization of the tasks of assessment, formation, and correction of dynamic states of technical objects under conditions of intense loads. This approach has opened up the possibility to clarify the idea of how the distributions of the amplitudes of vibrations in the coordinates of control points depend on the connectivity of external disturbances.

Parameters of external vibration disturbances determine the possibilities of implementing dynamic effects that can act in different directions:

- constitute a danger to the performance of technical facilities;
- increase the process performance.

An example of a negative effect is exceeding the permissible values of the vibration amplitudes. Useful effects include a significant decrease in the amplitudes of coordinate vibrations and the establishment of a certain amplitude distribution.

In the tasks of vibration hardening of long-length parts, dynamic effects can be understood as the coincidence of the vibration patterns of the control points of the working bodies of vibrating production machines. This maintains the one-dimensionality and uniformity of the vibration field, which is consistent with the requirements for the dynamic quality of the interactions of the working medium and the surface of the hardened part. The required motion mode of the working body can be expressed using the conditions of equality of the vibration amplitudes of the control points. To study the concept of a vibrational field, the concept of a dynamic state at a point is generalized — at the same time, a set of points distributed over a certain variety of points of a solid body or a system of solids is considered [16].

In problems of vibrational interactions, a number of dynamic effects can be displayed using lever, elastic, and interpartial unilateral constraints. All of them are factors of specific dynamic effects that manifest themselves under the influence of external disturbances of a special configuration. To determine such configurations of external disturbances providing dynamic effects, it is proposed to develop a methodological framework that allows building mathematical models of vibration fields, taking into account the system of requirements for the features of interactions of system elements. The proposed methodological framework should have:

- an effective mathematical apparatus;
- a tool for visual display of structural features;
- capabilities to build dynamic analogies to generalize the developed methods to a broad class of physical processes.

Materials and Methods. A structural approach based on a comparison of mechanical vibratory systems and automatic control systems can serve as a methodological framework [17]. In this case, the mechanical vibratory system is considered as a design scheme of a technical object. It is compared to the structural scheme of a dynamically equivalent automatic control system. The established correspondence makes it possible to analyze and evaluate the dynamic characteristics of technical objects, taking into account the ideas about the steady-state forms of vibrations of a mechanical system based on the apparatus of the theory of automatic control [18]. The technology of structural mathematical modeling has features related to the assessment of dynamic states. Transfer functions of structural schemes are used for it. The input signals for these functions are external disturbances, the output signals are vibrations in the coordinates of the object being evaluated. Each coordinate of the system can be correlated with an indicator of the amplitude of the steady-state vibration. This allows us to consider the distribution of amplitudes over the points of the system as a vibration field of a technical object. The construction of a vibration field, taking into account a number of requirements, belongs to the class of inverse problems of dynamics, which in general may be incorrect. One of the methods for solving ill-posed problems is related to the regularization of the initial problem by introducing optimality criteria.

The listed features of the assessment of the dynamic states of technical objects indicate the need to develop a common approach in the methodology of constructing vibration fields, taking into account the criteria of optimality. At the same time, the methodology for the formation, evaluation, and correction of vibration fields with specified characteristics is not sufficiently detailed. Specifically, it is not possible to build vibration fields according to optimality criteria.

The presented research is devoted to the development of the techniques of structural mathematical modeling. For this purpose, we solve a class of specific problems of constructing vibration fields of technical objects with conditions for vibration amplitudes that reflect the requirements for dynamic effects and take into account the criteria of optimality.

Basic provisions. Formulation of the problem. A model mechanical vibratory system formed by a set of solids under conditions of vibrational loading of a kinematic origin is considered. The model system (Fig. 1) has 5 degrees of freedom, consists of 4 links in the form of solid-state rods with masses M_i , moments of inertia J_i , centers of gravity at point O_i , spaced from extreme points A_i and A_{i+1} at distances l_{1i} and l_{2i} , where $i = 1 \dots 4$.

Solid bodies in the form of rods are articulated at the extreme points — these are the attachment points of elastic elements mounted on support surfaces that perform in-phase harmonic vibrations (Fig. 1).

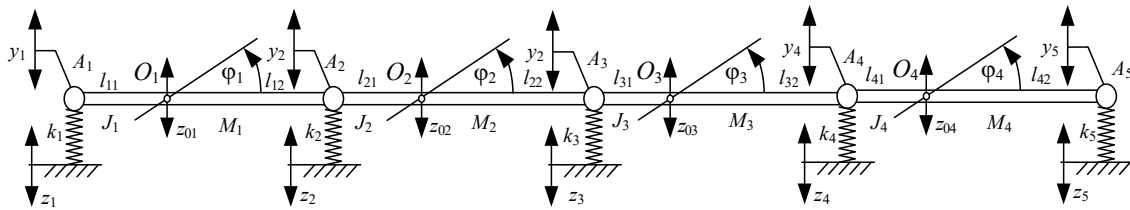


Fig. 1. Mechanical vibratory system formed by solids $A_1 A_2, A_2 A_3, A_3 A_4, A_4 A_5$: A — articulation points of solids; O_i — centers of gravity; z_i — support surfaces; J_i — moments of inertia

Under the influence of external kinematic disturbances z_i from the support surfaces, the system performs small steady-state vibrations relative to the static equilibrium position. External kinematic disturbances are connected in-phase vibrations:

$$z_i = z_g \gamma_i. \quad (1)$$

Here, z_g — harmonic disturbance of type $Asin(\omega t)$, where ω — frequency and γ_i — connection coefficients of external disturbances; $i = 1 \dots 5$. In general, the connection coefficients (1) are external disturbances of a certain structure.

The required dynamic effects are provided by a set of model conditions, namely: the vibration amplitudes of the coordinates of the control points of a technical object take fixed values regardless of the frequency of external disturbances.

The task is to determine for a mechanical vibratory system such external kinematic disturbances that the corresponding vibration field at the control points satisfies a given set of conditions in the form of fixed vibration amplitudes.

Research Results

Mathematical model. To compile a system of differential equations, the coordinates $\{y_1, y_2, y_3, y_4, y_5\}$ of the displacements of point $A_i, i = 1 \dots 5$ relative to the positions of static equilibrium are studied. The following coordinates are considered along with coordinates $\{y_i\}$:

- coordinates $\{z_{01}, z_{02}, z_{03}, z_{04}, z_{05}\}$, displaying the displacements of the centers of gravity O_i of rods relative to the positions of static equilibrium;
- coordinates $\{\varphi_1, \varphi_2, \varphi_3, \varphi_4, \varphi_5\}$ of small rotation angles around the centers of gravity.

Coordinates z_{0i} , φ_i , y_i are related by expressions:

$$\begin{cases} z_{0i} = a_i y_i + b_i y_{i+1}, \\ \varphi_i = c_i (y_{i+1} - y_i), \end{cases} \quad (2)$$

Here, $a_i = \frac{l_{i2}}{l_{i1} + l_{i2}}$, $b_i = \frac{l_{i1}}{l_{i1} + l_{i2}}$, $c_i = \frac{1}{l_{i1} + l_{i2}}$.

A mathematical model in the form of Lagrange differential equations of the 2nd kind is based on expressions for potential and kinematic energy. They can be represented in a matrix form using the scalar product \langle, \rangle vectors in R^n :

$$\Pi = \frac{1}{2} \langle K(\bar{y} - \bar{z}), (\bar{y} - \bar{z}) \rangle, T = \frac{1}{2} \langle M \dot{\bar{z}}_0, \dot{\bar{z}}_0 \rangle + \frac{1}{2} \langle J \dot{\bar{\varphi}}, \dot{\bar{\varphi}} \rangle, \quad (3)$$

here, $\dot{\bar{z}}_0, \dot{\bar{\varphi}}$ — coordinate derivatives $\dot{\bar{z}}_0, \dot{\bar{\varphi}}$.

$$K = \begin{pmatrix} k_1 & & & 0 \\ & k_2 & & \\ & & k_3 & \\ 0 & & & k_4 \end{pmatrix}, J = \begin{pmatrix} J_1 & & & 0 \\ & J_2 & & \\ & & J_3 & \\ 0 & & & J_4 \end{pmatrix}, M = \begin{pmatrix} M_1 & & & 0 \\ & M_2 & & \\ & & M_3 & \\ 0 & & & M_4 \end{pmatrix},$$

$$\bar{\varphi} = \begin{pmatrix} \varphi_1 \\ \varphi_2 \\ \varphi_3 \\ \varphi_4 \end{pmatrix}, \bar{z}_0 = \begin{pmatrix} z_{01} \\ z_{02} \\ z_{03} \\ z_{04} \end{pmatrix}, \bar{y} = \begin{pmatrix} y_1 \\ y_2 \\ y_3 \\ y_4 \\ y_5 \end{pmatrix}, \bar{z} = \begin{pmatrix} z_1 \\ z_2 \\ z_3 \\ z_4 \\ z_5 \end{pmatrix}.$$

Vectors $\bar{z}_0 \in R^4$, $\bar{\varphi} \in R^4$, $\bar{y} \in R^5$ taking into account (2), are interconnected through the following relations:

$$\bar{z}_0 = U \bar{y}, \bar{\varphi} = V \bar{y}. \quad (4)$$

$$\text{Here, } U = \begin{pmatrix} a_1 & b_1 & & & 0 \\ & a_2 & b_2 & & \\ & & a_3 & b_3 & \\ 0 & & & a_4 & b_4 \end{pmatrix}, V = \begin{pmatrix} -c_1 & c_1 & & & 0 \\ & -c_2 & c_2 & & \\ & & -c_3 & c_3 & \\ 0 & & & -c_4 & c_4 \end{pmatrix}.$$

In coordinates $\{y_i\}$, kinetic energy (3) takes the form:

$$T = \frac{1}{2} \langle (U^T M U + V^T J V) \dot{\bar{y}}, \dot{\bar{y}} \rangle. \quad (5)$$

Taking into account expressions (2)–(5), Lagrange equations of the 2nd kind take the form:

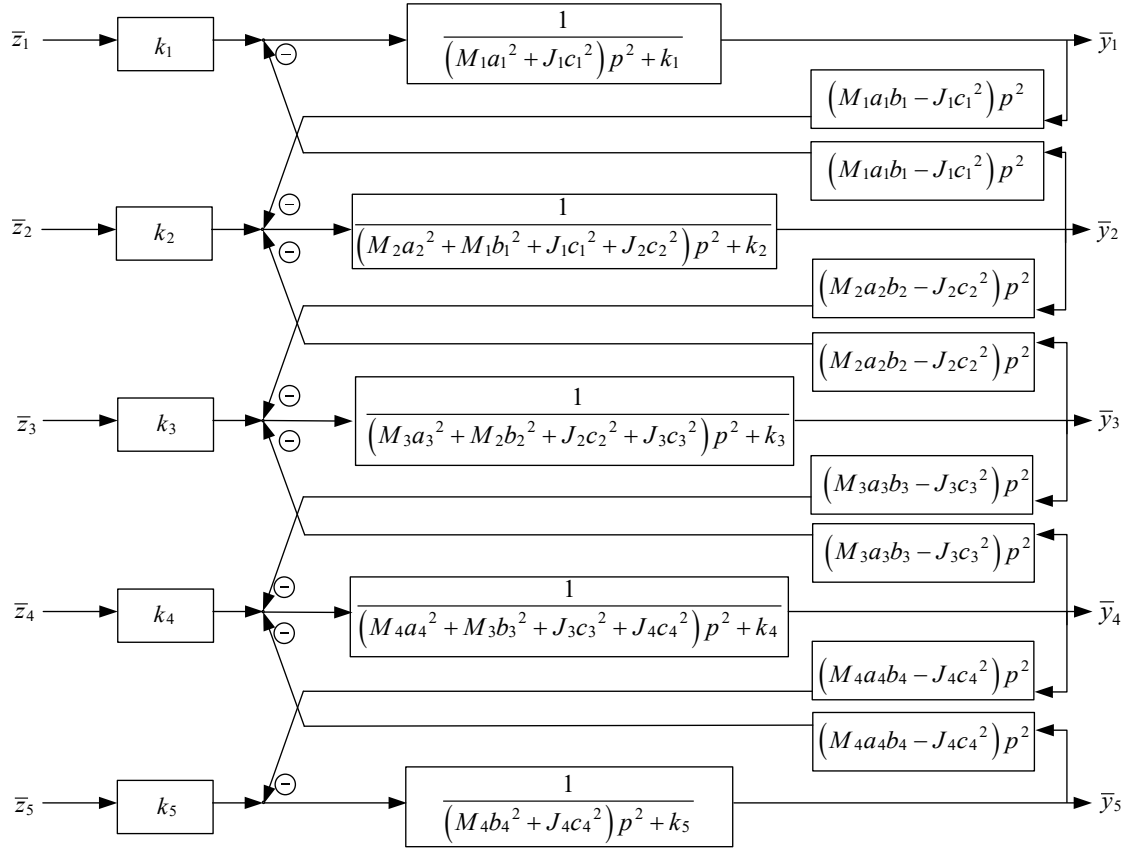
$$(U^T M U + V^T J V) \ddot{\bar{y}} + K \bar{y} = K \bar{z}. \quad (6)$$

It is assumed that the initial conditions are zero. In this case, the integral Laplace transformations lead (6) to a system of algebraic equations:

$$(M_0 p^2 + K) \bar{y} = K \bar{z}, \quad (7)$$

where $M_0 = U^T M U + V^T J V$ — matrix of the system, sign “—” above vectors y and z denotes the Laplace transformation [19].

Using the methods of [18], algebraic system (7) can be represented as a block diagram of a dynamically equivalent automatic control system (Fig. 2).


 Fig. 2. Block diagram of mechanical vibratory system (Fig. 1): $p = j\omega$, $j = \sqrt{-1}$

Transfer functions can be constructed based on a block diagram for a fixed set of connection coefficients γ_i . They are determined by the selection of an object, whose dynamic state is estimated by the expressions:

$$W_1(p) = \frac{\bar{y}_1}{\bar{z}_g}, W_2(p) = \frac{\bar{y}_2}{\bar{z}_g}, W_3(p) = \frac{\bar{y}_3}{\bar{z}_g}, W_4(p) = \frac{\bar{y}_4}{\bar{z}_g}, W_5(p) = \frac{\bar{y}_5}{\bar{z}_g}. \quad (8)$$

Physically, we consider the amplitude-frequency characteristics of transfer functions (8) as lever connections representing the ratio of the amplitudes of the coordinate vibrations $\{y_i\}$ to the vibration amplitude of the external kinematic disturbance $\{z_g\}$.

Within the framework of the lever interpretation, the positive branches of the amplitude-frequency response display lever connections of the 1st kind (implemented by double-arm levers). Negative branches represent lever connections of the 2nd kind (implemented by double-arm levers). The modes of resonance and dynamic damping of vibrations display degenerate lever connections, which can be represented by conditional virtual levers with zero or infinite arms.

The selection of the structure of external kinematic disturbances through setting the connection coefficients $\{\gamma_i\}$ uniquely determines the amplitudes of system coordinate vibrations. At the same time, the requirements imposed on the vibration amplitudes may:

- either imply ambiguity of the solution;
- either directly contradict each other;
- or, due to large errors, allow only partial compliance.

In these cases, criteria for the selection of external disturbances, which uniquely determine the vibration field according to the set of requirements, are needed. The logical approach for this task is based on the fact that external kinematic disturbances providing the required conditions can be determined by the criterion of optimality of vibration fields. The principle of this criterion is as follows: the vibration amplitudes of a technical object are selected in such a way that they deliver a minimum to a certain energy functional [20].

Formation of vibration fields of mechanical vibratory systems based on the optimality criterion. Within the framework of the model problem, it is assumed that a certain condition is set at points $A_{i1}, A_{i2}, \dots, A_{ik}$ of vibration field $\{y_i\}$, $i = 1 \dots n$ of the mechanical vibratory system. It consists in the fact that amplitudes $\{y_{ik}\}$, $k = 1 \dots m$ take fixed values $\{y_{01} \dots y_{0m}\}$:

$$\bar{y}_{ik} = y_{0k}. \quad (9)$$

Here, $k = 1 \dots m$, where m displays the number of points at which conditions for amplitudes are set; in this case, and further in the text, the sign “–” above y or z means the vibration amplitude of the steady component of the coordinate, unless otherwise specified. At the remaining points $\{y_i, i = 1 \dots n\} / \{y_{ik}, k = 1 \dots m\}$, the requirements for the values of the vibration field are not set.

Needed requirements (9) can be presented in the form:

$$A\bar{y} = b, \quad (10)$$

where A — matrix displaying the condition operator on the shape of the vibration field at the control points; b — vector of vibration field characteristics values [20].

In general, the conditions for vibration field (10) may be uncertain or incompatible. To rationally account for incompatible or uncertain requirements for the vibration field, a criterion of its optimality is introduced, as well as the assumption that the set of requirements can be fulfilled with some approximation.

Values $\bar{y}_1, \bar{y}_2 \dots \bar{y}_n$ mean the vibration amplitudes of the steady-state components; therefore, for each fixed frequency ω of external disturbances z , it is possible to set a variational task of constructing an optimal vibration field, which:

- delivers a minimum to the energy functional;
- displays representations of vibration patterns or values of potential or kinetic energy.

In general, the energy functional determines features of the distribution of the amplitudes of dynamic characteristics over the points of a mechanical vibratory system.

Within the framework of the considered model problem, the energy functional specified by operator T_e , displays the nonuniformity of the vibration field. Its indicator is the sum of the squares of the differences in the deviations of the vibration amplitudes of nearby points:

$$T_e(\bar{y}) = \sum_{i=1}^{n-1} (\bar{y}_{i+1} - \bar{y}_i)^2. \quad (11)$$

Zero value of energy functional (11) determines a uniform vibration field, whose vibration amplitudes of the points are equal to each other. Minimizing the energy functional, taking into account the specified conditions for the vibration amplitudes at the control points (10), determines the shape of the vibration field, extremely close to uniform.

We make allowance for a number of conditions:

- fixed frequency of external disturbances ω ;
- vibration field is optimal in the terms of the criterion given by the energy functional;
- amplitudes of the vibration field at the control points satisfy conditions (10).

In this case, the formal formulation of the problem of constructing a vibration field can be represented as:

$$y_\sigma(\omega) = \arg \min_{A\bar{y}=b, \bar{y} \in (-M_0\omega^2 + K)^{-1} K\bar{z}} T_e(\bar{y}), \quad (12)$$

where \bar{y} — vibration field defined by external kinematic disturbances \bar{z} , which are considered as independent variational parameters.

For fixed frequency ω , vibration field $y_\sigma(\omega)$, which exactly satisfies the set of requirements, is formally found as solution (12) to the conditional minimization of the quadratic function (11) taking into account linear conditions (10):

$$L(\bar{y}, \Lambda) = \langle T_{e0}\bar{y}, \bar{y} \rangle + \langle A\bar{y} - b, \Lambda \rangle \rightarrow \min_{\Lambda, \bar{y} \in (M_0 p^2 + K)^{-1} K\bar{z}}. \quad (13)$$

Here, \bar{y} — vibration field determined by external kinematic disturbance \bar{z} ; $\Lambda = (\lambda_1, \dots, \lambda_m)$ — Lagrange coefficients. Minimization in problem (13) proceeds according to the parameters \bar{z} of external disturbances. For fixed values \bar{z} of amplitudes of external disturbances, the created vibrational field \bar{y} is the solution to the problem:

$$(-M_0\omega^2 + K)\bar{y} = K\bar{z}, \quad (14)$$

where $M_0 = U^T M U + V^T J V$ — matrix of the system.

Vibration field \bar{y} , which exactly satisfies the set values (10), can be determined under the solution to the conditional minimum problem using the Lagrange function:

$$L(\bar{z}, \Lambda) = \langle T_{e0} (M_0 p^2 + K)^{-1} K\bar{z}, (M_0 p^2 + K)^{-1} K\bar{z} \rangle + \langle A (M_0 p^2 + K)^{-1} K\bar{z} - b, \Lambda \rangle \rightarrow \min_{\Lambda, \bar{z}}, \quad (15)$$

where \bar{z} — vector of vibration amplitudes of external kinematic disturbances; T_{e0} — matrix defining the quadratic form of the energy functional (11).

External disturbances \bar{z}_σ , forming the required vibrational field, the Lagrange multipliers Λ are the solution of the system:

$$\begin{pmatrix} K^T \left((-M_0\omega^2 + K)^{-1} \right)^T T_{e0} (-M_0\omega^2 + K)^{-1} K & A (-M_0\omega^2 + K)^{-1} K \\ A (-M_0\omega^2 + K)^{-1} K & 0 \end{pmatrix} \begin{pmatrix} \bar{z} \\ \Lambda \end{pmatrix} = \begin{pmatrix} 0 \\ b \end{pmatrix}. \quad (16)$$

Thus, z_σ — solution to the problem of conditional minimization (15), (16). The optimal vibration field y_σ is determined by external disturbance z_σ and has the form:

$$y_\sigma = (-M_0\omega^2 + K)^{-1} K z_\sigma. \quad (17)$$

Here, y_σ can be called an interpolating vibration field, since under the condition of compatibility (16), it exactly satisfies requirements (10). Taking into account the dependence on frequency ω , the compatibility and certainty of system (16) is characterized within the framework of the theorems of the existence and uniqueness of solutions to systems of equations of the theory of splines [20]. Under the condition of compatibility and certainty of the system (16) and (17), the optimal vibration field y_σ exactly satisfies the set of conditions (10).

Necessary conditions (10) may contain noise, errors, or be contradictory. Taking into account contradictory or unreliable requirements, the vibration field can be constructed by solving the smoothing problem. Its result is an optimal vibration field that satisfies conditions different from the initial requirements, but close to them.

Vibration field assessment with account of noisy or unreliable dynamic performance requirements. Vibration field $y_\sigma(\omega)$ (17) satisfying conditions (10) can be approximated using vibration field $y_\alpha(\omega)$ taking into account the unreliability or inconsistency of the necessary requirements (10):

$$y_\alpha(\omega) = \arg \min_{\bar{y} = (-M_0\omega^2 + K)^{-1} K \bar{z}} \left(\alpha T_e(\bar{y}) + \sum_{k=1}^m (\bar{y}_{ik} - y_{0k})^2 \right). \quad (18)$$

Here, $T_e \bar{y}$ — operator displaying the criterion of optimality of the shape of the vibration field; α — smoothing parameter indicating the priority of the criterion of optimality of the shape of the vibration field in relation to the requirements of conditions (10).

In expression (18), \bar{z} is considered as an independent variable. Vibration field $y_\alpha(\omega)$ can be called smoothing, since it approximately satisfies the necessary requirements of the system.

Vibration field y_α is determined by a system of equations obtained through minimizing the Lagrange function:

$$L_\alpha(\bar{y}(\bar{z})) = \alpha \langle T_{e0} \bar{y}, \bar{y} \rangle + \|A \bar{y} - b\|^2 \rightarrow \min_{\bar{z}}. \quad (19)$$

Here, $\bar{y}(\bar{z})$ is a vibration field formed by external kinematic disturbance \bar{z} :

$$(-M_0\omega^2 + K) \bar{y} = K \bar{z}. \quad (20)$$

A replacement based on (20) is made:

$$\bar{y} = (-M_0\omega^2 + K)^{-1} K \bar{z}. \quad (21)$$

Now, the Lagrange function (19), taking into account (20) and (21), is reduced to the form:

$$L_\alpha(\bar{z}) = \alpha \left\langle T_{e0} (-M_0\omega^2 + K)^{-1} K \bar{z}, (-M_0\omega^2 + K)^{-1} K \bar{z} \right\rangle + \|A (-M_0\omega^2 + K)^{-1} K \bar{z} - b\|^2 \rightarrow \min_{\bar{z}}, \quad (22)$$

where $\|\cdot\| = \sqrt{\langle \cdot, \cdot \rangle}$ — length of the vector in R^n , expressed in terms of the scalar product $\langle \cdot, \cdot \rangle$.

Consider the external kinematic disturbances z_α . They form optimal vibration field y_α , which smooths out the specified conditions (10) and is a solution to the minimization problem (22). Such disturbances are determined by the system:

$$K^T \left((-M_0\omega^2 + K)^{-1} \right)^T (\alpha T_{e0} + A^T A) (-M_0\omega^2 + K)^{-1} K z_\alpha = K^T \left((-M_0\omega^2 + K)^{-1} \right)^T A^T b. \quad (23)$$

After simplifications of system (23), the desired amplitudes of kinematic disturbances z_α are determined by the expression:

$$z_\alpha = K^{-1} (M_0\omega^2 + K) (\alpha T_{e0} + A^T A)^{-1} A^T b. \quad (24)$$

As shown above, external disturbances z_α (24) are a solution to problem (23), taking into account the selection of the smoothing parameter α . These disturbances provide the construction of vibration field y_α , which approximately satisfies the set of requirements (10), taking into account possible incompatibility or unreliability:

$$y_\alpha = (M_0\omega^2 + K)^{-1} K z_\alpha. \quad (25)$$

The type of vibration field y_α (25) is clearly independent of the frequencies of external disturbances ω :

$$\bar{y}_\alpha = (\alpha T_{e0} + A^T A)^{-1} A^T b. \quad (26)$$

External disturbance z_α , which provides the construction of an optimal smoothing vibration field y_α (24), can be used to construct an interpolation vibration field y_σ as $\alpha \rightarrow 0$. The selection of smoothing parameter α is determined from the conditions of smallness of the discrepancy:

$$\varphi(\alpha) = \|Ay_\alpha - b\|^2, \quad (27)$$

where $y_\alpha = (-M_0\omega^2 + K)^{-1} Kz_\alpha$, z_α — kinematic disturbance (27).

It should be noted that vibration field y_α depends on frequency ω implicitly, through the smoothing parameter $\alpha = \alpha(\omega)$, whose selection is determined by the frequency of external disturbance ω and the value of discrepancy (27).

Construction of a vibration field for a mechanical oscillatory system. Computational experiment. Let the parameters of the mechanical vibratory system (Fig. 1) be given by stiffness k_i , masses M_i , moments of inertia J_i and geometric characteristics l_{1i} , l_{2i} (Table 1).

Table 1

Parameters of the model mechanical vibratory system

No.	M , kg	J , kg·m ²	k , N/m	l_1 , m	l_2 , m
1	100	10	1,000	1	1
2	200	20	2,000	1	1
3	300	30	3,000	1	1
4	400	40	4,000	1	1

As requirements for the amplitudes of the vibration field, conditions are set for the values at points A_i (Table 2).

Table 2

Vibration amplitudes at the points of the vibration field (y , m)

Values	A_1	A_2	A_3	A_4	A_5
Required	0.002	–	–	–	0.005
Smoothed out	0.002	0.0027	0.0035	0.0043	0.005

Expression (11) is used as an energy functional, which can be represented using operator T_e :

$$T_e : \begin{pmatrix} \bar{y}_1 \\ \bar{y}_2 \\ \bar{y}_3 \\ \bar{y}_4 \\ \bar{y}_5 \end{pmatrix} \rightarrow \begin{pmatrix} \bar{y}_2 - \bar{y}_1 \\ \bar{y}_3 - \bar{y}_2 \\ \bar{y}_4 - \bar{y}_3 \\ \bar{y}_5 - \bar{y}_4 \end{pmatrix} = \begin{pmatrix} 1 & -1 & & & 0 \\ & 1 & -1 & & \\ & & 1 & -1 & \\ 0 & & & 1 & -1 \end{pmatrix} \begin{pmatrix} \bar{y}_1 \\ \bar{y}_2 \\ \bar{y}_3 \\ \bar{y}_4 \\ \bar{y}_5 \end{pmatrix}.$$

Expression $\langle T_e \bar{y}, T_e \bar{y} \rangle$ can be represented as:

$$\langle T_e \bar{y}, T_e \bar{y} \rangle = \langle T_e^T T_e \bar{y}, \bar{y} \rangle = \langle T_{e0} \bar{y}, \bar{y} \rangle = \left\langle \begin{pmatrix} 1 & -1 & & & 0 \\ -1 & 2 & -1 & & \\ & -1 & 2 & -1 & \\ & & -1 & 2 & -1 \\ 0 & & & -1 & 1 \end{pmatrix} \begin{pmatrix} \bar{y}_1 \\ \bar{y}_2 \\ \bar{y}_3 \\ \bar{y}_4 \\ \bar{y}_5 \end{pmatrix}, \begin{pmatrix} \bar{y}_1 \\ \bar{y}_2 \\ \bar{y}_3 \\ \bar{y}_4 \\ \bar{y}_5 \end{pmatrix} \right\rangle.$$

Here, T_{e0} — matrix that defines a quadratic shape. The value of operator $T_e \bar{y}$ is zero on a uniform vibration field $\bar{y} = \text{const}$. The vibration amplitudes of the points of this field are equal to each other for an external kinematic disturbance at an arbitrary frequency.

We set conditions (10) for the vibration field. For this purpose, data operator A_{15} can be used, which maps the amplitude values at points A_1 , A_5 to vibration field y :

$$A_{15} : \begin{pmatrix} \bar{y}_1 \\ \bar{y}_2 \\ \bar{y}_3 \\ \bar{y}_4 \\ \bar{y}_5 \end{pmatrix} \rightarrow \begin{pmatrix} 1 & 0 & 0 & 0 & 0 \\ 0 & 0 & 0 & 0 & 1 \end{pmatrix} \begin{pmatrix} \bar{y}_1 \\ \bar{y}_2 \\ \bar{y}_3 \\ \bar{y}_4 \\ \bar{y}_5 \end{pmatrix} = \begin{pmatrix} \bar{y}_1 \\ \bar{y}_5 \end{pmatrix}.$$

The vibration field interpolating the set values at points A_1, A_5 (Table 2), can be approximated using the smoothing vibration field \bar{y}_α for smoothing parameter $\alpha = 0.01$. We find the difference between the values of the vibration field and the required values for the selected smoothing coefficient α . It is determined by the residual function (27), whose value is approximately 0.00001 m, where $b = (0.002, 0.005)^T$. The constructed vibration field, smoothing the interpolation conditions, has a linear shape (Table 2). For fixed smoothing parameter $\alpha = 0.01$, the set of vibration amplitudes of the points of vibration field y_α , which provides proximity to the interpolated data with residual $\varphi(\alpha) = 0.00001$ m (Table 2), has the form of constant functions of the frequency of external disturbance ω (Fig. 3 a).

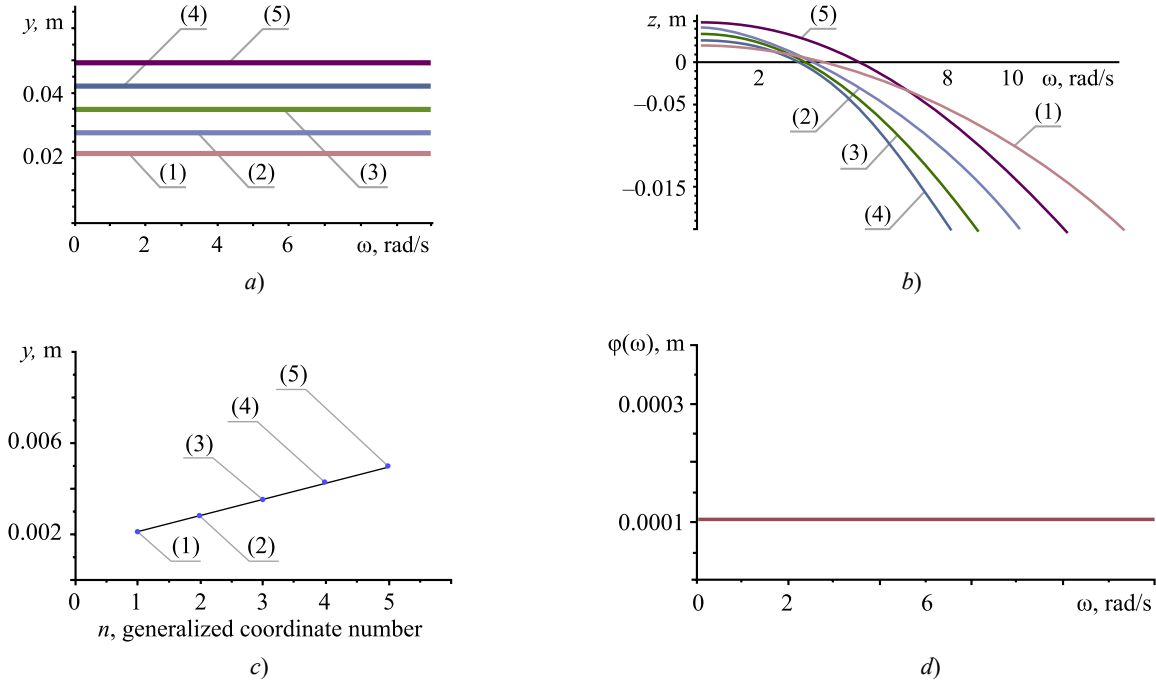


Fig. 3. Vibration field characteristics: *a* — values of vibration amplitudes of smoothing vibration field for frequencies of external disturbances in the range $\omega \in (0.100)$ rad/s; *b* — amplitudes of external kinematic disturbances providing the required vibration amplitudes depending on the frequency of disturbances ω ; *c* — shape of the vibration field for frequencies in the range $\omega \in (0...100)$; (1), (5) — required values of the vibration field; (2), (3), (4) — values based on the energy approach; *d* — deviation $\varphi(\omega)$ of the vibration field from the required amplitude values at fixed points of the technical object for constant smoothing coefficient $\alpha = 0.1$

In this case, the value of the vibration amplitudes of the generalized coordinates remains constant when the frequency of external kinematic disturbances z_α changes. These disturbances, which are needed to provide the required amplitudes at fixed points of the vibration field, depend significantly on frequency ω of external disturbances (Fig. 3 b).

We describe a vibration field for a fixed frequency or a frequency domain in which it remains unchanged. It can be represented by a graph of a function depending on the number of the generalized coordinate or the coordinate of the point of the system in which the vibration field is estimated. The shape of the vibration field is determined by the optimality criterion. Specifically, energy functional T_{e0} , which determines the optimality criterion, forms a linear shape of the vibration field (Fig. 3 c). It should be noted that the “interpolation” vibration field is constructed using a “smoothing” vibration field corresponding to smoothing parameter α . The deviation of the “smoothing” vibration field should be negligible. In the considered model example, for $\alpha = 0.1$, the deviation of the smoothing vibration field is represented by constant $\varphi(\alpha) = 0.0001$ m (Fig. 3 d). It should be noted that in the general case of the energy functional, the value of the smoothing coefficient α , which provides a fixed level of residual $\varphi(\alpha) = \varphi^*$, depends on frequency ω and the system of requirements.

Thus, the options for the formation of dynamic states of mechanical vibratory systems in the form of a vibration field satisfying a system of conditions depend on:

- energy functional reflecting the characteristics of the vibration field;
- operator displaying a set of requirements for the vibration field.

Other options for the formation of a vibration field based on the selection of an energy operator are also possible.

Correction of optimality criteria for shaping vibration fields using the weight coefficients of energy operators.

The shape of the vibration field with the possibility of equalizing the vibration amplitudes of the coordinates of a technical object is considered above. There are other approaches to minimizing the amplitudes of generalized coordinates, e.g., by selecting energy operator T_E in the form of an identity map:

$$T_E : \bar{y} \rightarrow E\bar{y},$$

where E — identity operator.

The formation of a vibrational field based on the energy operator is associated with minimizing or zeroing the quadratic function of the amplitudes of in-phase harmonic vibrations of a fixed frequency. As a result of solving the smoothing problem, a vibration field is formed for the energy functional corresponding to unit operator T_E . The amplitudes of its vibrations at points A_2, A_3, A_4 are zero (Fig. 4 a), i.e., at points A_2, A_3 and A_4 , a dynamic vibration damping mode is implemented.

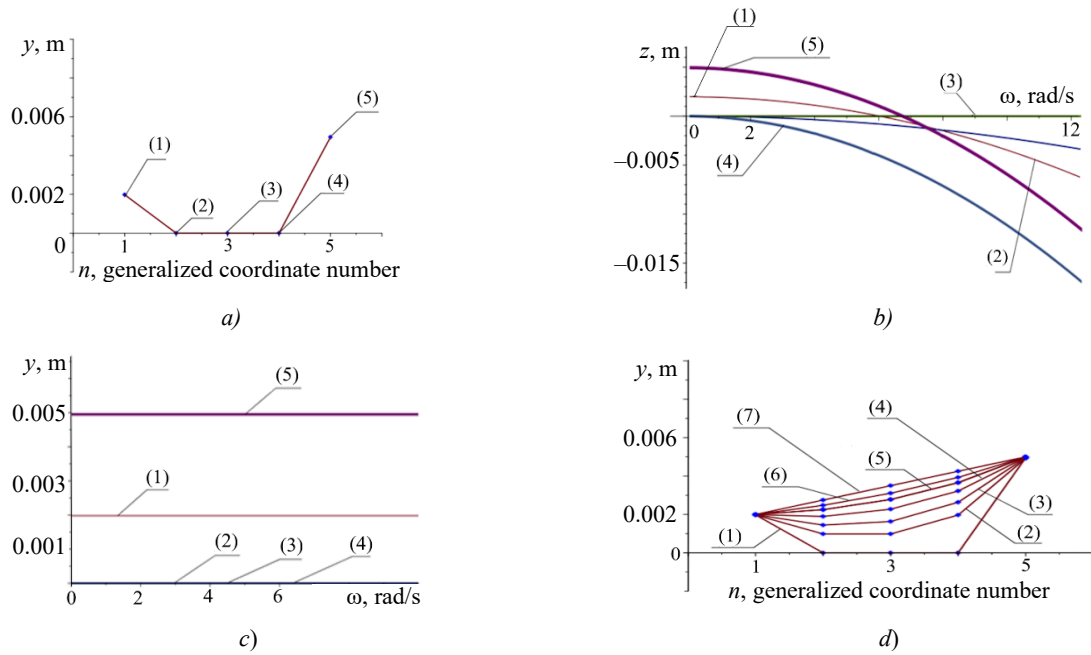


Fig. 4. Possibilities of vibration field correction: a — shape of vibration field for energy functional displays minimum possible vibration amplitudes, taking into account the necessary requirements; b — amplitudes of external kinematic disturbances z_i , providing the necessary requirements for dynamic features of vibration field; c — vibration amplitudes of vibration field of technical object depending on frequency of external disturbance; d — options of vibration fields depending on weight coefficient of energy operator T_β

The totality of external kinematic disturbances is a solution to the problem of minimizing the energy functional, generally defined on the dynamic states of mechanical vibratory systems, taking into account the requirements for vibration amplitudes at fixed points of the vibration field (Fig. 4 b).

The characteristic property of forced kinematic disturbances, which provide the required shape of the vibration field, is an increase in the vibration amplitude when the frequency of disturbances grows (Fig. 4 c). External kinematic disturbances z provide a fixed vibration field of a technical object at various frequencies ω (Fig. 4 d). Smoothing parameter $\alpha = 0.01$ provides an absolute deviation from the required values at level $\varphi(\alpha) = 0.000053$. This shows that the totality of the vibration amplitudes at the remaining points of the vibration field determines the characteristics of the energy operator based on the required values of the vibration field amplitudes at fixed points of the mechanical vibratory system. Specifically, operator T_e is aimed at forming a uniform vibration field, and operator T_E is aimed at zeroing the vibration field.

Weight coefficients that display a combination of optimality criteria can be used. This allows combining the following:

- requirements for convergence of vibration amplitudes of points of vibration fields;
- requirements aimed at zeroing the vibration amplitudes of the vibration field points.

Varying the weight coefficients that determine the combination of optimal criteria for the formation of a vibration field is actually a way to correct the vibration field.

We build a family of forms of vibration fields of a technical object that meet certain conditions. For this purpose, we use a combined optimality criterion implemented by a weighted sum of energy functionals, taking into account the weight factor:

$$\|T_{\beta} \bar{y}\|^2 = \|T_e \bar{y}\|^2 + \beta \|T_E \bar{y}\|^2. \quad (28)$$

Here, β — weight factor that determines the combination of the optimality criterion based on the smallness of the amplitudes and the criterion based on the uniformity of the amplitudes of the vibration fields. The variation of the weight coefficient β leads to the construction of a family of vibration fields. The criterion of their optimality has a complex structure that takes into account the differences and absolute values of the vibration amplitudes of the points of the vibration field. The selection of a set of weight coefficients determines the appropriate forms of vibration fields, which are realized under the influence of external disturbances, which are the solution to the variational problem [20].

Based on the set of weight coefficients β , it is possible to construct optimal vibration fields that meet the requirements for vibration amplitudes at fixed points with sufficient accuracy (Table 3).

Table 3

Forms of optimal vibration fields for weight coefficients of the energy functional

No	β	α	Residual $\varphi(\alpha)$, m	Frequency ω , rad/s	y_1 , m	y_2 , m	y_3 , m	y_4 , m	y_5 , m
1	1	0.01	0.0000841	10	0.0019704	0.0009850	0.0009845	0.0019686	0.0049213
2	0.5	0.01	0.0000503	10	0.0019847	0.0014467	0.0016322	0.0026337	0.0049521
3	0.25	0.01	0.0000305	10	0.0019940	0.0018969	0.0022740	0.0032196	0.0049701
4	0.125	0.001	0.0000195	10	0.0020000	0.0022503	0.0027818	0.0036611	0.0049980
5	0.0625	0.001	0.0000014	10	0.0020004	0.0024754	0.0031053	0.0039292	0.0049986

Combining optimal criteria for the formation of vibration fields is a way to correct the dynamic states of a technical object (Fig. 4 d). Note that the found kinematic disturbances z_i , considered as functions of frequency ω , have one zero each (Fig. 5 f).

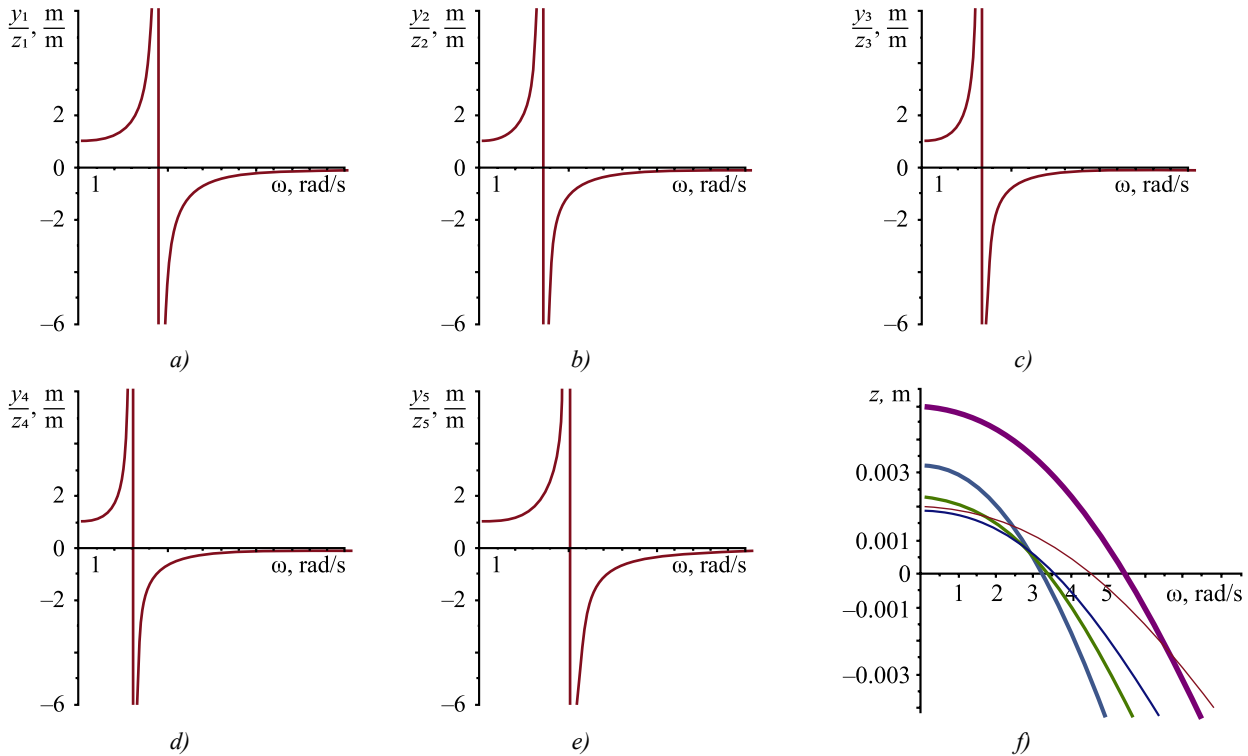


Fig. 5. Optimal vibration field characteristics for weight coefficient $\beta = 0.25$ and smoothing parameter $\alpha = 0.01$:
a — ratio of the vibration amplitudes of points of optimal vibration field $(y_{\alpha})_1$ to amplitude of kinematic disturbances $(z_{\alpha})_1$;
b — ratio of amplitudes $(y_{\alpha})_2$ to $(z_{\alpha})_2$; c — ratio of amplitudes $(y_{\alpha})_3$ to $(z_{\alpha})_3$; d — ratio of amplitudes $(y_{\alpha})_4$ to $(z_{\alpha})_4$;
e — ratio of amplitudes $(y_{\alpha})_5$ to $(z_{\alpha})_5$; f — value of amplitudes of external disturbances (z_{α}) depending on frequency ω

Amplitude ratios y_i/z_i , for which $y_i = y_i(\omega)$ and $z_i = z_i(\omega)$, are found on the basis of solution to the problem of determining optimal vibration fields, have one discontinuity of the 2nd kind (Fig. 5a–d).

The specified vibration amplitudes of fixed points of the vibration field of the mechanical vibration system should be provided. For this purpose, combined energy functionals with account for the weight coefficients can be selected, and, based on these indicators, the required external kinematic effects with account for the variational principles can be determined.

If the requirements for the vibration amplitudes of the vibration field are highly noisy or incompatible, it is possible to construct a vibration field that meets the requirements with a certain accuracy and is optimal for the combined criterion, but for other conditions.

Determination of the optimal criterion for shaping vibration fields based on the residual function. In general, the requirements for a vibration field can be a complex set of joint or incompatible conditions reflecting limitations on the amplitudes of displacements, velocities, and dynamic reactions, including non-retentive conditions.

Taking into account the criterion of optimality of the vibration field of a mechanical vibratory system, the set of joint conditions allows for a single solution in the form of a certain structure of external disturbances. In the case of incompatibility of conditions on the vibration field, the optimality criterion actually acts as a method of regularization of an incorrect inverse problem.

The energy functional determines the specifics of the formation of vibration fields based on the values of the vibration amplitudes of displacements, velocities, force disturbances, or reactions occurring between the elements of the system. Energy functionals can convey ideas about the maximum potential or kinetic energy, or serve as a combination of them with account for weight coefficients that act as methods for correcting vibration fields.

It is possible to add conditions according to the nature of the external kinematic or force disturbances themselves to the conditions for the values of the amplitudes of the vibration fields. They are expressed in the fact that the amplitudes of external disturbances take fixed absolute or relative values. The need to set requirements for input disturbances is due to the fact that to provide the specified forms of vibration fields, the amplitudes of external disturbances can increase indefinitely with growing frequency.

Thus, here is a complex task of selecting:

- an energy functional;
- an operator of requirements for a vibration field;
- an additional operator of requirements for external force or kinematic disturbances.

Within the framework of the development of the structural theory of the optimal vibration field, it is possible to set a generalized task of its construction:

$$y_{\sigma}(\omega) = \arg \min_{A\bar{y}=b, \bar{y} \in (-M_0\omega^2 + K)^{-1} K\bar{z}, C\bar{z}=f} T_e(\bar{y}),$$

where $C \cdot \bar{z} = f$ — additional connection limiting the dimension of external kinematic disturbances.

The technique for selecting an effective operator can be based on minimizing the function of additional residual, depending on the parameters of the energy operator:

$$\beta_{\sigma} = \arg \min_b \|By_{\beta} - c\|^2,$$

where y_{β} — solution to the problem of determining the vibration field with a combined optimality criterion T_{β} ((28) and Fig. 4) and conditions A (10); B — operator for determining values in a set of additional points; c — vector of values at additional points.

This problem can be considered as the problem of selecting a “natural” optimality criterion [21]. Thus, the presented set of tasks and solution techniques can be the fundamental basis for the structural theory of the construction of vibration fields.

Discussion and Conclusion. Elements of the structural theory of optimal vibration fields of mechanical vibratory systems have been developed. The main components of this theory are methods for constructing vibration fields of mechanical vibratory systems based on variational principles. The basic concept is the vibration field of a mechanical vibratory system. It represents the distribution of vibration amplitudes of generalized coordinates and other dynamic characteristics of a mechanical vibratory system over the points of an object with an estimated dynamic state.

It is assumed that a system of conditions is set at a number of points of the mechanical vibratory system. It is expressed in terms of absolute or relative values of displacements, velocities, and reactions. Conditions are requirements for the characteristics of the vibration field of a mechanical vibratory system. There is also a system of conditions related to the features of external force or kinematic disturbances, and it also reflects the requirements for a set of absolute and relative values of the amplitudes of kinematic or force disturbances.

For the development of the applied theory of optimal vibration fields within the framework of structural representations, an analogy can be established between the two pairs. The first one is formed from energy operator T and

condition operator A in the theory of abstract splines. The second one is formed by the criterion of optimality of the vibration field and a system of requirements for the characteristics of the vibration field at control points.

Interpolation, smoothing and mixed splines are distinguished within the framework of the theory of variational spline approximation. Within the framework of the concepts of vibration fields of mechanical vibratory systems based on structural representations, the role of the spline is performed by a set of amplitudes of external force and kinematic disturbances, and the role of interpolation conditions is performed by a set of requirements for the amplitudes of input or output signals.

It can be assumed that there are differences between the vibration fields of technical objects under conditions of external forced or kinematic disturbances, which are considered as a key factor in the formation of a dynamic state. At the same time, when constructing a vibration field, it is considered natural to estimate energy ratios depending on generalized coordinates. Their values are determined by an external force or kinematic disturbance. In fact, we need to find two vectors — generalized coordinates and external disturbances.

We take into account the variational approach, as well as the set of requirements for the vibration field and external disturbances. We present the problem of determining external disturbances that form a set of dynamic states in the form of a vibration field with account for a system of conditions. In this interpretation, we are talking about the optimization problem in different formulations within the framework of variational principles. Specifically, it is possible to set tasks similar to the tasks of constructing a smoothing or mixed spline. It depends on the compatibility of the conditions for the input and output signals. We note the following an essential feature of the problems of constructing vibration fields: the frequency of an external disturbance is a parameter of the optimization problem, and in the case of systems with concentrated parameters, amplitude vectors serve as elements of an n -dimensional Cartesian space.

Analogies between the tasks of approximation and construction of vibration fields provide developing techniques for the formation, assessment, and correction of dynamic states of technical objects.

The improved structural theory of optimal vibration fields will be in demand in the aviation and space industries. Its apparatus can be used to maintain flight safety and durability of structures. In addition, it is logical to use this approach in mechanical engineering, electronics, and the development of medical equipment. The theory will allow solving the problems of forming, evaluating, and correcting the states of technical systems and devices under conditions of vibration loading. Another area of its practical application is the creation and improvement of measuring methods and means of complex vibratory systems. We also believe that mathematical models of optimal vibration fields are of interest for the development of new technologies and materials, in particular, materials with high damping, which can reduce the level of vibrations and noise in technical systems.

As the main limitation of the technique, it is necessary to indicate that vibrations in the coordinates of an object, which are steady-state forms of harmonic vibrations or vibrations of a fixed amplitude, are considered.

References

1. Juan Carlos A Jauregui Correa, Alejandro A Lozano Guzman. Chapter One — Fundamentals of Mechanical Vibrations. *Mechanical Vibrations and Condition Monitoring*. Cambridge, MA: Academic Press; 2020. P. 1–26. <https://doi.org/10.1016/B978-0-12-819796-7.00001-9>
2. Jalal Torabi, Jarkko Niiranen. Nonlinear Finite Element Free and Forced Vibrations of Cellular Plates Having Lattice-Type Metamaterial Cores: A Strain Gradient Plate Model Approach. *Mechanical Systems and Signal Processing*. 2023;192:110224. <https://doi.org/10.1016/j.ymssp.2023.110224>
3. Keigo Ikeda, Kota Kamimori, Ikkei Kobayashi, Jumpei Kuroda, Deigo Uchino, Kazuki Ogawa, et al. Basic Study on Mechanical Vibration Suppression System Using 2-Degree-of-Freedom Vibration Analysis. *Vibration*. 2023;6(2):407–420. <https://doi.org/10.3390/vibration6020025>
4. Bolshakov RS. *Features of Vibration States of Transport and Technological Machines. Dynamic Reactions and Forms of Interaction of Elements*. Novosibirsk: Nauka; 2020. 411 p. (In Russ.).
5. Dumitriu M, Apostol II. Influence of Interference between Vertical and Roll Vibrations on the Dynamic Behaviour of the Railway Bogie. *Vibration*. 2022;5(4):659–675. <https://doi.org/10.3390/vibration5040039>
6. Sehner M, Seidi-Nigsch M, Valdés Nava LE, Loy H. Vibration Mitigation: Under-Ballast Mats in Heavy-Haul Applications. *Practice Periodical on Structural Design and Construction*. 2023;28(4):05023004. <https://doi.org/10.1061/PPSCFX.SCENG-1258>
7. Zhenhang Zhao, Ying Gao, Chenghui Li. Research on the Vibration Characteristics of a Track's Structure Considering the Viscoelastic Properties of Recycled Composite Sleepers. *Applied Sciences*. 2020;11(1):150. <https://doi.org/10.3390/app11010150>
8. Yu Zou, Yongpeng Wen, Qian Sun. Study on the Urban Rail Transit Sleeper Spacing Considering Vehicle System. *MATEC Web of Conferences*. 2019;296:01008. <https://doi.org/10.1051/mateconf/201929601008>
9. Yoshino Sh, Abe K, Koro K. An Analytic Solution of Mathematical Expectation for Bogie-Track Interaction Problems. *Mechanical Engineering Journal*. 2023;10(3):22–00300. <https://doi.org/10.1299/mej.22-00300>

10. Wenping Chu, Yang Song. Study on Dynamic Interaction of Railway Pantograph–Catenary Including Reattachment Momentum Impact. *Vibration*. 2020;3(1):18–33. <https://doi.org/10.3390/vibration3010003>
11. Maryam El Moueddeb, François Louf, Pierre-Alain Boucard, Franck Dadié, Gilles Saussine, Danilo Sorrentino. An Efficient Numerical Model to Predict the Mechanical Response of a Railway Track in the Low-Frequency Range. *Vibration*. 2022;5(2):326–343. <https://doi.org/10.3390/vibration5020019>
12. Korendiy V, Kachur O, Predko R, Kotsiumbas O, Stotsko R, Ostashuk M. Generating Rectilinear, Elliptical, and Circular Oscillations of a Single-Mass Vibratory System Equipped with an Enhanced Twin Crank-Type Exciter. *Vibroengineering Procedia*. 2023;51:8–14. <https://doi.org/10.21595/vp.2023.23657>
13. Krot P, Shiri H, Dąbek P, Zimroz R. Diagnostics of Bolted Joints in Vibrating Screens Based on a Multi-Body Dynamical Model. *Materials*. 2023;16(17):5794. <https://doi.org/10.3390/ma16175794>
14. Vishva Priya Vellingiri, Udhayakumar Sadasivam. Effect of Vibrator Parameters and Physical Characteristics of Parts on Conveying Velocity. *Strojniški vestnik — Journal of Mechanical Engineering*. 2023;69(7–8):352–363. <https://doi.org/10.5545/sv-jme.2022.510>
15. Korendiy V, Gursky V, Kachur O, Dmyterko P, Kotsiumba O, Havrylchenko O. Mathematical Model and Motion Analysis of a Wheeled Vibro-Impact Locomotion System. *Vibroengineering Procedia*. 2022;41:77–83. <https://doi.org/10.21595/vp.2022.22422>
16. Krupenin V, Astashev V. Properties of Vibration Fields in a Two-Dimensional Lattice Structure Colliding with an Obstacle. In: EJ Sapountzakis, M Banerjee, P Biswas, E Inan (eds). *Proc. 14th Int. Conf. on Vibration Problems (ICOVP)*. Singapore: Springer; 2020. P. 473–485. https://doi.org/10.1007/978-981-15-8049-9_30
17. Karnovsky IA, Lebed E. Structural Theory of Vibration Protection Systems. In book: *Theory of Vibration Protection*. Cham: Springer; 2016. 708 p. https://doi.org/10.1007/978-3-319-28020-2_12
18. Eliseev AV. *Structural Mathematical Modeling Applications in Technological Machines and Transportation Vehicles*. Hershey, PA: IGI Global; 2023. 288 p. <https://doi.org/10.4018/978-1-6684-7237-8>
19. Sarah Saeed. Laplace Transform: Basics and Main Properties. In book: J García (ed). *Encyclopedia of Electrical and Electronic Power Engineering*. Amsterdam: Elsevier; 2023. P. 645–651. <https://doi.org/10.1016/B978-0-12-821204-2.00062-3>
20. Bezhaev AYU, Vasilenko VA. *Variational Theory of Splines*. New York, NY: Springer; 2001. 208 p. <https://doi.org/10.1007/978-1-4757-3428-7>
21. Vasilenko VA, Elyseev AV. Abstract Splines with the Tension as the Functions of Parameters in Energy Operator. *Siberian Journal of Computational Mathematics*. 1998;1(4):301–311. URL: <https://www.mathnet.ru/links/be5b8fe7cfea1927a6fff34630f7de33/sjvm311.pdf> (accessed: 11.12.2023).

About the Authors:

Andrey V. Eliseev, Cand.Sci. (Eng.), Associate Professor of the Department of Mechanical Engineering Design and Standardization, Irkutsk National Research Technical University (83, Lermontov St., Irkutsk, 664074, RF), Associate Professor of the Mathematics Department, Irkutsk State Railway Transport Engineering University (15, ul. Chernyshevskogo, Irkutsk, 664074, RF), SPIN-code: [8781-1123](https://orcid.org/0000-0001-8781-1123), [ORCID](https://orcid.org/0000-0001-8781-1123), [ResearcherID](https://orcid.org/0000-0001-8781-1123), [ScopusID](https://orcid.org/0000-0001-8781-1123), eavsh@ya.ru

Nikolai K. Kuznetsov, Dr.Sci. (Eng.), Professor, Head of the Department of Mechanical Engineering Design and Standardization, Irkutsk National Research Technical University (83, Lermontov St., Irkutsk, 664074, RF), SPIN-code: [4875-9445](https://orcid.org/0000-0001-4875-9445), [ORCID](https://orcid.org/0000-0001-4875-9445), [ResearcherID](https://orcid.org/0000-0001-4875-9445), [ScopusID](https://orcid.org/0000-0001-4875-9445), knik@istu.edu

Claimed contributorship:

AV Eliseev: basic concept formulation, working with the text of the manuscript.

NK Kuznetsov: analysis and generalization of the research results.

Conflict of interest statement: the authors do not have any conflict of interest.

All authors have read and approved the final version of manuscript.

Received 18.12.2023

Revised 17.01.2024

Accepted 21.01.2024

Об авторах:

Елисеев Андрей Владимирович, кандидат технических наук, доцент кафедры конструирования и стандартизации в машиностроении Иркутского национального исследовательского технического университета (664074, РФ, г. Иркутск, ул. Лермонтова, 83), доцент кафедры математики Иркутского государственного

университета путей сообщения (664074, РФ, г. Иркутск, ул. Чернышевского, 15), [ResearcherID](#), [ScopusID](#),
SPIN-код: [8781-1123](#), [ORCID](#), eavsh@ya.ru

Кузнецов Николай Константинович, доктор технических наук, профессор, заведующий кафедрой
конструирования и стандартизации в машиностроении Иркутского национального исследовательского
технического университета (664074, РФ, г. Иркутск, ул. Лермонтова, 83), [ResearcherID](#), [ScopusID](#), [ORCID](#),
SPIN-код: [4875-9445](#), knik@istu.edu

Заявленный вклад авторов:

А.В. Елисеев — создание концепции, работа с текстом рукописи.

Н.К. Кузнецов — анализ и обобщение результатов исследования.

Конфликт интересов: авторы заявляют об отсутствии конфликта интересов.

Все авторы прочитали и одобрили окончательный вариант рукописи.

Поступила в редакцию 18.12.2023

Поступила после рецензирования 17.01.2024

Принята к публикации 21.01.2024

МЕCHANICS МЕХАНИКА



UDC 539.3

Research article

<https://doi.org/10.23947/2687-1653-2024-24-1-23-35>

Coupled Axisymmetric Thermoelastoelectricity Problem for a Round Rigidly Fixed Plate

Dmitriy A. Shlyakhin , Elena V. Savinova

Samara State Technical University, Samara, Russian Federation

slenax@yandex.ru

EDN: DUOERK

Abstract

Introduction. To describe the operation of temperature piezoceramic structures, the theory of thermoelastoelectricity is used, in which the mathematical model is formulated as a system of nonself-adjoint differential equations. The complexity of its integration in general leads to the study of problems in an unrelated formulation. This does not allow us to evaluate the effect of electroelastic fields on temperature. The literature does not present studies on these problems in a three-dimensional coupled formulation in which closed solutions would be constructed. At the same time, conducting such studies allows us to understand the interaction picture of mechanical, thermal and electric fields in a structure. To solve this problem, a new closed solution of a coupled problem for a piezoceramic round rigidly fixed plate has been constructed in this research. It provides for qualitative assessment of the cross impact of thermoelastoelectric fields in this electroelastic system.

Materials and Methods. The object of the study is a piezoceramic plate. The case of unsteady temperature change on its upper front surface is considered, taking into account the convection heat exchange of the lower plane with the environment (boundary conditions of the 1st and 3rd kind). The electric field induced as a result of the thermal strain generation is fixed by connecting the electrodated surfaces to the measuring device. The thermoelastoelectricity problem includes the equations of equilibrium, electrostatics, and the unsteady hyperbolic heat equation. It is solved by the generalized method of finite biorthogonal transformation, which makes it possible to construct a closed solution of a nonself-adjoint system of equations.

Results. A new closed solution of the coupled axisymmetric thermoelastoelectricity problem for a round plate made of piezoceramic material was constructed.

Discussion and Conclusion. The obtained solution to the initial boundary value problem made it possible to determine the temperature, electric and elastic fields induced in a piezoceramic element under arbitrary temperature axisymmetric external action. The calculations performed provided determining the dimensions of solid electrodes, which made it possible to increase the functionality of piezoceramic transducers. Numerical analysis of the results enabled us to identify new connections between the nature of external temperature action, the deformation process, and the value of the electric field in a piezoceramic structure. This can validate a proper program of experiments under their designing and significantly reduce the volume of field studies.

Keywords: thermoelastoelectricity problem, coupled problem, round piezoceramic rigidly fixed plate, biorthogonal finite integral transformations

Acknowledgements. The authors would like to thank the reviewers for the work done, which made it possible to improve the quality of the article.

For citation. Shlyakhin DA, Savinova EV. Coupled Axisymmetric Thermoelastoelectricity Problem for a Round Rigidly Fixed Plate. *Advanced Engineering Research (Rostov-on-Don)*. 2024;24(1):23–35. <https://doi.org/10.23947/2687-1653-2024-24-1-23-35>

Связанная осесимметричная задача термоэлектростатости для круглой жестко закрепленной пластины

Д.А. Шляхин , Е.В. Савинова  

Самарский государственный технический университет, г. Самара, Российская Федерация

 slenax@yandex.ru

Аннотация

Введение. Для описания работы температурных пьезокерамических конструкций используется теория термоэлектростатости, в которой математическая модель сформулирована в виде системы несамосопряженных дифференциальных уравнений. Сложность ее интегрирования в общем виде приводит к исследованию задач в несвязанной постановке. Это не позволяет оценить эффект влияния электростатических полей на температурное. В литературе не представлены исследования данных задач в трехмерной связанной постановке, в которых были бы построены замкнутые решения. При этом проведение именно таких исследований позволяет понять картину взаимодействия механических, тепловых и электрических полей в конструкции. Для решения данной проблемы в настоящей работе построено новое замкнутое решение связанной задачи для пьезокерамической круглой жестко закрепленной пластины, позволяющее качественно оценить взаимное влияние термоэлектростатических полей в данной электростатической системе.

Материалы и методы. Объектом исследования является пьезокерамическая пластина. Рассматривается случай нестационарного изменения температуры на ее верхней лицевой поверхности при учете конвекционного теплообмена нижней плоскости с окружающей средой (граничные условия 1 и 3 рода). Индуцируемое в результате образования температурных деформаций электрическое поле фиксируется путем подключения электродированных поверхностей к измерительному прибору. Задача термоэлектростатости включает уравнения равновесия, электростатики и нестационарное гиперболическое уравнение теплопроводности. Она решается обобщенным методом конечного биортогонального преобразования, позволяющего построить замкнутое решение несамосопряженной системы уравнений.

Результаты исследования. Построено новое замкнутое решение связанной осесимметричной задачи термоэлектростатости для круглой пластины, выполненной из пьезокерамического материала.

Обсуждение и заключение. Полученное решение начально-краевой задачи позволяет определить температурное, электрическое и упругое поля, индуцируемые в пьезокерамическом элементе при произвольном температурном осесимметричном внешнем воздействии. Проведенные расчеты позволяют определить размеры сплошных электродов, которые дают возможность повысить функциональные возможности пьезокерамических преобразователей. Численный анализ результатов позволяет выявить новые связи между характером внешнего температурного воздействия, процессом деформирования и величиной электрического поля в пьезокерамической конструкции. Это дает возможность обосновать рациональную программу экспериментов при их проектировании и значительно сократить объем натурных исследований.

Ключевые слова: задача термоэлектростатости, связанная осесимметричная задача, жестко закрепленная пластина, биортогональные конечные интегральные преобразования

Благодарности. Авторы выражают благодарность рецензентам за проведенную работу, которая позволила повысить качественный уровень статьи.

Для цитирования. Шляхин Д.А., Савинова Е.В. Связанная осесимметричная задача термоэлектростатости для круглой жестко закрепленной пластины. *Advanced Engineering Research (Rostov-on-Don)*. 2024;24(1):23–35. <https://doi.org/10.23947/2687-1653-2024-24-1-23-35>

Introduction. Various mathematical models are used to improve the functionality of piezoceramic sensors [1–3] based on the interdependence of thermoelectroelastic fields. To more accurately account for the effect of coupling of these fields, it is needed to construct closed solutions. Some simplifications are used to solve systems of initial nonself-adjoint differential equations. Thus, the problems can be considered in an uncoupled formulation, or the problems consider and analyze elements that have a degenerate geometry. An uncoupled stationary problem for a long electroelastic cylinder is considered in [4, 5], and article [6] is devoted to the analysis of thermal stresses in a hollow sphere. Papers [7, 8] are related to the determination of the temperature field in a piezoceramic shell and a round plate in solving uncoupled problems. Coupled dynamic problems for a homogeneous piezoceramic layer, as well as dynamic problems in a coupled formulation for a gradient-inhomogeneous piezoceramic layer, were considered in [9–10]. In [11, 12], fields in an

unbounded medium were analyzed. In [13, 14], a long hollow cylinder was considered, and thermoelectroelastic fields were analyzed.

Currently, the literature does not describe the results of constructing closed solutions to the mentioned non-stationary problems in a three-dimensional coupled formulation. Therefore, in this paper, we consider a round plate made of piezoceramic composition and having a rigid fixation, for which a new closed solution to the problem of thermoelectroelasticity is obtained. The use of a limit on the rate of temperature change on its front surface [10] makes it possible not to include the inertial characteristics of the system under study and apply the equilibrium equations in the calculated ratios.

Materials and Methods. In the process of solving, a generalized finite biorthogonal transformation was used, which provided the reduction of the dimension of a nonself-adjoint system of equations and the construction of a closed solution through significant simplifying research in the image space.

Mathematical model. Consider certain area $\Omega : \{0 \leq r_* \leq b, 0 \leq \theta \leq 2\pi, 0 \leq z_* \leq h^*\}$, which is occupied by a piezoceramic solid circular plate in the cylindrical coordinate system (r_*, θ, z_*) . Arbitrary temperature boundary conditions can be used for the problem under study. However, for the certainty of the solution, on the upper ($z_* = 0$) front surface, the temperature change $\omega_1^*(r_*, t_*)$ at a given ambient temperature ϑ^* on the lower ($z_* = h^*$) plane (t_* — time) is considered. The cylindrical thermally insulated surface is rigidly fixed: there is no radial component of the displacement vector and the angle of rotation, and its lower part is fixed in the vertical plane. The lower plane of the round plate in question is grounded. The front electrodated planes of the plate are connected to the measuring device. The design scheme of the plate is shown in Figure 1.

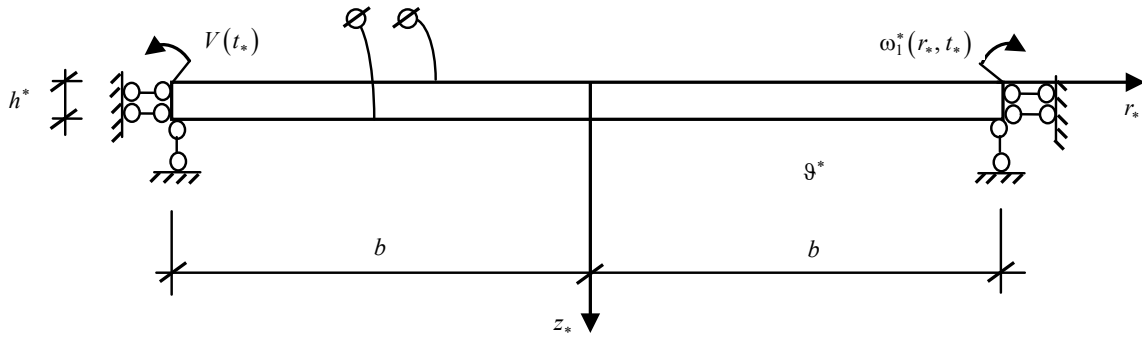


Fig. 1. Plate design diagram

The mathematical formulation of the problem under consideration in a dimensionless form for an axially polarized piezoceramic material with a hexagonal crystal lattice of 6 mm composition has the form:

$$\frac{\partial}{\partial r} \nabla U + a_1 \frac{\partial^2 U}{\partial z^2} + a_2 \frac{\partial^2 W}{\partial r \partial z} + a_3 \frac{\partial^2 \phi}{\partial r \partial z} - \frac{\partial \Theta}{\partial r} = 0, \quad (1)$$

$$\begin{aligned} a_1 \nabla \frac{\partial W}{\partial r} + a_4 \frac{\partial^2 W}{\partial z^2} + a_2 \nabla \frac{\partial U}{\partial z} + a_5 \nabla \frac{\partial \phi}{\partial r} + a_6 \frac{\partial^2 \phi}{\partial z^2} - a_7 \frac{\partial \Theta}{\partial z} &= 0, \\ -\nabla \frac{\partial \phi}{\partial r} - a_8 \frac{\partial^2 \phi}{\partial z^2} + a_9 \nabla \frac{\partial U}{\partial z} + a_{10} \nabla \frac{\partial W}{\partial r} + a_{11} \frac{\partial^2 W}{\partial z^2} + a_{12} \nabla \Theta + a_{13} \frac{\partial \Theta}{\partial z} &= 0, \\ \nabla \frac{\partial \Theta}{\partial r} + \frac{\partial^2 \Theta}{\partial z^2} - \left(\frac{\partial}{\partial t} + \beta \frac{\partial^2}{\partial t^2} \right) \left[\Theta + a_{14} \left(\nabla U + \frac{\partial W}{\partial z} \right) - a_{15} \frac{\partial \phi}{\partial z} \right] &= 0; \end{aligned}$$

$$r = 0, 1; \{U, W, \phi, \Theta\}_{|r=0} < \infty; \left\{ U, \frac{\partial W}{\partial r}, \frac{\partial \Theta}{\partial r} \right\}_{|r=1} = 0, \quad (2)$$

$$D_{r|r=1} = 0 \left\{ \left[-\frac{\partial \phi}{\partial r} + a_{10} \left(\frac{\partial W}{\partial r} + \frac{\partial U}{\partial z} \right) + a_{12} \Theta \right]_{|r=1} = 0 \right\};$$

$$r = 0, 1; \{U, W, \phi, \Theta\}_{|r=0} < \infty; \left\{ U, \frac{\partial W}{\partial r}, \frac{\partial \Theta}{\partial r} \right\}_{|r=1} = 0, \quad (2)$$

$$z = 0, h; \sigma_{zz} = 0 \left\{ a_{16} \nabla U + a_4 \frac{\partial W}{\partial z} + a_6 \frac{\partial \phi}{\partial z} - a_7 \Theta = 0 \right\}; \sigma_{rz} = 0 \left\{ \frac{\partial W}{\partial r} + \frac{\partial U}{\partial z} = 0 \right\}, \quad (3)$$

$$\begin{aligned} \phi|_{z=0} = \phi_0, \phi|_{z=h} = 0, \Theta|_{z=0} = \omega_1, \left(\frac{\partial \Theta}{\partial z} + a_{17} \Theta \right) \Big|_{z=h} = a_{17} \vartheta; \\ t = 0, \{U, W, \phi, \Theta\} = 0, \frac{\partial \{U, W, \phi\}}{\partial t} \Big|_{t=0} = 0, \frac{\partial \Theta}{\partial t} \Big|_{t=0} = \dot{\Theta}_0; \end{aligned} \quad (4)$$

where

$$\begin{aligned} \{U, W, r, z\} = \{U^*, W^*, r_*, z_*\} / b, \{\phi, \phi_0\} = \frac{e_{31}}{C_{11}b} \{\phi^*, \phi_0^*\}, \{\phi, \phi_0\} = \frac{e_{31}}{C_{11}b} \{\phi^*, \phi_0^*\}, \\ \{\Theta, \omega_1, \vartheta\} = \frac{\gamma_{11}}{C_{11}} \{\Theta^*, (\omega_1^* - T_0), (\vartheta^* - T_0)\}, a_1 = \frac{C_{55}}{C_{11}}, a_2 = \frac{C_{13} + C_{55}}{C_{11}}, a_3 = \frac{e_{15} + e_{31}}{e_{31}}, \\ a_4 = \frac{C_{33}}{C_{11}}, a_5 = \frac{e_{15}}{e_{31}}, a_6 = \frac{e_{33}}{e_{31}}, a_7 = \frac{\gamma_{33}}{\gamma_{11}}, a_8 = \frac{\varepsilon_{33}}{\varepsilon_{11}}, a_9 = \frac{e_{31}(e_{15} + e_{31})}{C_{11}\varepsilon_{11}}, a_{10} = \frac{e_{15}e_{31}}{C_{11}\varepsilon_{11}}, \\ a_{11} = a_{10} \frac{e_{33}}{e_{15}}, a_{12} = \frac{g_{11}e_{31}}{\gamma_{11}\varepsilon_{11}}, a_{14} = T_0 \frac{\gamma_{11}\gamma_{33}}{C_{11}k}, a_{15} = T_0 \frac{g_{33}\gamma_{11}}{e_{31}k}, a_{16} = a_2 - a_1, \end{aligned}$$

$a_{17} = \alpha \cdot b / \Lambda$, $\Theta^*(r_*, z_*, t_*)$ — temperature increment in dimensional form; $U^*(r_*, z_*, t_*)$, $W^*(r_*, z_*, t_*)$ — components of the displacement vector, electric field potential; $\sigma_{zz}(r, z, t)$, $\sigma_{rz}(r, z, t)$ — components of the mechanical stress tensor; $D_r(r, z, t)$ — radial component of the electric field induction vector; Λ, k, α_t — coefficients of thermal conductivity, volumetric heat capacity, and linear thermal expansion; $\phi_0^*(r, t)$ — electric potential induced on the upper front surface; γ_{ii}, g_{ii} — components of the tensor of temperature stresses and pyroelectric coefficients ($i = 1, 3, \gamma_{ii} = C_{ii}\alpha_t$); $e_{15}, e_{31}, e_{33}, \varepsilon_{11}, \varepsilon_{33}$ — piezoelectric modules and permittivity coefficients; $\Theta^* = T - T_0$; T, T_0 — current temperature and temperature of the original state of the body; β_{rel} — relaxation time; α — heat transfer coefficient, $\dot{\Theta}_0$ — known rate of temperature change; $\nabla = \frac{\partial}{\partial r} + \frac{1}{r}$.

To determine the potential of the electric field induced under deformation on the upper front surface $\phi_0^*(r, t)$, in the case of connecting electrodes to a measuring device with a large input resistance, an additional boundary condition is used:

$$\frac{\partial}{\partial t} \int_{(S)} D_{z|z=0} dS = 0 \quad (5)$$

where $D_z(r, z, t)$ — axial component of the induction vector; S — surface area.

Construction of a general solution. To fulfill the condition of fixing the cylindrical surface of the plate in the vertical plane, new functions $w(r, z, t)$, $W_1(t)$ are introduced:

$$W(r, z, t) = W_1(t) + w(r, z, t), \quad (6)$$

this makes it possible to form a boundary value problem with respect to functions U, w, ϕ, Θ , which is investigated by the method of finite Fourier-Bessel transformations:

$$u_H(n, z, t) = \int_0^1 U(r, z, t) r J_1(j_n r) dr, \quad (7)$$

$$\{w_H(n, z, t), \phi_H(n, z, t), N_H(n, z, t)\} = \int_0^1 \{w(r, z, t), \phi(r, z, t), \Theta(r, z, t)\} r J_0(j_n r) dr,$$

$$U(r, z, t) = 2 \sum_{n=1}^{\infty} \frac{u_H(n, z, t)}{J_0(j_n)^2} J_1(j_n r) \quad (8)$$

$$\{w(r, z, t), \phi(r, z, t), \Theta(r, z, t)\} = 2 \sum_{n=0}^{\infty} \frac{\{w_H(n, z, t), \phi_H(n, z, t), N_H(n, z, t)\}}{J_0(j_n)^2} J_0(j_n r),$$

where j_n — positive zeros of the function $J_1(j_n)$ ($n = \overline{0, \infty}$; $j_0 = 0$), $J_\nu(\dots)$ — Bessel functions.

It should be noted here that to satisfy the last boundary condition (2), it is necessary to assume that the original temperature of plate T_0 is equal to the ambient temperature ϑ^* , and the temperature increment function on the upper front surface $\omega_1(1, t) = 0$. These assumptions, without much error, allow assuming that on the cylindrical surface of the plate, $\Theta(1, z, t) = 0$.

As a result of using the transformation algorithm in the image area, the following initial boundary value problem is obtained:

$$-j_n^2 u_H + a_1 \frac{\partial^2 u_H}{\partial z^2} - a_2 j_n \frac{\partial w_H}{\partial z} + a_3 j_n \frac{\partial \phi_H}{\partial z} + j_n N_H = 0, \quad (9)$$

$$\begin{aligned} & -a_1 j_n^2 w_H + a_4 \frac{\partial^2 w_H}{\partial z^2} + a_2 j_n \frac{\partial u_H}{\partial z} - a_5 j_n^2 \phi_H + a_6 \frac{\partial^2 \phi_H}{\partial z^2} - a_7 \frac{\partial N_H}{\partial z} = 0, \\ & j_n^2 \phi_H - a_8 \frac{\partial^2 \phi_H}{\partial z^2} + a_9 j_n \frac{\partial u_H}{\partial z} - a_{10} j_n^2 w_H + a_{11} \frac{\partial^2 w_H}{\partial z^2} + a_{12} j_n N_H + a_{13} \frac{\partial N_H}{\partial z} = 0, \\ & -j_n^2 N_H + \frac{\partial^2 N_H}{\partial z^2} - \left(\frac{\partial}{\partial t} + \beta \frac{\partial^2}{\partial t^2} \right) \left[N_H + a_{14} \left(j_n u_H + \frac{\partial w_H}{\partial z} \right) - a_{15} \frac{\partial \phi_H}{\partial z} \right] = 0; \\ & z = 0, h; a_{16} j_n u_H + a_4 \frac{\partial w_H}{\partial z} + a_6 \frac{\partial \phi_H}{\partial z} - a_7 N_H = 0; \frac{\partial u_H}{\partial z} - j_n w_H = 0, \end{aligned} \quad (10)$$

$$\phi_H|_{z=0} = \phi_{0H}, \phi_H|_{z=h} = 0, N_H|_{z=0} = \omega_{1H}, \left(\frac{\partial N_H}{\partial z} + a_{17} N_H \right)_{|z=h} = a_{17} \vartheta_H;$$

$$t = 0, \{u_H, \phi_H, N_H\} = 0, w_H = w_{0H}, \frac{\partial \{u_H, \phi_H\}}{\partial t} \Big|_{t=0} = 0, \quad (11)$$

$$\frac{\partial w_H}{\partial t} \Big|_{t=0} = \dot{w}_{0H}, \frac{\partial N_H}{\partial t} \Big|_{t=0} = \dot{N}_{0H};$$

where $\{\phi_{0H}, \vartheta_H, w_{0H}, \dot{w}_{0H}, \dot{N}_{0H}\} = \int_0^1 \left\{ \phi_0, \vartheta, -W_1(0), -\frac{dW_1(t)}{dt} \Big|_{t=0}, \dot{\phi}_0 \right\} r J_0(j_n r) dr$.

At the next stage of the solution, the introduction of functions $U_H(n, z, t)$, $W_H(n, z, t)$, $\phi_H(n, z, t)$, $Q_H(n, z, t)$ using the following relations:

$$u_H(n, z, t) = H_1(n, z, t) + U_H(n, z, t), w_H(n, z, t) = H_2(n, z, t) + W_H(n, z, t), \quad (12)$$

$$\phi_H(n, z, t) = H_3(n, z, t) + \phi_H(n, z, t), N_H(n, z, t) = H_4(n, z, t) + Q_H(n, z, t),$$

allows the reduction of conditions (9) to homogeneous.

Here, $\{H_1 \dots H_4\} = \{H_1^* \dots H_4^*\} + \{f_9(z) \dots f_{12}(z)\} \phi_{0H}(t)$, $\{H_1^* \dots H_4^*\} = \{f_1(z) \dots f_4(z)\} \omega_{1H}(t) + \{f_5(z) \dots f_8(z)\} \vartheta_H$, $f_1(z) \dots f_{12}(z)$ — twice differentiable functions.

Substitution (12) in (9) – (11) when the conditions are satisfied:

$$z = 0, h; a_{16} j_n H_1 + a_4 \frac{\partial H_2}{\partial z} + a_6 \frac{\partial H_3}{\partial z} - a_7 H_4 = 0; j_n H_2 - \frac{\partial H_1}{\partial z} = 0, \quad (13)$$

$$H_3|_{z=0} = \phi_{0H}, H_3|_{z=h} = 0, H_4|_{z=0} = \omega_{1H}, \left(\frac{\partial H_4}{\partial z} + a_{17} H_4 \right)_{|z=h} = a_{17} \vartheta_H,$$

provides the formulation of the following task:

$$-j_n^2 U_H + a_1 \frac{\partial^2 U_H}{\partial z^2} - a_2 j_n \frac{\partial W_H}{\partial z} + a_3 j_n \frac{\partial \phi_H}{\partial z} + j_n Q_H = F_1, \quad (14)$$

$$-a_1 j_n^2 W_H + a_4 \frac{\partial^2 W_H}{\partial z^2} + a_2 j_n \frac{\partial U_H}{\partial z} - a_5 j_n^2 \phi_H + a_6 \frac{\partial^2 \phi_H}{\partial z^2} - a_7 \frac{\partial Q_H}{\partial z} = F_2,$$

$$j_n^2 \phi_H - a_8 \frac{\partial^2 \phi_H}{\partial z^2} + a_9 j_n \frac{\partial U_H}{\partial z} - a_{10} j_n^2 W_H + a_{11} \frac{\partial^2 W_H}{\partial z^2} + a_{12} j_n Q_H + a_{13} \frac{\partial Q_H}{\partial z} = F_3,$$

$$-j_n^2 Q_H + \frac{\partial^2 Q_H}{\partial z^2} - \left(\frac{\partial}{\partial t} + \beta \frac{\partial^2}{\partial t^2} \right) \left[Q_H + a_{14} \left(j_n U_H + \frac{\partial W_H}{\partial z} \right) - a_{15} \frac{\partial \phi_H}{\partial z} \right] = F_4,$$

$$z = 0, h; a_{16} j_n U_H + a_4 \frac{\partial W_H}{\partial z} + a_6 \frac{\partial \phi_H}{\partial z} - a_7 Q_H = 0; \frac{\partial U_H}{\partial z} - j_n W_H = 0, \quad (15)$$

$$\phi_H|_{z=0} = \phi_H|_{z=h} = 0, Q_H|_{z=0} = 0, \left(\frac{\partial Q_H}{\partial z} + a_{17} Q_H \right)_{|z=h} = 0;$$

$$t = 0; U_H = U_{0H}; W_H = W_{0H}; \varphi_H = \varphi_{0H}; Q_H = Q_{0H}, \quad (16)$$

$$\left. \frac{\partial U_H}{\partial t} \right|_{t=0} = \dot{U}_{0H}, \left. \frac{\partial W_H}{\partial t} \right|_{t=0} = \dot{W}_{0H}, \left. \frac{\partial \varphi_H}{\partial t} \right|_{t=0} = \dot{\varphi}_{0H}, \left. \frac{\partial Q_H}{\partial t} \right|_{t=0} = \dot{Q}_{0H};$$

where

$$\begin{aligned} F_1 &= j_n^2 H_1 - a_1 \frac{\partial^2 H_1}{\partial z^2} + a_2 j_n \frac{\partial H_2}{\partial z} - a_3 j_n \frac{\partial H_3}{\partial z} - j_n H_4, \\ F_2 &= a_1 j_n^2 H_2 - a_4 \frac{\partial^2 H_2}{\partial z^2} - a_2 j_n \frac{\partial H_1}{\partial z} + a_5 j_n^2 H_3 - a_6 \frac{\partial^2 H_3}{\partial z^2} + a_7 \frac{\partial H_4}{\partial z}, \\ F_3 &= -j_n^2 H_3 + a_8 \frac{\partial^2 H_3}{\partial z^2} - a_9 j_n \frac{\partial H_1}{\partial z} + a_{10} j_n^2 H_2 - a_{11} \frac{\partial^2 H_2}{\partial z^2} - a_{12} j_n H_4 - a_{13} \frac{\partial H_4}{\partial z}, \\ F_4 &= j_n^2 H_4 - \frac{\partial^2 H_4}{\partial z^2} + \left(\frac{\partial}{\partial t} + \beta \frac{\partial^2}{\partial t^2} \right) \left[H_4 + a_{14} \left(j_n H_1 + \frac{\partial H_2}{\partial z} \right) - a_{15} \frac{\partial H_3}{\partial z} \right], \\ U_{0H} &= -H_{1|t=0}, W_{0H} = w_{0H} - H_{2|t=0}, \varphi_{0H} = -H_{3|t=0}, Q_{0H} = -H_{4|t=0}, \\ \dot{U}_{0H} &= -\left. \frac{\partial H_1}{\partial t} \right|_{t=0}, \dot{W}_{0H} = \dot{w}_{0H} - \left. \frac{\partial H_2}{\partial t} \right|_{t=0}, \dot{\varphi}_{0H} = -\left. \frac{\partial H_3}{\partial t} \right|_{t=0}, \dot{Q}_{0H} = \dot{N}_{0H} - \left. \frac{\partial H_4}{\partial t} \right|_{t=0}. \end{aligned}$$

Using the biorthogonal finite transformation (CMD) [15], we obtain a solution to problem (14) – (16). CMD with unknown components of vector functions of transformations is introduced on the segment $[0, h]$ $K_1(\lambda_{in}, z) \dots K_4(\lambda_{in}, z), N_1(\mu_{in}, z) \dots N_4(\mu_{in}, z)$:

$$G(n, \lambda_{in}, t) = \int_0^h \left[Q_H + a_{14} \left(j_n U_H + \frac{\partial W_H}{\partial z} \right) - a_{15} \frac{\partial \varphi_H}{\partial z} \right] K_4(\lambda_{in}, z) dz, \quad (17)$$

$$\begin{aligned} \{U_H, W_H, \varphi_H, Q_H\} &= \sum_{i=1}^{\infty} G(n, \lambda_{in}, t) \frac{\{N_1(\mu_{in}, z), N_2(\mu_{in}, z), N_3(\mu_{in}, z), N_4(\mu_{in}, z)\}}{\|K_{in}\|^2}, \\ \|K_{in}\|^2 &= \int_0^h K_4(\lambda_{in}, z) N_4(\mu_{in}, z) dz, \end{aligned}$$

where λ_{in}, μ_{in} — the eigenvalues of the corresponding problems with respect to the components of the vector functions of the CMD ($k = 1 \dots 4$).

In the course of transformations, we obtain a task for determining transformants $G(n, \lambda_{in}, t)$:

$$\left(\beta \frac{d^2}{dt^2} + \frac{d}{dt} + \lambda_{in}^2 \right) G(n, \lambda_{in}, t) = -F_H(n, \lambda_{in}, t), \quad \left(i = \overline{1, \infty} \quad n = \overline{0, \infty} \right) \quad (18)$$

$$t = 0, G(\lambda_{in}, n, 0) = G_{0H}, \left. \frac{dG(\lambda_{in}, n, t)}{dt} \right|_{t=0} = G_0(\lambda_{in}, n), \quad (19)$$

whose solution has the following form:

$$\begin{aligned} G(n, \lambda_{in}, t) &= (m_{1in} - m_{2in})^{-1} \left\{ (\dot{G}_0 - G_0 m_{2in}) \exp(m_{1in} t) - (\dot{G}_0 - G_0 m_{1in}) \exp(m_{2in} t) + \right. \\ &\quad \left. + \beta^{-1} \int_0^t F_H(n, \lambda_{in}, \tau) \left[\exp(m_{2in}(t - \tau)) - \exp(m_{1in}(t - \tau)) \right] d\tau \right\}, \end{aligned} \quad (20)$$

in addition, two homogeneous problems with respect to components $K_1(\lambda_{in}, z) \dots K_4(\lambda_{in}, z)$,

$$\begin{aligned} -j_n^2 K_{1in} + a_1 \frac{d^2 K_{1in}}{dz^2} - a_2 j_n \frac{dK_{2in}}{dz} - a_9 j_n \frac{dK_{3in}}{dz} + \lambda_{in}^2 a_{14} j_n K_{4in} &= 0, \\ -a_1 j_n^2 K_{2in} + a_4 \frac{d^2 K_{2in}}{dz^2} + a_2 j_n \frac{dK_{1in}}{dz} - a_{10} j_n^2 K_{3in} + a_{11} \frac{d^2 K_{3in}}{dz^2} - \lambda_{in}^2 a_{14} \frac{dK_{4in}}{dz} &= 0, \\ j_n^2 K_{3in} - a_8 \frac{d^2 K_{3in}}{dz^2} - a_3 j_n \frac{dK_{1in}}{dz} - a_5 j_n^2 K_{2in} + a_6 \frac{d^2 K_{2in}}{dz^2} + \lambda_{in}^2 a_{15} \frac{dK_{4in}}{dz} &= 0, \\ (\lambda_{in}^2 - j_n^2) K_{4in} + \frac{d^2 K_{4in}}{dz^2} + j_n K_{1in} + a_7 \frac{dK_{2in}}{dz} + a_{12} j_n K_{3in} - a_{13} \frac{dK_{3in}}{dz} &= 0; \end{aligned} \quad (21)$$

$$z = 0, h, a_{16} j_n K_{1in} + a_4 \frac{dK_{2in}}{dz} + a_{11} \frac{dK_{3in}}{dz} - \lambda_{in}^2 a_{15} K_{4in} = 0, K_{3in|z=0} = K_{3in|z=h} = 0, \quad (22)$$

$$\frac{dK_{1in}}{dz} - j_n K_{2in} - \frac{a_{10}}{a_1} j_n K_{3in} = 0, K_{4in|z=0} = 0, \left(\frac{dK_{4in}}{dz} + a_{17} K_{4in} \right)_{|z=h} = 0;$$

and $N_1(\mu_{in}, z) \dots N_4(\mu_{in}, z)$:

$$-j_n^2 N_{1in} + a_1 \frac{d^2 N_{1in}}{dz^2} - a_2 j_n \frac{dN_{2in}}{dz} + a_3 j_n \frac{dN_{3in}}{dz} + j_n N_{4in} = 0, \quad (23)$$

$$-a_1 j_n^2 N_{2in} + a_4 \frac{d^2 N_{2in}}{dz^2} + a_2 j_n \frac{dN_{1in}}{dz} - a_5 j_n^2 N_{3in} + a_6 \frac{d^2 N_{3in}}{dz^2} - a_7 \frac{dN_{4in}}{dz} = 0,$$

$$j_n^2 N_{3in} - a_8 \frac{d^2 N_{3in}}{dz^2} + a_9 j_n \frac{dN_{1in}}{dz} - a_{10} j_n^2 N_{2in} + a_{11} \frac{d^2 N_{2in}}{dz^2} + a_{12} j_n N_{4in} + a_{13} \frac{dN_{4in}}{dz} = 0,$$

$$-j_n^2 N_{4in} + \frac{d^2 N_{4in}}{dz^2} + \mu_{in}^2 \left(N_{4in} + a_{14} j_n N_{1in} + a_{14} \frac{dN_{2in}}{dz} - a_{15} \frac{dN_{3in}}{dz} \right) = 0;$$

$$z = 0, h, a_{16} j_n N_{1in} + a_4 \frac{dN_{2in}}{dz} + a_6 \frac{dN_{3in}}{dz} - a_7 N_{4in} = 0, \frac{\partial N_{1in}}{\partial z} - j_n N_{2in} = 0, \quad (24)$$

$$N_{3in|z=0} = N_{3in|z=h} = 0, N_{4in|z=0} = 0, \left(\frac{\partial N_{4in}}{\partial z} + a_{17} N_{4in} \right)_{|z=h} = 0;$$

where

$$F_H(n, \lambda_{in}, t) = \int_0^h (F_1 K_{1in} + F_2 K_{2in} + F_3 K_{3in} + F_4 K_{4in}) dz,$$

$$\{G_{0H}, \dot{G}_{0H}\} = \int_0^h \left[\{Q_{0H}, \dot{Q}_{0H}\} + a_{14} \left(j_n \{U_{0H}, \dot{U}_{0H}\} + \frac{d\{W_{0H}, \dot{W}_{0H}\}}{dz} \right) - a_{15} \frac{d\{\Phi_{0H}, \dot{\Phi}_{0H}\}}{dz} \right] K_{4in} dz,$$

m_{1in}, m_{2in} — roots of the characteristic equation: $\beta m_{in}^2 + m_{in} + \lambda_{in}^2 = 0$.

Constructed homogeneous problem (23), (24) with respect to functions $N_1(\mu_{in}, z) \dots N_4(\mu_{in}, z)$ is invariant to the initial calculated relations (14), (15).

Systems (21), (23) are reduced to the following equations with respect to $K_2(\lambda_{in}, z), N_2(\mu_{in}, z)$:

$$\left(\frac{d^8}{dz^8} + e_{1in} \frac{d^6}{dz^6} + e_{2in} \frac{d^4}{dz^4} + e_{3in} \frac{d^2}{dz^2} + e_{4in} \right) \{K_{2in}, N_{2in}\} = 0. \quad (25)$$

In the paper, coefficients $e_{1in} \dots e_{4in}$ are not given due to the limitation of its volume.

In equation (25), the left part is decomposed into commutative factors, presented below:

$$\left(\frac{d^2}{dz^2} - A_{1in}^2 \right) \left(\frac{d^2}{dz^2} + A_{2in}^2 \right) \left(\frac{d^4}{dz^4} + m_{3in}^2 \frac{d^2}{dz^2} + m_{4in}^2 \right) \{K_{2in}, N_{2in}\} = 0, \quad (26)$$

where $A_{1in} = \sqrt{B_{1in}}, A_{2in} = \sqrt{S_{1in}}, m_{3in}^2 = e_{1in} + B_{1in} + S_{1in}, m_{4in}^2 = \frac{e_{4in}}{B_{1in} S_{2in}}, B_{1in}, S_{1in}$ — real positive roots of the following characteristic equations:

$$B_{in}^4 + e_{1in} B_{in}^3 + e_{2in} B_{in}^2 + e_{3in} B_{in} + e_{4in} = 0,$$

$$S_{in}^3 - (e_{1in} + B_{1in}) S_{in}^2 + (e_{1in} B_{1in} + B_{1in}^2 + e_{2in}) S_{in} - \frac{e_{4in}}{B_{1in}} = 0.$$

When examining a round rigidly fixed piezoceramic plate, the general integral of equations (26) has the following form:

$$\begin{aligned} \{K_{2in}, N_{2in}\} = & \{D_{1in}, E_{1in}\} \exp(A_{1in} z) + \{D_{2in}, E_{2in}\} \exp(-A_{1in} z) + \{D_{3in}, E_{3in}\} \sin(A_{2in} z) + \\ & + \{D_{4in}, E_{4in}\} \cos(A_{2in} z) + \{D_{5in}, E_{5in}\} \sin(A_{3in} z) + \{D_{6in}, E_{6in}\} \cos(A_{3in} z) + \\ & + \{D_{7in}, E_{7in}\} \sin(A_{4in} z) + \{D_{8in}, E_{8in}\} \cos(A_{4in} z), \end{aligned} \quad (27)$$

where

$$A_{3in} = \left(\frac{m_{3in}^2 + \sqrt{m_{3in}^4 - 4m_{4in}^2}}{2} \right)^{0.5}, \quad A_{4in} = \left(\frac{m_{3in}^2 - \sqrt{m_{3in}^4 - 4m_{4in}^2}}{2} \right)^{0.5}.$$

It should be noted here that the condition of the actual positive values of coefficients $B_{1in}, S_{1in}, A_{1in} \dots A_{4in}$ is fulfilled for most structures made of piezoceramic material. Otherwise, the formula structure (26), (27) simply changes.

Considering that the connections were previously obtained as a result of reducing (21), (23) to (25), we get expressions for functions $K_1(\lambda_{in}, z), K_3(\lambda_{in}, z), K_4(\lambda_{in}, z), N_1(\lambda_{in}, z), N_3(\lambda_{in}, z), N_4(\lambda_{in}, z)$.

Substituting $K_1(\lambda_{in}, z) \dots K_4(\lambda_{in}, z), N_1(\mu_{in}, z) \dots N_4(\mu_{in}, z)$ in conditions (22), (24) provides determining constants $D_{1in} \dots D_{8in}, E_{1in} \dots E_{8in}$ and eigenvalues λ_{in}, μ_{in} .

The final expressions of functions $U(n, z, t), W(n, z, t), \phi(n, z, t), \Theta(n, z, t)$ are obtained by applying the inversion formulas (17), (8). Then, taking into account (6), (12), we have:

$$\begin{aligned} U(r, z, t) &= 2 \sum_{n=1}^{\infty} \frac{J_1(j_n r)}{J_0(j_n)^2} \left[H_1(n, z, t) + \sum_{i=1}^{\infty} G(n, \lambda_{in}, t) N_1(\mu_{in}, z) \|K_{in}\|^{-2} \right], \\ W(r, z, t) &= W_1(t) + 2 \sum_{n=0}^{\infty} \frac{J_0(j_n r)}{J_0(j_n)^2} \left[H_2(n, z, t) + \sum_{i=1}^{\infty} G(n, \lambda_{in}, t) N_2(\mu_{in}, z) \|K_{in}\|^{-2} \right], \\ \phi(r, z, t) &= 2 \sum_{n=0}^{\infty} \frac{J_0(j_n r)}{J_0(j_n)^2} \left[H_3(n, z, t) + \sum_{i=1}^{\infty} G(n, \lambda_{in}, t) N_3(\mu_{in}, z) \|K_{in}\|^{-2} \right], \\ \Theta(r, z, t) &= 2 \sum_{n=0}^{\infty} \frac{J_0(j_n r)}{J_0(j_n)^2} \left[H_4(n, z, t) + \sum_{i=1}^{\infty} G(n, \lambda_{in}, t) N_4(\mu_{in}, z) \|K_{in}\|^{-2} \right]. \end{aligned} \quad (28)$$

Functions $f_1(z) \dots f_{12}(z)$ are calculated from the simplification condition $F_1 \dots F_4$ when conditions (13) are satisfied:

$$\begin{aligned} j_n^2 H_1 - a_1 \frac{\partial^2 H_1}{\partial z^2} + a_2 j_n \frac{\partial H_2}{\partial z} - a_3 j_n \frac{\partial H_3}{\partial z} - j_n H_4 &= 0, \\ a_1 j_n^2 H_2 - a_4 \frac{\partial^2 H_2}{\partial z^2} - a_2 j_n \frac{\partial H_1}{\partial z} + a_5 j_n^2 H_3 - a_6 \frac{\partial^2 H_3}{\partial z^2} + a_7 \frac{\partial H_4}{\partial z} &= 0, \\ -j_n^2 H_3 + a_8 \frac{\partial^2 H_3}{\partial z^2} - a_9 j_n \frac{\partial H_1}{\partial z} + a_{10} j_n^2 H_2 - a_{11} \frac{\partial^2 H_2}{\partial z^2} - a_{12} j_n H_4 - a_{13} \frac{\partial H_4}{\partial z} &= 0, \\ j_n^2 H_4 - \frac{\partial^2 H_4}{\partial z^2} &= 0. \end{aligned}$$

Function $W_1(t)$ is determined from condition $W(1, h, t) = 0$:

$$W_1(t) = -2 \sum_{n=0}^{\infty} \left[H_2(n, h, t) + \sum_{i=1}^{\infty} G(n, \lambda_{in}, t) N_2(\mu_{in}, h) \|K_{in}\|^{-2} \right] J_0(j_n)^{-1}.$$

For a qualitative assessment of the induced electric pulse on its upper front surface, it is required to form two electrodes with a radius of separation R and connect them to a measuring device. In this case, potential $\phi_0(r, t)$, induced on two equipotential surfaces is represented as:

$$\phi_0(r, t) = \phi_{01}(t) H(R - r) + \phi_{02}(t) H(r - R), \quad (29)$$

where $H(\dots)$ — the Heaviside step function.

Substituting (29) into (5) makes it possible to define expressions for determining potentials $\phi_0(t), \phi_{02}(t)$:

$$\int_0^R D_{z|z=0} r dr = \int_R^1 D_{z|z=0} r dr = 0. \quad (30)$$

As a result of solution (30), functions $\phi_0(t), \phi_{02}(t)$ are defined as follows:

$$\phi_{01}(t) = Q_{01}^{-1} [Q_1(t) + Q_2(t) + Q_3(t)], \quad \phi_{02}(t) = Q_{02}^{-1} \left[-Q_1(t) + \frac{1-R^2}{R^2} Q_2(t) + Q_4(t) \right],$$

where

$$Q_1(t) = R \sum_{n=1}^{\infty} \frac{J_1(j_n R)}{J_0(j_n)^2} \left\{ \frac{a_{10}}{a_5} H_1^*(n, 0, t) + \frac{a_{11}}{j_n} \frac{\partial H_2^*(n, z, t)}{\partial z} \Big|_{z=0} - \frac{a_8}{j_n} \frac{\partial H_3^*(n, z, t)}{\partial z} \Big|_{z=0} + \right.$$

$$\begin{aligned}
 & + \sum_{i=1}^{\infty} \frac{G(\lambda_{in}, 0, t)}{\|K_{in}\|^2} \left[\frac{a_{10}}{a_5} K_1(\lambda_{in}, 0) + \frac{a_{11}}{j_n} \frac{dK_2(\lambda_{in}, z)}{dz} \Big|_{z=0} - \frac{a_8}{j_n} \frac{dK_3(\lambda_{in}, z)}{dz} \Big|_{z=0} \right], \\
 Q_2(t) = & R^2 \left[a_{11} \frac{\partial H_2^*(0, z, t)}{\partial z} \Big|_{z=0} - a_8 \frac{\partial H_3^*(0, z, t)}{\partial z} \Big|_{z=0} + \sum_{i=1}^{\infty} \frac{G(\lambda_{i0}, 0, t)}{\|K_{i0}\|^2} \left[a_{11} \frac{dK_2(\lambda_{i0}, z)}{dz} \Big|_{z=0} - a_8 \frac{dK_3(\lambda_{i0}, z)}{dz} \Big|_{z=0} \right] \right], \\
 Q_3(t) = & a_{13} \int_0^R \omega_1(r, t) r dr, \quad Q_4(t) = a_{13} \int_R^1 \omega_1(r, t) r dr, \\
 Q_{01} = & - \left\{ \frac{R^4}{2} \left[a_{11} \frac{df_{10}(z)}{dz} \Big|_{z=0} - a_8 \frac{df_{11}(z)}{dz} \Big|_{z=0} \right] + 2R^2 \sum_{n=1}^{\infty} \left[\frac{J_1(j_n R)}{J_0(j_n)} \right]^2 \left[\frac{a_{10}}{a_5} f_9(z) + \frac{a_{11}}{j_n} \frac{df_{10}(z)}{dz} \Big|_{z=0} - \frac{a_8}{j_n} \frac{df_{11}(z)}{dz} \Big|_{z=0} \right] \right\}, \\
 Q_{02} = & - \left\{ \frac{(1-R^2)^2}{2} \left[a_{11} \frac{df_{10}(z)}{dz} \Big|_{z=0} - a_8 \frac{df_{11}(z)}{dz} \Big|_{z=0} \right] + 2R^2 \sum_{n=1}^{\infty} \left[\frac{J_1(j_n R)}{J_0(j_n)} \right]^2 \left[\frac{a_{10}}{a_5} f_9(z) + \frac{a_{11}}{j_n} \frac{df_{10}(z)}{dz} \Big|_{z=0} - \frac{a_8}{j_n} \frac{df_{11}(z)}{dz} \Big|_{z=0} \right] \right\}.
 \end{aligned}$$

In this case, the potential difference $V(t)$ is determined by the equality:

$$V(t) = \phi_{01}(t) - \phi_{02}(t). \quad (31)$$

Research Results. Numerical results are presented for a plate made of piezoceramics of the composition PZT-4 [4, 11, 16]:

$$\begin{aligned}
 \{C_{11}, C_{12}, C_{13}, C_{33}, C_{55}\} &= \{13.9, 7.78, 7.3, 11.5, 2.26\} \times 10^{10} \text{ Pa}, \quad \{\varepsilon_{11}, \varepsilon_{33}\} = \{6.46, 5.62\} \times 10^{-9} \text{ F/m}, \\
 \{e_{15}, e_{31}, e_{33}\} &= \{12.7, -5.2, 15.1\} \text{ C/m}^2, \quad \Lambda = 1.6 \text{ W/(m} \cdot \text{K)}, \quad \alpha_t = 0.4 \times 10^{-5} \text{ K}^{-1}, \\
 k &= 3 \times 10^6 \text{ J/(m}^3 \cdot \text{K)}, \quad g_{11} = g_{33} = -0.6 \times 10^{-4} \text{ C/(m}^2 \cdot \text{K)}, \quad \beta_{rel} = 10^{-4} \text{ s}, \quad \alpha = 5.6 \text{ W/(m}^2 \cdot \text{K)}.
 \end{aligned}$$

The following case of temperature change $\omega_1^*(r^*, t^*)$ is investigated:

$$\omega_1^*(r^*, t^*) = \left(1 - \frac{r^*}{b}\right) T_{max}^* \left[\sin\left(\frac{\pi}{2t_{max}^*} t^*\right) H(t_{max}^* - t^*) + H(t^* - t_{max}^*) \right],$$

where T_{max}^*, t_{max}^* — maximum temperature value and the corresponding time ($T_{max}^* = 100^\circ\text{C}$, $T_0 = 20^\circ\text{C}$).

Figure 2 shows graphs reflecting at various points in time ($t_{max}^* = 0.1 \text{ s}$) the change in temperature $\Theta^*(0, z, t)$ in the thickness of the plate ($b = 14 \times 10^{-3} \text{ m}$, $h^* = 1 \times 10^{-3} \text{ m}$).

According to the calculation result, it is observed that due to the high coefficient of thermal conductivity and the small thickness of the piezoceramic plate, the steady-state temperature regime is formed quite quickly ($t_{max}^* = 10 \text{ s}$) when it reaches $\Theta^*(0, z, t)$ on the lower front surface ($z = h$) 78°C (Fig. 2).

Figure 3 shows the change $\Theta^*(0, h/2, t)$ in time ($t_{max}^* = 3 \times 10^{-5} \text{ s}$) taking into account (represented by a solid line) and without account for (represented by dotted line, $\beta = 0$) the relaxation of the heat flux ($b = 14 \times 10^{-5} \text{ m}$, $h^* = 1 \times 10^{-5} \text{ m}$). It should be emphasized that the application of the hyperbolic Lord-Shulman heat conduction equation is needed only in the study of a piezoceramic micro-dimensional structure with a very rapid change $\omega_1^*(r^*, t^*)$.

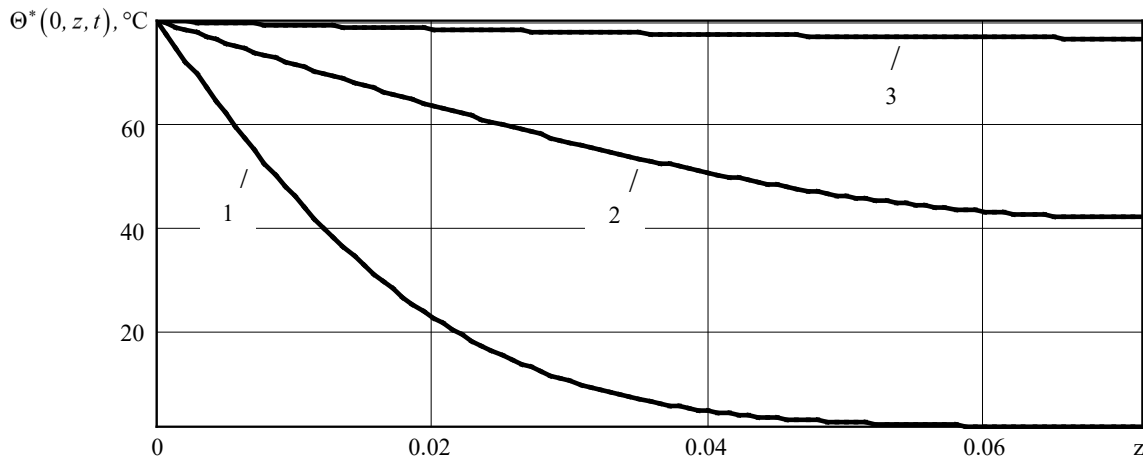
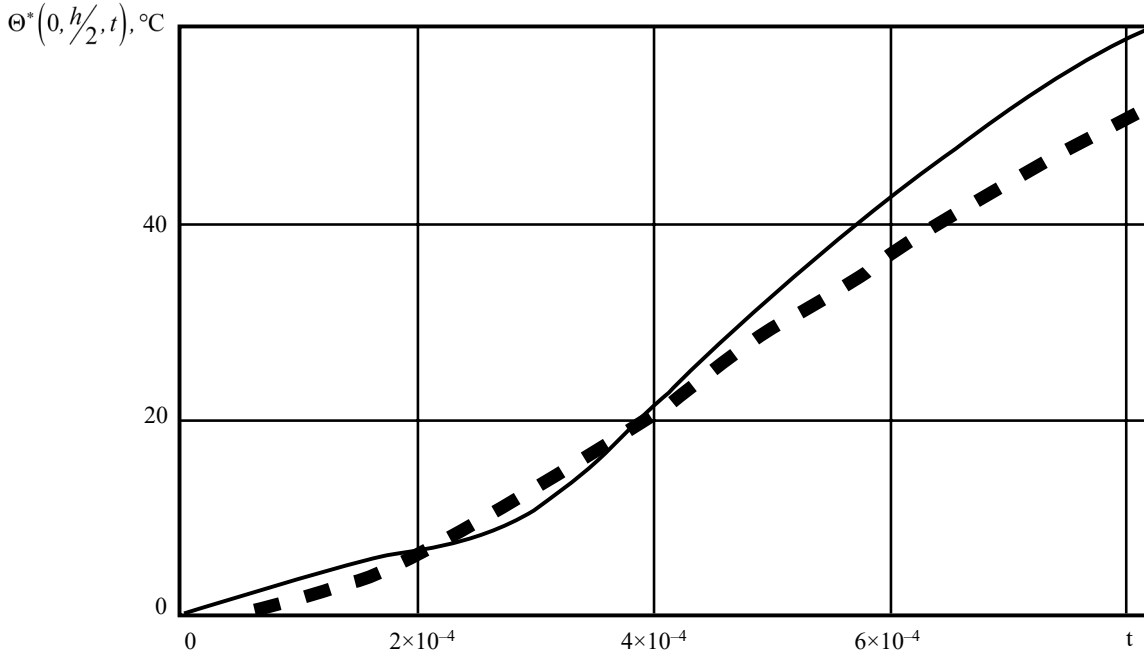


Fig. 2. Diagrams $\Theta^*(0, z, t) - z$: 1 — $t = t_{max}^*$, 2 — $t = 10t_{max}^*$, 3 — $t = 100t_{max}^*$

 Fig. 3. Diagrams $\Theta^*(0, h/2, t) - t \left(t = \frac{\Lambda}{kb^2} t^* \right)$:

 solid line — $\beta = 10^{-5} (s)$, dotted line — $\beta = 0$

The numerical results of determining function $\Theta^*(r, z, t)$ show that when conducting a study of a structure made of piezoceramic material, it is possible to neglect the impact of the rate of change of body volume and tension on the temperature field, i.e., to use only the equation of thermal conductivity in calculations.

Figure 4 shows a diagram of movements $W^*(0, z, t)$ over time t , and Figure 5 shows the dependence of the change in the radial component of normal stresses $\sigma_{rr}(r, z, t)$ along coordinate r at different points in time: 1 — $t = t_{max}$, 2 — $t = 10t_{max}$ ($t_{max}^* = 1 s$), solid line — $z = 0$, dotted line — $z = h$.

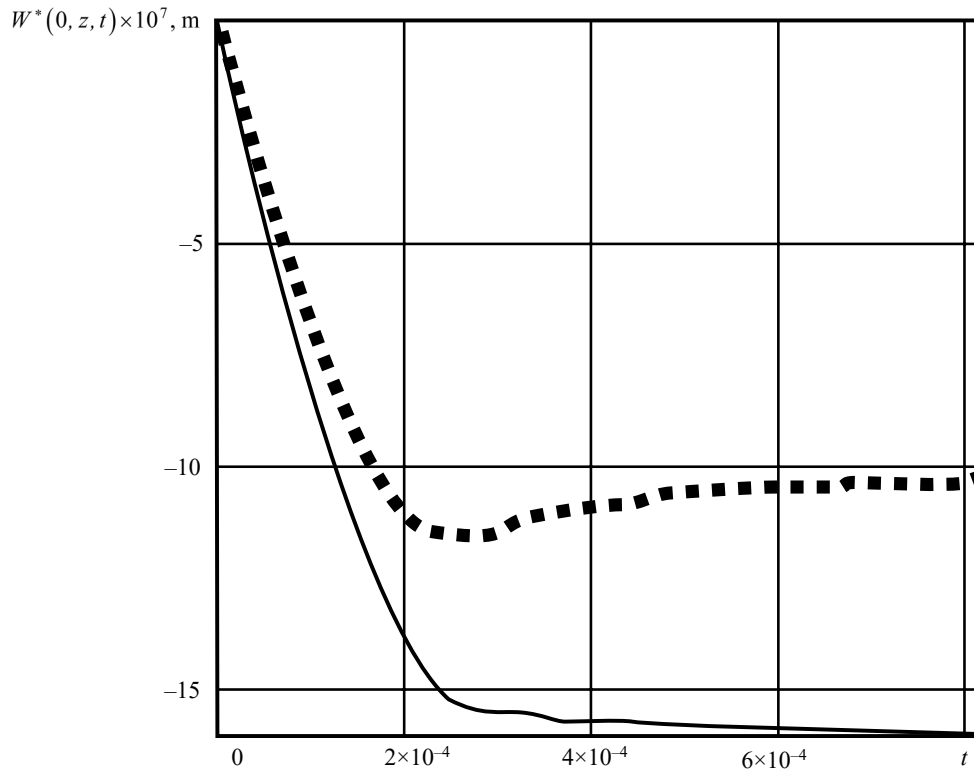


Fig. 4. Diagrams $W^*(0, z, t) - t$

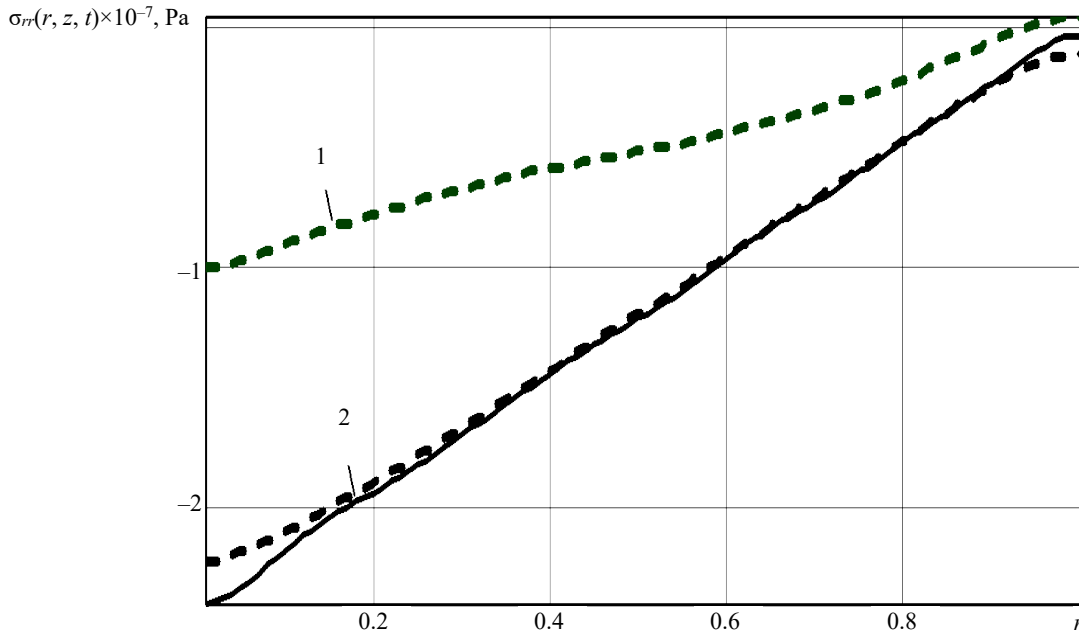


Fig. 5. Diagrams $\sigma_{rr}(r, z, t) - r$: 1 — $t = t_{max}$, 2 — $t = 10t_{max}$

It should be noted that under heating, the plate bends with increasing thickness; due to fixation, compressive normal stresses $\sigma_{rr}(r, z, t)$ are formed at all points. In the case of complete heating of the structure ($t = 10t_{max}$), the value of normal stresses $\sigma_{rr}(r, z, 10t_{max})$ in the height of the section practically coincide (Fig. 5, Diagram 2, solid and dotted lines). At this, $\sigma_{rr}(r, 0, t)$ remains constant over the entire time interval $t \geq t_{max}$ (Fig. 5, solid line), and on the lower plane at the initial moment of time $\sigma_{rr}(r, h, t)$, it is significantly less (Fig. 5, Diagram 1, dotted line).

For a qualitative assessment of the induced electric pulse in the form of a potential difference $V(t)$ (31), two electrodes with a radius of separation $R = 0.7$ and connected to a measuring device (Fig. 6, solid line) must be formed on the upper front surface of the element in question. At this, determination of $V(t)$ by connecting the upper and lower (grounded) solid electrodated surfaces of the plate to the voltmeter (Fig. 6, dotted line) is ineffective.

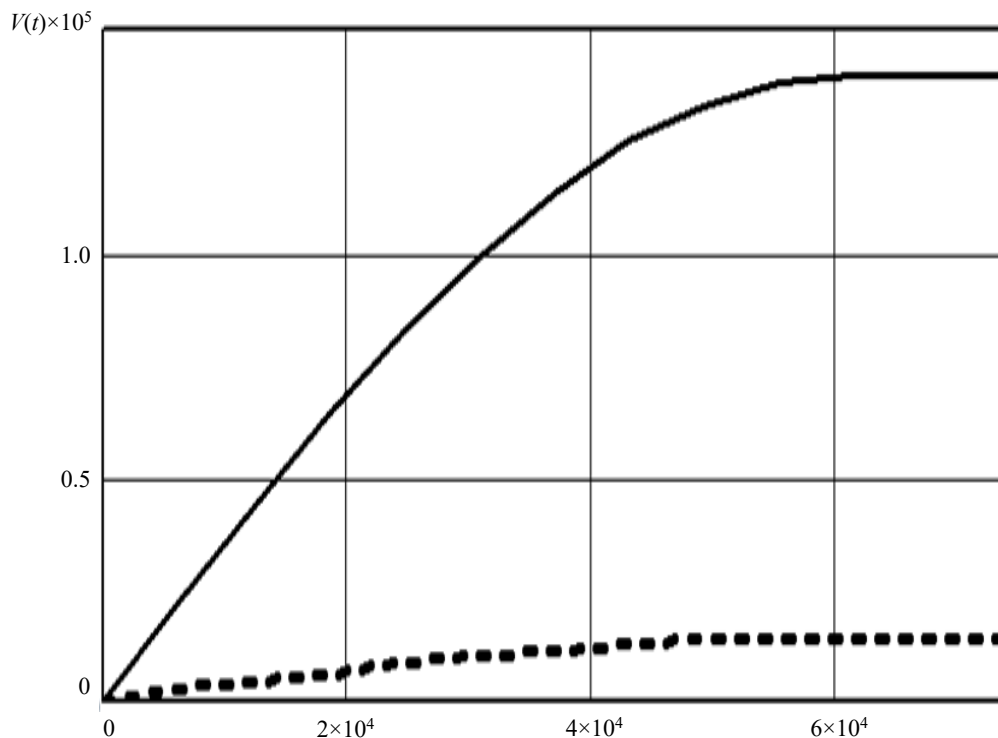


Fig. 6. Diagrams $V(t) - t$

Discussion and Conclusion. The developed closed solution of the coupled axisymmetric thermoelastoelectricity problem for a round plate made of piezoceramic material is more accurate than the solution that was developed when solving problems in an uncoupled formulation. This is due to the fact that the calculated ratios obtained make it possible to determine how the non-stationary temperature field affects the stress-strain state and the electric field of the element in question, which makes it possible to describe the behavior of a round piezoceramic plate under the influence of thermal and electrical loads with greater accuracy. In addition, it becomes possible to scientifically establish the dimensions of two uncoupled electrodes, which provides measuring the induced electric pulse most effectively.

References

1. Ionov BP, Ionov AB. Statistic-Spectral Approach to Noncontact Temperature Measurement. *Sensors & Systems*. 2009;117(2):9–12. URL: <https://rucont.ru/efd/600855> (accessed: 30.11.2023).
2. Kazaryan AA. Fine-Film Captive Pressure and Temperature. *Sensors & Systems*. 2016;(3):50–56. URL: <https://rucont.ru/efd/579511> (accessed: 30.11.2023).
3. Pan'kov AA. Resonant Diagnostics of Temperature Distribution by the Piezo-Electro-Luminescent Fiber-Optical Sensor according to the Solution of the Fredholm Integral Equation. *PNPRU Mechanics Bulletin*. 2018;(2):72–82. <https://doi.org/10.15593/perm.mech/2018.2.07>
4. Saadatfar M, Razavi AS. Piezoelectric Hollow Cylinder with Thermal Gradient. *Journal of Mechanical Science and Technology*. 2009;23:45–53. <https://doi.org/10.1007/s12206-008-1002-8>
5. Weiqiu Chen, Tadashi Shioya. Piezothermoelastic Behavior of a Pyroelectric Spherical Shell. *Journal Thermal Stresses*. 2001;24:105–120. <http://doi.org/10.1080/01495730150500424>
6. Podil'chuk YuN. Exact Analytical Solutions of Static Electroelastic and Thermoelastoelectric Problems for a Transversely Isotropic Body in Curvilinear Coordinate Systems. *International Applied Mechanics*. 2003;39(2):132–170. <https://doi.org/10.1023/A:1023953313612>
7. Shlyakhin DA, Kalmova MA. Uncoupled Problem of Thermoelastoelectricity for a Cylindrical Shell. In: P Akimov, N Vatin (eds). *XXX Russian-Polish-Slovak Seminar Theoretical Foundation of Civil Engineering (RSP 2021)*. Cham: Springer. 2022;189:263–271. https://doi.org/10.1007/978-3-030-86001-1_31
8. Shlyakhin DA, Savinova EV, Yurin VA. Dynamic Problem of Thermoelectricity for Round Rigidly Fixed Plate. *FEFU: School of Engineering Bulletin*. 2022;50(1):3–16. <https://doi.org/10.24866/2227-6858/2022-1/3-16>
9. Vatulyan AO. Heat Stroke on a Thermoelastoelectric Layer. *Vestnik of DSTU*. 2001;1(1):82–89. (In Russ.).
10. Vatulyan AO, Nesterov SA. The Dynamic Problem of Thermoelastoelectricity for Functionally Graded Layer. *Computational Continuum Mechanics*. 2017;10(2):117–126. <https://doi.org/10.7242/1999-6691/2017.10.2.10>
11. Shang F, Kuna M, Kitamura T. Theoretical Investigation of an Elliptical Crack in Thermopiezoelectric Material. Part 1: Analytical Development. *Theoretical and Applied Fracture Mechanics*. 2003;40(3):237–246. <https://doi.org/10.1016/J.TAFMEC.2003.08.003>
12. Kirilyuk VS. Thermostressed State of a Piezoelectric Body with a Plate Crack under Symmetric Thermal Load. *International Applied Mechanics*. 2008;44(3):320–330. <http://doi.org/10.1007/s10778-008-0048-8>
13. Shlyakhin DA, Kal'mova MA. The Coupled Non-Stationary Thermo-Electro-Elasticity Problem for a Long Hollow Cylinder. *Journal of Samara State Technical University, Ser. Physical and Mathematical Sciences*. 2020;24(4):677–691. <https://doi.org/10.14498/vsgtu1781>
14. Shlyakhin DA., Kalmova MA. The Nonstationary Thermoelectric Elasticity Problem for a Long Piezoceramic Cylinder. *PNPRU Mechanics Bulletin*. 2021;(2):181–190. <https://doi.org/10.15593/perm.mech/2021.2.16>
15. Senitsky YuE. Finite Integral Transformations Method – Generalization of Classic Procedure for Eigenvector Decomposition. *Izvestiya of Saratov University. Mathematics. Mechanics. Informatics*. 2011;11(3-1):61–89. <https://doi.org/10.18500/1816-9791-2011-11-3-1-61-89>
16. Selvamani R. Influence of Thermo-Piezoelectric Field in a Circular Bar Subjected to Thermal Loading due to Laser Pulse. *Materials Physics and Mechanics*. 2016;27(1):1–8. URL: https://www.ipme.ru/e-journals/MPM/no_12716/MPM127_01_selvamani.pdf (accessed: 30.11.2023).

About the Authors:

Dmitriy A. Shlyakhin, Dr.Sci. (Eng.), Associate Professor, Head of the Structural Mechanics, Engineering Geology, Foundation Engineering Department, Samara Polytech (244, Molodogvardeyskaya St., Samara, 443100, RF), SPIN-code: [7802-5059](https://orcid.org/7802-5059), [ORCID](https://orcid.org/0RCID), d-612-mit2009@yandex.ru

Elena V. Savinova, postgraduate student, senior lecturer of the Structural Mechanics, Engineering Geology, Foundation Engineering Department, Samara Polytech (244, Molodogvardeyskaya St., Samara, 443100, RF), SPIN-code: [7027-4822](https://orcid.org/7027-4822), [ORCID](https://orcid.org), slenax@yandex.ru

Claimed contributorship:

AD Shlyakhin: academic advising, basic concept formulation, research objectives and tasks, calculations, formulation of conclusions.

EV Savinova: text preparation, analysis of the research results, revision of the text, correction of the conclusions.

Conflict of interest statement: the authors do not have any conflict of interest.

All authors have read and approved the final version of the manuscript.

Received 15.12.2023

Revised 11.01.2024

Accepted 18.01.2024

Об авторах:

Дмитрий Аверкиевич Шляхин, доктор технических наук, доцент, заведующий кафедрой строительной механики, инженерной геологии, основания и фундаментов Самарского государственного технического университета (443100, РФ, г. Самара ул. Молодогвардейская, 244), SPIN-код: [7802-5059](https://orcid.org/7802-5059), [ORCID, d-612-mit2009@yandex.ru](https://orcid.org/d-612-mit2009@yandex.ru)

Елена Владимировна Савинова, аспирант, старший преподаватель кафедры строительной механики, инженерной геологии, основания и фундаментов Самарского государственного технического университета (443100, РФ, г. Самара ул. Молодогвардейская, 244), SPIN-код: [7027-4822](https://orcid.org/7027-4822), [ORCID, slenax@yandex.ru](https://orcid.org/slenax@yandex.ru)

Заявленный вклад авторов:

Д.А. Шляхин — научное руководство, формирование основной концепции, цели и задачи исследования, проведение расчетов, формирование выводов.

Е.В. Савинова — подготовка текста, анализ результатов исследования, доработка текста, корректировка выводов.

Конфликт интересов: авторы заявляют об отсутствии конфликта интересов.

Все авторы прочитали и одобрили окончательный вариант рукописи.

Поступила в редакцию 15.12.2023

Поступила после рецензирования 11.01.2024

Принята к публикации 18.01.2024

MECHANICS МЕХАНИКА





UDC 532.135, 624.04

Research article

<https://doi.org/10.23947/2687-1653-2024-24-1-36-47>

Prediction of Rheological Parameters of Polymers by Machine Learning Methods

Tatiana N. Kondratieva , Anton S. Chepurnenko 

Don State Technical University, Rostov-on-Don, Russian Federation

✉ ktn618@yandex.ru

EDN: HTOURY

Abstract

Introduction. All polymer materials and composites based on them are characterized by pronounced rheological properties, the prediction of which is one of the most critical tasks of polymer mechanics. Machine learning methods open up great opportunities in predicting the rheological parameters of polymers. Previously, studies were conducted on the construction of predictive models using artificial neural networks and the CatBoost algorithm. Along with these methods, due to the capability to process data with highly nonlinear dependences between features, machine learning methods such as the k -nearest neighbor method, and the support vector machine (SVM) method, are widely used in related areas. However, these methods have not been applied to the problem discussed in this article before. The objective of the research was to develop a predictive model for evaluating the rheological parameters of polymers using artificial intelligence methods by the example of polyvinyl chloride.

Materials and Methods. This paper used k -nearest neighbor method and the support vector machine to determine the rheological parameters of polymers based on stress relaxation curves. The models were trained on synthetic data generated from theoretical relaxation curves constructed using the nonlinear Maxwell-Gurevich equation. The input parameters of the models were the amount of deformation at which the experiment was performed, the initial stress, the stress at the end of the relaxation process, the relaxation time, and the conditional end time of the process. The output parameters included velocity modulus and initial relaxation viscosity coefficient. The models were developed in the Jupyter Notebook environment in Python.

Results. New predictive models were built to determine the rheological parameters of polymers based on artificial intelligence methods. The proposed models provided high quality prediction. The model quality metrics in the SVR algorithm were: MAE — 1.67 and 0.72; MSE — 5.75 and 1.21; RMSE — 1.67 and 1.1; MAPE — 8.92 and 7.3 for the parameters of the initial relaxation viscosity and velocity modulus, respectively, with the coefficient of determination R^2 — 0.98. The developed models showed an average absolute percentage error in the range of 5.9–8.9%. In addition to synthetic data, the developed models were also tested on real experimental data for polyvinyl chloride in the temperature range from 20° to 60°C.

Discussion and Conclusion. The approbation of the developed models on real experimental curves showed a high quality of their approximation, comparable to other methods. Thus, the k -nearest neighbor algorithm and SVM can be used to predict the rheological parameters of polymers as an alternative to artificial neural networks and the CatBoost algorithm, requiring less effort to preset adjustment. At the same time, in this research, the SVM method turned out to be the most preferred method of machine learning, since it is more effective in processing a large number of features.

Keywords: rheology, polymers, artificial intelligence, machine learning, k -nearest neighbors, support vector regression

Acknowledgements. The authors would like to thank the Editorial board and the reviewers for their attentive attitude to the article and the specified comments that improved its quality.

For citation. Kondratieva TN, Chepurnenko AS. Prediction of Rheological Parameters of Polymers by Machine Learning Methods. *Advanced Engineering Research (Rostov-on-Don)*. 2024;24(1):36–47. <https://doi.org/10.23947/2687-1653-2024-24-1-36-47>

Прогнозирование реологических параметров полимеров методами машинного обучения

Т.Н. Кондратьева  , А.С. Чепурненко 

Донской государственный технический университет, г. Ростов-на-Дону, Российская Федерация

 ktn618@yandex.ru

Аннотация

Введение. Для всех полимерных материалов и композитов на их основе характерны явно выраженные реологические свойства, прогнозирование которых является одной из важнейших задач механики полимеров. Большие возможности для прогнозирования реологических параметров полимеров открывают методы машинного обучения. Ранее проводились исследования на предмет построения прогнозных моделей с использованием искусственных нейронных сетей и алгоритма CatBoost. Наряду с этими методами, благодаря возможности обрабатывать данные с сильно нелинейными зависимостями между признаками, широкое применение в смежных областях находят методы машинного обучения — метод k -ближайших соседей и метод опорных векторов (SVM). Однако ранее к проблеме, рассмотренной в данной статье, эти методы не применялись. Целью работы явилась разработка прогнозной модели для оценки реологических параметров полимеров методами искусственного интеллекта на примере поливинилхлорида.

Материалы и методы. В работе применены метод k -ближайших соседей и метод опорных векторов для определения реологических параметров полимеров на основе кривых релаксации напряжений. Обучение моделей выполнялось на синтетических данных, сгенерированных на основе теоретических кривых релаксации, построенных с использованием нелинейного уравнения Максвелла-Гуревича. Входными параметрами моделей выступали величина деформации, при которой производился эксперимент, начальное напряжение, напряжение в конце процесса релаксации, время релаксации и условное время окончания процесса. Выходные параметры: модуль скорости и коэффициент начальной релаксационной вязкости. Модели разработаны в среде Jupyter Notebook на языке Python.

Результаты исследования. Построены новые прогнозные модели для определения реологических параметров полимеров на основе методов искусственного интеллекта. Предложенные модели обеспечивают высокое качество прогнозирования. Метрики качества модели в алгоритме SVR составляют: MAE — 1,67 и 0,72; MSE — 5,75 и 1,21; RMSE — 1,67 и 1,1; MAPE — 8,92 и 7,3 для параметров начальной релаксационной вязкости и модуля скорости соответственно с коэффициентом детерминации R^2 — 0,98. Разработанные модели показали среднюю абсолютную процентную ошибку в диапазоне 5,9–8,9 %. Помимо синтетических данных, разработанные модели также апробировались на реальных экспериментальных данных для поливинилхлорида в диапазоне температур от 20 до 60 °C.

Обсуждение и заключение. Апробация разработанных моделей на реальных экспериментальных кривых показала высокое качество их аппроксимации, сопоставимое с другими методами. Таким образом, алгоритмы k -ближайших соседей и SVM могут использоваться для прогнозирования реологических параметров полимеров как альтернатива искусственным нейронным сетям и алгоритму CatBoost, требующая меньших усилий по предварительной настройке. При этом в данном исследовании наиболее предпочтительным методом машинного обучения оказался метод SVM, так как он более эффективен в обработке большого числа признаков.

Ключевые слова: реология, полимеры, искусственный интеллект, машинное обучение, k -ближайшие соседи, опорная векторная регрессия

Благодарности. Авторы выражают благодарность редакции и рецензентам за внимательное отношение к статье и указанные замечания, которые позволили повысить ее качество.

Для цитирования. Кондратьева Т.Н., Чепурненко А.С. Прогнозирование реологических параметров полимеров методами машинного обучения. *Advanced Engineering Research (Rostov-on-Don)*. 2024;24(1):36–47. <https://doi.org/10.23947/2687-1653-2024-24-1-36-47>

Introduction. Polymers are used in various industries, including the production of plastics, textiles, packaging materials, and more. Accurate prediction of the rheological parameters of polymers is a complex task that is important for optimizing production processes and creating products with desired properties.

Today, machine learning methods have gained great popularity in various fields, including chemistry and materials science, due to their ability to efficiently process and analyze large amounts of data. These methods make it possible to

predict the properties of materials. In [1], a platform based on machine learning was described, and the integration of metrological support in the context of digital transformation was proposed. In [2], the local distribution of deformation, the development of plastic anisotropy, and fracture in additively manufactured alloys were predicted. The problems of developing measuring control regulators on digital platforms were formulated in [3]. An intelligent model for controlling the parameters of overlap joint welding was built in [4]. However, the issues of using machine learning methods to predict the rheological properties of polymers remain insufficiently investigated. This is caused by both technical and methodological difficulties, such as the heterogeneity of the polymer structure, their sensitivity to external conditions, and complex interactions between molecules during deformation.

Research in the field of rheological properties of polymers and composites using machine learning methods has great prospects in the construction industry [5]. For numerous polymers, the experimental data are well described by the generalized nonlinear Maxwell-Gurevich equation [6], which has the form for a uniaxial stress state [7]:

$$\begin{aligned}\frac{\partial \varepsilon^*}{\partial t} &= \frac{f^*}{\eta^*}, \\ f^* &= \sigma - E_\infty \varepsilon^*, \\ \frac{1}{\eta^*} &= \frac{1}{\eta_0^*} \exp\left(\frac{|f^*|}{m^*}\right),\end{aligned}\tag{1}$$

where ε^* — creep deformation, f^* — stress function, σ — stress, E_∞ — module of high elasticity, η_0^* — initial relaxation viscosity, m^* — velocity module.

Various intelligent machine learning models can be used to determine the rheological parameters of polymers, such as the initial relaxation viscosity (hereinafter just “viscosity”) and the velocity module [8, 9]. For example, one such model is a neural network that can be trained on generated datasets to determine optimal polymer parameters [10].

Prediction based on synthesized data is a fairly common practice, including for nonlinear optimization methods [11, 12]. One of the ways to generate data is the use of Rosenbrock, Himmelblau, and Booth functions [13], which are effectively applied to test optimization methods such as gradient descent methods, genetic algorithms, and the Newton method. This approach was applied in [14], where a data set based on theoretical stress relaxation curves using the nonlinear Maxwell-Gurevich equation was generated to test the efficiency of various optimization methods.

In [15], several machine learning approaches were given to predict the durability of a reinforced concrete beam, such as a neural network of back propagation, linear and ridge regression, a decision tree, and a random forest. The input parameters of the study were both various characteristics of the material and their properties, depending on the environment (temperature, humidity). Finally, according to the results of the study, the back propagation model determined a more accurate forecast (85%), the average values (MAE) and MAPE were 1.13% and 14.5%, respectively.

Another approach to solving inverse problems of creep theory using the neural network method is based on training a model on large amounts of experimental data. In [16], a neural network model was developed, which was trained on data obtained as a result of long-term experiments on polymer materials, and successfully predicted the viscoelastic behavior of these materials. The data obtained from experiments on samples of various materials were used for the study.

Unlike the above-mentioned papers, the presented research is intended to promote the development of more accurate and reliable methods for predicting polymer properties, such as the k -nearest neighbor method and the support vector machine, which is important for various industries and science.

The research objective was to develop a predictive model based on artificial intelligence methods for analyzing the rheological properties of polymers. Previously, the authors had already used a machine learning algorithm based on gradient boosting CatBoost to process stress relaxation curves [17, 18]. CatBoost is one of the most powerful machine learning algorithms applicable to solving not only regression problems, but also classification and ranking problems [19].

The CatBoost method can be useful for solving some tasks, but it also has its limitations and disadvantages. In this regard, there is an interest in using other algorithms mentioned earlier [20] to solve the problem.

Materials and Methods. The generated data array is partially presented in Table 1. This array was formed on the basis of theoretical stress relaxation curves described by the Maxwell-Gurevich equation, according to the technique presented in [14]. The variation ranges of the velocity modulus and the initial relaxation viscosity in the generated array correspond to the real ranges for polyvinyl chloride in the temperature interval from 20° to 60°C. The total number of numerical experiments (n) was 30,000.

Table 1

Table of initial data for training the model

No	Deformation, %	Stress at the beginning of the process σ_0 , MPa	Stress at the end of the process σ_∞ , MPa	Relaxation time t_n , h	Conditional end time of the process t_{95} , h	Velocity module m^* , MPa	Viscosity η_0^* , 10^6 , MPa·s
1	1.000	10.000	0.909	0.277	1.484	6.000	3.000
2	2.000	20.000	1.818	0.109	1.003	6.000	3.000
3	3.000	30.000	2.727	0.046	0.820	6.000	3.000
4	1.000	10.000	0.909	0.861	4.615	6.000	9.333
5	2.000	20.000	1.818	0.339	3.122	6.000	9.333
6	3.000	30.000	2.727	0.142	2.552	6.000	9.333
7	1.000	10.000	0.909	1.445	7.747	6.000	15.667
...							
29997	3	45	37.5	0.285	2.476	15	53.666
29998	1	15	12.5	1.003	4.255	15	60
29999	2	30	25	0.558	3.371	15	60
30000	3	45	37.5	0.319	2.769	15	60

The data set consisted of five input variables and two output variables. Input variables (unit measure): deformation — ε (%); stress at the beginning of the process — σ_0 (MPa); stress at the end of the process — σ_∞ (MPa); relaxation time — t_n (h); conditional end time of the process — t_{95} (h). Output variables (unit measure): velocity module — m^* (MPa); initial relaxation viscosity — η_0^* (in Table 1 and further, simply “viscosity”) (10^6 MPa·s).

Values σ_0 , σ_∞ , t_n , and t_{95} are schematically shown on the typical stress relaxation curve (Fig. 1).

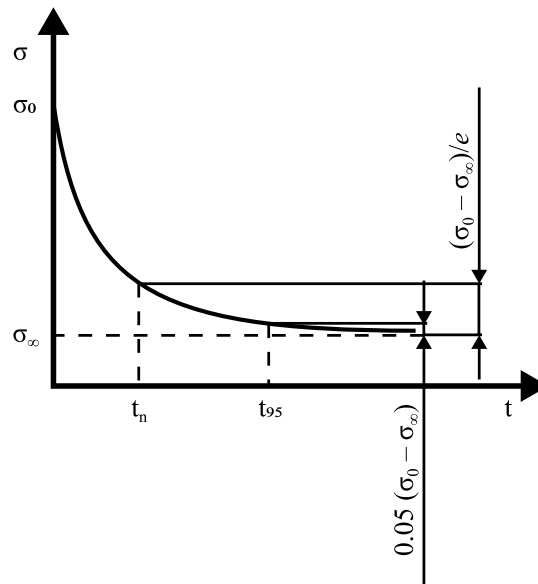


Fig. 1. Typical stress relaxation curve

The k -nearest neighbor (k -NN) algorithm is based on the similarity analysis of nearby objects. The k -NN method is in great demand for solving various types of machine learning tasks.

Formula (2) represents the general form of the algorithm, where $w(i, x)$ — weight function evaluating the importance of the i -th neighbor.

$$F(x) = \operatorname{argmax}_{y \in Y} \sum_{i=1}^m [x_{ix} = y] w(i, x). \quad (2)$$

The maximum total weight can be achieved for several objects at the same time. The entropy of this process can be adjusted using nonlinear sequence $w(i, x) = [i \leq k] q^i$ (exponentially weighted k -nearest neighbor method) provided that $0 \leq q \leq 0.5$.

Representing a fairly simple machine learning algorithm, k -NN is well applicable to solving classification and regression problems. The advantages of this method are ease of implementation, no need for pre-training of the model. It is used for all types of data, including categorical and numeric. Disadvantages: a tendency to over-training (provided that k is too small), poor performance with large amounts of data, it is not possible to take into account the relationship between the signs.

The support vector algorithm — support vector regression (SVR) — solves the problem of minimizing the sum of the mean absolute error. SVR is more resistant to outliers, unlike the least squares method, due to the regularization coefficient (C) and the “epsilon-insensitive tube” (ϵ). In this case, ϵ determines the width of the tube in which errors are ignored. Stochastic gradient descent is used to find the minimum of the function.

The support vector machine learning algorithm is function $F(x)$ of approximation and regularization of empirical risk, which converts training and test samples into output data for each object of the corresponding sample. Formula (3) represents the general form of the algorithm, (4) is a linearly separable sample, (5) is a linearly inseparable sample, where C — regularization coefficient, $M_i(w, w_0)$ — scalar product of vectors (feature and support vector), w_i — weight coefficients.

$$F(x) = C \sum_{i=1}^l (1 - M_i(w, w_0)) + \frac{1}{2} \|w\|^2 \rightarrow \min_{w, w_0} F(x). \quad (3)$$

$$\begin{cases} \frac{1}{2} \|w\|^2 \rightarrow \min_{w, w_0} F(x); \\ M_i(w, w_0) \geq 1, i = \{1: l\}. \end{cases} \quad (4)$$

$$\begin{cases} \frac{1}{2} \|w\|^2 + C \sum_{i=1}^l \epsilon_i \rightarrow \min_{w, w_0} F(x); \\ M_i(w, w_0) \geq 1 - \epsilon_i, i = \{1: l\}; \\ \epsilon_i \geq 0, i = \{1: l\}. \end{cases} \quad (5)$$

Function $K(x, x')$ is a function of a pair of objects (x, x') , π representable as a scalar product in some space H , for which transformation $\psi: X \rightarrow H$ takes place. Function $K: X \times X \rightarrow R$ — kernel if $K(x, x') = (\psi(x), \psi(x'))$, provided that K is symmetric: $K(x, x') = K(x', x)$ and nonnegative definite: $\iint K(x, x') g(x) g(x') dx dx', \forall g: X \rightarrow R$.

The regularization coefficient is determined by the sliding mode control method.

Advantages of the SVM method are as follows: high accuracy in classification problems in nonlinear spaces; ability to work with a large number of features (including categorical and numerical), generalize data (which provides applying the model to new data), work with data that are not linearly separable due to the use of kernel functions.

Disadvantages of the SVM method include inefficiency of working with large amounts of data; low interpretability of the model; the requirement to configure numerous parameters, such as the type of kernel (its parameters, regularization parameters), etc.

In this research, algorithms are developed in the Jupyter Notebook intelligent computing environment using machine learning methods.

As a learning algorithm, function $F(x)$ is considered. It transforms training sample $\{x_i\}_{i=1}^m \in X^m$ and test sample $\{x_i'\}_{i=1}^l \in X^l$ into output data when training $\{y_i\}_{i=1}^m \in X^m$ and testing $\{y_i'\}_{i=1}^l \in X^l$ for each object of the corresponding selection. The training of the vector of parameters $w_i \in W$ is embedded inside the algorithm.

Under the conditions of the presented problem: $\{y_i\}_{i=1}^m$ — actual values of viscosity η_0^* (at the beginning of the relaxation process) and velocity module m^* ; $\{y_i'\}_{i=1}^m$ — predicted values of viscosity η_0^* (at the beginning of the relaxation process) and velocity module m^* .

The selection of such a parameter as the number of neighbors affects the generalizing ability of the developed model and is important for its correct operation. The most suitable algorithm for calculating distance based on data is Distance, in which the weights of objects are inversely proportional to their distance. Accordingly, in the case of closer neighbors of the query object, they have more influence than their neighbors located at a greater distance from the object.

The data set was divided into training and test samples in a ratio of 75/25. In turn, 20% of the training sample became validation. The sample size was: training — $x_{train} = 20,400$; test — $x_{test} = 6,000$; validation — $x_{eval} = 3,600$. For variables y_{train} , y_{test} , y_{eval} , the data were distributed in a similar way.

To build the k -nearest neighbor model, the following parameters were selected: number of neighbors, sheet size, interval, and weight function. The range and functionality of the values for the configurable parameters are shown in Table 2.

Table 2

Parameter table for k -NN model

No	Parameter	Value	Functional
1	Number of neighbors (k)	3, 5, 7, 9	Determines optimal number of neighbors for query
2	Sheet size (n)	15, 20, 30	Determines speed of querying and required memory for storing the tree
3	Interval (p)	1 (11), 2 (12)	Defines power parameter (Minkowski metric)
4	Weight function (w)	'uniform', 'distance'	Predicting weights

To build the SVR model, the following parameters were selected: kernel type, kernel order, regularization coefficient (quadratic regularizer), ε . The range and functional values for the adjustable parameters are presented in Table 3.

Table 3

Parameter table for SVR model

No	Parameter	Value	Functional
1	Kernel type	'linear'; 'poly'; 'rbf'; 'sigmoid'	Defines type of hyperplane (linear/nonlinear)
2	Kernel order	1, 2, 3, 4, 5, 7	Defines degree of polynomial function of kernel
3	Quadratic regularizer (C)	2; 3; 4; 5; 7; 10	Solves problems of vector multicollinearity and model retraining
4	ε	0.1; 0.2; 0.5; 1; 1.5; 2; 3	Determines deviation of the object (proximity measure)

Research Results

Figure 2 shows the correlations between the variables.

The following types of linear correlations between individual input and output variables of the model can be noted:

- strong enough — between the variables “Deformation” and “Stress at the beginning” $\rho_{\sigma_0\varepsilon} = 0.93$; “Relaxation time” and “End time of the process” $\rho_{t_{n195}} = 0.93$;
- average — between the variables “Deformation” and “Stress at the end” $\rho_{\sigma_{\infty}\varepsilon} = 0.71$; “Stress at the beginning” and “Stress at the end” $\rho_{\sigma_0\sigma_{\infty}} = 0.75$;
- weak — between the variables “End time of the process” and “Viscosity” $\rho_{\eta^*t_{95}} = 0.58$; “Viscosity” and “Relaxation time” $\rho_{\eta^*\varepsilon} = 0.46$.

The presence of a moderate correlation between variables or its absence indicates only the absence of a linear relationship; therefore, it is possible to have a nonlinear relationship between variables.

Deformation	1	0.95	0.71	-0.39	-0.2	6.5e-11	8.4e-11
Stress at the beginning	0.95	1	0.75	-0.42	-0.24	5.4e-11	6.3e-13
Stress at the end	0.71	0.75	1	-0.54	-0.51	7.6e-13	5.6e-12
Relaxation time	-0.39	-0.42	-0.54	1	0.93	0.23	0.46
End time of the process	-0.2	-0.24	-0.51	0.93	1	0.13	0.58
Velocity module	6.5e-11	5.4e-11	7.6e-13	0.23	0.13	1	8.9e-17
Viscosity	8.4e-11	6.3e-13	5.6e-12	0.46	0.58	8.9e-17	1
	Deformation	Stress at the beginning	Stress at the end	Relaxation time	End time of the process	Velocity module	Viscosity

Fig. 2. Correlation matrix

Table 4 shows the statistical characteristics of the original data set.

Table 4

Statistical characteristics of the original data set

Parameter	ε	σ_0	σ_∞	t_n	t_{95}	m^*	η_0^*
Unit measure	%	MPa	MPa	h	h	MPa	10^6 MPa·s
<i>count</i>	30,000.00	30,000.00	30,000.00	30,000.00	30,000.00	30,000.00	30,000.00
<i>mean</i>	2.00	25.00	15.78	0.75	4.41	10.50	31.50
<i>std</i>	0.82	10.77	9.10	0.94	4.40	2.87	18.19
<i>min</i>	1.00	10.00	0.91	0.00	0.07	6.00	3.00
<i>max</i>	3.00	45.00	37.50	10.04	38.02	15.00	60.00

The best parameters for the k -nearest neighbor model were determined as a result of 5-block cross-validation (Table 5).

Table 5

Best k -NN model parameters

Parameter	Number of neighbors (k)	Sheet size (n)	Interval (p)	Weight function (w)
η_0^*	3	15	2	'distance'
m^*	5	15	2	'distance'

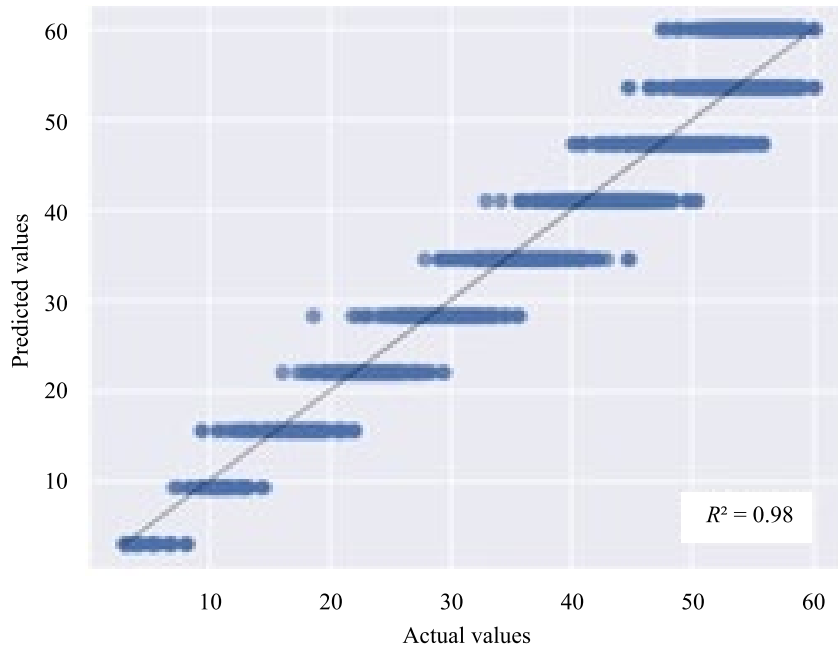
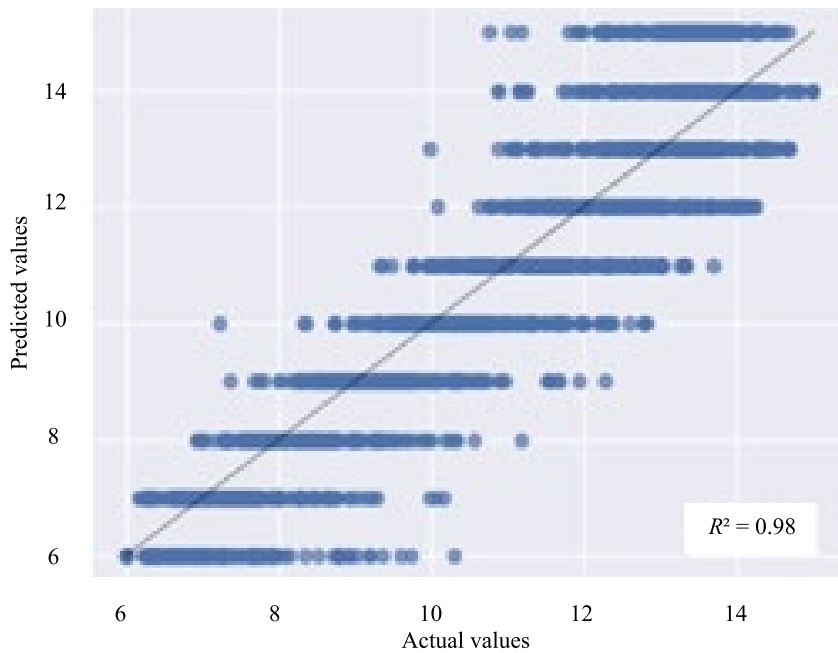
The best parameters of the SVR model for viscosity parameters η_0^* (at the beginning of the relaxation process) and velocity module m^* were obtained empirically (Table 6).

Table 6

Best parameters of SVR model

Parameter	Kernel type	Kernel order	Quadratic regularizer	ε
η_0^*	'rbf'	2	5	0.3
m^*	'rbf'	3	6	0.3

The ratio between the real and predicted values for the k -NN model in terms of the parameters “Viscosity” and “Velocity modulus” is shown in Figures 3, 4.

Fig. 3. Diagrams of prediction errors of k -NN, “Viscosity”Fig. 4. Diagrams of prediction errors of k -NN, “Velocity module”

The ratio between the real and predicted values for the SVR model according to the parameters “Viscosity” and “Velocity module” is shown in Figures 5, 6.

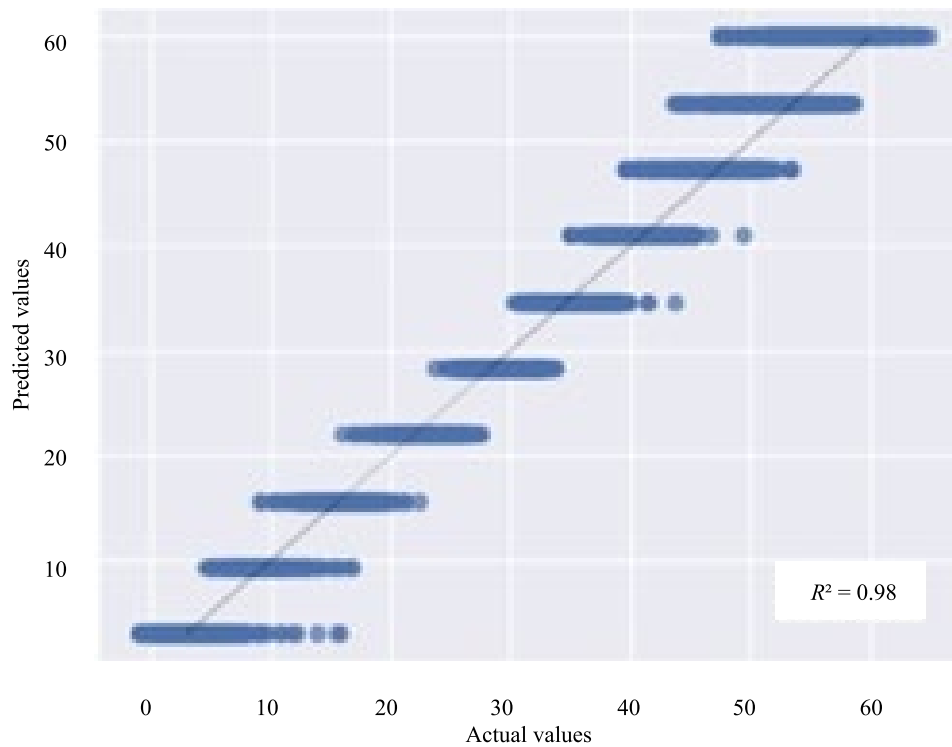


Fig. 5. Diagrams of prediction errors of k -NN, “Viscosity”

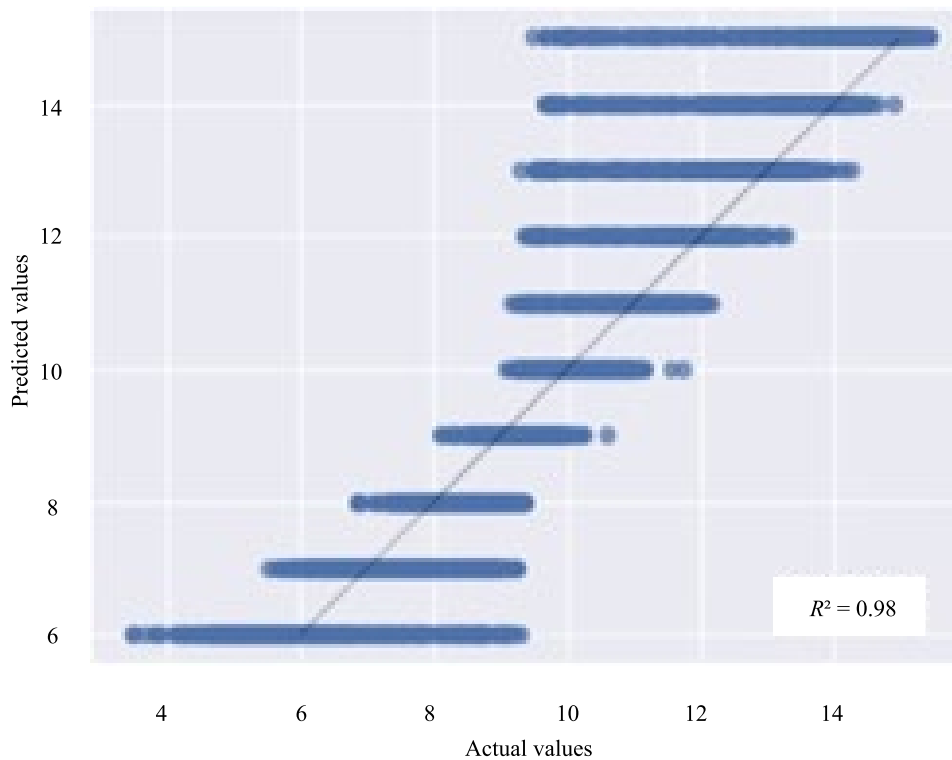


Fig. 6. Diagrams of prediction errors of k -NN, “Velocity module”

The metrics of the developed models of k -nearest neighbors and support vectors are presented in Tables 7 and 8, respectively.

Table 7

Metrics of the developed k -NN models

Parameter	MAE	MSE	RMSE	MAPE (%)	R^2 train	R^2 test
η_0^*	1.8	6.8	2.6	5.9	1.00	0.98
m^*	0.7	0.8	0.9	6.9	0.99	0.98

Table 8

Metrics of the developed SVR models

Parameter	MAE	MSE	RMSE	MAPE (%)	R^2 train	R^2 test
η_0^*	1.67	5.75	1.67	8.92	0.98	0.97
m^*	0.72	1.21	1.1	7.3	0.89	0.87

In addition to synthetic data, the developed models were also tested on real experimental data presented in [13]. Experimental relaxation curves of polyvinyl chloride were used for various temperatures in the range from 20° to 60°C. In Figure 7, the experimental stress values at different temperatures at different points in time are marked with felt-tip pens, and solid lines show stress relaxation curves based on values m^* and η_0^* predicted by the models.

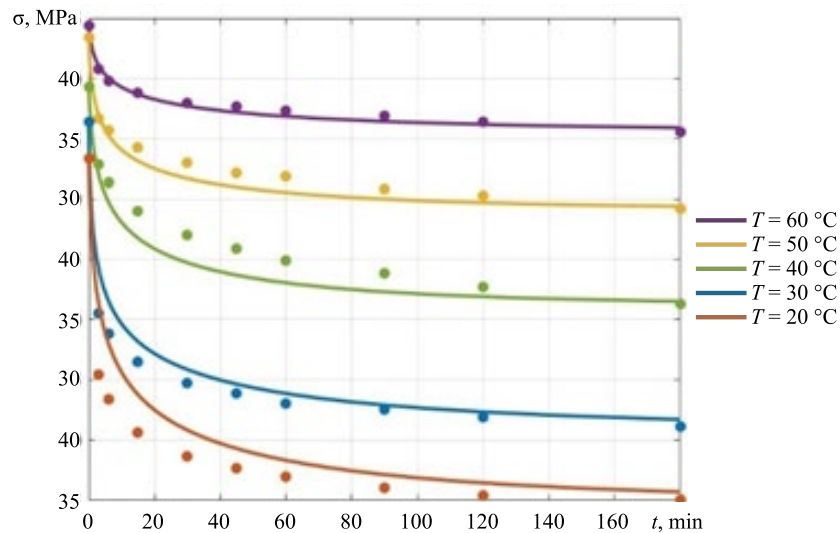


Fig. 7. Results of testing the model on experimental data

Discussion and Conclusion. Figure 5 shows that the quality of prediction based on experimental data is quite high, specifically, for temperatures of 30°C, 50°C and 60°C. For other temperatures, the prediction quality is somewhat lower, which is due to the quality of the experimental curves themselves. It was necessary to extend the experiment time and wait for the curves to reach the horizontal asymptote.

In this research, the most preferred method is the support vector machine (SVM). This is due to the fact that SVM can process data with a large number of features, which is important for the analysis of rheological parameters of materials. In addition, SVM works with nonlinear dependences between features, it is applicable to solve the regression problem, which is required to determine the rheological parameters of materials.

However, the CatBoost method can also be effective in this task, especially, if there are categorical features in the data. In addition, CatBoost can process missing data, which can be important for analyzing rheological parameters of materials.

The k -nearest neighbor method is less preferable in this task due to its low efficiency in processing a large number of features, as well as the presence of problems with high data dimensionality.

In the course of the investigation, it has been shown that the use of machine learning methods makes it possible to effectively analyze and process large amounts of data, including information about the characteristics of polymers and their rheological properties. The model developed on the basis of such an analysis maintains high accuracy in predicting the rheological parameters of polyvinyl chloride, which is confirmed by the results of cross-validation and comparison to experimental data.

One of the key advantages of this approach is the ability to automate the process of predicting the rheological parameters of polymers, which reduces the time and cost of research and development of new materials. In addition, the model can be easily adapted to analyze other types of polymers and predict their properties.

As a result of this research, a predictive model has been developed to evaluate the rheological parameters of polyvinyl chloride using artificial intelligence methods based on data of its characteristics and rheological properties. The model demonstrates high prediction accuracy and can be used to optimize the production and development of new polymer-based materials.

References

1. Dudukalov EV, Munister VD, Zolkin AL, Losev AN, Knishov AV. The Use of Artificial Intelligence and Information Technology for Measurements in Mechanical Engineering and in Process Automation Systems in Industry 4.0. *Journal of Physics: Conference Series*. IOP Publishing. 2021;1889(5):052011. <https://doi.org/10.1088/1742-6596/1889/5/052011>
2. Waqas Muhammad, Abhijit P Brahme, Olga Ibragimova, Jidong Kang, Kaan Inal. A Machine Learning Framework to Predict Local Strain Distribution and the Evolution of Plastic Anisotropy & Fracture in Additively Manufactured Alloys. *International Journal of Plasticity*. 2021;136:102867. <https://doi.org/10.1016/j.ijplas.2020.102867>
3. Won-Bin Oha, Tae-Jong Yuna, Bo-Ram Leea, Chang-Gon Kima, Zong-Liang Lianga, Ill-Soo Kim. A Study on Intelligent Algorithm to Control Welding Parameters for Lap-joint. *Procedia Manufacturing*. 2019;30:48–55. <http://doi.org/10.1016/j.promfg.2019.02.008>
4. Amit R Patel, Kashyap K Ramaiya, Chandrakant V Bhatia, Hetalkumar N Shah, Sanket N Bhavsar. Artificial Intelligence: Prospect in Mechanical Engineering Field—A Review. In book: *Data Science and Intelligent Applications*. Singapore: Springer; 2021. P. 267–282. https://doi.org/10.1007/978-981-15-4474-3_31
5. Amjadi M, Fatemi A. Creep and Fatigue Behaviors of High-Density Polyethylene (HDPE): Effects of Temperature, Mean Stress, Frequency, and Processing Technique. *International Journal of Fatigue*. 2020;141:105871. <http://doi.org/10.1016/j.ijfatigue.2020.105871>
6. Chepurnenko V, Yazyev B, Xuazhen Song. Creep Calculation for a Three-Layer Beam with a Lightweight Filler. *MATEC Web of Conferences*. 2017;129:05009. <https://doi.org/10.1051/mateconf/201712905009>
7. Litvinov SV, Yazyev BM, Turko MS. Effecting of Modified HDPE Composition on the Stress-Strain State of Constructions. *IOP Conference Series: Materials Science and Engineering*. 2018;463(4):042063. <https://doi.org/10.1088/1757-899X/463/4/042063>
8. Guangjian Xiang, Deshun Yin, Ruifan Meng, Siyu Lu. Creep Model for Natural Fiber Polymer Composites (NFPCs) Based on Variable Order Fractional Derivatives: Simulation and Parameter Study. *Journal of Applied Polymer Science*. 2020;137(24):48796. <http://doi.org/10.1002/app.48796>
9. Tugce Tezel, Volkan Kovan, Eyup Sabri Topal. Effects of the Printing Parameters on Short-Term Creep Behaviors of Three-Dimensional Printed Polymers. *Journal of Applied Polymer Science*. 2019;136(21):47564. <http://doi.org/10.1002/app.47564>
10. Litvinov SV, Trush LI, Yazyev SB. Flat Axisymmetrical Problem of Thermal Creepage for Thick-Walled Cylinder Made of Recyclable PVC. *Procedia Engineering*. 2016;150:1686–1693. <https://doi.org/10.1016/j.proeng.2016.07.156>
11. Dudnik AE, Chepurnenko AS, Litvinov SV. Determining the Rheological Parameters of Polyvinyl Chloride, with Change in Temperature Taken into Account. *International Polymer Science and Technology*. 2017;44(1):43–48. <https://doi.org/10.1177/0307174X1704400109>
12. Litvinov S, Yazyev S, Chepurnenko A, Yazyev B. Determination of Rheological Parameters of Polymer Materials Using Nonlinear Optimization Methods. In book: A. Mottaeva (ed). *Proceedings of the XIII International Scientific Conference on Architecture and Construction*. Singapore: Springer; 2020. P. 587–594. https://doi.org/10.1007/978-981-33-6208-6_58
13. Solovyova EB, Askadskiy AA, Popova MN. Investigation of Relaxation Properties of Primary and Secondary Polyvinyl Chloride. *Plasticheskie massy*. 2013;2:54–62. (In Russ.).
14. Chepurnenko A. Determining the Rheological Parameters of Polymers Using Artificial Neural Networks. *Polymers*. 2022;14(19):3977. <https://doi.org/10.3390/polym14193977>
15. Yu Xuan Rui. Developing an Artificial Neural Network Model to Predict the Durability of the RC Beam by Machine Learning Approaches. *Case Studies in Construction Materials*. 2022;17:e01382. <http://doi.org/10.1016/j.cscm.2022.e01382>
16. Nagababu Andraju, Greg W Curtzwiler, Yun Ji, Kozliak Evguenii, Prakash Ranganathan. Machine-Learning-Based Predictions of Polymer and Postconsumer Recycled Polymer Properties. A Comprehensive Review. *ACS Applied Materials & Interfaces*. 2022;14(38):42771–42790. <http://doi.org/10.1021/acsami.2c08301>

17. Chepurnenko AS, Kondratieva TN, Deberdeev TR, Akopyan VF, Avakov AA, Chepurnenko VS. Prediction of Rheological Parameters of Polymers Using CatBoost Gradient Boosting Algorithm. *All Materials: Encyclopedic Reference Book*. 2023;(6):21–29. (In Russ.).

18. Kondratieva T, Prianishnikova L, Razveeva I. Machine Learning for Algorithmic Trading. *E3S Web of Conferences*. 2020;224:01019. <https://doi.org/10.1051/e3sconf/202022401019>

19. Stelmakh SA, Shcherban EM, Beskopylny AN, Mailyan LR, Meskhi B, Razveeva I, et al. Prediction of Mechanical Properties of Highly Functional Lightweight Fiber-Reinforced Concrete Based on Deep Neural Network and Ensemble Regression Trees Methods. *Materials*. 2022;15(19):6740. <https://doi.org/10.3390/ma15196740>

20. Beskopylny AN, Stelmakh SA, Shcherban EM, Mailyan LR, Meskhi B, Razveeva I, et al. Concrete Strength Prediction Using Machine Learning Methods CatBoost, k-Nearest Neighbors, Support Vector Regression. *Applied Sciences*. 2022;12(21):10864. <https://doi.org/10.3390/app122110864>

About the Authors:

Anton S. Chepurnenko, Dr.Sci. (Eng.), Associate Professor, professor of the Strength of Materials Department, Don State Technical University (1, Gagarin sq., Rostov-on-Don, 344003, RF), SPIN-code: [7149-7981](#), [ORCID](#), [ResearcherID](#), [ScopusID](#), anton_chepurnenk@mail.ru

Tatiana N. Kondratieva, Cand.Sci. (Eng.), Associate Professor of the Mathematics and Informatics Department, Don State Technical University (1, Gagarin sq., Rostov-on-Don, 344003, RF), SPIN-code: [7794-2841](#), [ORCID](#), ktn618@yandex.ru

Claimed contributorship:

AS Chepurnenko: academic advising, analysis of the research results, the text revision, correction of the conclusions.

TN Kondratieva: basic concept formulation, research objectives and tasks, calculations, preparation of the text, formulation of the conclusions.

Conflict of interest statement: the authors do not have any conflict of interest.

All authors have read and approved the final version of the manuscript.

Received 28.12.2023

Revised 24.01.2024

Accepted 01.02.2024

Об авторах:

Антон Сергеевич Чепурненко, доктор технических наук, доцент, профессор кафедры сопротивления материалов Донского государственного технического университета (344003, РФ, г. Ростов-на-Дону, пл. Гагарина, 1), SPIN-код: [7149-7981](#), [ResearcherID](#), [ScopusID](#), [ORCID](#), anton_chepurnenk@mail.ru

Татьяна Николаевна Кондратьева, кандидат технических наук, доцент кафедры математики и информатики Донского государственного технического университета (344003, РФ, г. Ростов-на-Дону, пл. Гагарина, 1), SPIN-код: [7794-2841](#), [ORCID](#), ktn618@yandex.ru

Заявленный вклад авторов:

А.С. Чепурненко — научное руководство, анализ результатов исследований, доработка текста, корректировка выводов.

Т.Н. Кондратьева — формирование основной концепции, цели и задачи исследования, проведение расчетов, подготовка текста, формирование выводов.

Конфликт интересов: авторы заявляют об отсутствии конфликта интересов.

Все авторы прочитали и одобрили окончательный вариант рукописи.

Поступила в редакцию 28.12.2023

Поступила после рецензирования 24.01.2024

Запланирована в номер 01.02.2024

MACHINE BUILDING AND MACHINE SCIENCE МАШИНОСТРОЕНИЕ И МАШИНОВЕДЕНИЕ



UDC 621.181:621.184.244

Research article

<https://doi.org/10.23947/2687-1653-2024-24-1-48-57>

Application of Special Calculation Techniques in the Design of All-Welded Gastight Structures of Boiler Units

 Maxim P. Kurepin¹ , Mikhail Yu. Serbinovskiy² 
¹ Research and Design Institute of Nitrogen Industry and Products of Organic Synthesis, Moscow, Russian Federation

² Rostov State Transport University, Rostov-on-Don, Russian Federation
✉ mkurepin@gmail.com

EDN: IJMIOY

Abstract

Introduction. Improving the calculation methods of mechanical engineering facilities is an urgent and in-demand task. This fully applies to the techniques of calculating the strength of all-welded gastight boiler structures. Normative calculation techniques are based on simplified models that give limited possibilities for optimizing these structures. The low calculation accuracy inherent in such techniques is unacceptable under real design conditions, when an engineer is faced with the task of developing competitive structures in a short time, i.e., reducing metal consumption while providing the strength of these structures with limited development time. The use of simplified models was justified in the past, under conditions of insufficient development of computer technology. Application of the most advanced techniques based on computer modeling makes it possible to increase the accuracy of calculations, provide the optimization of such structures, and improve the quality of design. The objective of this study was to develop a new special procedure for calculating the strength of all-welded gastight structures based on computer modeling, using the most advanced methods of modeling the membrane wall and factors affecting it. The accompanying task was to verify the developed procedure based on comparing the results of calculations using the developed technique and the normative method.

Materials and Methods. The developed technique is based on the replacement of the membrane wall with an orthotropic plate or shell. Computer modeling was used applying the finite element method of all-welded gastight structures, and the impacts to which they were subjected during operation, as well as an effective method for assessing the technical condition of these structures.

Results. A new two-stage technique for calculating the strength of increased accuracy of all-welded gastight boiler structures was developed and patented. The calculation results were compared according to the proposed procedure and the normative method. It was shown that the proposed technique made it possible to increase the accuracy of modeling and calculation. The error in calculating all-welded gastight structures of a high-power boiler was reduced by more than 30% for the recommended steps between stiffeners. For specially reinforced membrane walls with steps exceeding the permissible values, the error reduction reached 70% or higher.

Discussion and Conclusion. The developed technique is used in the modeling and calculation of all-welded gastight structures. Its application makes it possible to optimize the step between the stiffeners of the structure of the support and connecting nodes of gastight membrane walls. Based on the results of the application of the two-stage calculation procedure, new designs were developed and patented. The developed technique has been used in the real design of boilers since 2014.

Keywords: boiler unit, all-welded gastight structures, membrane walls, plates, shells, orthotropic plates, mathematical modeling, finite element method

Acknowledgements. The authors would like to thank the Editorial board and reviewers for their attentive attitude to the article and the above comments, which made it possible to improve its quality.

For citation. Kurepin MP, Serbinovskiy MYu. Application of Special Calculation Techniques in the Design of All-Welded Gastight Structures of Boiler Units. *Advanced Engineering Research (Rostov-on-Don)*. 2024;24(1):48–57. <https://doi.org/10.23947/2687-1653-2024-24-1-48-57>

Научная статья

Применение специальных расчётных методик при проектировании цельносварных газоплотных конструкций котлоагрегатов

М.П. Курепин¹ , М.Ю. Сербиновский² 

¹ Научно-исследовательский и проектный институт азотной промышленности и продуктов органического синтеза ОАО «ГИАП», г. Москва, Российская Федерация

² Ростовский государственный университет путей сообщения, г. Ростов-на-Дону, Российская Федерация

✉ mkurepin@gmail.com

Аннотация

Введение. Совершенствование расчётных методик объектов машиностроения — актуальная и востребованная задача. В полной мере это относится и к методикам расчёта на прочность цельносварных газоплотных конструкций котлоагрегатов. Нормативные расчётные методики основаны на упрощённых моделях, имеющих ограниченные возможности для оптимизации этих конструкций. Низкая точность расчёта, присущая таким методикам, неприемлема в условиях реального проектирования, когда перед инженером стоят задачи разработки в сжатые сроки конкурентоспособных конструкций, то есть снижения металлоёмкости при обеспечении прочности этих конструкций и ограниченном времени разработки. Использование упрощённых моделей было оправдано в прошлом, в условиях недостаточного развития компьютерной техники. Применение наиболее совершенных методик, основанных на компьютерном моделировании, позволяет повысить точность расчётов, обеспечить оптимизацию таких конструкций, улучшить качество проектирования. Цель данного исследования — разработка новой специальной методики расчёта на прочность цельносварных газоплотных конструкций, основанной на компьютерном моделировании, с применением наиболее совершенных методик моделирования мембранного экрана и факторов, воздействующих на него. Сопутствующей задачей авторов статьи являлась верификация разработанной методики на основе сравнения результатов расчётов с применением разработанной методики и нормативного метода.

Материалы и методы. Разработанная методика основана на замене мембранного экрана ортотропной пластиной или оболочкой. Используются компьютерное моделирование с применением метода конечных элементов цельносварных газоплотных конструкций и воздействий, которым они подвержены в процессе эксплуатации, а также эффективный метод оценки технического состояния этих конструкций.

Результаты исследования. Разработана новая двухэтапная методика расчёта на прочность цельносварных газоплотных конструкций котлоагрегатов, получившая патент на изобретение. Проведено сравнение результатов расчётов по предложенной методике и по нормативному методу. Показано, что предложенная методика позволяет повысить точность моделирования и расчёта. Погрешность расчёта цельносварных газоплотных конструкций котла большой мощности снижена более чем на 30 % для рекомендованных шагов между поясами жесткости. Для подкреплённых специальным образом мембранных экранов с шагами, превышающими допустимые значения, снижение погрешности достигает 70 % и выше.

Обсуждение и заключение. Разработанная методика используется при моделировании и расчёте цельносварных газоплотных конструкций. Применение ее позволяет оптимизировать шаг между поясами жесткости конструкции опорных и соединительных узлов газоплотных экранов. По результатам применения двухэтапной расчётной методики были разработаны новые конструкции, получившие патенты на изобретения. Разработанная методика применяется в реальном проектировании котлоагрегатов с 2014 года.

Ключевые слова: котлоагрегат, цельносварные газоплотные конструкции, мембранные экраны, пластины, оболочки, ортотропные пластины, математическое моделирование, метод конечных элементов

Благодарности. Авторы выражают благодарность редакции и рецензентам за внимательное отношение к статье и указанные замечания, которые позволили повысить ее качество.

Для цитирования. Курепин М.П., Сербиновский М.Ю. Применение специальных расчётных методик при проектировании цельносварных газоплотных конструкций котлоагрегатов. *Advanced Engineering Research (Rostov-on-Don)*. 2024;24(1):48–57. <https://doi.org/10.23947/2687-1653-2024-24-1-48-57>

Introduction. The normative technique of the strength calculation of all-welded gastight structures¹ is based on replacing the screen with a structurally orthotropic Kirchhoff-Love plate with considerable simplifications. In this model, the orthotropy of the plate properties is taken into account only when calculating bending forces. The major objective of the introduced simplifications is to reduce the complexity of calculation formulas and, ultimately, the overall complexity of calculations. The models underlying the technique include a gastight screen in the form of an orthotropic plate, stiffener rings in the form of constant-section beams, and fasteners in the form of connections between the wall and the stiffener rings.

The following assumptions are made in the model²:

1. The orthotropy of the gastight wall is taken into account by introducing ratio D_z / D_x when calculating the bending moment M_z for an isotropic wall with cylindrical stiffness in a section perpendicular to pipes D_x , and in a section parallel to pipes D_z .

2. When determining stresses at the midpoint of the panel, there is a hinged connection of the gastight screens to each other in the screens of the all-welded box, since the fastening condition affects the nearest 6-8 pipes from the fixing point.

3. When determining the stresses in the corner of an all-welded box, there is pinching.

4. The action of two groups of forces is considered: active (boost and “buckling”) and reactive (emphasis on stiffener rings). The remaining impacts (from the internal pressure in the pipes, weight and temperature factors) are determined independently and taken into account at the stage of assessing the technical condition by the superposition of forces method.

5. The calculation is based on the principle of assessing the structural strength by bearing capacity, which is determined by the limiting state of the transition of the most loaded section from an elastic state to a plastic one. The calculation is performed according to a conditionally elastic scheme.

A significant disadvantage of this scheme is the use of simplified models that do not fully take into account the reinforcing, attached and other structural elements, their cross impact, as well as the effect of all influencing factors causing a complex stress-strain state of the membrane wall. This technique has limited modeling capabilities, specifically for membrane walls of complex shape, for which it is not applicable.

There are limits to the application of normative calculation formulas, constraining them due to design or loading features³. For membrane walls, standard calculation formulas are not applicable for any cross-sections, except for a pipe with a flat spacer. They are not applicable for membrane walls of complex shape. The maximum step size between stiffener rings is limited. It is noted in the normative technique that it is allowed to use other methods of calculating the strength of all-welded membrane structures, subject to providing the normative strength reserves. The technical regulations of the Customs Union enable using a number of calculation methods in addition to regulatory formulas, including computer modeling⁴. In regulatory documents, the strength calculation techniques that go beyond the application of regulatory formulas are called alternative, or special. In connection with the above, the objective set by the authors of this article — to develop a new special method for calculating all-welded gastight structures using computer modeling, which allows for high accuracy and reliability of modeling and calculation results — seems highly relevant.

In the papers of Russian authors, models have already been proposed in which the membrane wall is replaced by a statically indeterminate frame. Special calculation methods are successfully used to assess the strength and resource of elements of boilers and power plants [1]. In the studies devoted to the calculation of gastight membrane walls, it is noted that the methods based on the use of modern achievements in the area of numerical methods using computer modeling are promising [2].

Recent studies on boiler membrane walls include the works of Milošević-Mitić [3], Nagiar [4], Sertić [5], who proposed a method for calculating boiler strength and determining temperature displacements and loads of supports based on the Kirchhoff-Love theory and computer modeling using the finite element method (FEM) [6]. However, this technique is characterized by an increased error due to the application of significant simplifications in the membrane wall model (e.g., pipes are replaced with absolutely rigid bodies) [7]. The method of reverse transition from the plate to the wall and assessment of its technical condition has not been proposed [8].

¹ RD 10-249-98. Calculation Standards for the Strength of Stationary Boilers and Steam and Hot Water Pipelines. URL: <https://docs.cntd.ru/document/1200021653> (accessed: 15.12.2023) (In Russ.).

² RTM 24.031.06-73. Calculation and Design of Fastening Elements of the Wall System of Boiler Units with All-welded Panels: Technical Guides. Leningrad: RIO NPO TsKTI; 1974. 39 p. (In Russ.).

³ GOST 34233.1-2017. Vessels and Devices. Norms and Methods of Strength Calculations. Moscow: Standartinform; 2019. 30 p. (In Russ.).

⁴ CUTR 032/2013. Technical Regulations of the Customs Union. On the Safety of Equipment Operating under Excessive Pressure. URL: <http://docs.cntd.ru/document/499031170> (accessed: 15.12.2023) (In Russ.).

High calculation accuracy was obtained through modeling membrane walls based on the general mechanics of a deformed solid and measurements in numerical experiments with accurate solid-state models of the screen [9]. Effective methods for modeling loads [10] acting on all-welded gastight structures have been proposed, which make it possible to increase the accuracy and reliability of modeling these structures [11].

In general, modeling membrane walls using orthotropic plates is relevant if we take into account the complexity of modeling and calculating membrane walls with many pipes and spacers using traditional solid-state computer simulation techniques, for which there are strict limitations. These restrictions deal with the relative dimensions of the height of the solid-state element to its length and width, which cannot exceed $\frac{1}{8}$ (aspect ratio metric [12]), with a ratio of membrane wall thickness to its width of $\frac{1}{400}$ or more.

When developing the new technique, the following objectives were set: increasing accuracy, reducing the complexity of modeling and calculation, reducing the time of computational operations during optimization and evaluation of strength, rigidity, stability, and durability of structures. It is known that membrane walls operate under conditions of complex resistance and are simultaneously exposed to external forces, moments, pressure or rarefaction from the inside of the boiler, pressure in pipes, an uneven temperature field, taking into account the cyclic effect of these parameters and creep of materials at high temperatures. An additional, but rather important task of this development was to create a convenient tool for cyclic optimization of the structure, which includes visualization of the results of making changes to the structure in the form of stress, strain, and displacement fields.

Materials and Methods. The technique proposed by the authors involves replacing the membrane wall with an orthotropic plate or shell. The membrane wall has a regular structure and a section that periodically changes in the direction perpendicular to the pipes. Such a membrane wall can be considered as a structurally orthotropic plate, i.e., a plate in a flat stressed state with elastic characteristics that differ in mutually perpendicular directions. The membrane wall is a plate, and the bent screen is a shell since the diameter of the pipes, which determines the thickness of the screen, is small compared to its other dimensions. The structural elements of a gastight boiler, which can be represented as structurally orthotropic plates, are, first of all, membrane walls of the furnace, the transition flue, the convective shaft of the boiler, and membrane superheaters.

The authors previously developed a two-stage modeling and calculation technique for all-welded gastight structures, which received a patent for the invention [13]. It is based on the replacement of the membrane wall with an orthotropic plate or shell, reliable modeling of all-welded gastight structures and the impacts to which they are exposed during operation, and on an effective method for assessing the technical condition of these structures. Through the developed technique, there are opportunities to optimize structures and reduce their metal consumption [14], which have not existed before. New designs are worked out, the complexity of design is significantly reduced [15]. The problem of assessing the technical condition of boiler structures containing membrane walls is solved by applying the most advanced modern practices based on achievements in numerical modeling.

The method of calculating the strength of all-welded gastight structures consists of two stages. At the first stage, a model of a box structure with screens in the form of orthotropic plates and/or shells is formed with a preliminary calculation of their dimensional and physico-mechanical characteristics. The attached elements, including pipe connectors with headers, festoons, stiffener rings, various fasteners, supports, reinforcement elements are modeled in the form of rods, shells, connections, and boundary conditions. Then, local zones of orthotropic plates and/or shells with increased displacements and deformations are determined, and the technical condition of the attached elements is assessed. At the second stage, models are formed for places with exceeding the specified parameters, in which local zones of screens with attached elements with increased displacements, stresses, and deformations are modeled by solid-state elements (submodeling of local zones [12]). Conditionally elastic analysis is carried out. Health assessment in critical sections is provided according to static strength conditions and optimization of the structure.

Research Results. The calculation of all-welded gastight boiler structures with a steam capacity of 810 tons of steam per hour (TPE-360/T model) with dimensions of 14.48×14.24 m was performed. In the course of the work, the authors compared the calculation results using the proposed procedure and the normative method.

Initial data for the calculation: the boiler membrane walls were welded from a 60×6 mm pipe of steel 20 with flat spacers 80 mm wide, made of sheets of steel 20 with a thickness of 6 mm. The membrane wall was exposed to heating from a furnace with a cooling medium in pipes with the following parameters: 16.3 MPa, 349°C (Fig. 1). The calculation was carried out for buckling 3,000 Pa and emergency rarefaction 5,000 Pa.

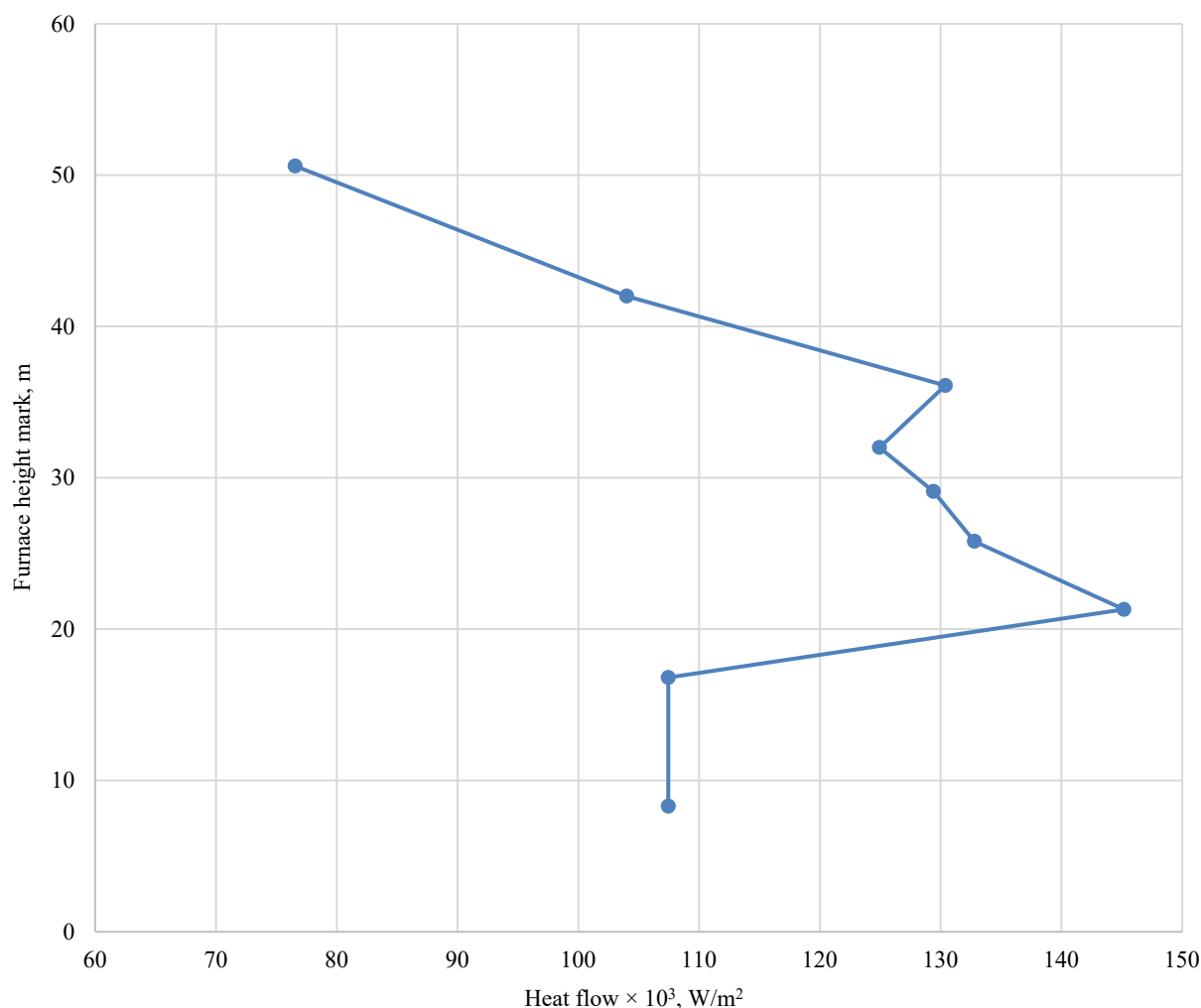


Fig. 1. Initial data for the calculation: heat flow perceived by the screen surface

The calculation was carried out in accordance with the requirements and formulas of normative documents (“Calculation standards for the strength of stationary boilers and steam and hot water pipelines”, “Calculation and design of fastening elements of the screen system of boiler units with all-welded panels”, “Technical Regulations of the Customs Union”).

The permissible step between the stiffener rings, according to the calculation results, is 4,012 mm at the furnace level and 4,050 mm in the upper part of the furnace at marks 16.8 and 50.6, respectively.

The calculation of the boiler box using the technique presented in this paper was performed in two stages. The model of the first stage included gastight screens of a furnace, a convective shaft, a gas reversing chamber, an aerodynamic nose, and a ceiling superheater, made in the form of shells with elasticity parameters calculated using numerical methods [9]. The stiffener rings, festoons No. 1 and No. 2 with suspensions, suspensions of boiler screens, wall superheater were modeled with beam-rod elements (Fig. 2). When comparing the results of the two calculations, it was reported that the problem areas of the structures, determined by the first stage of modeling, converged with the design points of the standard calculation: in the middle of the screen under the stiffener rings (point No. 1, Fig. 2 C), in the corner of the furnace between stiffener rings (point no. 2, Fig. 2 B). At the same time, the new technique based on a more advanced model of the boiler box made it possible to take into account the following technical solutions applied in the design of the boiler box and aimed at optimizing and strengthening it: design of corner bracing in the form of lever mechanisms that allow the force to be transmitted strictly along the axis of the adjacent screen; intermediate fasteners reinforced with combs-ribs, providing free thermal expansion of the screen; longitudinal ribs under the stiffener rings in places where the standard values of the steps between the stiffener rings are exceeded [15]; special designs of stiffener rings [16]; angle brackets; seal boxes]. In addition, the model made it possible to take into account the effect of a wall-mounted radiant superheater (attached to the screens through welding), festoons, stiffen boxes, and other structural elements.

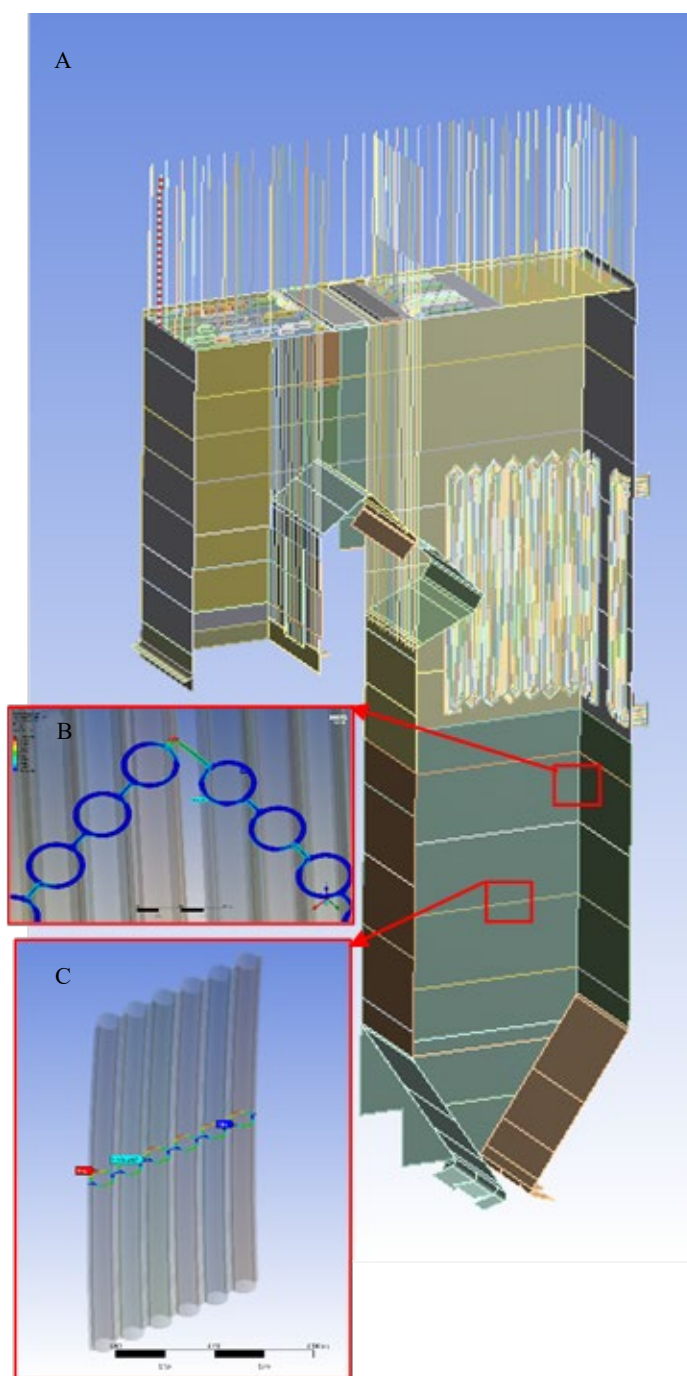


Fig. 2. Calculation of the boiler box of TPE-360/T model according to the developed technique:

A — shell-rod model (first stage of modeling); B — solid model of the box corner (second stage of modeling); C — solid model of the midpart of the screen under the stiffener (second stage of modeling)

The model includes structures of a ceiling superheater, an aerodynamic nose, a convective shaft, a gas reversing chamber, and other elements, whose technical condition is difficult to assess using the normative technique due to its limitations. The permissible step between the stiffener rings, according to the calculation, is 4,500 mm at the furnace level, and 6,000 mm at the top of the furnace, which is higher than the values obtained through the normative technique.

Thus, it can be concluded that the impact of design solutions aimed at optimizing and strengthening the boiler box (without increasing the number of stiffener rings) is significant. The results of the calculation according to the normative technique, which does not allow taking into account these decisions, are excessively conservative. The calculation results using the proposed method are more reliable, as they enable us to fully take these decisions into account.

A comparison of the calculation results obtained through different methods was carried out at two characteristic points of the structure specified in the normative technique: point 1, for which the influence of attached and reinforcing elements is minimal, at the calculated point 2, for which the influence of reinforcing elements is most significant (Table 1).

Table 1

Calculated stresses in screen sections according to the normative and new technique, MPa

Design section, mark, m	16.8		50.6	
Permissible stresses in the cross section of 1–2 screen, MPa	149.8		152.6	
Permissible stresses in the cross section of 5–6 screen, MPa	158.4		161.8	
Calculated combination of loads: weight, overpressure in pipes, buckling in the furnace space				
Setting-out point according to the requirements of the normative technique	1*	2**	1*	2**
Equivalent stresses in the cross section of 1–2 screen according to the requirements of the normative technique, MPa	119.3	121.7	141.4	145.9
Equivalent stresses in the cross section of 5–6 screen according to the requirements of the normative technique, MPa	10.4	97.0	21.9	175.9
Equivalent stresses in the cross section of 1–2 screen according to the requirements of the developed technique, MPa	135.6	109.2	149.0	114.4
Equivalent stresses in the cross section of 5–6 screen according to the requirements of the developed technique, MPa	18.1	55.4	27.4	92.8
Calculated combination of loads: weight, overpressure in pipes, emergency rarefaction in the furnace space				
Permissible stresses in the cross section of 1–2 screen, MPa	199.8		203.5	
Permissible stresses in the cross section of 5–6 screen, MPa	217.8		222.5	
Equivalent stresses in the cross section of 1–2 screen according to the normative technique, MPa	138.6	142.7	175.8	183.4
Equivalent stresses in the cross section of 5–6 screen according to the normative technique, MPa	15.6	160.5	31.1	289.3
Equivalent stresses in the cross section of 1–2 screen according to the developed technique, MPa	147.6	109.6	182.8	109.0
Equivalent stresses in the cross section of 5–6 screen according to the developed technique, MPa	19.1	87.8	30.9	125.8
* in the middle of the wall, between the stiffener rings				
** in the corner of the box				

At point 1, a good coincidence of the results was obtained — with respect to the permissible stresses, the voltage difference was no more than 11%. At point 2, the stress difference ranged from 33% for small and medium steps between the stiffener rings to 73% for large steps between the stiffener rings. High stress values in all cases were given by the normative technique.

The proposed method and model increase the reliability of simulating the behavior of the structure and the accuracy of the calculation. One of the results of the calculations and optimization of the design is the distribution of stiffener rings according to the height of the boiler furnace of TPE-360/T model. Table 2 shows the results of calculating the step of stiffener rings: 1 — according to the normative technique, without taking into account the design features; 2 — according to the calculation results using the developed techniques that provide more reliable simulation of the behavior of the structure, taking into account the influence of all its elements, including additional reinforcing elements in the form of stiffener rings, etc.

Table 2

Calculated and accepted steps between the stiffener rings

Design section ¹ , m	8.3	16.8	21.3	25.8	29.1	32	36.1	42	50.6
Maximum permissible step between stiffener rings ² , mm	4,012	4,012	3,961	3,974	3,979	3,971	3,962	4,000	4,050
The adopted step between the stiffener rings following the results of design optimization, mm	2,660	4,500	4,400	4,250	2,700	3,520	3,300	3,500	6,000
Fulfillment of the strength conditions for the accepted step (yes/no)	yes	yes	yes	yes	yes	yes	yes	yes	yes
1 — mark for the height of the furnace, where 0 — the floor level									
2 — as per calculation according to the normative technique									

It can be observed that the use of special calculation methods makes it possible to avoid the installation of additional stiffener rings for at least two characteristic places of the boiler furnace: at the place of installation of the burners (marks from 16.8 to 25.8 m) and at the place of the reversing flue (50.6 m mark). This avoids overspending of metal and complication of the structure due to the difficulties of simultaneous placement of burner devices and stiffener rings, and elements of the reversing flue.

An assessment of the metal consumption was carried out. In this case, the weight of one stiffener ring with fasteners is on average 3,500 kg. To meet the requirements of the regulatory calculation for the step between the stiffener rings, it is required to install at least three additional stiffener rings at the furnace height from 16.8 to 25.8 m and 50.6 m. The total metal consumption of such a constructive solution is 10,500 kg. Thus, the use of new special calculation techniques provides ample opportunities for optimization and reduction of metal consumption while maintaining sufficient strength of all-welded gastight boiler structures.

Discussion and Conclusion. A new technique for calculating and analyzing the technical condition and optimization of membrane wall structures of boiler units has been developed on the basis of modern, most effective methods of mathematical modeling of membrane walls with equivalent orthotropic plates, calculation of their geometric and physico-mechanical parameters, special loads and impacts inherent in all-welded gastight structures. The use of new special calculation techniques provides ample opportunities for optimization and reduction of metal consumption while maintaining sufficient strength of all-welded gastight boiler structures.

The results of verification of the replacement of membrane walls with orthotropic plates were compared to the results of field experiments on determining the angles of rotation of the vertices of the ribs under the action of a unit moment. They showed that the displacement error did not exceed 14% for shell models implemented through the proposed technique. At the same time, solid-state models give an error of up to 10%, i.e., slightly less when the number of finite elements of the models is an order of magnitude larger (and the dimension of the model is up to 100 times higher, depending on the type of element — linear or quadratic). This modeling error fully meets the requirements of modern design, since the errors associated with manufacturing tolerances are in the range of 10–15% of the wall thicknesses of pipes, sheets, and the weld leg [9].

The significant disadvantages of the normative technique are the scant possibilities for optimizing the design and strength requirements in other ways, except for increasing the number of stiffener rings, which significantly increases the metal consumption and causes growth of cost. This means that simplified models adopted in the normative calculation at the time when computer engineering was insufficiently developed, limit the possibilities of optimizing structures in modern design. This necessitates using special calculation techniques based on numerical computer modeling.

The technique proposed by the authors during the actual design of boiler units has shown its high accuracy and efficiency, wide possibilities for optimizing the design, reducing metal consumption under maintaining sufficient strength, the ability to significantly reduce the complexity of model formation and machine calculation time. In addition, the reliability of behavioral modeling and calculation accuracy of all-welded gastight structures have been increased through the use of modern numerical simulation techniques. They provide most accurate accounting of the features of structures and their cross impact, and the effect of all influencing factors, as well as calculating screens of complex shape. Through the developed techniques, the calculation error has been reduced by more than 30% for the recommended steps between the stiffener rings. For specially reinforced membrane walls with steps exceeding the permissible values, the error reduction reaches 70% or higher.

The application of the proposed technique makes it possible to decrease the number of finite elements of models of structures with screens by several orders of magnitude compared to similar solid-state models of the screen, reduce the complexity of forming models of structures with screens. The time of computational operations in calculating the stress-strain state of all-welded gastight structures is significantly improved. And finally, the complexity of modeling and calculation is significantly reduced while maintaining sufficient accuracy [13].

The authors note that the technique they developed for calculating the strength of all-welded gastight structures is generally intended for the use in the design and optimization of thin-walled structures with periodically changing cross-section and internal channels in the walls, which can be simultaneously exposed to external forces, moments. In this particular case, these are thin-walled structures made of tubular membrane walls of steam and hot water boilers, i.e., all-welded gastight structures with all structural elements attached to them, e.g., elements of the support and suspension system, fasteners, burners, blast nozzles, etc.

This technique is implemented on medium-powered personal computers and can be put into practice of real design of boiler-building enterprises and design organizations of other branches of mechanical engineering, which use plates and/or shells with regularly changing cross-sections.

The proposed technique has been used in the real design of boiler units since 2014, including power boilers Pp-1030-25.0-570/570GM, E-220-9.8-540GM, E-500-13.8-560G (model TGE-440), PP-1900-25.8-568/568 KT, E-540-13.8-560GN (model TGE-225, E-540-13.8-560GN (model TGE-224/S7), E-810-13.8-560BT (model TPE-360/T).

References

1. Kurepin MP, Serbinovskiy MYu, Kolesnikov AA, Dotsenko VE. Using 3D Modeling in an Automated System for Diagnosing the Technical Condition, Assessing the Strength and Resource of Components of Boilers and Power Plants. In: *Proc. II Int. Sci.-Tech. Conf. "Diagnostics and Forecasting of the Technical Condition of Power Plant Equipment"*. Moscow: "VTI" OJSC; 2021. P. 48–54. (In Russ.).
2. Kurepin MP, Serbinovskiy MYu. Efficient Methods of Finite-Element Analysis of Energetic Machinery Complex Structures. *Modern High Technologies*. 2017;(10):19–25. URL: <https://top-technologies.ru/ru/article/view?id=36822> (accessed: 15.12.2023). (In Russ.).
3. Gaćeša B, Milošević-Mitić V, Maneski T, Kozak D, Sertić J. Numerical and Experimental Strength Analysis of Fire-Tube Boiler Construction. *Tehnicki vjesnik — Technical Gazette*. 2011;18(2):237–242. URL: https://www.researchgate.net/publication/265201672_Numerical_and_experimental_strength_analysis_of_fire-tube_boiler_construction (accessed: 15.12.2023).
4. Nagiar HM, Maneski T, Milošević-Mitić V, Gaćeša B, Andelić N. Modeling of the Buckstay System of Membrane-Walls in Watertube Boiler Construction. *Thermal Science*. 2014;18(1):59–72. <http://doi.org/10.2298/TSCI120204174N>
5. Konjatić P, Dautović S, Ostojić Z, Sertić J. Seismic Action Influence on the Pressure Parts of the Watertube Steam Boiler Construction. *Machines. Technologies. Materials*. 2019;13(5):210–213. URL: <https://stumejournals.com/journals/mtm/2019/5/210.full.pdf> (accessed: 15.12.2023).
6. Sertić J, Kozak D, Samardžić I. Calculation of Reaction Forces in the Boiler Supports Using the Method of Equivalent Stiffness of Membrane Wall. *The Scientific World Journal*. 2014;2014(3):392048. <http://doi.org/10.1155/2014/392048>
7. Sertić J, Kozak D, Damjanovic D, Konjatic P. Homogenization of Steam Boiler Membrane Wall. In: *Proc. 7th Int. Congress of Croatian Society of Mechanics*. Zagreb: Hrvatsko Društvo za Mehaniku; 2012. P. 207–208.
8. Sertić J, Gelo I, Kozak D, Damjanović D, Konjatić P. Theoretical Determination of Elasticity Constants for Steam Boiler Membrane Wall as the Structurally Orthotropic Plate. *Tehnicki vjesnik — Technical Gazette*. 2013;20(4):697–703.
9. Kurepin MP, Serbinovskiy MYu. Simulation and Optimization of Water-Wall Tube Panels Design for Power Boilers. *MATEC Web Conferences*. 2019;298:0011210. <http://doi.org/10.1051/mateconf/201929800112>
10. Kurepin MP, Serbinovskiy MYu. Boiler Dry-Bottom Ash Hopper Load Calculation Methods. *Modern High Technologies*. 2016;(7):32–39. URL: <https://toptechnologies.ru/ru/article/view?id=36059&ysclid=liolq7zv6e178655419> (accessed: 15.12.2023). (In Russ.).
11. Kurepin MP, Serbinovskiy MYu. Simulation of One-Sided Heating of Boiler Unit Membrane-Type Water Walls. *Thermal Engineering*. 2017;(3):60–68. <https://doi.org/10.1134/S0040363617030055> (In Russ.).
12. Basov KA. *ANSYS: User Reference*. Moscow: DMK Press; 2014. 640 p. (In Russ.).
13. Kurepin MP, Serbinovskij MYu, Ivanenko VV. *Analysis and Optimisation of Designs and Boilers with Tube-in-Sheet Shields*. RF Patent No. 2 568 783 C1. 2015. URL: https://patents.s3.yandex.net/RU2568783C1_20151120.pdf (accessed: 15.12.2023). (In Russ.).
14. Serbinovskij MYu, Kurepin MP. *Convective Shaft of Boiler with Node for Sealing of Passage of Vertical Pipes*. RF Patent No. 2 702 3142019 C1. 2019. URL: https://patents.s3.yandex.net/RU2702314C1_20191007.pdf (accessed: 15.12.2023). (In Russ.).
15. Serbinovskij MYu, Kurepin MP. *Membrane Screen of Steam Boiler*. RF Patent No. 2 668 048 C1. 2018. URL: https://patents.s3.yandex.net/RU2668048C1_20180925.pdf (accessed: 15.12.2023). (In Russ.).
16. Kumar PR, Thiruselvan MG, Babu JM, Rajagopal M. Weight Optimization of Buck Stays using Castellated Beams. *International Journal of Engineering and Advanced Technology (IJEAT)*. 2014;3(5):200–203.

About the Authors:

Maxim P. Kurepin, lead technician designer, Research and Design Institute of Nitrogen Industry and Products of Organic Synthesis (OJSC GIAP) (50A/8, bld. 4, Zemlyanoy Val St., Moscow, 109028, RF), [ORCID](https://orcid.org/0000-0001-9151-1120), mkurepin@gmail.com

Mikhail Yu. Serbinovskiy, Dr.Sci. (Eng.), Professor of the Fundamentals of Machine Design Department, Rostov State Transport University (2, Rostovskogo Strelkovogo Polka Narodnogo Opolcheniya Sq., Rostov-on-Don, 344038, RF), SPIN-code: [9003-8798](https://orcid.org/0003-8798), [ORCID](https://orcid.org/0003-8798), serb-m@mail.ru

Claimed contributorship:

MP Kurepin: research objective and task formulation, development of calculation methods, modeling and calculations, initial version of the main text, formulation of conclusions.

MYu Serbinovskiy: development of calculation methods and new design solutions based on the results obtained, analysis of the research results.

Conflict of interest statement: the authors do not have any conflict of interest.

All authors have read and approved the final manuscript.

Received 10.01.2024

Revised 06.02.2024

Accepted 12.02.2024

Об авторах:

Максим Павлович Курепин, ведущий специалист, расчетчик научно-исследовательского и проектного института азотной промышленности и продуктов органического синтеза ОАО «ГИАП» (109028, РФ, г. Москва, ул. Земляной вал, д. 50а/8, стр. 4), [ORCID](#), mkurepin@gmail.com

Михаил Юрьевич Сербиновский, доктор технических наук, профессор кафедры основ проектирования машин Ростовского государственного университета путей сообщения (344038, РФ, г. Ростов-на-Дону, пл. Ростовского Стрелкового Полка Народного Ополчения, 2), SPIN-код: [9003-8798](#), [ORCID](#), serb-m@mail.ru

Заявленный вклад авторов:

М.П. Курепин — формирование цели и задачи исследования, разработка расчётных методик, проведение моделирования и расчётов, начальная версия основного текста, формулирование выводов.

М.Ю. Сербиновский — разработка расчётных методик и новых конструктивных решений на основе полученных результатов, анализ результатов исследований.

Конфликт интересов: авторы заявляют об отсутствии конфликта интересов.

Все авторы прочитали и одобрили окончательный вариант рукописи.

Поступила в редакцию 10.01.2024

Поступила после рецензирования 06.02.2024

Принята к публикации 12.02.2024

MACHINE BUILDING AND MACHINE SCIENCE МАШИНОСТРОЕНИЕ И МАШИНОВЕДЕНИЕ



UDC 669.1:66.04

Research article

<https://doi.org/10.23947/2687-1653-2024-24-1-58-65>

Stress Martensite Nucleation in a State of Premartensitic Lattice Instability

Yuri V. Dolgachev^{ID}, Viktor N. Pustovoi^{ID}, Yuri M. Vernigorov^{ID}

Don State Technical University, Rostov-on-Don, Russian Federation

✉ yuridol@mail.ru

EDN: KQSXLQ

Abstract

Introduction. The combined effect on the phase transformation process, involving a combination of heat treatment and external action, is a major technology solution for obtaining the required properties of steel products. When hardening steel in a constant magnetic field with a strength of 1–2 MA/m, martensite formation is observed at higher temperatures. In addition, when compared to conventional hardening, there are changes in structure and properties. Such effects cannot be explained only in terms of thermodynamics, since the expected shift in the equilibrium temperature between austenite and martensite in a magnetic field of such strength does not exceed 4–8°C. To explain the effects that occur during hardening in a magnetic field, it is proposed to consider the features of martensitic transformation in highspeed steel when exposed to an external magnetic field in the temperature range of austenite superplasticity. This research was aimed at identifying the features of martensitic transformation in the presence of a constant magnetic field in steel with account for the phenomena occurring in the premartensitic state.

Materials and Methods. Samples made of steel R6M5 were used. Characteristics of the martensitic transformation were studied using the potentiometric method of electrical resistance. The data were recorded using an L-CARD E14-440 analog-to-digital converter with the LGraph2 software package. The sample was heated by passing current. The sample was placed in the interpolar space of an open-type laboratory electromagnet FL-1, which provided the creation of a magnetic field with a strength of 1.2 MA/m.

Results. The obtained differentiated dependences were characterized by electrical resistance anomalies (low-temperature peaks) at a temperature corresponding to the appearance of a ferromagnetic phase as a result of martensitic transformation. In a magnetic field, the development of martensitic transformation began at a higher temperature, which could not be explained in terms of thermodynamics. Thus, the formation of stress martensite was observed in microvolumes of austenite with ferromagnetic ordering, which perceived the energy of the external field through magnetostrictive stresses. Under conditions of superplastic austenite, such stresses were sufficient to initiate shear transformation. The minimum possible size of lattice instability fluctuations (1.372 nm) was determined.

Discussion and Conclusion. Exposure to a magnetic field under hardening intensified the processes of some magnetic decomposition of austenite. At temperatures close to the beginning of the martensitic transformation, the existing areas of magnetic inhomogeneity were superimposed on the effects of the phenomenon of instability of the crystal lattice. In the temperature range M_d – M_s , when austenite exhibited superplasticity, the formation of stress martensite in microvolumes of austenite with ferromagnetic ordering was significantly facilitated.

Keywords: stress martensite, magnetic field, superplasticity, lattice instability, steel, hardening

Acknowledgements. The authors appreciate the reviewers, whose critical assessment of the submitted materials and suggestions helped to significantly improve the quality of this article.

For citation. Dolgachev YuV, Pustovoi VN, Vernigorov YuM. Stress Martensite Nucleation in a State of Premartensitic Lattice Instability. *Advanced Engineering Research (Rostov-on-Don)*. 2024;24(1):58–65. <https://doi.org/10.23947/2687-1653-2024-24-1-58-65>

Зарождение мартенсита напряжения в состоянии предмартенситной неустойчивости решетки

Ю.В. Долгачев  , В.Н. Пустовойт , Ю.М. Вернигорov 

Донской государственный технический университет, г. Ростов-на-Дону, Российская Федерация

 yuridol@mail.ru

Аннотация

Введение. Комбинированное влияние на процесс фазового превращения, предполагающее сочетание термической обработки с внешним воздействием, является актуальным технологическим решением для получения необходимых свойств стальной продукции. При закалке стали в постоянном магнитном поле напряженностью 1–2 МА/м наблюдается образование мартенсита при более высоких температурах. Помимо этого, по сравнению с обычной закалкой, происходят изменения в структуре и свойствах. Подобные эффекты не могут объясняться только с термодинамических позиций, так как предполагаемый сдвиг температуры равновесия между аустенитом и мартенситом в магнитном поле такой напряженности не превышает 4–8 °С. Для объяснения эффектов, возникающих при закалке в магнитном поле, предлагается рассмотреть особенности мартенситного превращения в быстрорежущей стали при воздействии внешним магнитным полем в температурном интервале сверхпластичности аустенита. Целью данной работы стало выявление особенностей мартенситного превращения в присутствии постоянного магнитного поля в стали с учетом явлений, возникающих в предмартенситном состоянии.

Материалы и методы. Использовались образцы стали марки Р6М5. Исследование особенностей мартенситного превращения осуществляли потенциометрическим методом электросопротивления. Данные фиксировались с помощью аналого-цифрового преобразователя L-CARD E14-440 с использованием программного комплекса LGraph2. Нагрев образца проводился проходящим током. Образец размещался в межполюсном пространстве лабораторного электромагнита открытого типа ФЛ-1, который обеспечивал создание магнитного поля напряженностью 1,2 МА/м.

Результаты исследования. На полученных дифференцированных зависимостях присутствовали аномалии электросопротивления (низкотемпературные пики) при температуре, соответствующей появлению ферромагнитной фазы в результате мартенситного превращения. В магнитном поле развитие мартенситного превращения начинается при более высокой температуре, что не может найти объяснения с термодинамических позиций. Таким образом, наблюдали образование мартенсита напряжения в микрообъемах аустенита с ферромагнитным упорядочением, которые воспринимают энергию внешнего поля через магнитострикционные напряжения. В условиях сверхпластичного аустенита такие напряжения оказываются достаточными для инициирования сдвигового превращения. Определен минимально возможный размер флуктуаций неустойчивости решетки (1,372 нм).

Обсуждение и заключение. Воздействие магнитным полем при закалке приводит к усилению процессов своеобразного магнитного расслоения аустенита. При температурах, близких к началу мартенситного превращения, имеющиеся области магнитной неоднородности накладываются на эффекты от явления неустойчивости кристаллической решетки перед мартенситным превращением. В температурном интервале M_o – M_n , когда аустенит проявляет сверхпластичность, существенно облегчается образование мартенсита напряжения в микрообъемах аустенита с ферромагнитным упорядочением.

Ключевые слова: мартенсит напряжения, магнитное поле, сверхпластичность, неустойчивость решетки, сталь, закалка

Благодарности. Авторы выражают благодарность рецензентам, чья критическая оценка представленных материалов и высказанные предложения по их совершенствованию, способствовали значительному повышению качества настоящей статьи.

Для цитирования: Долгачев Ю.В., Пустовойт В.Н., Вернигорov Ю.М. Зарождение мартенсита напряжения в состоянии предмартенситной неустойчивости решетки. *Advanced Engineering Research (Rostov-on-Don)*. 2024;24(1):58–65. <https://doi.org/10.23947/2687-1653-2024-24-1-58-65>

Introduction. Before starting the martensitic transformation, instability of the crystal lattice is detected in metals and alloys [1] expressed in a specific premartensitic state of the initial lattice [2]. The thermodynamic analysis of the state of the initial phase before point M_s [3] shows the possibility of the emergence of separate micro regions having their own short-range ordering in the arrangement of atoms. Such micro regions retain their atomic order only near the fluctuation nucleus. At a distance from it, there are no obvious boundaries between phases, the order gradually degrades. The experimentally described micro regions manifest themselves in the form of diffusion scattering effects during X-ray

diffraction. The presence of regions with a near atomic order explains the decrease in elastic constants near point M_s and the convergence of structures [4] involved in the phase transformation.

In the case where an applied external stress is present, the martensitic transformation can be initiated by deformation at a temperature above point M_s . The maximum temperature at which the deformation of the initial phase causes the formation of martensite is indicated by point M_d . It has been found [5] that a maximum of plasticity is observed in the temperature range $M_d - M_s$, which is due to the manifestation of superplasticity associated with the hardening transition. The imposition of a constant magnetic field under these conditions causes the appearance of forced magnetostriction and corresponding stresses in the austenite nanodomains having a ferromagnetic order [6], which induces the appearance of crystals of the hardening phase called stress martensite (by analogy with deformation martensite) [7]. The imposition of a constant magnetic field changes the initial magnetic state of austenite [8], increasing the number and size of ferromagnetically ordered clusters, which are possible sites of nucleation of the ferromagnetic α -phase [6]. Thus, in the temperature range $M_d - M_s$, the integration of magnetic and a number of special structural states occurs, which is undoubtedly of interest to investigate.

This research was aimed at studying the features of martensitic transformation in the presence of a constant magnetic field in steel taking into account the phenomena occurring in the premartensitic state.

Materials and Methods. In the course of the research, samples of steel P6M5 were used, for which there was information about the development of superplasticity [5] associated with phase transformation [9]. The chemical composition was monitored using a Q8Magellan optical emission spectrometer (Bruker). The average composition of samples from one melt is shown in Table 1.

Table 1

Average content of elements in samples, %

<i>C</i>	<i>Si</i>	<i>Mn</i>	<i>S</i>	<i>P</i>	<i>Cr</i>	<i>Mo</i>	<i>V</i>	<i>W</i>
0.844	0.421	0.420	0.019	0.023	3.946	4.918	2.018	5.922

To analyze the course of hardening transformation without a field and with the imposition of a magnetic field, the potentiometric method of resistometry was used [10], since changes in the alloy structure were reflected in the measured values ρ with a fairly high sensitivity. And although it is difficult to quantify the relationships between the transforming phases, the establishment of the start and finish points of the transition can be done quite accurately. The applied method is highly sensitive to the appearance of a ferromagnetic phase (during phase transformations of the 1st or 2nd kind), which is shown in abnormal behavior on curve ρ due to electronic interactions at “*s*” and “*d*” sublevels [11] determining the presence of spontaneous magnetization [12].

An S-type thermocouple (PTC) was used as a temperature sensor. The thermocouple was spot-welded in the central part of the sample to a single point to eliminate the occurrence of side stresses under separate welding due to the passage of current through the sample during measurement. The data was recorded using an analog-to-digital converter L–CARD E14–440 and the LGraph2 software package. The sample was heated by passing current from the RNO-250–5 autotransformer.

The sample was placed in an interpolar space (Fig. 1). An open-type electromagnet (FL-1) provided the generation of a magnetic field with a strength of 1.2 MA/m. When conducting the experiment without a field, the power supply of the electromagnet was turned off, and the poles were bridged with an ARMCO-iron plate.

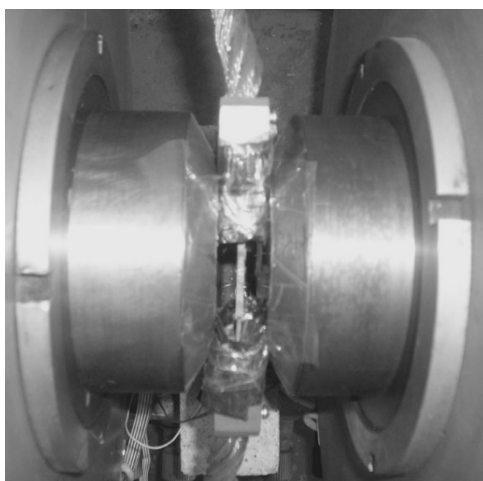


Fig. 1. Sample with connected copper contacts in the interpolar space of the magnet

The experimental data ($\rho(\tau)$ and $T(\tau)$ in Fig. 2), recorded with a sampling rate of 400 kHz, were numerically differentiated and approximated to obtain function $d\rho/dT(T)$, which reflected the characteristic anomalies when a ferromagnetic phase appeared.

Research Results. Primary dependences $\rho(\tau)$ and $T(\tau)$ shown in Figure 2 already demonstrate the shift of anomalies, corresponding to the phase transformation, to the high-temperature region when a constant magnetic field is applied.

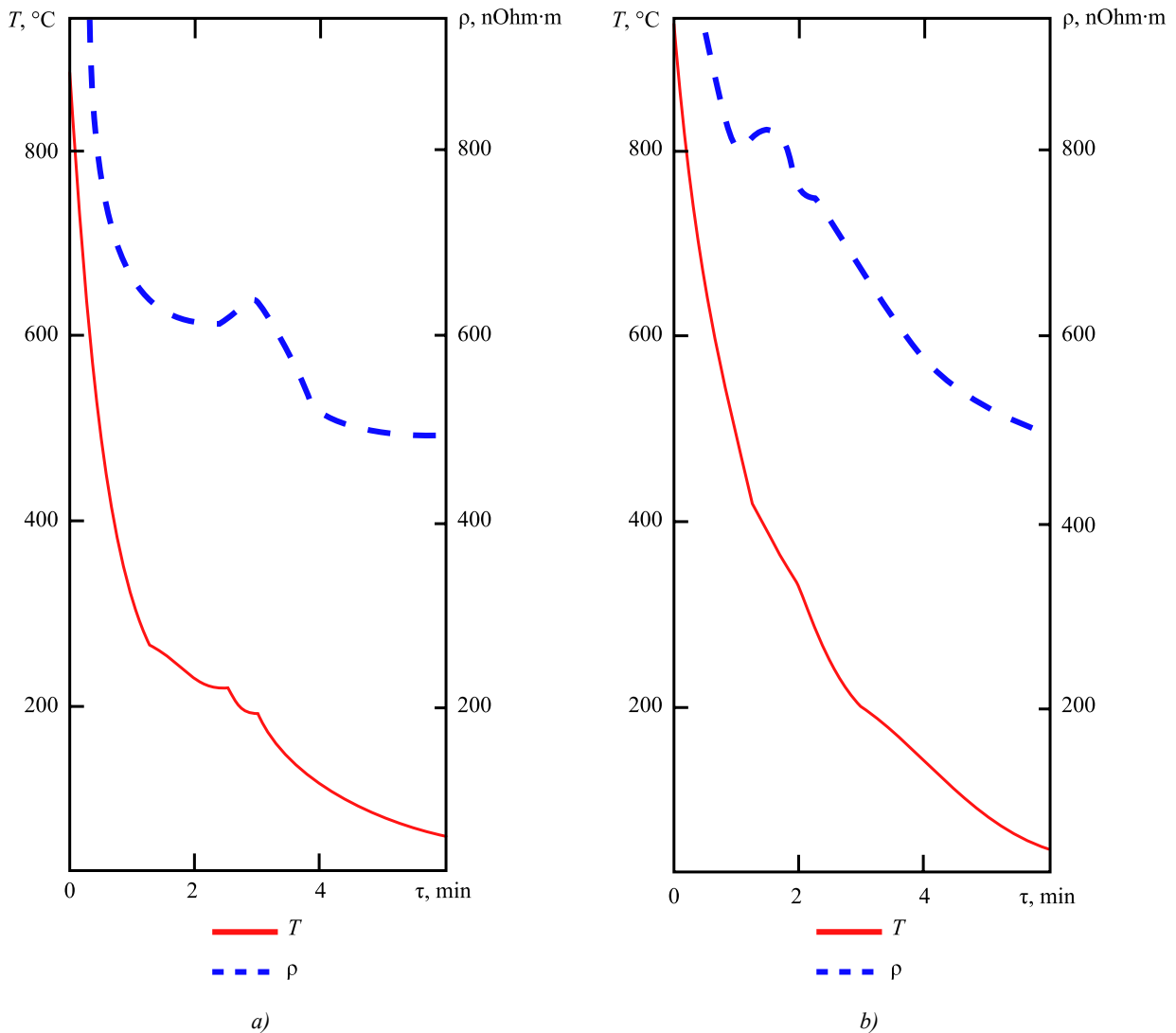


Fig. 2. Dependences $\rho(\tau)$ and $T(\tau)$ for steel P6M5 under cooling:
a — without field; b — in magnetic field of 1.2 MA/m

According to the reference data [13], for samples of steel P6M5 corresponding to the chemical composition indicated in Table 1, temperature of 140°C corresponds to the initiation of the martensitic transformation. This is confirmed by the data obtained as a result of differentiation in Figure 3, which illustrate the characteristic features of the analyzed transformation.

The formation of a ferromagnetic phase corresponds to the appearance of a peak at low temperatures (Fig. 3), which makes it possible to record the start of the martensitic reaction. In the case of treatment with the imposition of a magnetic field, the start of the formation of the martensitic phase is noted at a temperature of 185°C, which cannot be explained solely from the point of view of changes in the thermodynamic potentials of the phases. For a magnetic field with a strength of 1.2 MA/m, the effect of the equilibrium temperature shift is $\sim 4.5^\circ\text{C}$ [14]. It can be argued that the imposition of a magnetic field in the temperature range of superplasticity causes the formation of stress martensite higher than the starting point of transformation known for this steel as a result of forced magnetostriction in nanodomains with a near magnetic order in austenite. In this case, the stresses arising in the austenitic matrix are about 10 MPa [15], which, under conditions of the crystal lattice instability, contributes to the initiation of a phase reaction.

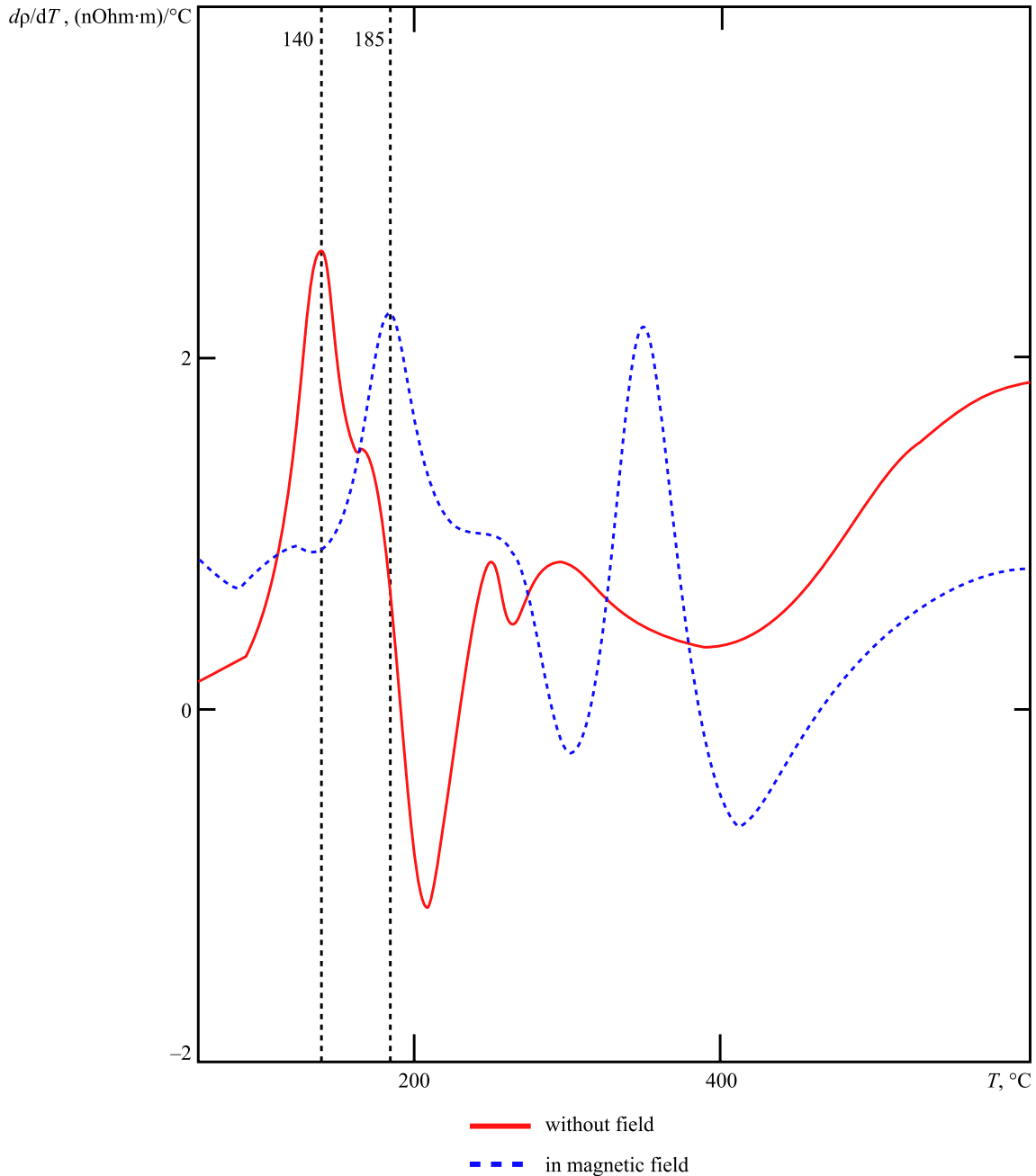


Fig. 3. Results of differentiation of experimental data obtained under cooling of steel P6M5:
1 — without a field; 2 — in a magnetic field with a strength of 1.2 MA/m

The phenomenon associated with the occurrence of instability of the crystal lattice of the initial phase, as it approaches the transition point, is reflected in the differentiated dependences in the form of a peak in the high-temperature area of the curve. The appearance of this peak under cooling indicates the approach of the superplastic state of austenite. The effect of an external magnetic field enhances the magnetic decomposition of austenite [8], contributing to an increase in the number and size of ferromagnetic nanoclusters [15], which causes a shift of this peak to higher temperatures. Anisotropic fields arise in local regions with unidirectional spins. They introduce elastic distortions due to the fact that the magnetization energy differs in different directions — this reduces the stability of γ -phase lattice. The average diameter of a ferromagnetic nanocluster determined in [8] is about 1.7 nm for a given field strength, which is comparable to the wavelengths of electrons. It can deflect them and, accordingly, cause distortions in the curves. The results obtained indicate the presence of heterogeneity in the magnetic state of austenite, and that this heterogeneity increases when an external magnetic field is applied.

The transformation under hardening is characterized by a diffusionless shear mechanism of atomic restructuring; therefore, external action increases the driving force of the transition. In a state where the lattice of the initial phase becomes unstable before point M_s , spontaneous atomic displacements occur in local regions (preparing the lattice for $\gamma \rightarrow \alpha$ transition), where magnetostrictive stresses can act as a trigger for the start of the transformation.

The conditions describing the possibility of fluctuations of atomic displacements in the premartensitic state were considered in [16]. The type of function, whose minimum corresponded to the transition state, was derived on the basis of diffuse scattering patterns and existing options for restructuring the crystal lattice. Oscillation frequencies and anharmonicity parameters were expressed in terms of elastic modulus, whose values determined the adjustment option.

The analysis suggests that micro regions of atomic displacements are shaped like plates of densely packed planes that can experience shear. The expression for estimating the minimum possible fluctuation size H can be derived using matrix elasticity coefficients:

$$H \cong 6d \sqrt{\frac{c_{11} + c_{44} - 2c'}{2c' + c_{44}}}, \quad (1)$$

where d — interplanar spacing; $c' = 1/2(c_{11} - c_{12})$ — elastic constant; c_{11} , c_{12} , c_{44} — elastic coefficients.

Values for calculation according to formula (1) were selected for the temperature of martensitic transformation in steel P6M5. Lattice constant a was estimated taking into account the instructions in [17]. The interplanar spacing was determined for the case of a FCC lattice, when the first reflecting planes were a family of planes $\{111\}$, having the maximum interplanar spacing $d = \frac{a}{\sqrt{3}} = 2.1 \text{ \AA}$. Based on the data on the elastic characteristics of steel P6M5 [9], the

elasticity coefficients and constant were determined through known ratios [18]. The calculation results based on dependence (1) allow us to estimate the minimum diameter of the region where instability $H \cong 1.372 \text{ nm}$ may occur, which is commensurate with the average diameter of a ferromagnetic cluster in austenite.

Discussion and Conclusion. The following script for the development of martensitic transformation can be assumed. Above point M_s in γ -phase, there are regions with ferromagnetic ordering [15]. If waves of atomic displacements are superimposed in or near these places, then, in the presence of an external magnetic field, under such conditions, forced magnetostriction is able to affect the fields of elastic forces in the crystal lattice and lower the energy barrier for the formation of a critical martensite nucleus.

The experimental results indicate the existence of magnetic heterogeneity in the state of γ -phase, whose degree affects the running of the martensitic transformation. The imposition of a constant magnetic field under quench cooling enhances the existing magnetic inhomogeneity in austenite. Near point M_s , the phenomenon of lattice instability in combination with magnetostrictive effects from the field initiates the appearance of stress martensite crystals. Thus, the effect of intensification of martensitic transformation under hardening in a magnetic field with a strength of 1–2 MA/m can be explained, which is of great importance for the practice of heat treatment of steel.

The research results showed the following. Exposure to a magnetic field under quench cooling made it possible to achieve greater completeness of the martensitic reaction, reducing the amount of residual austenite, whereas the early formation of stress martensite provided its longer presence in the area of elevated temperatures, which contributed to the flow of tempering processes directly under hardening.

References

1. Yongmei M Jin, Yu U Wang, Yang Ren. Theory and Experimental Evidence of Phonon Domains and Their Roles in Pre-Martensitic Phenomena. *npj Computational Materials*. 2015;1(1):15002. URL: <https://www.nature.com/articles/npjcompumats20152> (accessed: 20.11.2023).
2. Muslov SA, Khachin VN, Pushin VG, Chumlyakov YuI. Elastic Properties and Structure of Alloys TiNi-TiFe prior Martensitic Transformations. *Letters on Materials*. 2015;5(4):420–423. URL: <https://lettersonmaterials.com/Upload/Journals/794/420-4231.pdf> (accessed: 20.11.2023).
3. Kondratyev VV, Pushin VG, Romanova RR, Tyapkin YuD. Elastic Properties and Stability of FCC Lattices near the Martensitic Transformation Temperature. *The Physics of Metals and Metallography*. 1977;44(3):468–479. (In Russ.).
4. Estrin EI. Lattice Stability and Martensitic Transformations. In: *Proc. Int. Conf. "Martensitic Transformations"*. Kiev: Naukova dumka; 1978. P. 29–33. (In Russ.).
5. Gulyaev AP. *Superplasticity of Steel*. Moscow: Metallurgiya; 1982. 56 p. (In Russ.).
6. Pustovoi VN, Dolgachev YuV. Ferromagnetically Ordered Clusters in Austenite as the Areas of Martensite Formation. *Emerging Materials Research*. 2017;6(2):249–253. <https://doi.org/10.1680/jemmr.17.00042>
7. Frolova AV, Tsarenko YuV, Rubanik VV Jr., Rubanik VV, Stolyarov VV. Tensile Strain of Alloys with the Martensitic Transformation under the External Impact. *Bulletin of the Russian Academy of Sciences: Physics*. 2019;83(10):1289–1293. <https://doi.org/10.1134/S0367676519100107>
8. Dolgachev YuV, Pustovoi VN. The Model of Austenite Structure State Taking into Account Fluctuations of Magnetic Nature. *CIS Iron and Steel Review*. 2022;24(2):74–78. URL: https://rudmet.net/media/articles/Article_CIS_2022_24_pp.74-78.pdf (accessed: 20.11.2023).

9. Gvozdev AE. *Production of Blanks of High-Speed Tools under Conditions of Superplasticity*. Moscow: Mashinostroenie; 1992. 176 p. (In Russ.).
10. Cherepin VT. *Experimental Technique in Physical Metallurgy*. Kiev: Tekhnika; 1968. 279 p. URL: <https://search.rsl.ru/ru/record/01006388994?ysclid=lozixgfkxj355220445> (accessed: 20.11.2023) (In Russ.).
11. Vonsovskiy SV. *Magnetism: Magnetic Properties of Dia-, Para-, Ferro-, Antiferro-, and Ferrimagnets*. Moscow: Nauka; 1971. 1032 p. URL: <https://search.rsl.ru/ru/record/01007305776?ysclid=lozipmaxya147070803> (accessed: 20.11.2023) (In Russ.).
12. Livshits BG, Kraposhin VS, Linetskii YaL. *Physical Properties of Metals and Alloys*. Moscow: Metallurgiya; 1980. 320 p. (In Russ.).
13. Popova LE, Popov AA. *Diagrams of the Transformation of Austenite in Steels and beta Solution in Titanium Alloys*. 3rd ed., reprint. and add. Moscow: Metallurgiya; 1991. 411 p. (In Russ.).
14. Krivoglaz MA, Sadovskiy VD, Smirnov LV, Fokina EA. *Hardening of Steel in a Magnetic Field*. Monograph. Moscow: Nauka; 1977. 120 p. URL: <https://www.imp.uran.ru/?q=ru/content/zakalka-stali-v-magnitnom-pole> (accessed: 20.11.2023) (In Russ.).
15. Pustovoit VN, Dolgachev YuV. *Magnetic Heterogeneity of Austenite and Transformations in Steels*. Monograph. OV Kudryakova (ed). Moscow: IPR Media; 2022. 190 p. <https://doi.org/10.23682/117033> (In Russ.).
16. Kondratyev VV, Tyapkin YuD. Elastic Properties and Quasi-Static Displacements of Atoms near the Point of Martensitic Transformation. In: *Proc. Int. Conf. "Martensitic Transformations"*. Kiev: Naukova dumka; 1978. P. 43–46. URL: <https://search.rsl.ru/ru/record/01007789971?ysclid=loziaf1a8v964754252> (accessed: 20.11.2023) (In Russ.).
17. Seki I, Nagata K. Lattice Constant of Iron and Austenite Including Its Supersaturation Phase of Carbon. *ISIJ International*. 2005;45(12):1789–1794. <https://doi.org/10.2355/isijinternational.45.1789>
18. Elmanov GN, Zaluzhnyi AG, Skrytnyi VI, Smirnov EA, Perlovich YuA, Yal'tsev VN. *Physical Materials Science: Vol. 1. Solid State Physics*. 3rd ed., reprint. Moscow: National Research Nuclear University MEPhI; 2021. 764 p. (In Russ.).

About the Authors:

Yuri V. Dolgachev, Cand.Sci. (Eng.), Associate Professor of the Materials Science and Technology of Metals Department, Don State Technical University (1, Gagarin sq., Rostov-on-Don, 344003, RF), SPIN-code: [2774-5346](#), [ORCID](#), [ScopusID](#), [ResearcherID](#), yuridol@mail.ru

Viktor N. Pustovoit, Dr.Sci. (Eng.), Professor of the Materials Science and Technology of Metals Department, Don State Technical University (1, Gagarin sq., Rostov-on-Don, 344003, RF), SPIN-code: [7222-6100](#), [ORCID](#), [ScopusID](#), [Researcher ID](#), pustovoyt45@gmail.com

Yuri M. Vernigorov, Dr.Sci. (Eng.), Professor of the Physics Department, Don State Technical University (1, Gagarin sq., Rostov-on-Don, 344003, RF), [ORCID](#), [ScopusID](#), jvernigorov@donstu.ru

Claimed contributorship:

YuV Dolgachev: preparation of samples for research, obtaining experimental data, calculations, text preparation, formulation of conclusions.

VN Pustovoit: basic concept formulation, research objectives and tasks, academic advising, revision of the text, correction of the conclusions.

YuM Vernigorov: analysis of the research results, the text revision.

Conflict of interest statement: the authors do not have any conflict of interest.

All authors have read and approved the final manuscript.

Received 23.12.2023

Revised 19.01.2024

Accepted 24.01.2024

Об авторах:

Юрий Вячеславович Долгачев, кандидат технических наук, доцент кафедры материаловедения и технологии металлов Донского государственного технического университета (344003, РФ, г. Ростов-на-Дону, пл. Гагарина, 1), SPIN-код: [2774-5346](#), [ORCID](#), [ScopusID](#), [ResearcherID](#), yuridol@mail.ru

Виктор Николаевич Пустовойт, доктор технических наук, профессор кафедры материаловедения и технологии металлов Донского государственного технического университета (344003, РФ, г. Ростов-на-Дону, пл. Гагарина, 1), SPIN-код: [7222-6100](#), [ORCID](#), [ScopusID](#), [Researcher ID](#), pustovoyt45@gmail.com

Юрий Михайлович Вернигоров, доктор технических наук, профессор кафедры физики Донского государственного технического университета, (344003, РФ, г. Ростов-на-Дону, пл. Гагарина, 1), [ORCID](#), [ScopusID](#), jvernigorov@donstu.ru

Заявленный вклад авторов:

Ю.В. Долгачев — подготовка образцов для исследования, получение экспериментальных данных, проведение расчетов, подготовка текста, формирование выводов.

В.Н. Пустовойт — формирование основной концепции, цели и задач исследования, научное руководство, доработка текста, корректировка выводов.

Ю.М. Вернигоров — анализ результатов исследований, редактирование текста.

Конфликт интересов: авторы заявляют об отсутствии конфликта интересов.

Все авторы прочитали и одобрили окончательный вариант рукописи.

Поступила в редакцию 23.12.2023

Поступила после рецензирования 19.01.2024

Принята к публикации 24.01.2024

MACHINE BUILDING AND MACHINE SCIENCE МАШИНОСТРОЕНИЕ И МАШИНОВЕДЕНИЕ



UDC 621.9

Research article

<https://doi.org/10.23947/2687-1653-2024-24-1-66-77>

Improving the Principles of Identifying Critical Requirements for the Assembly of High-Precision Products

 Alexandr V. Nazaryev¹ , Pyotr Yu. Bochkarev^{2,3} 
¹ Industrial Association “Korpus”, SPC branch, Saratov, Russian Federation² Kamyshin Technological Institute, VSTU branch, Kamyshin, Russian Federation³ Saratov State Vavilov Agrarian University, Saratov, Russian Federation✉ alex121989@mail.ru

EDN: NMXQLA

Abstract

Introduction. The problem of improving the manufacturing of high-precision products is currently becoming a key one, since the requirements for them are constantly being tightened. Maintaining assembly quality and accuracy is an important aspect of manufacturing precision products. Standard approaches to this process do not always have sufficient versatility. Existing studies that aim to develop universal approaches, such as end-to-end production design or the application of parallel engineering principles, also have a number of shortcomings. These include the fact that the given approaches do not fully take into account information about the technology capabilities of a particular production when making design decisions, and do not consider the relationship between the manufacturing preparation of machining and mechanical assembly industries. That is why studies aimed at developing such universal approaches have high applicability. To solve these problems, the authors conceptually developed a set of formalized design procedures for a system of accounting requirements for the assembly of high-precision products in the design of machining processes. However, to effectively identify the numerous requirements for the assembly of high-precision products (output parameters) and select those that cannot be provided by the method of complete interchangeability (critical elements), additional research is needed. The research objective is to develop principles for identifying the output parameters of high-precision products and detecting critical elements. To achieve this goal, it is required to solve the following problems: to formulate principles for constructing generalized surface graphs of high-precision products; to develop standards for classifying output parameters and identifying critical ones.

Materials and Methods. To conduct the research, a high-precision assembly unit was selected — “Stator Package 2”. The research was carried out under real conditions of the existing multiproduct manufacture. For this assembly, a generalized surface graph was constructed, including information about the nature and sequence of surfaces, requirements for the assembly, dimensional tolerances and tolerances of shape and location, with its subsequent analysis.

Results. This paper presents the results of research on improving the enlarged block of design procedures for analyzing requirements for the assembly of high-precision products of the designed system. The paper established the relationship between the accuracy of dimensional tolerances and the tolerances of the shape and location of the surfaces of the product to which these dimensions belonged. Based on the relationship obtained, an order was determined for the unambiguous identification of critical elements.

Discussion and Conclusion. The application of this technique makes it possible to increase the reliability of the source information obtained during the implementation of an enlarged block of design procedures, as well as the validity and efficiency of identifying rational manufacturing technologies at subsequent stages of the system implementation, while providing the specified quality, accuracy of products, and reducing the complexity and cost of their manufacture.

Keywords: mechanical assembly production, process design, generalized surface graph, assembly, high-precision product, design dimensional analysis

Acknowledgements. The authors would like to thank the Editorial board of the journal and the reviewer for attentive attitude to the article and suggestions made that helped to improve its quality.

For citation. Nazaryev AV, Bochkarev PYu. Improving the Principles of Identifying Critical Requirements for the Assembly of High-Precision Products. *Advanced Engineering Research (Rostov-on-Don)*. 2024;24(1):66–77. <https://doi.org/10.23947/2687-1653-2024-24-1-66-77>

Научная статья

Технологическое обеспечение сборки на основе принципов выявления критичных требований к высокоточным изделиям

А.В. Назарьев¹ , П.Ю. Бочкарев^{2,3} 

¹ ПО «Корпус» — филиал АО «НПЦАП», г. Саратов, Российская Федерация

² Камышинский технологический институт — филиал Волгоградского государственного технического университета, г. Камышин, Российская Федерация

³ Саратовский государственный университет генетики, биотехнологии и инженерии имени Н.И. Вавилова, г. Саратов, Российская Федерация

✉ alex121989@mail.ru

Аннотация

Введение. Проблема совершенствования производства высокоточных изделий в настоящее время становится ключевой, поскольку требования к ним постоянно ужесточаются. Обеспечение качества и точности сборки является важным аспектом производства высокоточной продукции. Стандартные подходы к этому процессу не всегда обладают достаточной универсальностью. Существующие исследования, целью которых является разработка универсальных подходов, таких как сквозное технологическое проектирование или применение принципов параллельной инженерной разработки, также обладают рядом недостатков. К их числу можно отнести то, что в них не в полной мере обеспечен учет информации о технологических возможностях конкретного производства при принятии конструкторских решений и не учитывается связь между технологической подготовкой механообрабатывающего и механосборочного производств. Именно поэтому исследования, направленные на разработку универсальных подходов, обладают высокой актуальностью. Для решения обозначенных проблем авторами был концептуально разработан комплекс формализованных проектных процедур системы учета требований к сборке высокоточных изделий при проектировании технологических процессов механической обработки. Однако для эффективного выявления множества требований к сборке высокоточных изделий (выходных параметров) и выбора из них тех, которые не могут быть обеспечены методом полной взаимозаменяемости (критичных элементов), требуется проведение дополнительных исследований. Целью данной работы является разработка принципов выявления выходных параметров высокоточных изделий и определения критичных элементов. Для достижения поставленной цели необходимо решить следующие задачи: сформировать принципы построения обобщенных графов поверхностей высокоточных изделий, сформировать стандарты классификации выходных параметров и выявления из них критичных.

Материалы и методы. Для проведения исследования была выбрана высокоточная сборочная единица — «Пакет статора 2». Исследования проводились в реальных условиях действующего многономенклатурного производства. Для данной сборки был построен обобщенный граф поверхностей, включающий в себя информацию о характере и последовательности поверхностей, предъявляемые требования к сборке, допуски размеров и допуски формы и расположения с последующим его анализом.

Результаты исследования. В данной статье представлены итоги исследований по совершенствованию укрупненного блока проектных процедур анализа требований к сборке высокоточных изделий проектируемой системы. В работе установлена взаимосвязь между точностью допусков на размеры и допусков формы и расположения поверхностей изделия, которым принадлежат данные размеры. На основе полученной взаимосвязи был определен порядок для однозначного выявления критичных элементов.

Обсуждение и заключение. Применение данной методики позволяет повысить достоверность исходной информации, полученной при реализации укрупненного блока проектных процедур, а также обоснованность и эффективность выявления рациональных технологий изготовления на последующих этапах реализации системы при обеспечении заданных качества, точности изделий и снижении трудоемкости и себестоимости их изготовления.

Ключевые слова: механосборочные производства, технологическая подготовка производства, обобщенный граф поверхностей, сборка, высокоточное изделие, конструкторский размерный анализ

Благодарности. Авторы выражают благодарность редакции за внимательное отношение к содержанию статьи и высказанные предложения, которые позволили повысить ее качество.

Для цитирования. Назарьев А.В., Бочкарев П.Ю. Технологическое обеспечение сборки на основе принципов выявления критичных требований к высокоточным изделиям. *Advanced Engineering Research (Rostov-on-Don)*. 2024;24(1):66–77. <https://doi.org/10.23947/2687-1653-2024-24-1-66-77>

Introduction. The production of modern devices and machines requires a clear organization of the assembly process with careful manufacturing preparation [1]. This requirement is particularly urgent in the manufacture of high-precision products in precision machine tool industry, aerospace industry, military-industrial complex, bearing industry, etc. [2]. In this paper, high-precision products mean such products, whose assembly process is complex due to difficulties in meeting specified requirements (critical assembly requirements, or critical elements), such as dimensional, dynamic and other characteristics, which may result in the need to manufacture a large number of spare parts and kits. This, in turn, causes an increase in the volume of work in progress and requires more time and resources to complete the assembly production process (PP) [3].

Modern technology makes it possible to improve the quality and accuracy of production, reduce material costs, and introduce resource-saving technologies. However, today there is no unified concept of an integrated approach to solving the above-mentioned problems. When assembling products, classical methods of maintaining accuracy are often used, which in most cases are not universal. They depend on the type of production and are often economically unjustified. In such cases, it is necessary to develop unique assembly approaches that take into account the specifications of a particular product and provide the required accuracy without unreasonable costs. In addition, it should be borne in mind that the traditional PP design of mechanical processing and assembly is subjective. This is primarily due to time constraints and physical capabilities, which make it impossible for a person to compete with modern computing technology [4]. To solve these problems, it is needed to develop unique approaches that combine various aspects of production and assembly of products, as well as taking into account economic factors. Only a comprehensive solution can provide achieving optimal results and effectively cope with the tasks set.

Currently, a system of automated process planning (SAPP) has been conceptually developed [5]. Nevertheless, the weakness of this automated system is the lack of correlation between the multiple-alternate design of the manufacturing process for parts included in the assembly unit and the requirements for the technology and accuracy of assembly of a high-precision assembly unit, based on which it is possible to efficiently solve the problem of reducing the volume of work in progress and the cost of assembly. At the same time, the correlation between design and manufacturing preparation of production has not yet been fully worked out. As a result, research in this area is urgent for the modern development of mechanical assembly production systems. The objective of the article is to develop principles for identifying the output parameters of high-precision products and determining critical elements. To do this, it is needed to formulate the principles of constructing generalized graphs of surfaces of high-precision products, determine the standards for classifying output parameters and identifying critical ones from them.

Materials and Methods. To solve the above problems, a system with account for the requirements for the assembly of high-precision products in the design of manufacturing processes of mechanical processing was developed (SRPPMP) [6]. However, to provide a more comprehensive integration of this system into the SAPP structure, it is required to actively look for options of upgrading the development strategies used. This will allow us to move on to the analysis of the manufacturability of products and provide a more effective implementation of the system into the production structure.

As part of the research to improve the methodology of formalization of the block under consideration, strategies for performing the procedures of this block were formed, and the one that provides identifying the maximum number of critical elements was selected. This strategy is a combined one and matches up the advantages of the other approaches. In addition, for a more accurate calculation of dimensional chains, a special size indexing system has been introduced, which is most effective. The specified indexing is considered in detail in [7] and is not fully cited in this paper.

According to this strategy, detailed segmentation of high-precision products is performed, which provides determining the required parameters for the formation of a set of assembly requirements ($M_{T.C}$), carrying out a design dimensional analysis and, based on its results, identifying critical elements. To implement the described procedures, first, it is needed to identify those elements from the set $M_{T.C}$ that satisfy the following condition:

$$TB_{k_1,l}^{i,j} < \sum_{i=1}^{n_0} TA_{k_1,m}^{i,j}, \quad (1)$$

where B — assembly requirements (closing links); A — component links.

The above condition makes it possible to identify those elements that cannot be provided by the method of complete interchangeability, i.e., critical elements. The specified elements are included in the corresponding subset M_1 . The remaining elements are provided by the method of complete interchangeability. They form subset $M_{II.B.}$ and are no longer considered.

$$M_1 = \frac{M_{T.C.}}{M_{II.B.}}. \quad (2)$$

Next, it is necessary to determine methods for maintaining accuracy for each critical element and distribute them into appropriate subsets: $M_{H.B.}$ — critical elements provided by the method of incomplete interchangeability; $M_{Г.В.}$ — critical elements provided by the method of selective assembly; $M_{H.II.}$, $M_{P.E.}$ — critical elements provided by compensation.

Research Results. For the distribution of critical elements into groups, a technique based on the construction of a generalized graph of surfaces of high-precision assembly units and nodes has been developed, and distribution rules have been formulated.

The classification of modules of working and connecting surfaces of parts and assembly units (PAU), proposed by Professor Bazrov B.M. [8], is shown in Figure 1.

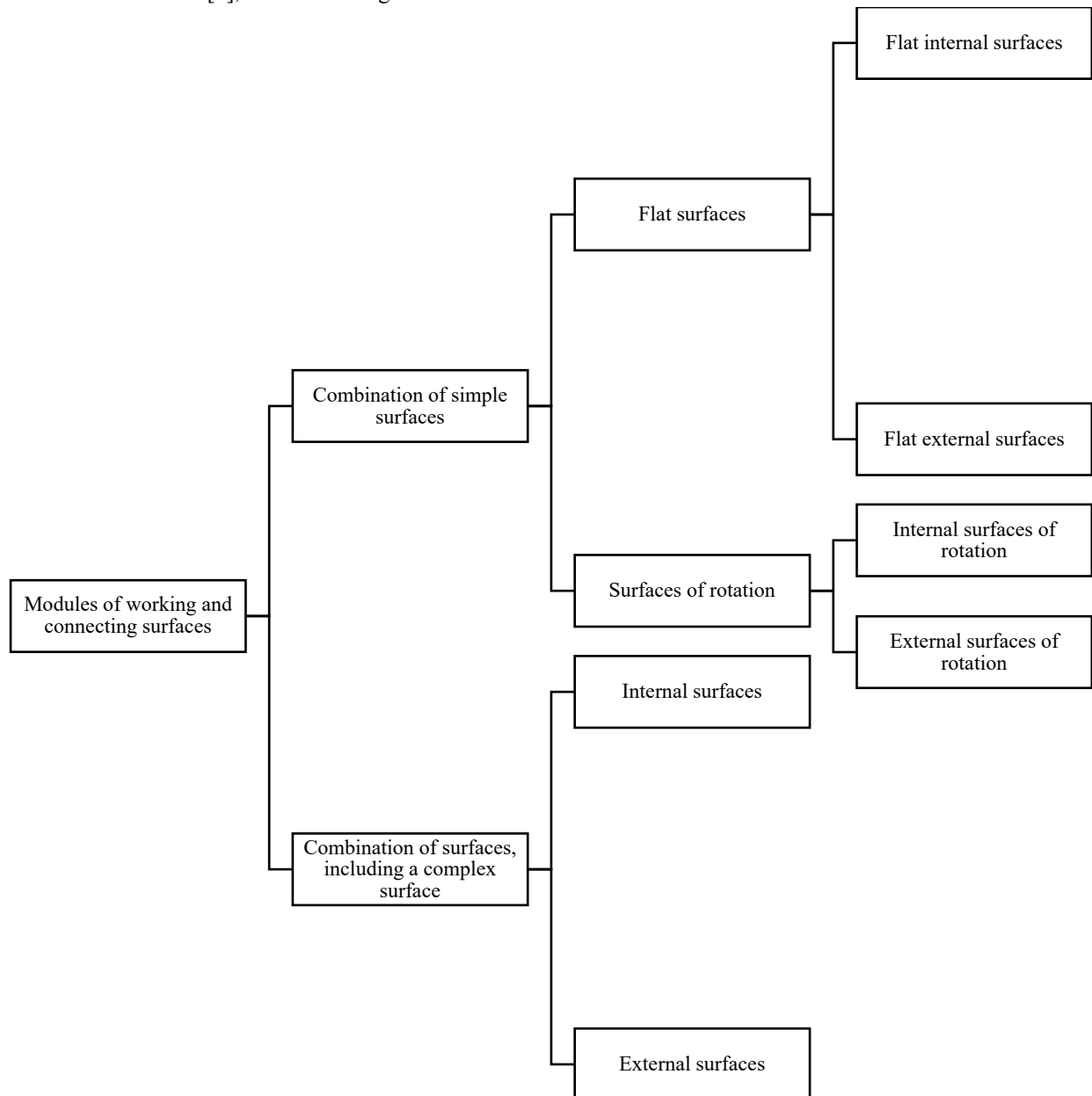


Fig. 1. Modules of working and connecting surfaces of PAU [8]

Consider the principles of constructing a generalized graph of surfaces using the example of the assembly unit (AU) “Stator Package 2”, which is part of the high-precision “Gyromotor” product. Figure 2 shows an axonometric projection of the AU “Stator Package 2” and a schematic representation of this AU, indicating the basic assembly requirements, shape and location tolerances imposed on it, as well as the PAU of which it consists.

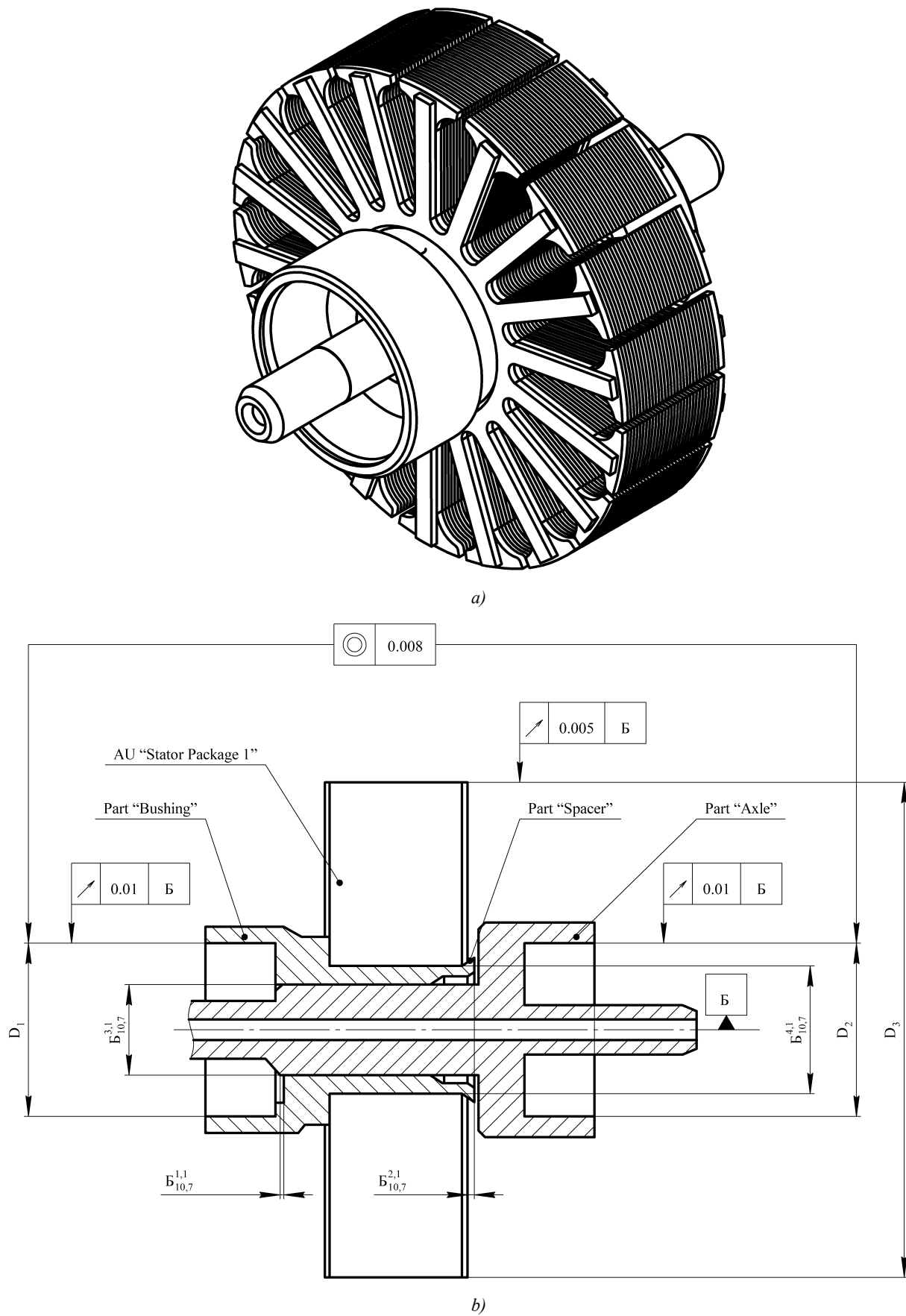


Fig. 2. AU "Stator Package 2":
 a — axonometric projection; b — composition and basic assembly requirements,
 shape and location tolerances

Figure 3 shows a sketch of the AU “Stator Package 2”, on which the surfaces of the composite PAU are numbered, and a code is indicated for each surface in accordance with the requirements of the SAPP [9] (Table 1).

Based on the information obtained about the nature and sequence of the PAU surfaces, a graph of the AU surfaces “Stator Package 2” is constructed. In this graph, the surfaces of the PAU included in the considered AU are indicated. For the surfaces of the PAU, parallel to the axis of rotation of the AU (marked “01” in the graph), the connection with this axis is conditionally shown. Additionally, the PAU surfaces that are in direct contact in the assembly unit are marked (e.g., surfaces 1.7 and 3.3 in Figure 4a). Further, the assembly requirements (dimensional chains) posed on this AU are presented on the specified graph, indicating the closing links and the directions of the constituent links. It is important to note that the components and closing links going to or from the group of contacting surfaces are assembly dimensions. Also, the graph indicates the basic shape and location tolerances required for the AU assembly (Fig. 4b). The assembly requirements and basic tolerances of shape and location are taken from Figure 2b. As a result, a generalized graph of AU surfaces “Stator Package 2” is formed.

Thus, the presented graph provides obtaining the required data on the dimensional relationships between individual surfaces (groups of surfaces) of PAU, as well as the surfaces of the mating PAU in contact with each other. The obtained data form the initial information for the further stages of the implementation of the SAPP procedures.

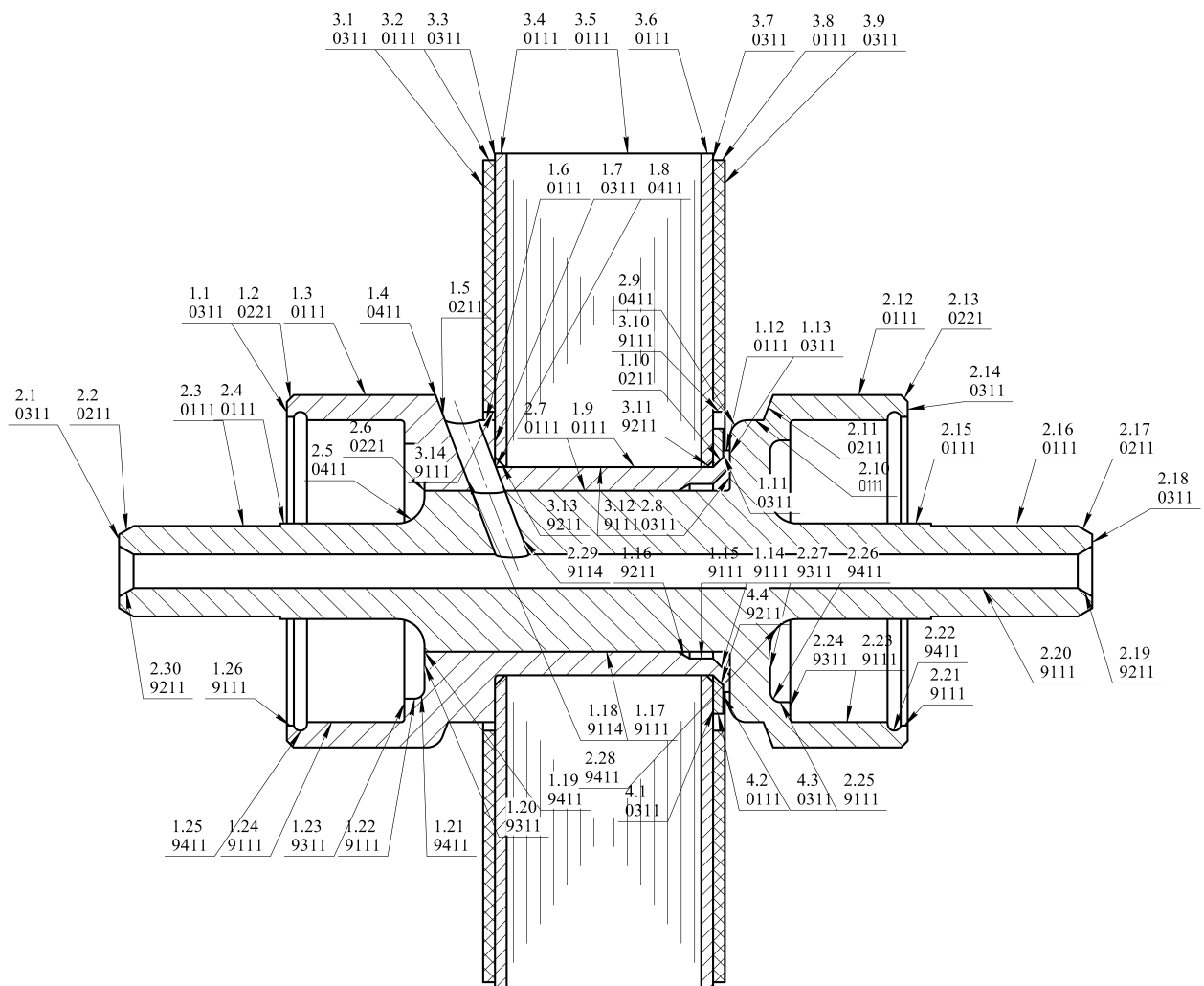


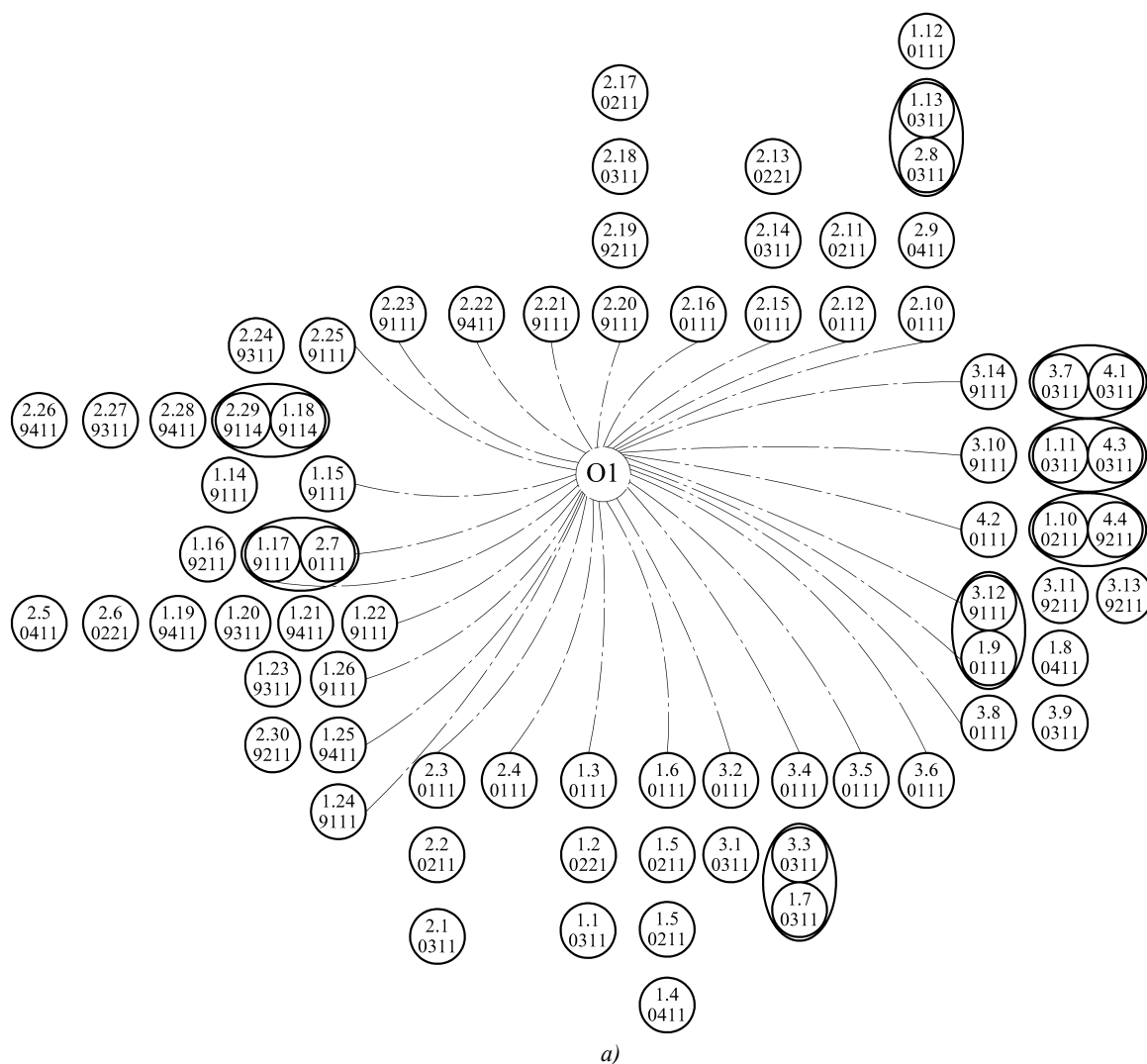
Fig. 3. Numbering of AU surfaces “Stator Package 2”

Table 1

No. of PAU, surfaces	Code	Type
Part “Bushing”		
1.1	0311	Outer end
1.2	0221	External chamfer
1.3	0111	External cylindrical

1.4	0411	Curved external
1.5	0211	Outer cone
1.6	0111	Outer cylindrical
1.7	0311	Outer end
1.8	0411	Outer curve
1.9	0111	External cylindrical
1.10	0211	Outer cone
1.11	0311	Outer end
1.12	0111	External cylindrical
1.13	0311	Outer end
1.14	9211	Internal cone
1.15	9111	Internal cylindrical
1.16	9211	Internal cone
1.17	9111	Internal cylindrical
1.18	9114	Cylindrical hole at an angle to the axis of rotation
1.19	9411	Curvilinear internal
1.20	9311	Inner end
1.21	9411	Curvilinear internal
1.22	9111	Internal cylindrical
1.23	9311	Inner end
1.24	9111	Internal cylindrical
1.25	9411	Curvilinear internal
1.26	9111	Internal cylindrical
Part “Axle”		
2.1	0311	Outer end
2.2	0211	Outer cone
2.3	0111	External cylindrical
2.4	0111	External cylindrical
2.5	0411	Outer curve
2.6	0221	External chamfer
2.7	0111	External cylindrical
2.8	0311	Outer end
2.9	0411	Outer curve
2.10	0111	External cylindrical
2.11	0211	Outer cone
2.12	0111	External cylindrical
2.13	0221	External chamfer
2.14	0311	Outer end
2.15	0111	External cylindrical
2.16	0111	External cylindrical
2.17	0211	Outer cone

2.18	0311	Outer end
2.19	9211	Internal cone
2.20	9111	Internal cylindrical
2.21	9111	Internal cylindrical
2.22	9411	Curvilinear internal
2.23	9111	Internal cylindrical
2.24	9311	Inner end
2.25	9111	Internal cylindrical
2.26	9411	Curvilinear internal
2.27	9311	Inner end
2.28	9411	Curvilinear internal
2.29	9114	Cylindrical hole at an angle to the axis of rotation
2.30	9211	Internal cone
Part “Spacer”		
4.1	0311	Outer end
4.2	0111	External cylindrical
4.3	0311	Outer end
4.4	9211	Internal cone





The performed approbation of the developed graph construction techniques and the formed rules on the example of the analysis of the requirements for the AU “Stator Package 2” under the conditions of the current multiproduct

² GOST 8908-81. *Standard Angles and Angle Tolerances. Basic Norms of Interchange Ability*. URL: <https://docs.cntd.ru/document/1200011833> (accessed: 29.11.2023) (In Russ.).

manufacture showed their operability. Identified critical assembly requirements that do not meet the conditions of complete interchangeability include:

- permissible value of the deformable (rolled) part of the “Bushing” workpiece obtained during the assembly of the AU “Stator Package 2”;
- permissible value of the chamfer protrusion of the “Axle” part in the AU “Stator Package 2”.

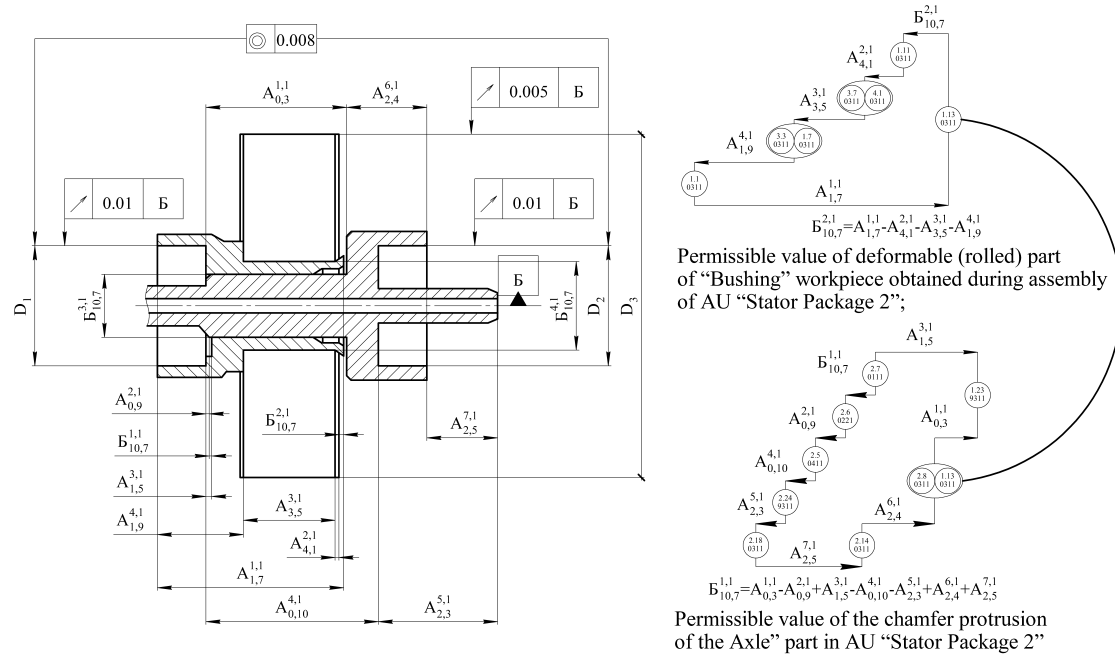


Fig. 5. Requirements for assembly of AU “Stator Package 2” with indication of surfaces between which the corresponding chain links are located

As a result of the implementation of this enlarged block of SRPPMP, initial information is formulated, including numerous assembly requirements (closing links of dimensional chains) that cannot be provided by the method of complete interchangeability. The dimensions of the PAU are the constituent links of the dimensional chains of the specified set and the set of SRPPMP to which these closing and constituent links belong. In the example under consideration, such a set will consist of “Bushing”, “Axle”, “Stator Package 1”. The dimensions of the part “Spacer” are not involved in the calculation of critical assembly requirements. At the next stages of the implementation of the SRPPMP for the received set of PAU in the SAPP, all possible options for PP are generated, and their in-process dimensional analysis is carried out. Next, the most rational options are selected from the resulting set of PP using the multicriteria optimization method. To carry out the selection procedure, a system of criteria was developed. The criterion for obtaining the maximum number of assembly kits is the basic from them. The technique of generation procedures, in-process dimensional analysis, and selection is described in detail in [6]. It should also be noted that the improvement of the methodological apparatus of the SRPPMP will allow us to proceed to the assessment of the production manufacturability of the product [11].

Discussion and Conclusion. The paper proposes the principles of constructing generalized graphs of high-precision AU surfaces and nodes, develops standards for classifying high-precision output parameters into appropriate groups and identifying critical elements of high-precision products from them. The described technique creates conditions for the complete formalization of the considered design procedure and the clarity of the graphical results of dimensional analysis. This technique makes it possible to increase the reliability of the initial information obtained during the implementation of an enlarged block of design procedures, as well as the validity and efficiency of identifying rational manufacturing methods for PAU at subsequent stages of the SRPPMP implementation, while providing the specified properties, accuracy of products, and reducing the complexity and cost of their manufacture.

The improvement of the scientific principles of the implementation of this enlarged block of design procedures of the SRPPMP increases the level of digital transformation of design and manufacturing preparation, and, along with the issues of automation of design, production and assembly, creates prerequisites for the implementation of a systematic approach to assessing the manufacturability of the products.

The next stage in the development of the proposed study is planned to supplement the generalized graph with information about the design and processing bases of the PAU, and the nature of combinations of mating connecting and working surfaces according to the classification of Professor B.M. Bazrov. The introduction of the specified information into the generalized graph will make it possible to finally form the methodological support for this enlarged block of design procedures.

References

1. Bazrov BM. Classification of Objects of Technological Preparation in the Machining Production. *IOP Conference Series: Materials Science and Engineering*. 2021;1047:12048. <https://doi.org/10.1088/1757-899X/1047/1/012048>
2. Suslov A, Fedonin O, Petreshin D. Basic Fundamentals to Ensure and Increase Quality of Mechanical Engineering and Aerospace Products. *Bulletin of Bryansk State Technical University*. 2020;87(2):4–10. <https://doi.org/10.30987/1999-8775-2020-2-4-10>
3. Osetrov VG, Slashchev ES. *Assembly in Mechanical Engineering, Instrumentation. Theory, Technology and Organization*. Monograph. Izhevsk: Izhevskii institut kompleksnogo priborostroeniya; 2015. 328 p. (In Russ.).
4. Peng Lin, Ming Li, Xiangtianrui Kong, Jian Chen, George Q. Huang, Meilin Wang. Synchronisation for Smart Factory — Towards IOT-Enabled Mechanisms. *International Journal of Computer Integrated Manufacturing*. 2017;31(7):624–635. <https://doi.org/10.1080/0951192X.2017.1407445>
5. Mitin SG. *Synthesis of Production Operations with a Complex Structure in Multi-Nomenclature Machining Systems*. Dr.Sci. (Engineering) diss. Saratov; 2017. 270 p. (In Russ.).
6. Nazaryev AV. *Improving the Manufacturing Preparation of Multitopic Machining Industries Based on Requirements for the Assembly of High-Precision Products*. Cand.Sci. (Engineering) diss. Saratov; 2019. 163 p. (In Russ.).
7. Nazarev A, Bochkarev P, Mitin S. Formal Characterization of the Strategy for Identifying Critical Assembly Requirements When Staging Multipart Machinery Productions. *Science Intensive Technologies in Mechanical Engineering*. 2022;136(10):42–48. <https://doi.org/10.30987/2223-4608-2022-10-42-48>
8. Bazrov BM. *Basis of Manufacturing Preparation of Machine-Building Production*. Moscow: KURS; 2023. 324 p. (In Russ.).
9. Ivanov AA. *Development of Models and Algorithms of Design Procedures for Production Management in the Planning System of Multiproduct Machining Processes*. Cand.Sci. (Engineering) diss. Saratov; 2016. 601 p. (In Russ.).
10. Suslov AG, Bezyazychny VF, Bazrov BM, Babichev AP, Bochkarev PYu, Guzeev VI, et al. AG Suslov (ed). *Technologist's Handbook*. Moscow: Innovatsionnoe mashinostroenie; 2019. 800 p. (In Russ.).
11. Bokova AK, Bokova LG. Product Quality Improvement Based on the Assessment of Production Manufacturability. In: *Coll. of Sci. Papers of All-Russian Sci.-Tech. Conf. "Modern Technologies, Materials and Equipment"*. Voronezh: Voronezh State Technical University; 2023. P. 91–96. (In Russ.).

About the Authors:

Alexandr V. Nazaryev, Cand.Sci. (Eng.), Head of the Design Sector, Industrial Association “Korpus”, Branch of FSUE “Academician Pilyugin Scientific-Production Center of Automatic and Instrument Making” (1, Osipov St., Saratov, 410019, RF), SPIN-code: [5363-6836](#), [ORCID](#), [ScopusID](#), alex121989@mail.ru

Pyotr Yu. Bochkarev, Dr.Sci. (Eng.), Professor of the Mechanical Engineering Department, Kamyshin Technological Institute, VSTU branch (6a, Lenin St., Kamyshin, Volgograd Region, 403805, RF), Professor of the AIC Engineering Support Department, Saratov State Vavilov Agrarian University (1, Teatralnaya Sq., Saratov, 410012, RF), SPIN-code: [1696-3045](#), [ORCID](#), [ScopusID](#), bpy@mail.ru

Claimed contributorship:

AV Nazaryev: development of principles of classification and requirements for the assembly of high-precision products, formalization of rules for identifying assembly requirements, industrial testing, text preparation.

PYu Bochkarev: academic advising, methodological approach to planning machining and assembly production, finalization of the text.

Conflict of interest statement: the authors do not have any conflict of interest.

All authors have read and approved the final version of the manuscript.

Received 19.01.2024

Revised 13.02.2024

Accepted 22.02.2024

Об авторах:

Александр Викторович Назарьев, кандидат технических наук, начальник конструкторского сектора ПО «Корпус» — филиала АО «НПЦАП» (410010, РФ, г. Саратов, ул. Осипова, 1), SPIN-код: [5363-6836](#), [ORCID](#), [ScopusID](#), alex121989@mail.ru

Петр Юрьевич Бочкарёв, доктор технических наук, профессор кафедры технологии машиностроения Камышинского технологического института (филиала) Волгоградского государственного технического университета (403874, Волгоградская обл., г. Камышин, ул. Ленина, 6а), профессор кафедры технического обеспечения АПК Саратовского государственного университета генетики, биотехнологии и инженерии имени Н.И. Вавилова (410068, г. Саратов, просп. Петра Столыпина, 4, стр. 3), SPIN-код: [1696-3045](#), [ORCID](#), [ScopusID](#), bpy@mail.ru

Заявленный вклад авторов:

А.В. Назарьев — разработка принципов классификации и учета требований к сборке высокоточных изделий, формализация правил выявления требований к сборке, промышленная апробация, подготовка текста.

П.Ю. Бочкарёв — научное руководство, методический подход к планированию механообрабатывающих и сборочных производств, доработка текста.

Конфликт интересов: авторы заявляют об отсутствии конфликта интересов.

Все авторы прочитали и одобрили окончательный вариант рукописи.

Поступила в редакцию 19.01.2024

Поступила после рецензирования 13.02.2024

Принята к публикации 22.02.2024

INFORMATION TECHNOLOGY, COMPUTER SCIENCE AND MANAGEMENT ИНФОРМАТИКА, ВЫЧИСЛИТЕЛЬНАЯ ТЕХНИКА И УПРАВЛЕНИЕ



UDC 004.032.22,621.438:62-253.51

Research article

<https://doi.org/10.23947/2687-1653-2024-24-1-78-87>

Approximation of the Profile of Gas Turbine Engine Blades

Mikhail E. Soloviev¹ , Yulia N. Shuleva¹ , Sergey L. Baldaev² , Lev Kh. Baldaev² 
¹ Yaroslavl State Technical University, Yaroslavl, Russian Federation² “Technological Systems of Protective Coatings” LLC, Shcherbinka, Moscow, Russian Federation✉ me_s@mail.ru

EDN: QOELMG

Abstract

Introduction. Increasing the durability of gas turbine engine (GTE) blades is achieved through the use of special protective coatings on their surface. For the development of such coatings, the basic source information is the geometric profile of the blade section. To transfer a given blade cross-section profile to the appropriate CAD/CAM system or engineering analysis package, parametric modeling methods are used to automate this operation. However, the known approaches to creating a parametric model of a blade profile are not without a number of disadvantages, and a generally accepted method for creating it does not currently exist. The research was aimed at creating a technique for approximating the profile of gas turbine engine blades, convenient for use in the subsequent analysis of the operating conditions of special coatings on the surface of the blades.

Materials and Methods. When constructing parametric models of the profile of gas turbine engine blades, a method based on the orthogonal Legendre polynomials was used. This made it possible to provide high accuracy of approximation and construction of a continuous mapping for the parameters of the blade profile approximation. A Python application was created for automated processing of source profiles. It provided the calculation of the coefficients of approximating polynomials for the contour lines of the blade, visualization of the calculation results, and creation of a dxf file based on the points of approximating functions to transfer it to the CAD system. Next, geometric models of blades were used to solve the problem of a stationary aerodynamic flow around a blade. The results of solving this problem were used to study the effect of the blade profile on its cooling in an aerodynamic flow.

Results. As an example, three options of blade profiles belonging to different types of GTE were considered. It was shown that for all three studied profiles, the proposed technique provided obtaining parametric models that maintained high accuracy in constructing approximating lines, which was confirmed by the values of the determination coefficients close to unity. To illustrate the possibility of using the obtained models, examples of solving the gas dynamic problem with a potential flow around a blade in a stationary aerodynamic flow were given. The distributions of pressure and temperature on the surface of the blade were calculated using the finite element method.

Discussion and Conclusion. The calculation results show that the proposed technique of approximating the profile of the GTE blade, based on the use of orthogonal polynomials, is a convenient tool to automate the creation of a geometric model of the blade and compare different types and profiles of blades, solving the corresponding gas dynamic problems. At the same time, for a given blade profile and GTE operating conditions, it is possible to obtain the distribution of temperatures and forces acting on the surface of the blade, which is required for predicting the durability of special coatings.

Keywords: blades of gas turbine engines, section profile, approximation, orthogonal polynomials

Acknowledgments. The authors would like to thank the Editorial board and the reviewers for their attentive attitude to the article and for the specified comments that improved the quality of the article.

For citation. Soloviev ME, Shuleva YuN, Baldaev SL, Baldaev LKh. Approximation of the Profile of Gas Turbine Engine Blades. *Advanced Engineering Research (Rostov-on-Don)*. 2024;24(1):78–87. <https://doi.org/10.23947/2687-1653-2024-24-1-78-87>

Научная статья

Аппроксимация профиля лопаток газотурбинных двигателей

М.Е. Соловьев¹ , Ю.Н. Шулева¹ , С.Л. Балдаев² , Л.Х. Балдаев² 

¹ Ярославский государственный технический университет, г. Ярославль, Российская Федерация

² ООО «Технологические системы защитных покрытий», г. Москва, г. Щербинка, Российская Федерация

✉ me_s@mail.ru

Аннотация

Введение. Повышение долговечности лопаток газотурбинных двигателей (ГТД) достигается за счет применения специальных защитных покрытий их поверхности. Для разработки таких покрытий основной исходной информацией является геометрический профиль сечения лопатки. Для передачи заданного профиля сечения лопатки в соответствующую CAD/CAM-систему или пакет инженерного анализа применяются методы параметрического моделирования, позволяющие автоматизировать данную операцию. Однако известные подходы к созданию параметрической модели профиля лопатки не лишены ряда недостатков, и общепринятой методики ее создания в настоящее время не существует. Целью данной работы является создание методики аппроксимации профиля лопаток ГТД, удобной для использования при последующем анализе условий работы специальных покрытий поверхности лопаток.

Материалы и методы. При построении параметрических моделей профиля лопаток газотурбинных двигателей авторами использован метод, основанный на применении ортогональных полиномов Лежандра. Это позволило обеспечить высокую точность аппроксимации и построение непрерывного отображения для параметров аппроксимации профиля лопатки. Для автоматизированной обработки исходных профилей создано приложение на языке Python, позволяющее вычислять коэффициенты аппроксимирующих полиномов для линий контура лопатки, визуализировать результаты расчета и создавать по точкам аппроксимирующих функций dxf-файл для передачи его в CAD-систему. Далее геометрические модели лопаток использовали для решения задачи обтекания лопатки стационарным аэродинамическим потоком. Результаты решения этой задачи использованы при исследовании влияния профиля лопатки на ее остывание в аэродинамическом потоке.

Результаты исследования. В качестве примера рассмотрены три варианта профилей лопаток, относящихся к разным типам ГТД. Показано, что для всех трех изученных профилей предложенная методика позволяет получать параметрические модели, обеспечивающие высокую точность построения аппроксимирующих линий, что подтверждается близкими к единице значениями коэффициентов детерминации. Для иллюстрации возможности использования полученных моделей приведены примеры решения задачи газовой динамики при потенциальном обтекании лопатки в стационарном аэродинамическом потоке. Методом конечных элементов рассчитаны распределения давлений и температур на поверхности лопатки.

Обсуждение и заключение. Результаты вычислений показали, что предлагаемая методика аппроксимации профиля лопатки ГТД, основанная на использовании ортогональных многочленов, является удобным инструментом, позволяющим автоматизировать создание геометрической модели лопатки и проводить сравнение различных типов и профилей лопаток, решая соответствующие задачи газовой динамики. При этом для заданного профиля лопаток и условий работы ГТД можно получить распределение температур и усилий, действующих на поверхности лопатки, что необходимо для прогнозирования долговечности специальных покрытий.

Ключевые слова: лопатки газотурбинных двигателей, профиль сечения, аппроксимация, ортогональные многочлены

Благодарности. Авторы выражают благодарность редакции и рецензентам за внимательное отношение к статье и указанные замечания, устранение которых позволило повысить ее качество.

Для цитирования. Соловьев М.Е., Шулева Ю.Н., Балдаев С.Л., Балдаев Л.Х. Аппроксимация профиля лопаток газотурбинных двигателей. *Advanced Engineering Research (Rostov-on-Don)*. 2024;24(1):78–87. <https://doi.org/10.23947/2687-1653-2024-24-1-78-87>

Introduction. Turbine blades are the most highly loaded parts of a gas turbine engine (GTE), the durability of which mainly determines the engine overhaul time [1]. One of the ways to increase the durability of turbine blades is to apply special protective coatings on their surfaces [2]. The coating is a complex composite structure. To select materials for it and determine its optimal geometric characteristics, it is necessary to know the operating conditions of the part: the distribution of temperatures, pressures, and shear stresses on the surface of the blade.

The highest requirements are posed on the shape of the blades, as well as on the selection of materials, their manufacturing technique, and special coatings [3]. When designing special coatings, the basic initial information is the geometric profile of the surface of the part, since the parameters of the coating manufacturing process are set on its basis.

Among the characteristic elements of the profile, the following can be distinguished: chord — distance between the most distant points with a horizontal arrangement of the blade, like an airplane wing; suction side — upper part of the profile; pressure side — lower part of the profile; leading and trailing edges [4].

The shape of the blade cross-section profile is selected both on the basis of experimental studies of pilot units and actual engines [5], as well as on the results of numerical experiments on models [6]. In the course of numerical simulation, we study the task of creating a geometric model of the blade based on a given cross-section profile and transferring it to the appropriate CAD/CAM system [7], or an engineering analysis package [8], in which the parameters of the physical properties of the materials of the parts are set, the boundary conditions of the problem are determined, and calculations are performed.

Traditionally, when creating a blade drawing, its profile is described by a set of circular arcs, which is then transferred point-by-point to the module for developing a geometric model and generating a grid of finite elements. The disadvantage of this approach is that when building each new model, you have to manually create its profile in the graphical editor. In this regard, methods of parametric modeling of the blade cross-section profile are proposed to automate this operation. One of the most well-known models is the nine-parameter RATD (Rapid Axial Turbine Design) model described in [9]. At the same time, the practice of using RATD has revealed certain disadvantages inherent in this model, specifically, the inconvenience of using it when optimizing the geometry of the profile, as well as insufficient accuracy. On this basis, the authors [10] proposed a modified version of this model, which included a larger number of parameters. Methods of parametric modeling of blade cross-section profiles are also actively used in domestic practice. Thus, in [11, 12], algorithms for the automated construction of the blade profile using approximation by curves from a set of parabolas and Bezier curves of the second order were proposed. In [13], a method for designing a grid of GTE profiles based on these algorithms was described. The use of parametric models of blade profiles in solving optimization problems was considered by the authors in [14, 15].

At the same time, it should be noted that the existing methods of parameterization of the blade profile are not without a number of disadvantages. The main disadvantage of traditional blade profile parameterization schemes based on the use of second-order curves is that different functions have to be used for different parts of the workpiece to maintain the accuracy of the description. At the same time, these functions do not form an orthogonal system, and the values of the parameters determined by the approximation of the existing profile by the least squares method turn out to be correlated. This leads to the fact that it is not possible to construct a continuous mapping for a set of parameters when the system approximates the cross sections of the three-dimensional surface of the blade of double curvature.

It should also be noted that there is currently no universal technique for parametric modeling of GTE blade profiles, and the selection of a specific technique depends both on the goals of modeling and on the characteristics of the specific type of engine being designed. However, the forms of input information can vary significantly. It can be a geometric model in the form of a file in the format of one of the CAD systems, or just a set of points from a database of profiles of the type [16].

Thus, an additional requirement for the parametric modeling technique of the blade profile, due to the purpose of the model, is versatility with respect to the format of the source data.

This research was aimed at the creation of the technique for approximating the profile of the GTE blades, free from the above disadvantages and convenient for use in the subsequent analysis of the working conditions of special coatings on the surface of the blades. This was demonstrated by the example of solving the problem of gas dynamics for three different blade models, whose profile was parameterized through the proposed technique.

Materials and Methods. The authors used an option of parametric models of the blade profile based on the orthogonal Legendre polynomials [17]. A Python application was created for automated processing of source profiles. This made it possible to calculate the coefficients of approximating polynomials for the contour lines of the blade, visualize the calculation results in the form of graphs of initial points and approximation curves for the suction and pressure sides of the blade, save the initial points of the profile, an array of coefficients of approximating polynomials and the coefficient of determination of the model in the database, and create a dxf file based on the points of approximating functions to transfer it to the CAD system and an engineering analysis package.

The constructed two-dimensional geometric models of the blades were used to solve the problem of a stationary aerodynamic flow around the blade in the approximation of potential flow. The velocity distributions calculated as a result of solving this problem in the flow were used to study the effect of the blade profile on its cooling in the aerodynamic flow.

Calculation method. The orthogonal polynomial systems used as the basis of the proposed method provide linear independence of the approximation coefficients and are devoid of a disadvantage that causes difficulties in constructing

models that are continuous in parameters. The degree of polynomials is selected to be high enough — of the ninth order, so that the set of two polynomials for two parts of the profile (suction and pressure sides) is twenty parameters, which is sufficient for approximating very complex profiles. The type of the approximating function and the method of calculating estimates of its coefficients are described below.

We denote the approximating line of the blade profile using function $y(x)$. The expression of this line in the case of a number of Legendre polynomials of the ninth degree is represented as:

$$y(x) = \sum_{i=0}^9 a_i L_i(x), \quad (1)$$

where a_i — coefficients that are parameters of the model; $L_i(x)$ — Legendre polynomials calculated by formulas:

$$\begin{aligned} L_0 &= 1; \\ L_1 &= x; \\ L_2 &= (3x^2 - 1)/2; \\ L_3 &= (5x^3 - 3x)/2; \\ L_4 &= (35x^4 - 30x^2 + 3)/8; \\ L_5 &= (63x^3 - 70x^3 + 15x)/8; \\ L_6 &= 231/16x^6 - 315/16x^4 + 105/16x^2 - 5/16; \\ L_7 &= 429/16x^7 - 693/16x^5 + 315/16x^3 - 35/16x; \\ L_8 &= 6435/128x^8 - 3003/32x^6 + 3465/64x^4 - 315/32x^2 + 35/128; \\ L_9 &= \frac{12155}{128x^9} - \frac{6435}{32x^7} + \frac{9009}{64x^5} - \frac{1155}{32x^3} + \frac{315}{128x}. \end{aligned} \quad (2)$$

Let the coordinates of the initial blade profile be given by a set of points $y_i^c = y^c(x_i)$, $i = 1, \dots, N$. Substituting values x_i in functions (2), we obtain matrix X of size $N \times 10$. The coefficients of the approximating polynomial for the given blade profiles were found by the least squares method from the minimum condition of the sum of squared deviations of the given values y_i^c and calculated through the regression equation (1):

$$\hat{a}_i = \sum_{i=1}^N (y_i^c - y(a_i, x_i))^2 \rightarrow \min. \quad (3)$$

The estimates of coefficients \hat{a}_i were calculated using the well-known regression analysis formula:

$$a = (X^T X)^{-1} X^T y, \quad (4)$$

where a — notation for the vector of coefficient estimates; y — for the vector of points of given profile y_i^c .

The approximation accuracy was estimated by the determinacy coefficient of the model (the coefficient of determination R^2), which, with a good approximation, should be close to unity:

$$R^2 = 1 - \frac{\sum (y(x_i) - y_i^c)^2}{\sum (\bar{y}^c - y_i^c)^2}, \quad (5)$$

where \bar{y}^c — average value of y_i^c .

In design practice, it is customary to describe the leading and trailing edges of the contour of the blades with the radii of circles. In this regard, the coordinates of the points of the approximated profiles between the arcs of the circles of the leading and trailing edges were considered in this paper. For the purposes of approximation, the contour of the blade in question was assumed to be horizontal, so that the blade chord line coincided with the abscissa axis of the Cartesian coordinate system. To preserve the orthogonality condition of the models, size normalization is mandatory. In this regard, all dimensions were normalized by the length of the blade chord, so that the abscissas of the profile points lay in the range of 0.1. This provided the orthogonality of functions (2) with coefficients calculated by formulas (4).

Research Results. Table 1 shows the coefficients of approximating polynomials for blade profiles belonging to different types of GTE to study the heat fatigue of a thermal-protective coating consisting of two metal and ceramic layers: profile of the compressor blade C8626 [13], profile of the NASA blade of a highly efficient high-pressure GTE [18], and profile of the simulator blade used in [19].

Table 1

Coefficients of approximating polynomials for blade profiles from different sources

Coefficients	[13]		[18]		[19]	
	suction side	pressure side	suction side	pressure side	suction side	pressure side
a_0	142.4250	-123.0993	-1275.6471	717.8336	-1043.6707	527.0915
a_1	-374.3446	324.9875	3328.6126	-1868.9670	2719.5055	-1369.9895
a_2	477.9332	-417.7186	-4181.1239	2338.1048	-3406.1466	1707.9198
a_3	-444.4554	392.7204	3794.0526	-2108.4202	3077.0694	-1531.8025
a_4	324.6819	-292.0489	-2684.7257	1479.0172	-2164.2992	1066.1471
a_5	-189.2284	174.3673	1502.4170	-818.4219	1201.7203	-583.7501
a_6	86.8260	-82.4103	-654.4877	351.5869	-518.2516	247.3087
a_7	-30.0775	29.5457	211.8930	-111.9355	165.6344	-77.2958
a_8	7.1533	-7.3024	-46.0284	23.8450	-35.3931	16.0493
a_9	-0.9024	0.9652	5.1021	-2.5861	3.8411	-1.6752
R^2	0.9999	0.9993	0.9896	0.9990	0.9982	0.9994

Figure 1 shows the starting points of these profiles and the corresponding approximating lines.

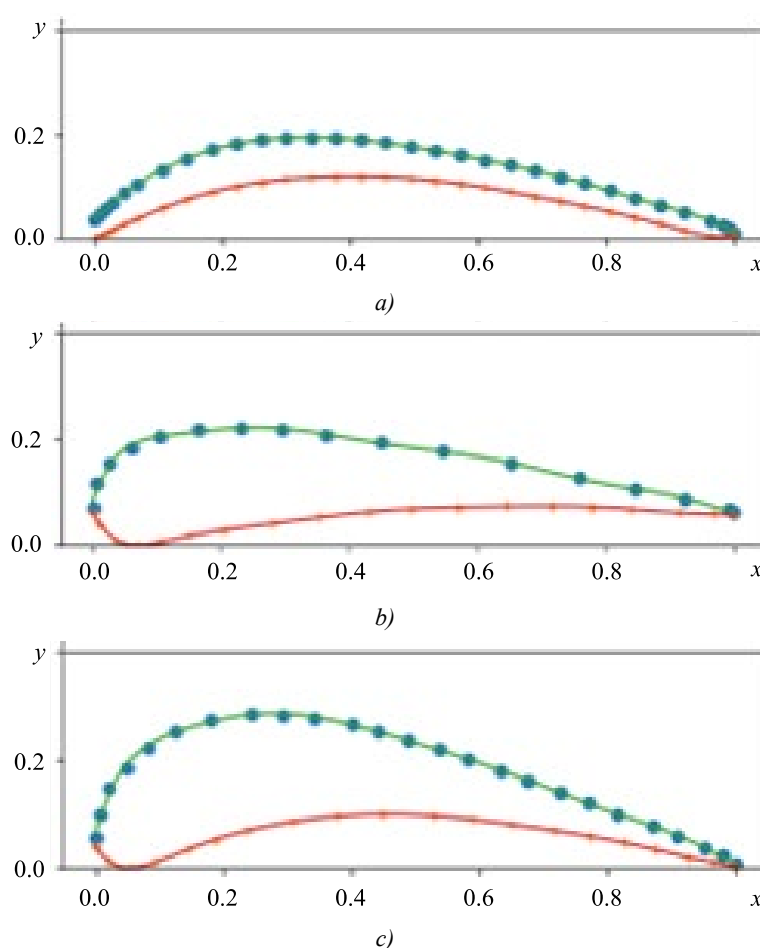


Fig. 1. Initial points and approximating lines of blade profiles presented in Table 1, sources of blade profiles: a — [13]; b — [18]; c — [19]

As mentioned above, the aim of parameterization in this paper is to approximate the profile by a continuous function followed by modeling the distribution of external parameters over the surface of the blade. To illustrate the possibility of solving this problem, we consider a simple two-dimensional model of a blade in a stationary aerodynamic flow, in the approximation of potential flow. In this case, the distribution of the velocities of flow $v(x, y)$ is described by the equation:

$$v = \begin{pmatrix} \frac{\partial \psi}{\partial x} \\ -\frac{\partial \psi}{\partial y} \end{pmatrix}, \quad (6)$$

where function ψ is found from the solution to the Laplace equation:

$$\Delta \psi = 0, \quad (7)$$

which in this case corresponds to the incompressibility condition ($\nabla \cdot v = 0$) and vortex-free flow ($\nabla \times v = 0$).

The boundary condition for function ψ will be equal-zero velocity in the normal direction of the blade surface, which means that ψ is constant on this surface.

We denote the profile line of the blade surface by S and search for a solution to equation (7) in region Ω , bounded by the outer part with respect to S and the inner part with respect to circle C of a sufficiently large diameter, compared to the length of the blade chord, so that the flow is homogeneous on surface C . That is, the conditions are set at the boundary of the domain $\partial\Omega = S \cup C$:

$$\psi|_S = 0, \quad \psi|_C = v_\infty \cdot x^\perp, \quad (8)$$

where v_∞ — uniform flow velocity vector.

After calculating the velocities, the pressure distribution can be found using the Bernoulli equation:

$$p = B - \frac{\rho v^2}{2}, \quad (9)$$

where ρ — gas density; B — Bernoulli's constant, which can be set equal to $p_\infty + \frac{\rho v_\infty^2}{2}$, where p_∞ — pressure at an infinite distance from the blade.

The variational formulation of problem (7) looks like this:

$$\int_{\Omega} \nabla \psi \nabla w = 0, \quad \forall w \in H_0^1(\Omega). \quad (10)$$

The solution to this problem was carried out by the finite element method. For comparison, the calculation was performed for three variants of blade profiles, shown in Table 1, with the same chord length l .

The obtained results were further used in solving the problem of cooling the blade in an aerodynamic flow. Such a task makes sense for thermocyclic testing of coatings on simulator blades. In this case, the problem statement looked as follows:

$$\partial_t T - \nabla \cdot (\kappa \nabla T) + v \cdot \nabla T = 0, \quad (11)$$

where T — temperature; t — time; κ — thermal diffusivity coefficient.

Initial temperature distribution:

$$T(t=0, x) = T_0(x) \quad (12)$$

was assumed to be as follows: inside the blade, a constant temperature was 400°C , ambient temperature was 0°C . The boundary conditions corresponded to the absence of heat flow on the outer contour C :

$$\frac{\partial T}{\partial n} \Big|_{C, v \cdot n > 0} = 0, \quad T|_{C, v \cdot n < 0} = 0. \quad (13)$$

The distribution of flow velocities in problem (11) was calculated when solving problem (10), while the velocity on contour C was assumed to be $v = 10[l/s]$ (length dimension in units of chord length). The thermal conductivity coefficients of the blade and gas were assumed to be 0.1 and 0.01 $[l^2/s]$, respectively.

The program code for solving problems (10), (11) was written in the input language of the universal finite element package FreeFem++ [20].

Figure 2 shows the pressure and temperature distributions calculated as a result of solving problems (11), (12), when the blade cools down for 25 seconds in the aerodynamic flow for the three studied blade profiles shown in Figure 1. Table 2 shows the calculated values of the minimum relative pressures near the blade surfaces and the maximum temperatures of the blades.

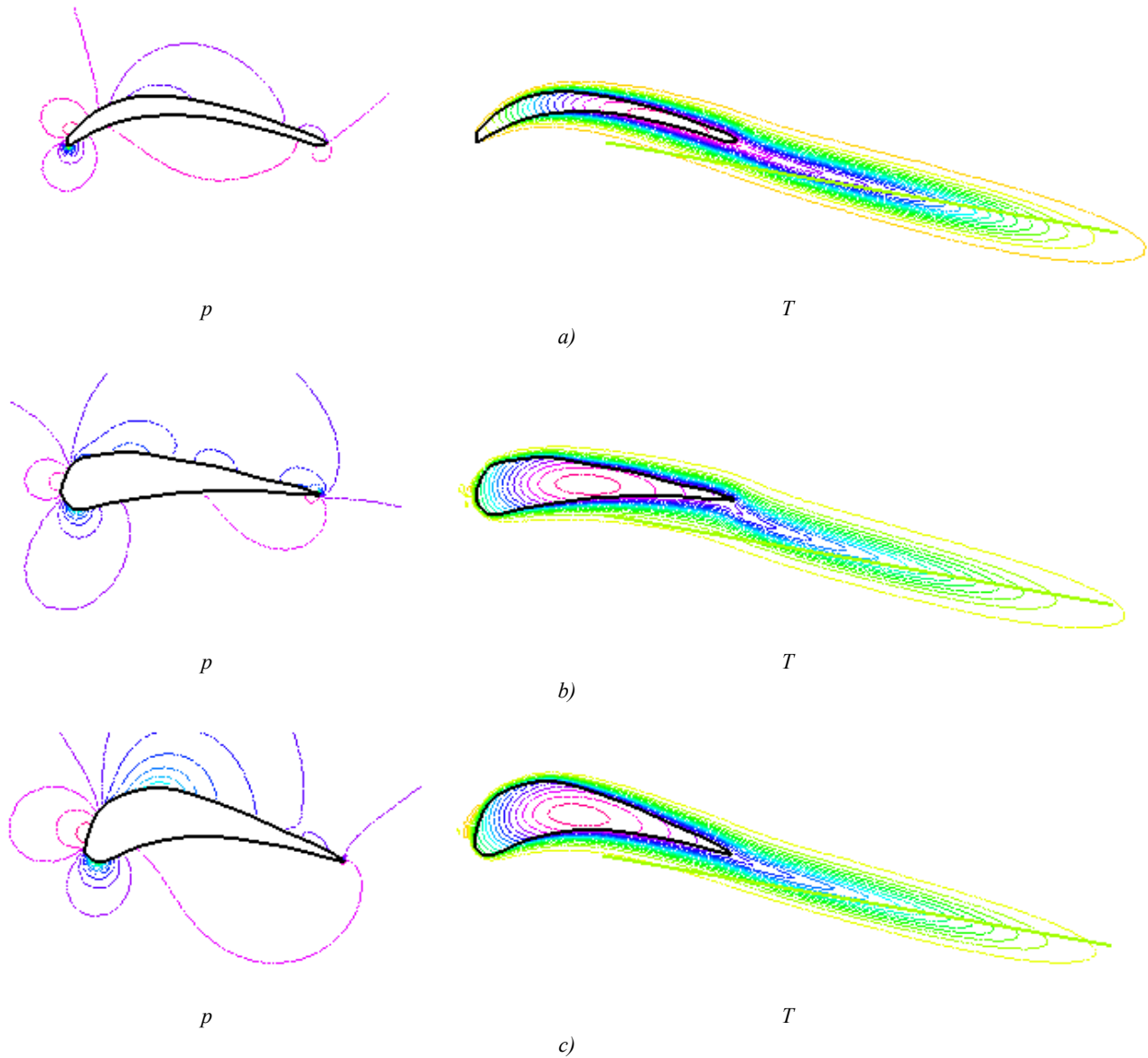


Fig.2. Calculated distributions of pressure (p, left) and temperature (T, right) when modeling the flow and cooling in the flow of the blades of the studied profiles (profile designations — as in Fig. 1). Flow vector direction angle with blade chord direction was 10°

Table 2

Minimum relative pressure near the surface of the blade
and maximum temperature of the blade after 25 s cooling
in the aerodynamic flow

Parameters	Blade profile		
	[13]	[18]	[19]
p_{min} / p_∞	0.599	0.699	0.720
$T_{max}(t = 25), ^\circ\text{C}$	156.9	245.2	263.4

Discussion and Conclusion. Judging by the data presented in Table 1, the coefficients of determination R^2 for all studied blade profiles were close to unity, despite the fact that the shapes of the profiles differed significantly. This confirms the good quality of the approximation and is also illustrated by the data in Figure 1. Thus, the proposed method makes it possible to construct approximating blade profile lines for various types of GTE with high accuracy.

The paper also illustrates the possibility of using approximating functions under calculating the distribution of pressures and temperatures on the surface of the blade on the basis of solution to the problem of gas dynamics. Further, this distribution can be used to optimize the structure of special blade coatings, such as heat-protective coatings. The data shown in Figure 2 and in Table 2, confirm that this task can also be successfully solved. The patterns of pressure and temperature distributions for different blade profiles have common features, but the detailed picture differs. It can be seen, specifically, that the blade of the profile [19], which has a larger cross-sectional area compared to the others, is characterized by a higher value of relative pressure in the area of the outlet edge and a lower cooling rate. This is also illustrated by the data given in Table 2. Since, from the point of view of the strength of the adhesive bond of the coating with the substrate, the most dangerous forces are directed normally away from the surface of the blade, the relative minimum pressure near the surface is relevant. Its values are presented in Table 2. With account to the calculation obtained, it is possible to reasonably approach the design of a special coating for the surface of a blade of a specific profile: adjust the materials and thickness of the coating depending on the degree of loading of individual surface areas.

Note that these calculation results are presented only as an illustration of the possibilities of the proposed profile approximation technique. Therefore, the model of gas dynamics used in the work is quite simplified. In a specific task, it is necessary to use a more rigorous model with parameters corresponding to the specified type and mode of the GTE operation.

Thus, the proposed technique for approximating the blade profile of the GTE, based on the use of orthogonal polynomials, is a convenient tool that provides automating the development of a geometric model of the blade and comparing different types and profiles of blades, solving the corresponding problems of gas dynamics. At the same time, for a given blade profile and working conditions of a GTE, it is possible to obtain a distribution of temperatures and forces acting on the blade surface, which is required to predict the durability of special coatings [21]. Based on this calculation, it is possible to optimize the coating technology by varying its thickness and/or composition, increasing the coefficient of durability in the most dangerous areas.

References

1. Krymov VV, Eliseev YuS, Zudin KI. *Production of Gas Turbine Engine Blades*. Moscow: Mashinostroenie; 2002. 376 p. (In Russ.).
2. Pankov VP, Babayan AL, Kulikov MV, Kossoy VA, Varlamov BS. Heat-Protective Coatings for Turbine Blades of Aircraft Gas Turbine Engines. *Polzunovskiy Vestnik*. 2021;1:161–172.
3. Nirmith Kumar Mishra, Shyam Raja Puppala, Laxmi Teja Kolanu, Jyoshnavi Amudapuram, Ratan Makthal. Design and Analysis of a Gas Turbine Blade. *AIP Conference. Proceedings*. 2023;2492(1):020040. <https://doi.org/10.1063/5.0113346>
4. Cohen H, Rogers GFC, Straznicky P, Saravanamuttoo HHH, Nix A. *Gas Turbine Theory*, 7th Ed. London: Pearson; 2017. 606 p.
5. Jabbar A, Rai AK, Reddy PR, Dakhil MH. Design and Analysis of Gas Turbine Rotor Blade Using Finite Element Method. *International Journal of Mechanical and Production Engineering Research and Development*. 2014;4(1): 91–112.
6. Win Lai Htwe, Htay Htay Win, Nyein Aye San. Design and Thermal Analysis of Gas Turbine Blade. *International Journal of Mechanical and Production Engineering*. 2015;3(7):62–66. URL: https://www.iraj.in/journal/journal_file/journal_pdf/2-165-143653913462-66.pdf (accessed: 14.12.2023).
7. Leloudas SN, Eskantar AI, Lygidakis GN, Nikolos LK. Low Reynolds Airfoil Family for Small Horizontal Axis Wind Turbines Based on RG15 Airfoil. *SN Applied Sciences*. 2020;2:371. <https://doi.org/10.1007/s42452-020-2161-1>
8. Eftekhari S, Al-Obaidi ASM. Investigation of a NACA0012 Finite Wing Aerodynamics at Low Reynold's Numbers and 0° to 90° Angle of Attack. *Journal of Aerospace Technology and Management*. 2019;11(1):e1519. URL: <https://www.scielo.br/j/atm/a/JdnMCtH6R3PhTBZ69YNqNfd/?format=pdf&lang=en> (accessed: 14.12.2023).
9. Pritchard LJ. An Eleven Parameter Axial Turbine Airfoil Geometry Model. In: *Proc. ASME International Gas Turbine Conference and Exhibition. Vol. 1: Aircraft Engine; Marine; Turbomachinery; Microturbines and Small Turbomachinery*. New York: ASME; 1985. <https://doi.org/10.1115/85-GT-219>
10. Mengistu T, Ghaly W, Mansour T. Aerodynamic Shape Optimization of Turbine Blades Using a Design-Parameter-Based Shape Representation. In: *Proc. ASME Turbo Expo 2007: Power for Land, Sea, and Air. Vol. 6: Turbo Expo 2007, Parts A and B*. New York: ASME; 2007. <https://doi.org/10.1115/GT2007-28041>
11. Vinogradov LV, Alekseev AP, Kostjukov AV. Turbine Blade Profile of Curves Bezier. *RUDN Journal of Engineering Research*. 2013;(3):10–15.

12. Vinogradov LV, Mamaev VK, Oschepkov PP. CAD of Turbine Profile Type A3K7 NACA by the Method of Nonlinear Transformation. *RUDN Journal of Engineering Research*. 2017;18(3):299–307.
13. Mamaev VK, Vinogradov LV, Oschepkov PP. Modeling the Set of Blade Profiles of a Gas Turbine Engine. *RUDN Journal of Engineering Research*. 2019;20(2):140–146. <https://doi.org/10.22363/2312-8143-2019-20-2-140-146>
14. Shabliy L, Kolmakova D, Krivtsov A. Parametric Modeling of Blade Machines during Optimization. *Izvestia RAS SamSC*. 2013;15(6–4):1013–1018.
15. Blinov VL, Brodov YuM, Sedunin VA, Komarov OV. Parametric Profiling of 2D Compressor Rows for Multicriteria Optimization Task. *Power Engineering: Research, Equipment, Technology*. 2015;(3–4):86–95.
16. Schnoes M, Nicke E. Exploring a Database of Optimal Airfoils for Axial Compressor Design. *ISABE*. 2017;21493:1–17.
17. Beals R, Wong R. *Special Functions and Orthogonal Polynomials*. Cambridge: Cambridge University Press; 2016. 473p. <https://doi.org/10.1017/CBO9781316227381>
18. Timko LP. *Energy Efficient Engine High Pressure Turbine Component Test Performance Report*. Washington, DC: NASA; 1984. 173 p.
19. Tikhomirova EA, Budinovskiy SA, Zhivushkin AA, Sidokhin EF. Features of Thermal Fatigue Development in Detail, Produced from Heat-Resistant Alloys with Coatings. *Aviation Materials and Technologies*. 2017;48(3):20–25.
20. Hecht F. *FreeFEM Documentation. Release 4.6*. Paris: Sorbonne University; 2021. 673 p.
21. Soloviev ME, Raikhvargher AB, Baldaev SL, Baldaev LKh. Kinetic Model of Destruction of Adhesive Bounding of Power Coating and Metal Host Material. *Science Intensive Technologies in Mechanical Engineering*. 2023;139(1): 9–19. <https://doi.org/10.30987/2223-4608-2023-1-9-19>

About the Authors:

Mikhail E. Soloviev, Dr.Sci. (Phys.-Math.), Professor of the Department of Information Systems and Technologies, Yaroslavl State Technical University (88, Moskovsky Ave., Yaroslavl, 150023, RF), SPIN-code: [7444-3564](#), [ORCID](#), [ResearcherID](#), [ScopusID](#), me_s@mail.ru

Yulia N. Shuleva, Teaching Assistant of the Department of Information Systems and Technologies, Yaroslavl State Technical University (88, Moskovsky Ave., Yaroslavl, 150023, RF), [ORCID](#), [ResearcherID](#), yuliya5153063506@mail.ru

Sergey L. Baldaev, Cand.Sci. (Eng.), Deputy General Director for Technology, “Technological Systems for Protective Coatings” LLC (9A, Yuzhnaya St., Scherbinka, Moscow, RF) SPIN-code: [6954-6407](#), [ORCID](#), [ResearcherID](#), s.baldaev@tspc.ru

Lev Kh. Baldaev, Dr.Sci. (Eng.), General Director, “Technological Systems for Protective Coatings” LLC (9A, Yuzhnaya St., Scherbinka, Moscow, RF), SPIN-code: [8991-5015](#), [ORCID](#), l.baldaev@tspc.ru

Claimed contributorship:

ME Soloviev: formulation of the concept and theoretical part of the study.

YuN Shuleva: data processing, calculations, revision of the article.

SL Baldaev: literature analysis, discussion of the results, revision of the article.

LKh Baldaev: research objective, analysis of the research results, correction of the conclusions.

Conflict of interest statement: the authors do not have any conflict of interest.

All authors have read and approved the final version of manuscript.

Received 25.01.2024

Revised 14.02.2024

Accepted 22.02.2024

Об авторах:

Михаил Евгеньевич Соловьев, доктор физико-математических наук, профессор кафедры информационных систем и технологий Ярославского государственного технического университета (150023, РФ, г. Ярославль, Московский пр-т, 88), SPIN-код: [7444-3564](#), [ORCID](#), [ResearcherID](#), [ScopusID](#), me_s@mail.ru

Юлия Николаевна Шулева, ассистент кафедры информационных систем и технологий Ярославского государственного технического университета (150023, РФ, г. Ярославль, Московский пр-т, 88), [ORCID](#), [ResearcherID](#), yuliya5153063506@mail.ru

Сергей Львович Балдаев, заместитель генерального директора по технологиям ООО «Технологические системы защитных покрытий» (108851, РФ, г. Москва, г. Щербинка, ул. Южная, 9а), SPIN-код: [6954-6407](#), [ORCID](#), [ResearcherID](#), s.baldaev@tspc.ru

Лев Христофорович Балдаев, генеральный директор ООО «Технологические системы защитных покрытий» (108851, РФ, г. Москва, г. Щербинка, ул. Южная, 9а), SPIN-код: [8991-5015](#), [ORCID](#), l.baldaev@tspc.ru

Заявленный вклад авторов:

М.Е. Соловьев — формулировка концепции и теоретической части исследования.

Ю.Н. Шулева — обработка данных, проведение расчетов, редактирование статьи.

С.Л. Балдаев — анализ литературы, обсуждение результатов, редактирование статьи.

Л.Х. Балдаев — постановка задачи, анализ результатов исследований, корректировка выводов.

Конфликт интересов: авторы заявляют об отсутствии конфликта интересов.

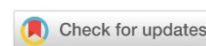
Все авторы прочитали и одобрили окончательный вариант рукописи.

Поступила в редакцию 25.01.2024

Поступила после рецензирования 14.02.2024

Принята к публикации 22.02.2024

INFORMATION TECHNOLOGY, COMPUTER SCIENCE AND MANAGEMENT ИНФОРМАТИКА, ВЫЧИСЛИТЕЛЬНАЯ ТЕХНИКА И УПРАВЛЕНИЕ



UDC 621.311

Research article

<https://doi.org/10.23947/2687-1653-2024-24-1-88-97>

Design of Instrumentation and Control Components of Power Distribution Systems

Yuri A. Klimenko , Yakov E. Lvovich , Andrey P. Preobrazhensky 

Voronezh Institute of High Technologies, Voronezh, Russian Federation

✉ klm71165@mail.ru



EDN: RZSDQA

Abstract

Introduction. In recent years, the development of high-voltage power systems has received a boost due to the need for infrastructural support for priority development areas. Universal models and algorithms are required to implement processes in power components and identify their optimal parameters. However, there are no such solutions. Accordingly, there are no ready-made subsystems with control and optimization algorithms adequate to the tasks under consideration. The objective of the presented research is to develop an optimization subsystem for the design of control and measurement components of power distribution systems.

Materials and Methods. Methods for constructing automated design systems, optimization, system analysis, mathematical modeling, and adaptive control were used. When selecting methods, we proceeded from the fact that the components of power distribution systems consisted of a finite number of elements. The synthesis of a power system includes tens or hundreds of sequential operations. This was taken into account in the developed models and algorithms.

Results. The possibilities of managing and monitoring manufacturing processes (MP) for the production of components of low-voltage power distribution systems were shown in terms of checking the operability and correct functioning of processing equipment. A modular structure was created to allow the integration of CAD output files into the manufacturing processes of energy distribution system components. A functional diagram of a subsystem for control and monitoring of the manufacturing processes of the production of components of power distribution systems was developed. The proposed schematic diagram of production control showed how the data collection subsystem, management system, and operating mechanisms were involved in the control of operations. The multi-level optimization module model created within the framework of this research sequentially optimized the service intensity of the i -th block, the input flow separation coefficients, and the priorities of the original data flows that form the input flow of the i -th block.

Discussion and Conclusion. The combined application of modeling, system analysis, and optimization methods maintains control of the accuracy of the generated power components. The algorithm for controlling electrical loads opens up opportunities for creating a mathematical model of a power supply system that combines management, control, and monitoring, which ultimately leads to an improvement in the quality of electric power. The solution can be in demand in the development of power systems of priority development areas.

Keywords: improvement of electric power quality, power distribution system, data flow in the optimization module, multi-level optimization model

Acknowledgments. The authors would like to thank colleagues of Voronezh Institute of High Technologies for their help in preparing the manuscript of this article.

For citation. Klimenko YuA, Lvovich YaE, Preobrazhensky AP. Design of Instrumentation and Control Components of Power Distribution Systems. *Advanced Engineering Research (Rostov-on-Don)*. 2024;24(1):88–97. <https://doi.org/10.23947/2687-1653-2024-24-1-88-97>

Проектирование контрольно-измерительных компонент распределительных энергетических систем

Ю.А. Клименко , Я.Е. Львович , А.П. Преображенский 

Воронежский институт высоких технологий, г. Воронеж, Российская Федерация

✉ klm71165@mail.ru

Аннотация

Введение. В последние годы развитие высоковольтных энергетических систем получило новый импульс в связи с необходимостью инфраструктурного обеспечения территорий опережающего развития. Нужны универсальные модели и алгоритмы для реализации процессов в энергетических компонентах и выявления их оптимальных параметров. Однако такие решения отсутствуют. Соответственно, нет готовых подсистем с алгоритмами управления и оптимизации, адекватными рассматриваемым задачам. Цель представленного исследования — разработка подсистемы оптимизации при проектировании контрольно-измерительных компонент распределительных энергетических систем.

Материалы и методы. Используются методы построения автоматизированных систем проектирования, оптимизации, системного анализа, математического моделирования и адаптивного управления. При выборе методов исходили из того, что компоненты распределительных электрических систем состоят из конечного числа элементов. Синтез энергетической системы включает десятки или сотни последовательных операций. Это учтено в разработанных моделях и алгоритмах.

Результаты исследования. Показаны возможности управления и контроля технологических процессов (ТП) производства компонент низковольтных распределительных энергетических систем в плане проверки работоспособности и корректности функционирования технологического оборудования. Создана модульная структура, позволяющая интегрировать выходные файлы САПР в процессы производства. Разработана функциональная схема подсистемы управления и контроля технологических процессов производства компонент распределительных энергетических систем. Предложенная принципиальная схема контроля производства показывает, каким образом в контроле операций задействованы подсистема сбора данных, система управления и управляющие механизмы. Созданная в рамках данной работы многоуровневая модель модуля оптимизации последовательно оптимизирует интенсивность обслуживания i -го блока, коэффициенты разделения входного потока и приоритеты исходных потоков данных, образующих входной поток i -го блока.

Обсуждение и заключение. Комплексное применение методов моделирования, системного анализа, оптимизации обеспечивает контроль точности формируемых энергетических компонент. Алгоритм управления электрическими нагрузками открывает возможности для создания математической модели системы энергоснабжения, которая объединяет управление, контроль, мониторинг, что в конечном счете ведет к улучшению качества электроэнергии. Решение может быть востребовано при развитии энергетических систем территорий опережающего развития.

Ключевые слова: улучшение качества электроэнергии, распределительная энергетическая система, поток данных в модуле оптимизации, многоуровневая оптимизационная модель

Благодарности. Авторы благодарны Воронежскому институту высоких технологий за помощь при подготовке статьи.

Для цитирования. Клименко Ю.А., Львович Я.Е., Преображенский А.П. Проектирование контрольно-измерительных компонент распределительных энергетических систем. *Advanced Engineering Research (Rostov-on-Don)*. 2024;24(1):88–97. <https://doi.org/10.23947/2687-1653-2024-24-1-88-97>

Introduction. The creation and development of power distribution systems with the required parameters is an important science and technology task. Active theoretical and applied developments are underway in the high-voltage energy area. In recent years, priority development areas have been formed and developing in Russia. These are production clusters that need to be provided with high-quality infrastructure, including energy infrastructure. In most cases, we are talking about small settlements that initially lag behind in economic, social and infrastructural terms. The solution of power problems under such conditions should be facilitated by the use of universal models and algorithms that will, in particular, identify the optimal parameters of the components of power processes. Such solutions are not presented in the literature. Accordingly, there are no management and optimization subsystems developed on their basis.

The high cost of modern power equipment should be noted. Its effectiveness assumes that the setting provides optimal parameters for the operation of the components. When designing monitoring-and-measuring components of power

distribution systems, it is important to specify control and tolerance points regarding the quality parameters of the corresponding process steps [1]. During production, processing sequence should be determined.

Let us consider the last situation, i.e., production, in greater detail. A large number of process steps can create difficulties associated with control and management [2]. Therefore, when releasing components of power equipment, it is important to specify the requirements for the subsystem of control and optimization of manufacturing processes (MP). Such a subsystem is used in the manufacture of prototypes. Another recommended approach is the examination of power modules. It provides determining adequate output parameters. It is also important to take into account the influence of external actions [3].

The selection of algorithms should be based on the methods of mathematical statistics. This makes it possible to control and optimize the quality parameters of processes and use appropriate management procedures [4]. Versatility should be noted as an advantage of the algorithms. By the provision of it, within the framework of a systematic approach, it is possible to plan and implement research in this direction [5]. It is known that the start of manufacturing new power equipment is not always provided with the required statistical data. In this case, it makes sense to apply adaptive management methods. Self-optimization procedures are convenient to use when there are changes in the requirements for MP, as well as when external conditions vary [6]. The objective of the presented research is to create an optimization subsystem in the design of monitoring-and-measuring components of power distribution systems.

Materials and Methods. Methods of creating automated systems for design, optimization, system analysis, mathematical modeling, and adaptive management are used. When selecting methods, it was taken into account that the components of power distribution systems consist of a finite number of elements. In more detail, the task can be presented as follows. It is planned to produce equipment components for power distribution systems. It is required to create a subsystem that will manage and optimize engineering MP. The analysis provides selecting and using the adaptive control method of such a subsystem [7].

The synthesis of the entire power system involves dozens or hundreds of sequential operations, and this is taken into account in modeling and algorithmization.

In the production of components of power complexes, it is proposed to use simulation modeling based on the MP optimization module [8]. At the same time, the quality of the components is considered in relation to the parameters of the created power distribution system. Uncontrolled MP parameters can also be taken into account.

Figure 1 shows the integration of computer-aided design (CAD) output files into the production of components of power distribution systems in the form of modules.

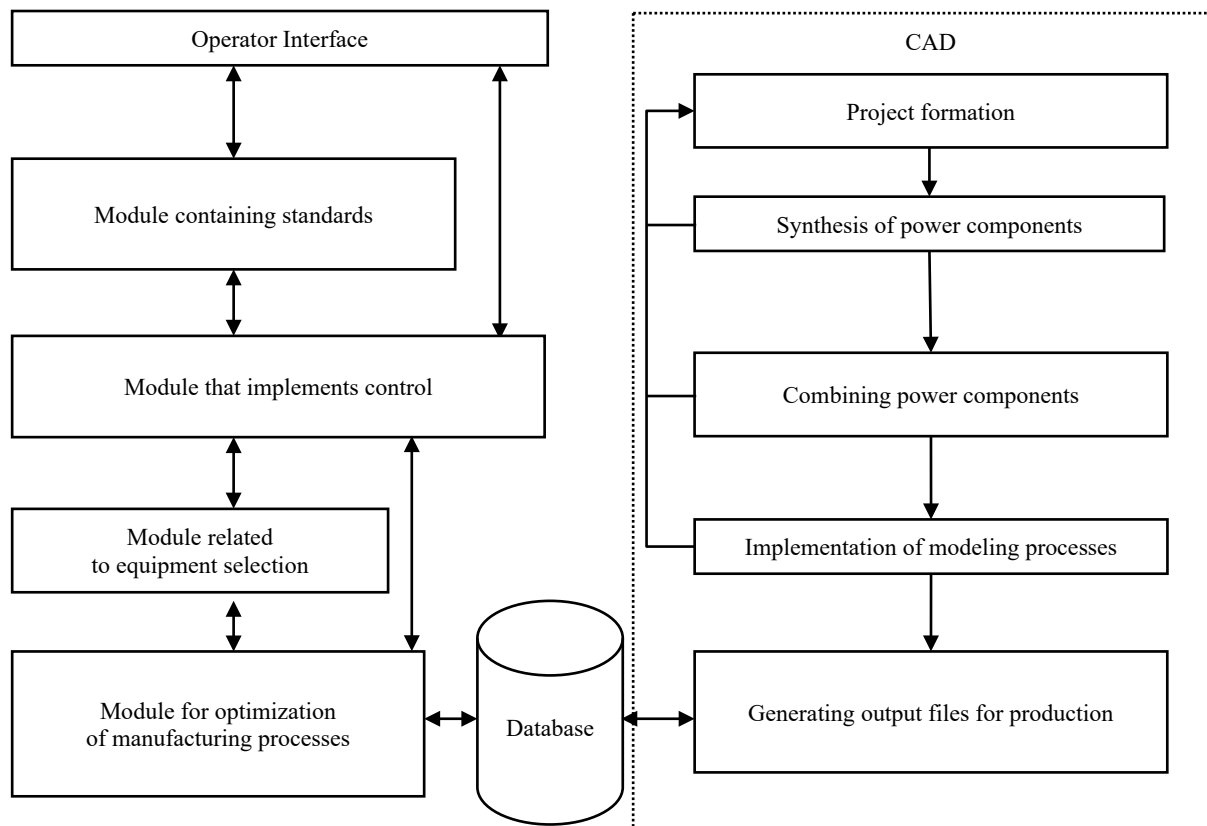


Fig. 1. Modular structure of integration of CAD output files and production of components of power distribution systems

The control module provides transmitting the process data to an automated control system (ACS) [9]. During the MP, operators receive data on the reliability of the power components being created. At the same time, the results of the physicotchnical expertise are taken into account, and the optimization module is used. The impact of various factors on the efficiency of power equipment is monitored. The data on previously manufactured components are analyzed. In further developments, the proposed module will make it possible to save and take into account several types of hardware settings. They can be used in production to determine tolerance ranges for each process step [10].

The ACS should include four modules.

1. Subsystem of interoperative control support.
2. Transport operations management module.
3. Subsystem for managing MP modes.
4. Subsystem of process steps management.

Such ACS translates information from designers to production. In practice, various quality management systems are used for the components of power distribution systems being created, including those with production control subsystems [11].

In this paper, an automated subsystem for control and optimization of monitoring-and-measuring components of power complexes is proposed. It provides different types of impacts on MP for any stage of production. The previously obtained data allow the subsystem to reduce the number of defective elements, i.e., to improve the quality of products.

Figure 2 illustrates the structure of this subsystem. It was formed on the basis of the requirements for the efficiency of production processes. In addition, different types of components being formed were taken into account. Previously used values of MP parameters can be applied for analysis. The operator has the opportunity to change them.

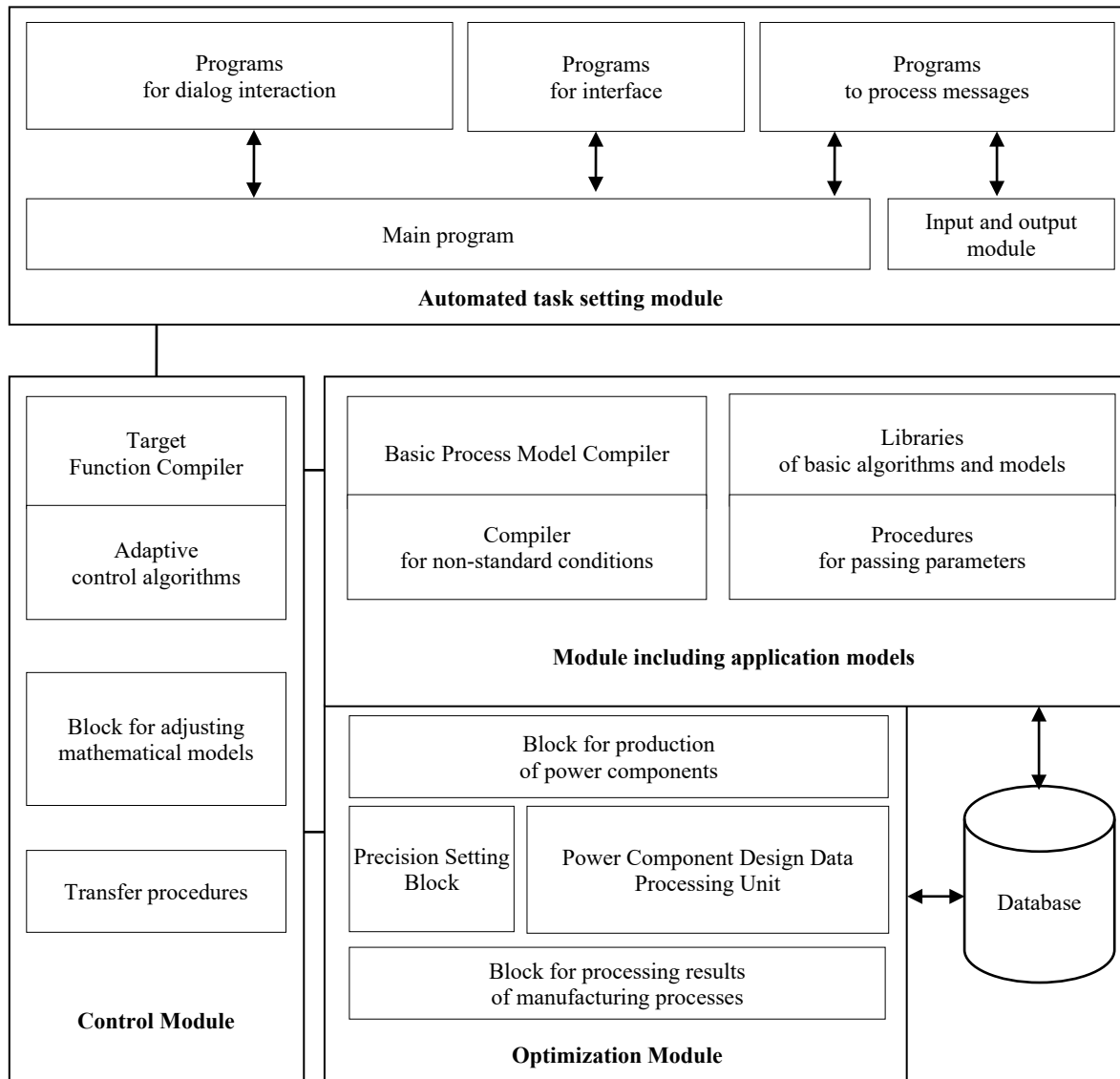


Fig. 2. Functional diagram of subsystem for management and control of MP components of power distribution systems

The main program is considered as the basis of the automated task module, and for the processes of setting up and transferring MP parameters. An analysis is carried out to identify the need to adjust equipment settings. A special role is played by programs for processing messages and supporting dialog interaction. They make it possible to adjust the MP manually. The operator has the ability to download current settings from the database. They are set manually or through an input and output module.

The optimization module generates a list of top-level management operations for a specific MP. Then, the operations are analyzed, the optimization accuracy and production parameters are set. According to the information received, the application models are transferred to the module. At the same time, analytical and statistical models of basic MP operations are used. For each such operation, the input and output parameters are determined in the corresponding part of the system.

The control module develops and refines the mathematical model of production processes [12]. It is then used to determine the tolerance for quality parameters within the framework of individual process steps. The model is developed in the module of applied models. The automated task module is designed for procedures to maximize the target function.

The received settings for equipment, management and process parameters are recorded in the database. Then, during the production of power components, the process is analyzed, and the current settings of the equipment elements are adjusted.

The study of MP management and control is required to verify the operability of processing equipment, the correctness of its operation and the organization of production.

Research Results. The monitoring-and-measuring components of power distribution systems consist of a finite number of elements. The component production involves dozens or hundreds of sequential operations and relies on solving the problem of forming components with maximum accuracy. At the same time, uncontrolled parameters should be taken into account for any step. For this purpose, correlation analysis, adaptive management, and optimization are used.

Particular models are combined into a general model for creating power components, which can be adjusted (e.g., with account of experimental testing of equipment or requirements for specific components). Some algorithms are created on the basis of the results of monitoring the formation of components and, as a result, provide improving the quality with changes in operating modes. The main indicators of the efficiency and stability of production can be considered the values of the output indicator of valid power components.

The following are three key features of managing the processes of component formation.

1. It is important to maintain the specifications at the required levels for input and output components for different batches.

2. Algorithms affect the shutdown of each processing step.

3. Constant wear of equipment requires regular adjustment of process parameters.

We describe the model based on the MP of creating power components [13].

Suppose that the $(i-1)$ -th operation of MP is being considered:

$$u_i = F(u_{i-1}, v_i). \quad (1)$$

Here, u_i — quality parameter of the power components of the current operation; v_i — production option.

It is important to take into account that in practice not the quality parameters of the power components are critical, but the design parameters that depend on them (e.g., highspeed response). Then:

$$g_i = F^*(u_{i-1}, k_i). \quad (2)$$

Here, g_i — controlled parameters of the current operation; k_i — design parameters.

The production of power components is described as a trajectory with a change of state. According to the final state, the adjustment of the MP is carried out. Within the framework of trajectory management, the corresponding tasks are solved. The optimal solution is selected from a variety of solutions [14]. At the same time, the specified characteristics of the generated power components are taken into account. In this case, the control actions should provide the best match of the required and output characteristics of the components being formed K_i^n . Here, n — number of MP operations.

The basic industrial technology determines the initial data, the processing sequence, and sets limits on control variables.

When selecting the number of MP operations $(n-1)$, the target function is as follows:

$$F_q = G(K_1 \dots K_n, c_1 \dots c_n). \quad (3)$$

Here, $c_1 \dots c_n$ — selectable process control variables.

We introduce parameter φ_i , which characterizes the corresponding goals associated with the i -th operation. For $(n-1)$ operations in MP, the following expression is valid:

$$f_{n-1}(K_n) = \min_{c_{n-1}} (\varphi_{n-1}[K_n, c_{n-1}] + f_{n-2}(K_{n-1})) = \min_{c_{n-1}} C_{n-1}(K_n, c_{n-1}). \quad (4)$$

If there is one operation in the MP, then:

$$f_1(K_2) = \min_{c_1}(K_2, l_1). \quad (5)$$

Significantly,

$$f_0(K_1) = 0. \quad (6)$$

Under such conditions for MP, the target function is defined as follows:

$$C_1(K_2, c_1) = \varphi(K_2, c_1). \quad (7)$$

The schematic diagram in Figure 3 shows how the power components are generated. The MP data acquisition subsystem (sensor system and instrumentation) transmits the values of input and output parameters for each processing step n to the control system. This happens before and after each step n ($n = 0, 1, 2, \dots, m$). The values are recorded in the data collection subsystem.

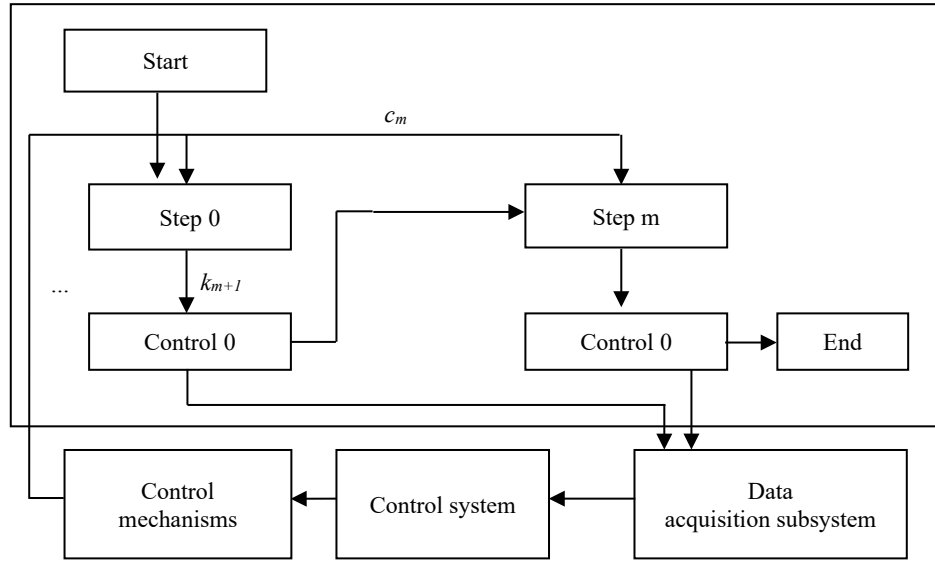


Fig. 3. Schematic diagram of control of production of power components

In total, m steps are considered. The work ends after performing $m+1$ steps.

The use of the optimization model makes it possible to form technologies for converting the input data flow (x_{BX}). The main channels for processing input data are:

- process department (PD);
- production department (PRD), $n = 1$;
- N of structural subdivisions (SS^n).

Figure 4 shows the block diagram of the transformation of the input data flow.

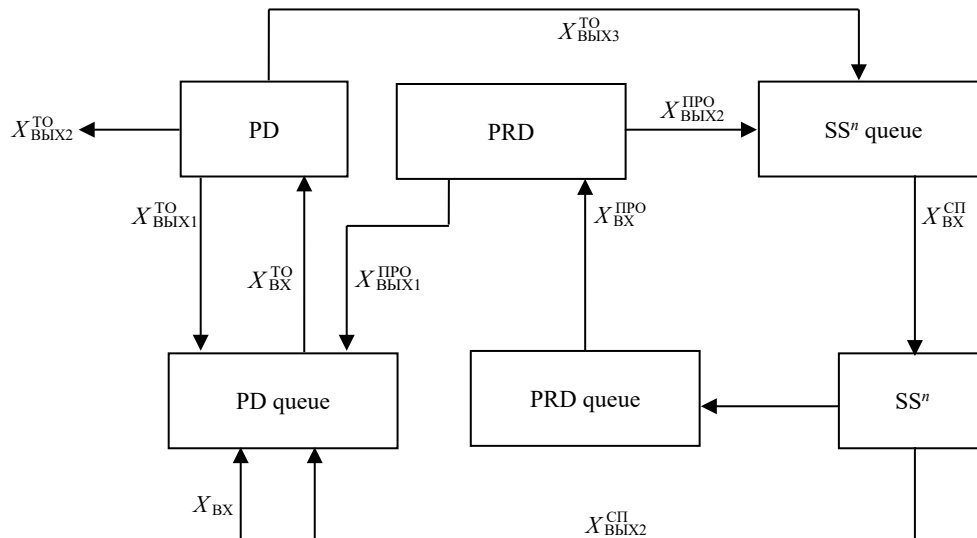


Fig. 4. Block diagram of data flow distribution in the optimization module

Here, X_{BX} — input data flow to be processed in PD; $X_{BbIX1}^{TO}, X_{BbIX2}^{TO}, X_{BbIX3}^{TO}$ — data flows at the output of PD; X_{BbIX}^{IPO} — input data flow for processing in PRD; $X_{BbIX1}^{IPO}, X_{BbIX2}^{IPO}$ — data flow at the output of PRD; X_{BX}^{CI} — input data flow for processing in the n -th ($n = 1, N$) SSⁿ; $X_{BbIX1}^{CI}, X_{BbIX2}^{CI}$ — data flows at the output of SSⁿ. At the same time, the flow at the output of the optimization module $X_{BbIX} = X_{BbIX2}^{TO}$.

The scheme efficiency is determined by three factors.

1. For all types of input data flows for any block in the system, the intensity and maintenance mechanisms are considered.
2. Input flow for each block is divided into several output data flows.
3. Depending on the level and priority, it is needed to observe the data queue in each block.

It is possible to analyze these processes using a multilevel optimization model (Fig. 5).

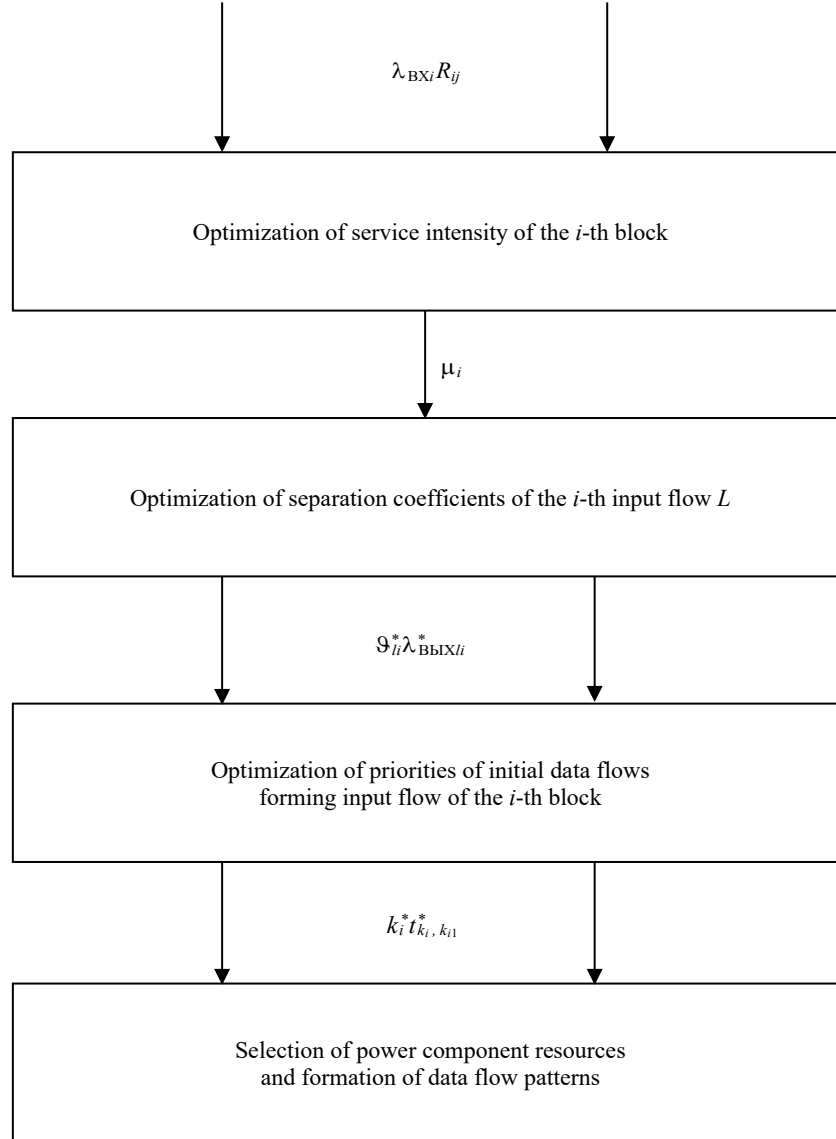


Fig. 5. Multilevel optimization model of the optimization module

Here, λ_{BXi} , $i = \overline{1, I}$ — intensity of the input data flow associated with X_{BXi} i -th block; $i = \overline{1, I}$ — block numbers for power components; R_{ij} — guaranteed level for the j -th ($j = \overline{1, J}$) resource in the i -th block; $j = \overline{1, J}$ — numbers related to resource provision; μ_i , $i = \overline{1, I}$ — intensity of data management associated with the i -th block; μ_i^* — optimal intensity value; v_{li} — data separation coefficient of the i -th flow to the 1st output; $l = \overline{1, L}$ — designation of numbers in output flows; v_{li}^* — optimal value in the separation coefficient; $k = \overline{1, K}$ — values of the numbers of source data flows for the input flow in the i -th block; $k^* = \overline{1, K^*}$ — numbers of the source flows that will show the optimal priorities; $t_{ki, ki1}$ — time of interruption of data k_i management by data k_{i1} with mixed priorities; $t_{ki, ki1}^*$ — optimal time for interruption of data k_i management by data k_{i1} .

The optimal pattern of priorities for the lower level is determined. The optimality problem is solved according to the Bellman principle, i.e., the optimality principle is proved to the contrary. It is accepted that part of the process is not optimal according to the quality criterion. The criteria of the initial and optimal processes are compared. Based on this comparison, a conclusion is drawn about the proof of the optimality principle [15]. The selection is made during the processing of different types of data according to optimal, absolute, and mixed priorities. The task scheduler can use various algorithms to make decisions about the order of tasks. In some cases, optimal priorities are useful, in others, absolute ones. Tasks with a higher priority are completed earlier, and, accordingly, the response to them is faster. When combining (mixing) priorities for individual applications, non-priority service is possible.

The optimal mechanism for dividing into several output flows at the middle level is selected by the input data flow for each block.

At the upper level, the following are selected:

- input flow balanced in intensity;
- resource provision of the module for optimizing the intensity of management for each block.

In this case, a gradient approach can be applied.

For energy components, a three-level parametric optimization is used in the selection of resources and the formation of data flow patterns for each block.

Discussion and Conclusion. A subsystem for the management and control of MP for the production of monitoring-and-measuring components of power distribution systems is created. It provides data collection and defect analysis depending on the hardware settings. In addition, the solution can obtain requirements for equipment settings to achieve a given level of component quality.

Optimization of the design is required, specifically, when modeling the control of electric loads to improve the quality parameters of electrical power in 0.4 kV power distribution networks. The algorithm of the electric load control process was studied in an adaptive system of control and management of the power quality [15]. Its operability has been confirmed; therefore, the solution can be used in the development of equipment for 0.4 kV distribution networks. In addition, this algorithm can be applied to develop a mathematical model of the power supply system, which is a set of functions: monitoring, management, control. The use of modeling, system analysis and optimization methods, maintains control of the accuracy of the generated power components. Adequate implementation of this approach can improve the quality of electric power.

The results of the presented research are practically applicable, in particular, for solving problems related to the power supply of the priority development areas.

References

1. Yizhou Zhou, Mohammad Shahidehpour, Zhinong Wei, Zhiyi Li, Guoqiang Sun, Sheng Chen. Distributionally Robust Unit Commitment in Coordinated Electricity and District Heating Networks. *IEEE Transactions on Power Systems*. 2020;35(3):2155–2166. <https://doi.org/10.1109/TPWRS.2019.2950987>
2. Hechuan Liu, Xiaoxin Zhou, Xiaoyu Yang, Yalou Li, Xiong Li. Influence Evaluation of Integrated Energy System on the Unit Commitment in Power System. *IEEE Access*. 2020;8:163344–163356. URL: <https://ieeexplore.ieee.org/stamp/stamp.jsp?arnumber=9181509> (accessed: 25.11.2023).
3. Rakipour D, Barati H. Probabilistic Optimization in Operation of Energy Hub with Participation of Renewable Energy Resources and Demand Response. *Energy*. 2019;173:384–399. <https://doi.org/10.1016/j.energy.2019.02.021>
4. Farahani SS, Bleeker C, Wijk A, Lukszo Z. Hydrogen-Based Integrated Energy and Mobility System for a Real-Life Office Environment. *Applied Energy*. 2020;264:114695. <https://doi.org/10.1016/j.apenergy.2020.114695>
5. Sadeghi H, Rashidinejad M, Moeini-Aghaie M, Abdollahi A. The Energy Hub: An Extensive Survey on the State-of-the-Art. *Applied Thermal Engineering*. 2019;161:114071. <https://doi.org/10.1016/j.applthermaleng.2019.114071>
6. Junkai Liang, Wenyuan Tang. Interval Based Transmission Contingency-Constrained Unit Commitment for Integrated Energy Systems with High Renewable Penetration. *International Journal of Electrical Power & Energy Systems*. 2020;119:105853. <http://doi.org/10.1016/j.ijepes.2020.105853>
7. Klimenko YuA, Preobrazhensky AP. Simulation of the Control Process Electric Loads in the Distribution Network of 0.4 kv. *Control Systems and Information Technologies*. 2021;86(4):95–100. <https://doi.org/10.36622/VSTU.2021.86.4.020>
8. Alqunun K, Guesmi T, Albaker AF, Alturki MT. Stochastic Unit Commitment Problem, Incorporating Wind Power and an Energy Storage System. *Sustainability*. 2020;2(23):10100. <https://doi.org/10.3390/su122310100>

9. Shuai Lu, Wei Gu, Ke Meng, Zhaoyang Dong. Economic Dispatch of Integrated Energy Systems with Robust Thermal Comfort Management. *IEEE Transactions on Sustainable Energy*. 2021;12(1):222–233. <https://doi.org/10.1109/TSTE.2020.2989793>
10. Voropai NI, Stennikov VA, Barakhtenko EA, Voitov ON. Methodology of Demand Management of Electricity and Heat in an Integrated Energy System with Active Consumers. *Proceedings of the RAS. Power Engineering*. 2020;4:11–23. <https://doi.org/10.31857/S0002331020040081>
11. Antonov SN, Adoshev AI. Experience of Conducting Energy Audits of State and Municipal Objects. *Agricultural Bulletin of Stavropol Region*. 2014;13(1):49–52. URL: <https://cyberleninka.ru/article/n/opyt-provedeniya-energeticheskikh-obsledovaniy-gosudarstvennyh-i-munitsipalnyh-obektov/viewer> (accessed: 25.11.2023).
12. Antonov SN, Adoshev AI, Sharipov IK. Energy Audit of Agricultural Enterprises. In: *Proc. 78th Sci.-Prac. Conf. "Methods and technical means of increasing the efficiency of the use of electrical equipment in industry and agriculture"*. Stavropol: AGRUS; 2014. P. 26–29. (In Russ.).
13. Mo Zo Twe. Adaptive Control System for a Cluster of Alternative Energy Sources. In: *Proc. 19th All-Russian Interuniversity Sci.-Tech. Conf. Of Students and Postgraduates "Microelectronics and Computer Science"*. Moscow: MIET; 2012. P. 180. (In Russ.).
14. Kirikova EA, Razzhivina AA. Risk Assessment of Energy Saving Projects Based on Simulation Methods. In: *Proc. XII Int. Sci.-Prac. Conf. "Russian Regions in the Focus of Change"*. Ekaterinburg: UrFU; 2017. P. 428–434. (In Russ.).
15. Mo Zo Twe. Development of Adaptive Algorithms for Managing the Energy Complex. *Defense Complex. Interindustry Scientific and Technical Journal*. 2011;4:48–51. (In Russ.).

About the Authors:

Yuri A. Klimenko, Postgraduate student of the Information Systems and Technologies Department, Voronezh Institute of High Technologies (73-A, Lenin St., Voronezh, 394043, RF), SPIN-code: [8457-7141](#), [ORCID](#), klm71165@mail.ru

Yakov E. Lvovich, Dr.Sci. (Eng.), Professor of the Information Systems and Technologies Department, Voronezh Institute of High Technologies (73-A, Lenin St., Voronezh, 394043, RF), SPIN-code: [9029-3251](#), [ORCID](#), [ResearcherID](#), office@vivt.ru

Andrey P. Preobrazhensky, Dr.Sci. (Eng.), Professor of the Information Systems and Technologies Department, Voronezh Institute of High Technologies (73-A, Lenin St., Voronezh, 394043, RF), SPIN-code: [2758-1530](#), [ResearcherID](#), app@vivt.ru

Claimed contributorship:

YuI. Klimenko: description of the construction of the modular structure of the system.

YaE Lvovich: description of the construction of the functional structure of the system.

AP Preobrazhensky: description of the multilevel optimization model of the optimization module.

Conflict of interest statement: the authors do not have any conflict of interest.

All authors have read and approved the final version of the manuscript.

Received 13.12.2023

Revised 09.01.2024

Accepted 15.01.2024

Об авторах:

Юрий Алексеевич Клименко, аспирант кафедры информационных систем и технологий Воронежского института высоких технологий (394043, РФ, г. Воронеж, ул. Ленина, 73а), SPIN-код: [8457-7141](#), [ORCID](#), klm71165@mail.ru

Яков Евсеевич Львович, доктор технических наук, профессор кафедры информационных систем и технологий Воронежского института высоких технологий (394043, РФ, г. Воронеж, ул. Ленина, 73а), SPIN-код: [9029-3251](#), [ORCID](#), [ResearcherID](#), office@vivt.ru

Андрей Петрович Преображенский, доктор технических наук, профессор кафедры информационных систем и технологий Воронежского института высоких технологий (394043, РФ, г. Воронеж, ул. Ленина, 73а), SPIN-код: [2758-1530](#), [ResearcherID](#), app@vivt.ru

Заявленный вклад авторов:

Ю.А. Клименко — описание построения модульной структуры системы.

Я.Е. Львович — описание построения функциональной структуры системы.

А.П. Преображенский — описание многоуровневой оптимизационной модели модуля оптимизации.

Конфликт интересов: авторы заявляют об отсутствии конфликта интересов.

Все авторы прочитали и одобрили окончательный вариант рукописи.

Поступила в редакцию 13.12.2023

Поступила после рецензирования 09.01.2024

Принята к публикации 15.01.2024

INFORMATION TECHNOLOGY, COMPUTER SCIENCE AND MANAGEMENT ИНФОРМАТИКА, ВЫЧИСЛИТЕЛЬНАЯ ТЕХНИКА И УПРАВЛЕНИЕ



УДК 51-76, 004.424.4

Research article

<https://doi.org/10.23947/2687-1653-2024-24-1-98-108>

Computer Program for Primer Design for Loop-Mediated Isothermal Amplification (LAMP)

Liana U. Akhmetzianova 

Ufa State Petroleum Technological University, Ufa, Russian Federation

✉ www.lianab@mail.ru

EDN: TRWNOM

Abstract

Introduction. To date, numerous methods of nucleic acid amplification have been proposed, and each method has a number of advantages and disadvantages. One of the most popular methods is Loop-mediated isothermal AMplification (LAMP). Unlike thermocyclic reactions, such as PCR (polymerase chain reaction), which require three temperature changes and expensive equipment, in LAMP, the entire reaction takes place at one and the same temperature and at the maximum rate possible. An important component of LAMP is primers (usually 20–25 nucleotides), which need to be matched to a specific part of the nucleotide sequence. It is known that DNA sequence contains four nucleotides: A — adenine and T — thymine, G — guanine and C — cytosine. There is a huge variety of permutations of these nucleotides, and it is practically impossible to analyze such a large amount of data manually. Therefore, there is a need to use modern computer technologies. More than 150 computer programs have been proposed for the design of PCR primers, while for LAMP primers there are less than 10 of them, and each of them has a number of drawbacks, e.g., in terms of the length of the analyzed site. Therefore, this work is aimed at developing a new domestic computer program for the design of specific primers for LAMP.

Materials and Methods. The primer search algorithm was based on a linear search for a substring in a string, taking into account the criteria of primer selection for LAMP. The program complex of LAMP-primer design was implemented in Python programming language. The bioPython library was used to work with various DNA and RNA, and the Qt framework was used to develop the interface.

Results. A modification of the direct sampling method using a stencil approach was proposed, taking into account the GC composition and annealing temperature of primers depending on their structure. A software package with a friendly interface was developed. It took into account the design criteria of primers: certificates of registration of computer programs (LAMPrimers iQ No. 2022617417 dated April 20, 2022, LAMPrimers iQ_loop No. 2023662840 dated June 14, 2023) were received. The program is in the public domain at <https://github.com/Restily/LAMPrimers-iQ>

Discussion and Conclusion. The developed software packages can be used for research and analysis in molecular biology and genetics, to create diagnostic test systems that provide high sensitivity and reliability of detection of specific DNA and RNA. The software packages can be used in research institutes and laboratories engaged in the amplification of nucleic acids. The results of evaluating the selected sets of primers for the LAMP reaction were tested, and the effectiveness of working sets using the LAMPrimers iQ program was experimentally proven by the example of the detection of genetic material of the SARS-CoV-2 coronavirus.

Keywords: primer design, loop primers, python, C++, loop-mediated isothermal amplification, LAMP

Acknowledgements. The author would like to thank his supervisor Professor I.M. Gubaidullin, Dr.Sci. (Phys.-Math.), and colleagues from the Institute of Biochemistry and Genetics, Ufa Federal Research Center, Russian Academy of Sciences, for the consultations during the execution of the work, as well as for the experimental testing of the results in laboratory conditions together with the author of the article.

Funding information. The research is done with the financial support from RFFI (grant No. 20–37–90091 “Development of a primer design program for Loop AMPlification — loop mediated isothermal amplification based on machine learning technologies”). https://www.rfbr.ru/rffi/ru/contest/o_2088005

For citation. Akhmetzianova LU. Computer Program for Primer Design for Loop-Mediated Isothermal Amplification (LAMP). *Advanced Engineering Research (Rostov-on-Don)*. 2024;24(1):98–108. <https://doi.org/10.23947/2687-1653-2024-24-1-98-108>

Научная статья

Компьютерная программа подбора праймеров для петлевой изотермической амплификации (LAMP)

Л.У. Ахметзянова 

Уфимский государственный нефтяной технический университет, г. Уфа, Российская Федерация

✉ www.lianab@mail.ru

Аннотация

Введение. На сегодняшний день существует множество способов амплификации нуклеиновых кислот и у каждого способа есть ряд достоинств и недостатков. Одним из наиболее популярных способов является петлевая изотермическая амплификация (Loop-mediated isothermal AMPlification, LAMP). В отличие от термоциклических реакций, таких как ПЦР (полимеразная цепная реакция), для которых требуется смена трех температурных режимов и дорогостоящее оборудование, в LAMP вся реакция проходит при одной температуре и с максимальной на данный момент скоростью. Важным компонентом проведения LAMP-амплификации являются праймеры (обычно 20–25 нуклеотидов), которые необходимо подбирать к определенному участку нуклеотидной последовательности. Известно, что последовательность ДНК содержит четыре нуклеотида: А — аденин и Т — тимин, Г — гуанин и Ц — цитозин. Вариантов перестановок этих нуклеотидов огромное множество, и проанализировать вручную такое большое количество данных практически невозможно, поэтому возникает необходимость в использовании современных компьютерных технологий. Для дизайна ПЦР-праймеров предложено более 150 компьютерных программ, в то время как для LAMP-праймеров их менее 10, и каждая из них имеет ряд недостатков, например, по длине анализируемого участка. Поэтому целью данной работы является разработка новой отечественной компьютерной программы дизайна специфичных праймеров именно для LAMP.

Материалы и методы. В основе алгоритма поиска праймеров лежит линейный поиск подстроки в строке с учетом критериев подбора праймеров для LAMP. Программный комплекс дизайна LAMP-праймеров разработан на языке программирования Python. Для работы с различными ДНК и РНК использовалась библиотека bioPython, а для разработки интерфейса — фреймворк Qt.

Результаты исследования. Предложена модификация метода прямого перебора с использованием трафаретного подхода, учитывающего GC-состав и температуру отжига праймеров в зависимости от их структуры. Разработан комплекс программ с дружелюбным интерфейсом, учитывающий критерии дизайна праймеров: получены свидетельства о регистрации программ для ЭВМ (LAMPprimers iQ № 2022617417 от 20 апреля 2022 года, LAMPprimers iQ_loop № 2023662840 от 14 июня 2023 года). Программа есть в открытом доступе по адресу: <https://github.com/Restily/LAMPprimers-iQ>

Обсуждение и заключение. Разработанные программные комплексы могут использоваться для исследований и анализа в области молекулярной биологии и генетики, для создания диагностических тест-систем, обеспечивающих высокую чувствительность и достоверность обнаружения специфических ДНК и РНК. Программные комплексы могут применяться в научно-исследовательских институтах и лабораториях, занимающихся амплификацией нуклеиновых кислот. Результаты оценки подобранных наборов праймеров для реакции LAMP апробированы, и эффективность рабочих наборов с помощью программы LAMPprimers iQ доказана экспериментально на примере обнаружения генетического материала коронавируса SARS-CoV-2.

Ключевые слова: дизайн праймеров, петлевые праймеры, python, C++, петлевая изотермическая амплификация, LAMP

Благодарности. Автор благодарит своего научного руководителя, доктора физико-математических наук, профессора И.М. Губайдуллина и коллег из Института биохимии и генетики УФИЦ РАН за консультации в ходе выполнения работы, а также за экспериментальную апробацию результатов в лабораторных условиях совместно с автором статьи.

Финансирование. Работа выполнена при финансовой поддержке РФФИ в рамках гранта № 20-37-90091 «Разработка программы дизайна праймеров для Loop AMPlification — петлевой изотермической амплификации на основе технологий машинного обучения», https://www.rfbr.ru/rffi/ru/contest/o_2088005

Для цитирования. Ахметзянова Л.У. Компьютерная программа подбора праймеров для LAMP-амплификации. *Advanced Engineering Research (Rostov-on-Don)*. 2024;24(1):98–108. <https://doi.org/10.23947/2687-1653-2024-24-1-98-108>

Introduction. Nucleic acid amplification is a valuable molecular tool not only in fundamental research, but also in applied areas, such as the diagnosis of infectious diseases, hereditary pathologies, establishing kinship, etc. Currently, amplification methods are intensively developing, and their application areas are expanding. The most popular and most frequently used amplification method is polymerase chain reaction (PCR) [1]. PCR is a reaction that takes place under three different temperature conditions: denaturation (95°C), annealing of primers (from 50° to 60°C), elongation (72°C). To quickly change these modes, a special device is needed — a DNA thermocycler [2]. At this, temperature variation in the amplifier does not occur instantly, but starts only when the desired temperature is reached, and this causes artificial containment of the reaction. As a rule, the duration of PCR is 1–1.5 hours.

The second most popular amplification method is loop-mediated isothermal amplification (LAMP) [3]. A water bath or thermostat is sufficient for LAMP, since the reaction takes place at one and the same temperature, and the first results can be seen in 15 minutes.

For both LAMP and any other type of amplification, the key component is primers, which are short sequences of nucleic acid. They serve as a starting point for increasing copies of a specific region of DNA. It is the primers that determine which DNA sequence will be copied.

The main difference of LAMP implementation is the number of primers. For a conventional LAMP, at least four primers are required (two external, two internal), while for a conventional PCR, two are sufficient (direct, reverse).

To increase the specificity and accuracy of the reaction, it is important to select the right primers. For the automatic selection of primers for PCR, more than 150 different computer programs have been developed that provide the selection of primers for any modifications of this reaction [4]. However, there are very few such programs for LAMP, no more than ten, and only two of them are available online. These programs also have a number of disadvantages, such as restrictions on the length of the analyzed sequence; they do not exclude the possibility of formation of homo- and heterodimers of primers, repeats of nucleotides in one primer. And none of the programs take into account the close arrangement of primers in one set, which, in turn, reduces the quality of primers and the accuracy of reaction results [5].

Thus, an urgent task is to develop a new computer program to select (model) high-quality sets of primers for LAMP with tougher conditions for choosing primers for nucleotide sequences of any length.

Materials and Methods. The authors of [3] proposed using two external, F3 (Forward), B3 (Backward), and two internal primers, FIP (Forward Inner Primer), BIP (Backward Inner Primer). It was assumed that the internal primers had double length (FIP: F1c/F2, BIP: B1c/B2) and were annealed at four regions of the nucleotide sequence. Schematically, the location of LAMP primers can be seen in Figure 1.

External primers are only needed at the initial stage. They are designed to limit the analyzed region of the nucleotide sequence and form a single-stranded structure of this region. A pair of internal primers, F1c and B1c, start their work already at the second stage, as they are annealed after the formation of new DNA chains.

Later, the same authors proposed a modified method offering the use of not four, but six primers, annealed already at eight regions of the target nucleotide sequence [7]. It was proposed to add two more loop primers (Loop B, Loop F), which should react at the third stage after the formation of a dumbbell-like DNA structure and anneal between regions F1/F2 and B1/B2, respectively. The use of additional primers implies an increase in sensitivity and reliability of the reaction.

Any amplification reaction has its own sensitivity threshold, and the spread of this indicator is very large due to the fact that numerous factors affect the course of both PCR and LAMP. Some papers have noted that LAMP is significantly more sensitive than PCR. The authors of [8], e.g., claim that LAMP is 10 times more sensitive than PCR. The authors of other studies have found that LAMP is 100 times more sensitive than PCR [9], and in some investigations, this indicator reaches 1,000 times [10].

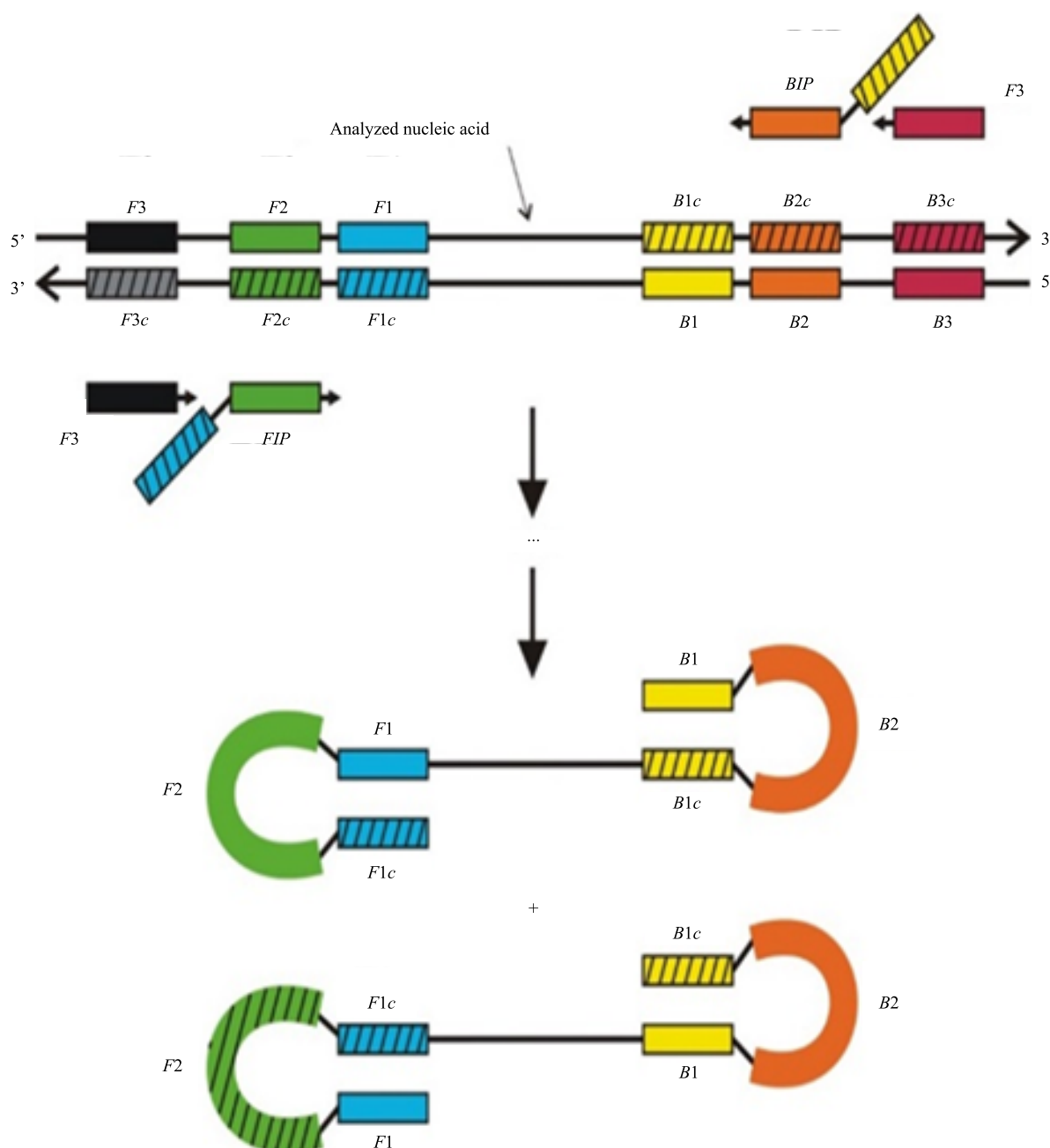


Fig. 1. Schematic arrangement of the annealing regions of external and internal primers for LAMP [6]

In addition to sensitivity, any amplification reaction has another equally important indicator — its specificity. And here, questions have recently begun to arise about the LAMP method [11], including due to the emergence of the so-called primer homo- and heterodimers, which are more difficult to exclude in this reaction than in PCR, because of the larger number of primers used and their increased length [12].

For successful amplification, it is necessary to select the right primers. When using the LAMP method, the main difficulty is in modeling primers with account for all recommended conditions, namely:

- 1) length of the primer (18–35 nucleotides for external primers, 30–55 nucleotides for internal ones);
- 2) content of guanine (G) and cytosine (C) (GC composition ranging from 40 to 60%);
- 3) optimal primer annealing temperature (55–65°C);
- 4) close arrangement of primers in one set: the average size of the amplicon (120–220 bp);
- 5) exclusion of the formation of dimers of primers;
- 6) elimination of nucleotide repeats in one primer (no more than three).

Table 1 provides brief characteristics and features of the most popular LAMP primer design programs [5].

Table 1

Brief characteristics of popular computer programs for LAMP primer design

	Development language	Length of the analyzed region, nucleotides	Selection of loop primers	Configuration of loop primers	Graphical interface	Free access
Primer Explorer (V4, V5), Japanese company Eiken Chemical Co. LTD, Tokyo	Java	up to 2,000	+	no	yes	yes
FastPCR, Finnish company Primer Digital Ltd	Java	from 12 up to 500	–	no	no	no
GLAPD. Shanghai Jiao Tong University, China	C, CUDA C, Perl OS Linux	unlimited	+	+	no	yes
LAMP Designer, American company Premier Biosoft		up to 15,000,000	+	only T _m	yes	no
Lamprim	Python		–	–	–	no access
NEB LAMP, New England Biolabs, Ipswich, Massachusetts, USA	Java	from 100 up to 2,000	+	–	yes	yes
LAMPPrimer iQ. LAMPPrimer iQ-loop, Ufa, Russia	Python 3.10	unlimited	+	yes	yes	yes

The design of primers for LAMP is a very difficult task and requires the development of a special computer program with proper functionality, taking into account all recommended conditions, and with the possibility of an extended selection of primers and a user-friendly interface.

The computer program for primer design is developed in the Python programming language. This language has the bioPython library, which allows working with nucleotide sequences, as well as the Qt framework for interface development.

Research Results. With account for the structural features of nucleotide sequences and the criteria for selecting LAMP primers, a modification of the direct sampling method using a stencil approach has been proposed. It considers the GC composition, the annealing temperature of the primers, and reducing the complexity of the sampling.

As is known, the GC composition of primers should be in the range from 40 to 60%. This is one of the important criteria for selecting LAMP primers, which depends on the sequence being analyzed, the length of the primer, and it partially affects the annealing temperature (T_m , °C).

In this paper, the following formula is used to calculate the annealing temperature of primers:

$$T_m = 81.5 + 16.6 \cdot \left(\log_{10} [Na^+] \right) + 0.41 \cdot (\%G + \%C) - 548/L, \quad (1)$$

where $[Na^+]$ — molar concentration of sodium ions; $(\%G + \%C)$ — GC composition in the analyzed sequence, expressed as a percentage; L — length of the primer. It was based on a well-known dependence:

$$T_m = 81.5 + 16.6 \cdot \left(\log_{10} [Na^+] \right) + 0.41 \cdot (\%G + \%C) - 600/\text{length}. \quad (2)^1$$

Formula (1) was selected empirically, the calculated values were compared to the values obtained through the convenient OligoAnalyzer² utility, which provided a high-quality selection of primers for all types of nucleotide acid amplification. Through determining the length of the primers, GC composition and annealing temperature, all possible primers can be found in a nucleotide sequence of any length that will meet the specified criteria.

¹ Oligo Calc: Oligonucleotide Properties Calculator. URL: <http://biotools.nubic.northwestern.edu/OligoCalc.html> (accessed: 10.12.2023).

² OligoAnalyzer™ Tool. URL: <https://eu.idtdna.com/pages/tools/oligoanalyzer?returnurl=%2Fcalc%2Fanalyzer> (accessed: 10.12.2023).

If we imagine the primer as a substring, and the analyzed nucleotide sequence as a longer string, this task can be represented as a search of all possible options (direct search), but complicating it through calculating the GC composition and annealing temperature of the primers.

Figure 2 shows a complete block diagram of the direct search algorithm, taking into account:

- length of the primers (bp);
- GC-composition, %;
- annealing temperature of the primers, T_m , °C;
- homodimers on both DNA strands.

The total complexity of the modified algorithm in the worst case is $O(m \cdot n)$, where n — length of the primer, m — length of the nucleotide sequence. It should be understood that the running time of the algorithm directly depends on how often the nucleotide fragments that meet the requirements are found.

Table 2 shows the search data for all possible primers in nucleotide sequences of different structures over time.

Further, it is necessary to form sets from all the primers found, taking into account the close distance between the primers, the heterodimeric properties in one set, as well as the minimum temperature difference between the annealing of the primers.

The design scheme for forming primers into the LAMP sets is shown in Figure 3.

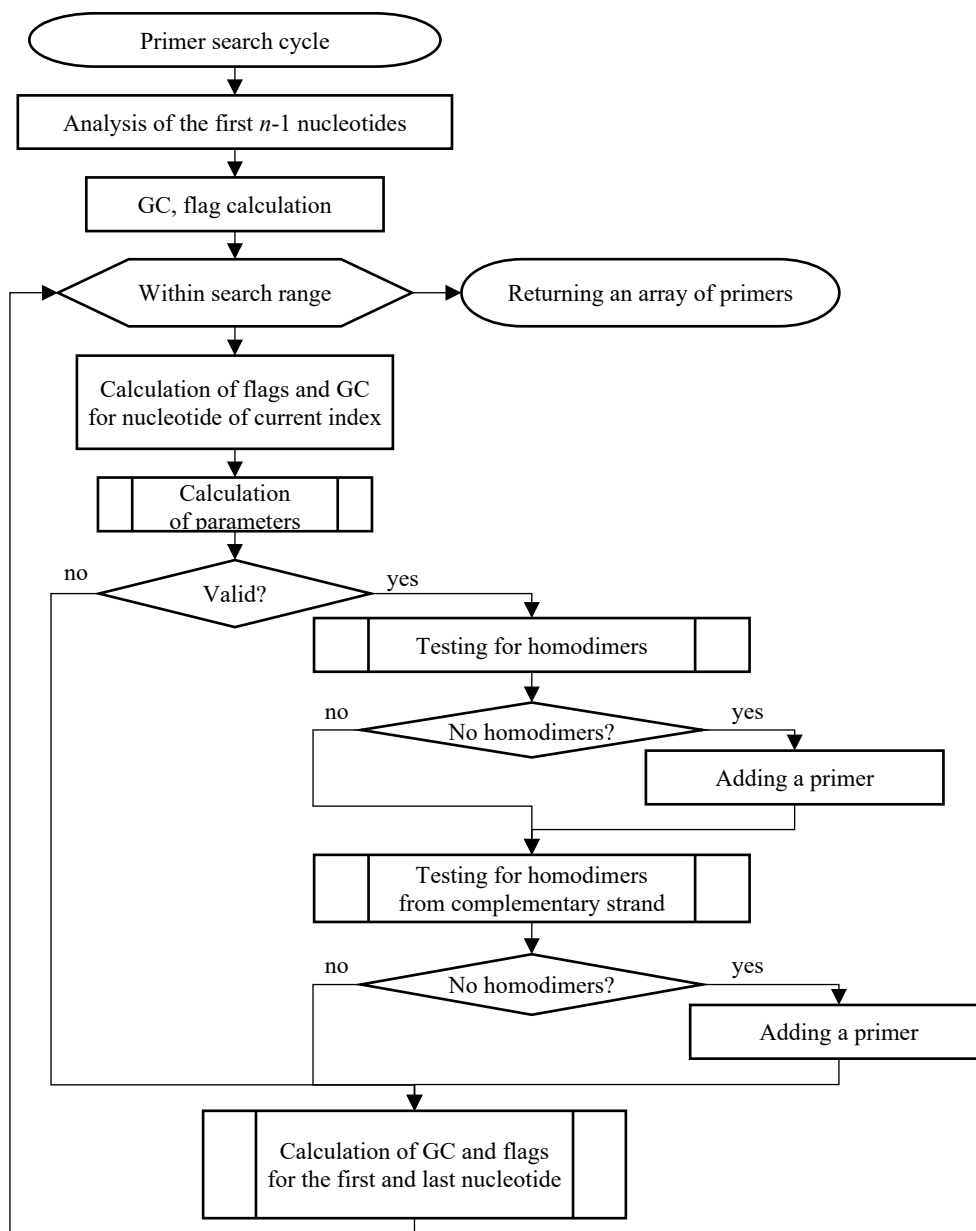


Fig. 2. Complete flowchart of the algorithm

Table 2

Time spent searching for valid primers in nucleotide sequences of different lengths

Genome name	Nucleotide sequence size, bp	Search for primers, s
SARS-CoV-2	29,903	0.31
Escherichia virus T4	168,903	1.73
Mycoplasma	580,076	5.43
Helicobacter pylori	1,624,458	18.11
Escherichia coli	4,641,652	71.68 (1.2 min)
Caenorhabditis	100,286,401	1,082.53 (18 min)



Fig. 3. Block diagram of the formation of primer sets for LAMP

At the input, the program reads the nucleotide sequence, either the desired file is loaded, or a fragment is inserted through the clipboard. Next, configurations are set, such as primer length, GC composition, primer annealing temperature, and temperature difference in one set. Then, all possible parameters satisfying the set configurations are searched, the selected primers are sorted into sets and displayed to the user.

The operation of the computer program:

1. Uploading a file (simple text format, FASTA format, GenBank), or a fragment of a sequence via the clipboard.
2. Search for all possible primers: primers are combined according to the following criteria:
 - length of the analyzed region;
 - distances between primers (F3/F2 — 1–10 nucleotides, F2/F1c — 10–25 nucleotides, F1c/B1c — 0–30 nucleotides);
 - temperature difference of primer annealing (<3);
 - heterodimers.

If all of the above conditions are met, the set is considered to be working.

3. Displaying simulated primer sets to the user's screen and/or saving to a file.

The LAMP program is registered in the Register of Computer Programs under the name LAMPprimers iQ, No. 2022617417 on April 20, 2022, and LAMPprimers iQ-loop, No. 2023662840 on June 14, 2023. The program code is publicly available³.

The developed software product has a user-friendly and intuitive interface, which can be used directly by end users — experimenters engaged in LAMP.

Discussion and Conclusion. The number of primer sets issued depends on the specified search parameters. The stricter the parameters, the fewer sets will be found. In case of hard restrictions, the program may not output a single set. The number of primer sets with different selection parameters for the genome of the bacteriophage lambda [13], whose length is ~48,500 nucleotides, is shown in Table 3.

For relatively short nucleotide sequences (up to 2,000 nucleotides), the selection of primers takes less than a second. With increasing sequence length, the duration of the primer search grows exponentially.

Table 3

Number of the primer sets for the bacteriophage lambda genome,
depending on the set selection parameters

GC, %	ΔT_m , °C	Maximum length of amplified region, bp		
		300	230	160
40–60	5	213	119	3
	2	198	184	3
45–55	5	132	80	0
	2	116	64	0
50–60	5	195	185	4
	2	181	164	4
55–65	5	160	147	4
	2	134	105	0

Figure 4 shows the effect of the length of the nucleotide sequence on the duration of the selection of primer sets. The data for the nucleotide sequence of the bacteriophage lambda on a laptop with the parameters are as follows: Intel(R) Core(TM) i7-10750H CPU, 2.60GHz, 6 cores. 16 GB RAM. The parameters of the soft selection of primers are indicated (40–60 % GC, $\Delta T_m = 5$, length of the analyzed region is up to 300 bp).

³ LAMPprimers-iQ. URL: https://github.com/Restily/LAMPprimers-iQ/blob/main/lamp/start_lamp.py (accessed: 10.12.2023).

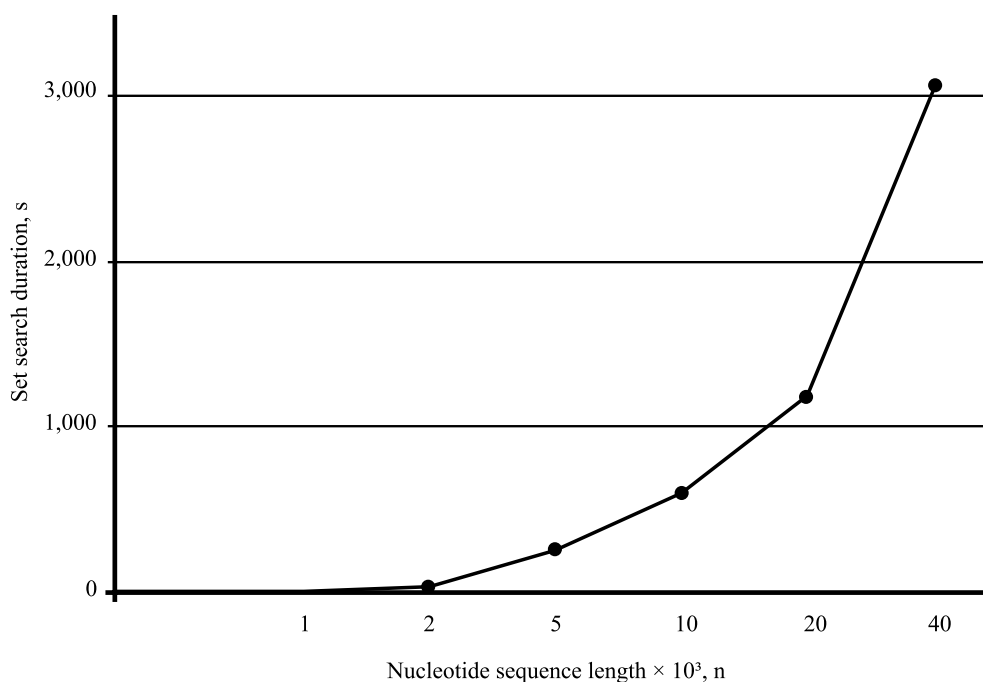


Fig. 4. Effect of length of nucleotide sequence on duration of selection of primer sets

It should be noted that the duration of the search for primers depends on the power of the computer.

To compare and determine the quality of the simulated primer sets, a number of field experiments were conducted to detect the RNA of the SARS-CoV-2 coronavirus, whose length was ~ 30,000 nucleotides. To do this, sets of LAMP primers were selected for the same region of the nucleotide sequence of the coronavirus using the LAMPprimers iQ program and two popular and accessible online utilities from New England Biolabs (NEB LAMP)⁴ and PrimerExplorer⁵. The designations L, N and P correspond to the sets of primers LAMPprimers iQ, NEB LAMP Primer Design and PrimerExplorer; “+” — samples contained RNA of SARS-CoV-2 coronavirus, “–” — samples did not contain nucleic acids. Figure 5 shows the curves of this experiment.

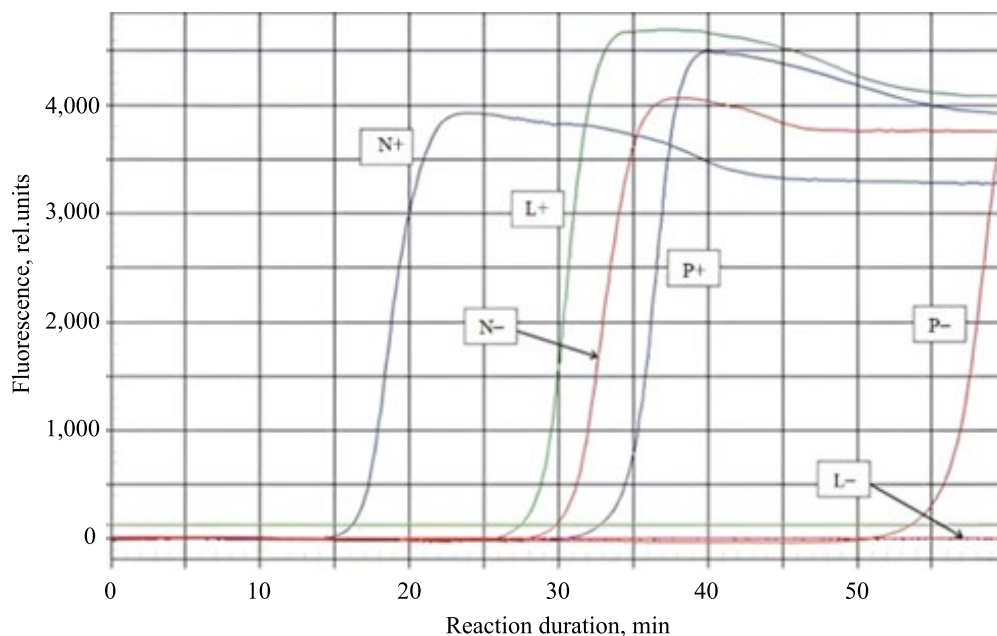


Fig. 5. Graph of the comparative experiment (the author's figure):
L — primers obtained using LAMPprimers iQ, N — NEB LAMP Primer Design,
P — PrimerExplorer, samples contained RNA of SARS-CoV-2 coronavirus,
“–” — control samples without matrix (did not contain nucleic acids)

⁴ NEB LAMP Primer Design Tool. URL: <https://lamp.neb.com/#/> (accessed: 24.11.2023).

⁵ LAMP primer designing software Primer Explorer. URL: <http://primerexplorer.jp/e> (accessed: 25.11.2023).

The primers obtained through PrimerExplorer, showed the latest rise in amplification curves (P+) compared to NEB LAMP (N+) and LAMPprimers iQ (L+). The primers obtained through LAMPprimers iQ, provided a later rise in the amplification curves (L+) compared to (N+). However, samples that did not contain virus RNA (P–), showed a later rise compared to the set (N–), while (L–) showed no rises even after 50 minutes, thereby providing the highest reliability of viral RNA detection.

The performed experiments showed a higher accuracy and specificity of the primer sets selected through LAMPprimers iQ computer program, caused by a decrease in the reaction rate with negative control samples. The amplification curves had later rises, or did not have them at all, even after 50 minutes of reaction time.

References

1. Gilmiyarova FN, Kolotyeva NA, Gusyakova OA, Sidorova IF. Polymerase Chain Reaction. History of Discovery. New Stage of Development. *Konsilium. Laboratornaya diagnostika*. 2017;154(4):17–21. URL: <https://cyberleninka.ru/article/n/polimeraznaya-tsepnaya-reaksiya-istoriya-otkrytiya-novyy-etap-razvitiya/viewer> (accessed: 05.11.2023). (In Russ.).
2. Garafutdinov RR, Baymiev AKh, Maleev GV, Alexeyev YaI, Zubov VV, Chemeris DA, et al. Diversity of PCR Primers and Principles of Their Design. *Biomics*. 2019;11(1):23–70. URL: https://biomicsj.ru/upload/iblock/ddf/bmcs19111023_1_.pdf?ysclid=lruepfy4zf297918053 (accessed: 05.11.2023).
3. Notomi T, Okayama H, Masubuchi H, Yonekawa T, Watanabe K, Amino N, et al. Loop-Mediated Isothermal Amplification of DNA. *Nucleic Acids Research*. 2000;28(12):e63 <https://doi.org/10.1093/nar/28.12.e63>
4. Chemeris DA, Kiryanova OYu, Gubaydullin IM, Chemeris AV. Design of Primers for Polymerase Chain Reaction (Brief Review of Software and Databases). *Biomics*. 2016;8(3):215–238. URL: <https://biomicsj.ru/upload/iblock/b05/3.pdf> (accessed: 05.11.2023).
5. Akhmetzianova LU, Davletkulov TM, Garafutdinov RR, Gubaydullin IM. Application of the Aho-Korasik Algorithm for the Selection of Primers for Loop Isothermal Amplification. *Mathematical Biology and Bioinformatics*. 2022;17(2):250–265. <https://doi.org/10.17537/2022.17.250>
6. Akhmetzianova LU, Davletkulov TM, Sakhabutdinova AR, Chemeris AV, Gubaydullin IM, Garafutdinov RR. LAMPprimers iQ: New Primer Design Software for Loop-Mediated Isothermal Amplification (LAMP). *Analytical Biochemistry*. 2023;684:115376. <https://doi.org/10.1016/j.ab.2023.115376>
7. Nagamine K, Hase T, Notomi T. Accelerated Reaction by Loop-Mediated Isothermal Amplification Using Loop Primers. *Molecular and Cellular Probes*. 2002;16(3):223–229. <https://doi.org/10.1006/mcpr.2002.0415>
8. Zhiyong Chen, Yuxue Liao, Xuemei Ke, Jie Zhou, Yixiong Chen, Lulu Gao, et al. Comparison of Reverse Transcription Loop-Mediated Isothermal Amplification, Conventional PCR and Real-Time PCR Assays for Japanese Encephalitis Virus. *Molecular Biology Reports*. 2011;38(6):4063–4070. <https://doi.org/10.1007/s11033-010-0525-0>
9. Nkere CK, Oyekeani JO, Silva G, Bömer M, Atiri GI, Onyeka J, et al. Chromogenic Detection of Yam Mosaic Virus by Closed-Tube Reverse Transcription Loop-Mediated Isothermal Amplification (CT-RT-LAMP). *Archives of Virology*. 2018;163(4):1057–1061. <https://doi.org/10.1007/s00705-018-3706-0>
10. Wang C, Shen X, Lu J, Zhang L. Development of a Reverse Transcription-Loop-Mediated Isothermal Amplification (RT-LAMP) System for Rapid Detection of HDV Genotype 1. *Letters in Applied Microbiology*. 2013;56(3):229–235. <https://doi.org/10.1111/lam.12039>
11. Hardinge P, Murray JAH. Lack of Specificity Associated with Using Molecular Beacons in Loop Mediated Amplification Assays. *BMC Biotechnology*. 2019;19(1):55. <https://doi.org/10.1186/s12896-019-0549-z>
12. Bodulev OL, Sakharov IYu. Isothermal Nucleic Acid Amplification Techniques and Their Use in Bioanalysis. *Biochemistry*. 2020;85(2):174–196. <https://doi.org/10.31857/S0320972520020037>
13. Rebolskaya YuA, Vasenko EA, Melnik SV, Sabirov DKh, Sarygina EV. Bacteriophage Lambda as a Model Object in Genetic Research. In: *Proc. X Int. Student Electronic Sci. Conf. "Student Scientific Forum-2018"*. Saratov: LLC Nauchno-izdatel'skii tsentr "Akademiya Estestvoznaniya"; 2018. URL: <https://scienceforum.ru/2018/article/2018002259> (accessed: 09.10.2023). (In Russ.).

About the Author:

Liana U. Akhmetzianova, teaching assistant of the Department of Computer Science and Engineering Cybernetics, Ufa State Petroleum Technological University (1, Kosmonavtov St., Ufa, 450064, RF). The research was carried out in the Laboratory of Mathematical Chemistry, Institute of Petrochemistry and Catalysis, UFRS RAS (141, pr. Oktyabrya, Ufa, 450075, RF), SPIN-code: [5800-5465](https://orcid.org/5800-5465), [ORCID](https://orcid.org/5800-5465), [ScopusID](https://orcid.org/5800-5465), www.lianab@mail.ru

Conflict of interest statement: the author does not have any conflict of interest.

The author has read and approved the final version of manuscript.

Received 14.12.2023

Revised 09.01.2024

Accepted 16.01.2024

Об авторе:

Лиана Ульфатовна Ахметзянова, ассистент кафедры вычислительной техники и инженерной кибернетики Уфимского государственного нефтяного технического университета (450062, РФ, г. Уфа, ул. Космонавтов, 1). Работа выполнялась в лаборатории математической химии Института нефтехимии и катализа Уфимского федерального исследовательского центра Российской академии наук. (450075, РФ, г. Уфа, проспект Октября, 141), SPIN-код: [5800-5465](https://orcid.org/5800-5465), [ORCID](https://orcid.org/5800-5465), [ScopusID](https://orcid.org/5800-5465), www.lianab@mail.ru

Конфликт интересов: автор заявляет об отсутствии конфликта интересов.

Автор прочитал и одобрил окончательный вариант рукописи.

Поступила в редакцию 14.12.2023

Поступила после рецензирования 09.01.2024

Принята к публикации 16.01.2024

INFORMATION TECHNOLOGY, COMPUTER SCIENCE AND MANAGEMENT ИНФОРМАТИКА, ВЫЧИСЛИТЕЛЬНАЯ ТЕХНИКА И УПРАВЛЕНИЕ



UDC 004.942, 004.02, 519.622, 544.3, 544.2

Research article

<https://doi.org/10.23947/2687-1653-2024-24-1-109-118>

Optimal Temperature Calculation for Multicriteria Optimization of the Hydrogenation of Polycyclic Aromatic Hydrocarbons by NSGA-II Method



EDN: VNTDAG

Anastasiya A. Alexandrova , Sergey N. Koledin 
Ufa State Petroleum Technical University, Ufa, Russian Federation
 nastena1425@gmail.com

Abstract

Introduction. Multicriteria optimization, taking into account contradicting criteria, is used to improve production efficiency, reduce costs, improve product quality and environmental safety of processes. The literature describes the application of multicriteria optimization for production purposes, including the selection of reaction conditions and improvement of technological processes. In the presented paper, the object of research is the process of hydrogenation of polycyclic aromatic hydrocarbons (PAH) in the production of high-density fuels. To determine the optimal conditions of the process, the problem of multicriteria optimization based on the kinetic model is solved. The criteria include maximizing the yield of targeted naphthenes and conversion of feedstock. The research objective is to create a program implementing the multicriteria optimization non-dominated sorting genetic algorithm-II (NSGA-II). Due to this, it is possible to calculate the optimal temperature for the PAH hydrogenation process on the basis of the kinetic model.

Materials and Methods. The NSGA-II genetic algorithm was used to solve the multicriteria optimization problem. Modified parental and survival selection within the Pareto front was also used. If it was necessary to divide the front, solutions based on the Manhattan distance between them were selected. The program was implemented in Python.

Results. In the system of ordinary nonlinear differential equations of chemical kinetics, the concentration was designated y_i , the conditional contact time of the reaction mixture with the catalyst — τ . The system was solved for the hydrogenation reaction of polycyclic aromatic hydrocarbons. The calculations showed that at $\tau = 0$ $y_1(0) = 0.025$; $y_2(0) = 0.9$; $y_6(0) = 0.067$; $y_9(0) = 0.008$; $y_i(0) = 0$, $i = 3-5, 7, 8, 10-20$; $Q(0) = 1$. The process temperature was considered as a control parameter according to two optimality criteria: maximizing the yield of target naphthenes (f_1) at the end of the reaction, and maximizing the conversion of feedstock (f_2). Values f_1 were in the range of 0.43–0.79; conversion — 0.01–0.03; temperature — 200–300 K. The growth of temperature was accompanied by an increase in the yield of target naphthenes and a decrease in the conversion of feedstock. Each solution obtained was not an unimprovable one. When modeling the process of hydrogenation of PAH, an algorithm was launched with a population size of 100 and a number of generations of 100. A program implementing the NSGA-II algorithm was developed. The optimal set of values of the PAH hydrogenation reaction temperature was calculated, which made it possible to obtain unimprovable values of the optimality criteria — maximizing the yield of target naphthenes and conversion of feedstock.

Discussion and Conclusion. The NSGA-II algorithm is effective for solving the problem of non-dominance, and deriving the optimal solution for all criteria. Future research should be devoted to the selection of optimal algorithm parameters to increase the speed of the solution. Based on the obtained theoretical optimal conditions of the PAH hydrogenation reaction, it is possible to implement the process in industry.

Keywords: hydrogenation of polycyclic aromatic hydrocarbons, multicriteria process optimization, nonlinear programming problem, Pareto front, NSGA-II method

Acknowledgements. The authors would like to thank the reviewers for valuable comments that contributed to the improvement of the article.

For citation. Alexandrova AA, Koledin SN. Optimal Temperature Calculation for Multicriteria Optimization of the Hydrogenation of Polycyclic Aromatic Hydrocarbons by NSGA-II Method. *Advanced Engineering Research (Rostov-on-Don)*. 2024;24(1):109–118. <https://doi.org/10.23947/2687-1653-2024-24-1-109-118>

Научная статья

Расчет оптимальной температуры при многокритериальной оптимизации процесса гидрирования полициклических ароматических углеводородов методом NSGA-II

А.А. Александрова  , С.Н. Коледин 

Уфимский государственный нефтяной технический университет, г. Уфа, Российская Федерация

 nastena1425@gmail.com

Аннотация

Введение. Многокритериальную оптимизацию с учетом противоречащих друг другу критериев задействуют для улучшения эффективности производства, сокращения затрат, повышения качества продукции и экологической безопасности процессов. В литературе описано использование многокритериальной оптимизации для производственных целей, в том числе при выборе условий реакции и улучшении технологических процессов. В представленной работе объект исследования — это процесс гидрирования полициклических ароматических углеводородов (ПАУ) при получении высокоплотных топлив. Для определения оптимальных условий процесса решается задача многокритериальной оптимизации на основе кинетической модели. Критерии: максимизация выхода целевых нафтен и конверсия исходного сырья. Цель работы — создание программы, реализующей алгоритм многокритериальной оптимизации NSGA-II (англ. non-dominated sorting genetic algorithm II). Благодаря этому на основе кинетической модели можно рассчитать оптимальную температуру для процесса гидрирования ПАУ.

Материалы и методы. Для решения многокритериальной задачи оптимизации применялся генетический алгоритм NSGA-II. Используется также измененный отбор родителей и выживания в рамках фронта Парето. При необходимости разделения фронта решения выбирались по манхэттенскому расстоянию между ними. Программа реализована на языке Python.

Результаты исследования. В системе обыкновенных нелинейных дифференциальных уравнений химической кинетики концентрацию обозначили y_i , условное время контакта реакционной смеси с катализатором — τ . Систему решили для реакции гидрирования полициклических ароматических углеводородов. Расчеты показали, что при $\tau = 0$ $y_1(0) = 0,025$; $y_2(0) = 0,9$; $y_6(0) = 0,067$; $y_9(0) = 0,008$; $y_i(0) = 0$, $i = 3-5, 7, 8, 10-20$; $Q(0) = 1$. В качестве управляемого параметра рассматривали температуру процесса по двум критериям оптимальности: максимизация выхода целевых нафтен (f_1) в конце реакции и максимизация конверсии исходного сырья (f_2). Значения f_1 были в границах 0,43–0,79; конверсии — 0,01–0,03; температуры — 200–300 К. Рост температуры сопровождается увеличением выхода целевых нафтен и снижением конверсии исходного сырья. Каждое полученное решение — неулучшаемое. При моделировании процесса гидрирования ПАУ запустили алгоритм с размером популяции — 100, количеством поколений — 100. Разработана программа, реализующая алгоритм NSGA-II. Рассчитано оптимальное множество значений температуры реакции гидрирования ПАУ, позволяющее получить неулучшаемые значения критериев оптимальности — максимизации выхода целевых нафтен и конверсии исходного сырья.

Обсуждение и заключение. Алгоритм NSGA-II эффективен для решения задачи недоминирования и вывода оптимального решения для всех критериев. Будущие исследования следует посвятить подбору оптимальных параметров алгоритма, позволяющих увеличить скорость решения. Опираясь на полученные теоретические оптимальные условия реакции гидрирования ПАУ, можно реализовать процесс в промышленности.

Ключевые слова: гидрирование полициклических ароматических углеводородов, многокритериальная оптимизация технологического процесса, задача нелинейного программирования, фронт Парето, метод NSGA-II

Благодарности. Авторы выражают признательность рецензентам за ценные замечания, способствовавшие улучшению статьи.

Для цитирования. Александрова А.А., Коледин С.Н. Расчет оптимальной температуры при многокритериальной оптимизации процесса гидрирования полициклических ароматических углеводородов методом NSGA-II. *Advanced Engineering Research (Rostov-on-Don)*. 2024;24(1):109–118. <https://doi.org/10.23947/2687-1653-2024-24-1-109-118>

Introduction. Optimization of multistage reactions is used in chemical, oil and gas, food, and other industries. In practice, optimization tasks are multicriteria, and the criteria are often contradictory and have an optimum at different points. Multicriteria optimization remains urgent, as it provides taking into account several parameters and selecting the best solution from a variety of options.

Within the framework of this study, the object of research is the catalytic hydrogenation reaction of polycyclic aromatic hydrocarbons (PAH). They are a class of organic compounds whose molecules contain at least two benzene rings [1]. PAH are common in the interstellar medium. They are part of heavy oil fractions, and are formed by laser irradiation of carbon materials. The study of these compounds is of interest from the point of view of establishing the dependences between their chemical structure and physico-chemical properties. In addition, the data obtained as a result of such scientific research can be used to create new organic and hybrid compounds with a strong carbon frame, which are applicable in nanoarchitectonics.

Applied science correlates the presence of PAH with the production purposes. As an example, the presence of PAH in raw materials is desirable if it is used to produce coke with a given structure [2]. However, in the production of fuel, PAH can negatively affect the performance characteristics of the product, specifically, the density [3].

Extremely strict requirements are imposed on the production of high-density jet fuel. At high density, it should have a boiling point no higher than the upper limit of the boiling point of the kerosene fraction. Another mandatory criterion is the low content of aromatic hydrocarbons. We also note the high cost of well-known technologies for producing high-density fuels.

Considering the above, the problem must be solved according to the Pareto dominance principle to determine the set of unimprovable options using a genetic algorithm of non-dominated sorting [4].

The research objective is to develop a program that implements NSGA-II (Non-dominated sorting genetic algorithm II) multicriteria optimization algorithm and provides calculating the optimal temperature for the PAH hydrogenation process based on a kinetic model.

Materials and Methods

Mathematical Model. We describe the changes in the concentrations of the components depending on the reaction time. To do this, the equations of chemical kinetics are used, which are a system of ordinary nonlinear differential equations (SONDE):

$$\frac{dy_i}{d\tau} = \sum_{j=1}^J v_{ij} w_j, i = 1, \dots, I, \quad (1)$$

$$w_j = k_j \cdot \prod_{i=1}^I (y_i)^{\alpha_{ij}} - k_{-j} \cdot \prod_{i=1}^I (y_i)^{\beta_{ij}}, k_j = A_j \cdot \exp\left(-\frac{E_j^+}{RT}\right), k_{-j} = A_{-j} \cdot \exp\left(-\frac{E_j^-}{RT}\right). \quad (2)$$

Here are the initial conditions: $y_i(0) = y_i^0$ at $\tau = 0$; $\tau \in [0, \tau^*]$; y_i — reagent concentrations, mole fractions; τ — conditional contact time of the reaction mixture with the catalyst, kg·min/mol; J — number of stages; I — number of substances; v_{ij} — stoichiometric matrix; w_j — speed of the j -th stage, 1/min or mol/(kg·min); k_j, k_{-j} — speed constants of the stages (given), 1/min; α_{ij} — negative elements of matrix v_{ij} ; β_{ij} — positive elements v_{ij} ; A_j, A_{-j} — pre-exponential multipliers, 1/min; E_j^+, E_j^- — activation energies of direct and reverse reactions, kcal/mol; R — gas constant, 2 cal/(mol·K); T — temperature, K; τ^* — reaction duration, kg·min/mol.

The model of catalytic hydrogenation of PAH takes into account the dynamics of the molar composition and volume of the reaction mixture. Therefore, changes in the concentration of components at each point in time are considered [3]:

$$\frac{dQ}{d\tau} = \sum_{i=1}^I \frac{dy_i}{d\tau}, \quad Q(0) = Q^0, \quad (3)$$

$$w_j = k_j \cdot \prod_{i=1}^I \left(\frac{y_i}{Q}\right)^{\alpha_{ij}} - k_{-j} \cdot \prod_{i=1}^I \left(\frac{y_i}{Q}\right)^{\beta_{ij}}.$$

To describe a nonstationary reaction that occurs with a change in the volume of the reaction mixture, it is necessary to solve a system of nonlinear differential equations at each moment of time. The direct kinetic problem is the solution to SONDE (1)–(3).

In the process of hydrogenation of PAH, naphthenes are obtained from the source aromatic hydrocarbons, which have a higher density and can be used as rocket fuel. For this purpose, nickel catalysts are used, and the control or variable parameter is the process temperature, which should be within 200–500 K. Optimality criteria — maximizing the output of target naphthenes at the end of the reaction and maximizing the conversion of feedstock.

Research Algorithm. Multicriteria optimization is the selection of the best solution from a variety of alternatives, taking into account several criteria. The importance of each of them is determined by the weight (priority).

Suppose, $f(x)$ — an objective function, and the constraints given in the form of equalities $h_1(x) \dots h_m(x)$ and inequalities $g_{m+1}(x) \dots g_p(x)$ are represented by a column vector of components $x = [x_1, \dots, x_n]^T$ in n -dimensional Euclidean space.

We formulate the problem of nonlinear programming [5].

Optimize

$$f(x) \rightarrow \text{extr}, x \in E^n \quad (4)$$

with m linear or nonlinear constraints in the form of equalities

$$h_j(x) = 0, j = 1, \dots, m \quad (5)$$

and with $(p - m)$ linear or nonlinear constraints in the form of inequalities

$$g_j(x) \geq 0, j = m + 1, \dots, p. \quad (6)$$

Decomposition (4)–(6) is the formulation and solution of a linear and quadratic programming problem. Each of them is determined by the type of equations (4)–(6). Thus, in the case of quadratic function (4) and linear equations (5), (6) — the quadratic programming problem described below.

We define the extremum of function

$$f(x) = a_0 + c^T x + x^T Q x \rightarrow \text{extr} \quad (7)$$

with constraints:

$$a^T x \geq b, x \geq 0. \quad (8)$$

In equations (7), (8) Q — nonnegatively defined quadratic symmetric matrix; a, b, c — coefficient matrices.

When setting multicriteria Pareto optimization problem, (4)–(6) will have the form:

$$\text{extr} F(x) = F(x^*) = F^*. \quad (9)$$

In equation (9), $Fx = (f_1(X), f_2(X), \dots, f_m(X))$ — vector-function of optimality criteria f_1 and f_2 . Set x^* — desired solution to the problem in the region of variation parameters. Set F^* represents the desired solution to the problem in the region of optimality criteria, which is unimprovable in terms of Pareto approximation. Then, x^* defines the Pareto set, F^* — Pareto front.

Priori and posteriori Pareto approximation algorithms were used to solve (9). One of them is the ideal point method, which represents the best solution according to all criteria [6]. To find it, we must first determine the minimum and maximum values of each criterion of all the solutions under consideration. Then, for each criterion, the maximum value of all the minimum and the minimum of all the maximum values are selected.

However, this approach has some drawbacks. Firstly, it may be ineffective if the ideal point is outside the range of acceptable criteria values. In this case, other methods of solving multicriteria optimization problems are used. In addition, the ideal point method does not take into account the relationship between the criteria and may cause the selection of a compromise solution that is not optimal for all criteria. Therefore, when using this method, it is needed to additionally analyze and verify the optimality of the solutions obtained [7].

The lexicographic ordering method is also used in solving multicriteria optimization problems. In this case, the criteria are ordered by priority and considered sequentially. If the solutions cannot be sorted by the first criterion, then they are sorted by the next criterion, etc. [7]. The advantages of lexicographic ordering are simplicity and transparency. Using this method, it is possible to obtain a single optimal solution that is easily interpreted. As for the disadvantages, we note, firstly, the inability to take into account compromise solutions that may turn out to be optimal by all criteria. Secondly, there is a risk of selecting an unfavorable solution if the first criterion has a lot of weight, but is not the most important for this task [8].

The presented work provides a solution to the problem of multicriteria optimization of the hydrogenation process of polycyclic aromatic hydrocarbons through the well-known NSGA-II method. It is based on a genetic algorithm and uses several techniques to solve the problem of non-dominance [9]. The main steps of the algorithm are described below [10].

1. Initialization of the population. The initial population is randomly generated.
2. Population assessment. Each element of the population is evaluated according to several criteria.
3. Sorting the population. The elements of the population are sorted by non-dominance level. Dominant and non-dominant elements are placed in the first level. Elements dominated only by elements of the first level are placed in the second level, etc.
4. Selecting parent elements. To create a new population, parent elements are selected from the first few levels.
5. Crossover and mutation. Parent elements undergo crossing-over and mutation to create new elements of the population.
6. Assessment of the new population. New elements are evaluated according to the criteria.

7. Sorting the new population. New items are sorted by non-dominance level.
8. Selection of a new population. Elements for the next generation are selected from the new population.
9. Repeat steps 4–8 until the stop criterion is reached.

NSGA-II allows working accurately and efficiently with multicriteria optimization tasks. It effectively solves the problem of non-dominance, which provides getting optimal solutions for all criteria.

NSGA-II is based on a genetic algorithm with parental selection and survival. Individuals are selected along the fronts, while the front is divided if not all individuals can survive. Solutions in the split front are selected on the basis of the distance between them, which is the Manhattan distance in the criteria space [9]. The endpoints are saved at each generation and are assigned a conditionally infinite distance for use in subsequent iterations [11] (Fig. 1).

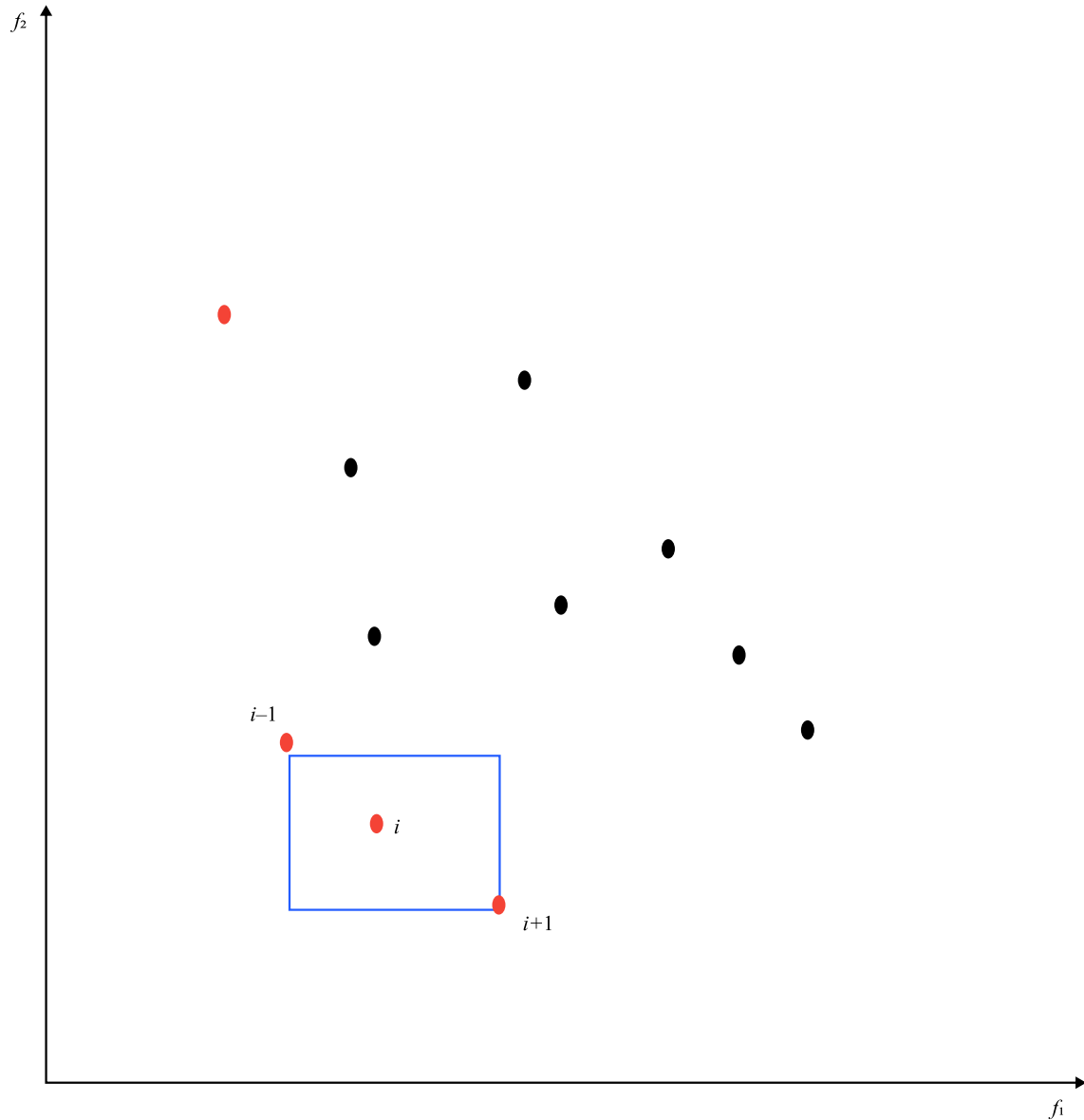


Fig. 1. Visualization of the Pareto front and selection of solutions based on distances

Figure 1 shows an example of a set of solutions for a multicriteria optimization problem using criteria f_1 and f_2 . The red dots represent the Pareto front. The calculation of the cluster distance for solution i is shown — this is the average length of the side of the cuboid in which solution i is located (marked with a blue frame).

To enhance the impact on the selection of parents, NSGA-II uses binary tournament selection [9]. Each individual is first compared by rank, and then — by the distance between them.

Research Results. The program implementing the algorithm for solving the multicriteria optimization problem is written in Python.

In the course of the study, a system of differential equations (1–3) was solved. For the hydrogenation reaction of polycyclic aromatic hydrocarbons, it has the form [12]:

$$\left\{ \begin{array}{l} \frac{dy_1}{d\tau} = (-w_1 - w_2 + w_{11}) \\ \frac{dy_2}{d\tau} = -3w_1 - w_2 - 2w_3 - 3w_4 - 3w_5 - 3w_6 - w_7 - w_8 - 3w_9 - w_{10} - w_{11} - w_{12} - w_{14} - w_{15} \\ \frac{dy_3}{d\tau} = w_1 \\ \frac{dy_4}{d\tau} = w_2 + w_8 - w_9 \\ \frac{dy_5}{d\tau} = w_2 \\ \frac{dy_6}{d\tau} = -w_3 + w_{16} \\ \frac{dy_7}{d\tau} = w_3 - w_9 - w_{10} - 2w_{16} \\ \frac{dy_8}{d\tau} = w_4 + w_{16} \\ \frac{dy_9}{d\tau} = -w_5 + w_{17} \\ \frac{dy_{10}}{d\tau} = w_5 - w_6 - w_8 - 2w_{17} \\ \frac{dy_{11}}{d\tau} = w_6 - w_7 + w_{17} \\ \frac{dy_{12}}{d\tau} = w_7 + w_7 + w_8 + w_9 - w_{13} - w_{15} \\ \frac{dy_{13}}{d\tau} = 0 \\ \frac{dy_{14}}{d\tau} = 0 \\ \frac{dy_{15}}{d\tau} = 0 \\ \frac{dy_{16}}{d\tau} = w_{10} - w_{11} - w_{12} \\ \frac{dy_{17}}{d\tau} = w_{12} \\ \frac{dy_{18}}{d\tau} = w_{13} - w_{14} \\ \frac{dy_{19}}{d\tau} = w_{14} \\ \frac{dy_{20}}{d\tau} = w_{15} \\ \frac{dQ}{d\tau} = \sum_{i=1}^{20} \frac{dy_i}{d\tau} \end{array} \right. , \quad \left\{ \begin{array}{l} w_1 = \frac{k_i y_1 \cdot y_2^3}{Q^3} - \frac{k_{21} \cdot y_3}{Q} \\ w_2 = \frac{k_2 \cdot y_1 \cdot y_2}{Q^2} \\ w_3 = \frac{k_3 \cdot y_6 \cdot y_2^2}{Q^3} - \frac{k_{18} \cdot y_7}{Q} \\ w_4 = \frac{k_4 \cdot y_7 \cdot y_2^3}{Q^4} \\ w_5 = \frac{k_5 \cdot y_9 \cdot y_2^3}{Q^4} - \frac{k_{19} \cdot y_{10}}{Q} \\ w_6 = \frac{k_6 \cdot y_{10} \cdot y_2^3}{Q^4} - \frac{k_{19} \cdot y_{10}}{Q} \\ w_7 = \frac{k_7 \cdot y_{11} \cdot y_2}{Q^2} \\ w_8 = \frac{k_8 \cdot y_{10} \cdot y_2}{Q^2} \\ w_9 = \frac{k_9 \cdot y_4 \cdot y_2^3}{Q^4} \\ w_{10} = \frac{k_{10} \cdot y_7 \cdot y_2}{Q^2} \\ w_{11} = \frac{k_{11} \cdot y_{16} \cdot y_2}{Q^2} \\ w_{12} = \frac{k_{12} \cdot y_{16} \cdot y_2}{Q^2} \\ w_{13} = \frac{k_{13} \cdot y_{12}}{Q} \\ w_{14} = \frac{k_{14} \cdot y_{18} \cdot y_2}{Q^2} \\ w_{15} = \frac{k_{15} \cdot y_{12} \cdot y_2}{Q^2} \\ w_{16} = \frac{k_{16} \cdot y_7^3}{Q^2} \\ w_{17} = \frac{k_{17} \cdot y_{10}^2}{Q^2} \end{array} \right. .$$

At $\tau=0$, $y_1(0)=0.025$; $y_2(0)=0.9$; $y_6(0)=0.067$; $y_9(0)=0.008$; $y_i(0)=0$, $i=3-5, 7, 8, 10-20$; $Q(0)=1$.

Figure 2 shows the calculated set of solutions satisfying the constraints of the system and the Pareto front, where f_1 — output of the target naphthenes, and f_2 — conversion of the feedstock.

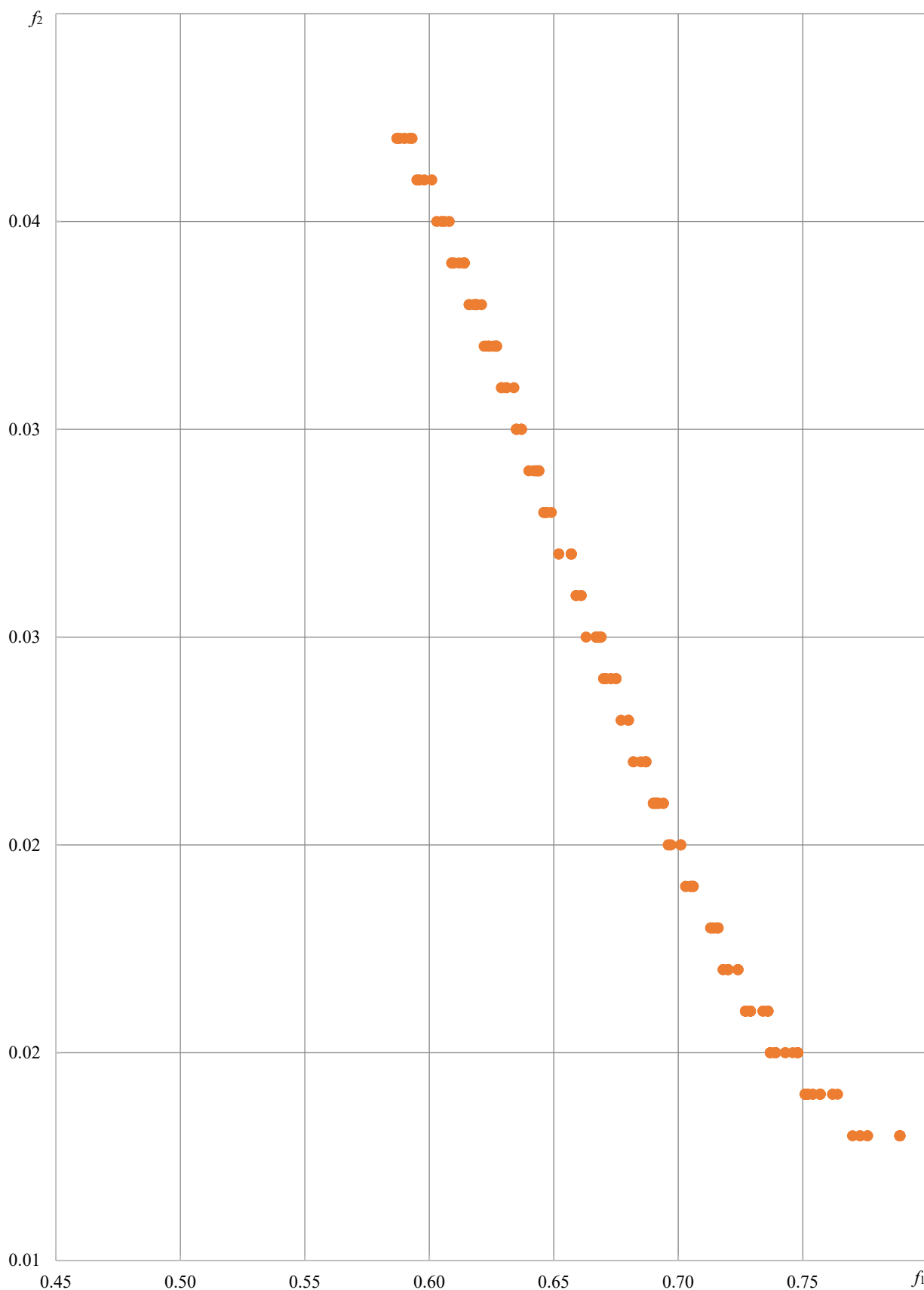


Fig. 2. Pareto front of the hydrogenation process of polycyclic aromatic hydrocarbons

The controlled parameter is the process temperature [13]. The optimality criteria are maximizing the output of target naphthenes at the end of the reaction and maximizing the conversion of feedstock [14]. Calculations using the proposed algorithm gave the results of matching the optimality criteria and the values of the temperature parameter, which are summarized in Table 1.

Table 1

Compliance of optimality criteria and temperature parameter value
of the hydrogenation of polycyclic aromatic hydrocarbons

Output of targeted naphthenes f_1	Feedstock conversion f_2	Temperature T, K
0.43	0.03	200.00
0.59	0.03	221.20
0.71	0.01	250.00
0.76	0.01	271.10
0.79	0.01	300.00

Thus, as the temperature grows, the output of the target naphthenes increases, and the conversion of the feedstock decreases. Each of these solutions is unimprovable, and the selection of specific values depends on the decision maker.

For NSGA-II to work successfully, it is required to select the algorithm parameters correctly. Specifically, the criteria of population size, number of generations, probability of crossover and mutation, should be optimized. When launching the algorithm on the model of the hydrogenation process of polycyclic aromatic hydrocarbons, the following parameters were used: population size — 100, number of generations — 100. An insufficiently large population may cause premature convergence of the algorithm to the local optimum. Too large population can slow down the optimization process [15]. An excessive number of generations potentially leads to retraining the algorithm, whereas with an insufficient number of generations there may not be enough time to achieve optimal solutions.

Discussion and Solution. A program has been created that implements the NSGA-II multicriteria optimization algorithm. Working with the corresponding problem within the framework of this method includes solving a system of differential equations, visualizing a set of solutions satisfying the constraints of the system, and constructing a Pareto front. In addition, the values of the variable parameters were found to achieve optimization goals. For the PAH hydrogenation process, based on the kinetic model, a set of temperature values has been calculated that are optimal for obtaining the unimprovable values of two optimality criteria: naphthene output and feedstock conversion. With increasing temperature, the reaction rate and the output of naphthenes increases. However, the conversion of raw materials is decreasing. In addition, too high temperatures can cause adverse reactions and decomposition of products.

The data obtained in the framework of the presented research can be useful for optimizing the process of hydrogenation of PAH under industrial conditions. It is important to take into account the impact of temperature on the output of naphthenes and the conversion of raw materials when developing a production strategy. In addition, other parameters, on which the kinetics of the reaction depends, should be considered. These are, e.g., pressure, flow rate of reagents, and the role of catalysts.

Thus, the developed program and the proposed algorithm make it possible to simultaneously analyze several criteria for the optimality of the process based on a kinetic model, and generate a set of unimprovable values of variable parameters.

References

1. Akhmetov AF, Akhmetov AV, Zagidullin ShG, Shayzhanov NS. Hydrofinery Processing Heavy Fraction of Aromatic Hydrocarbons C_{10+} on Catalyst Nickel on Kizelgur. *Bashkir Chemical Journal*. 2018;25(1):96–98. <https://doi.org/10.17122/bcj-2018-1-96-98>
2. Akhmetov AF, Akhmetov AV, Shayzhanov NS, Zagidullin ShG. Hydrogenolysis of Residual Fractions Obtained by Pyrolysis Process. *Bashkir Chemical Journal*. 2017;24(2):29–32. URL: <https://bcj.rusoil.net/files/slider/BCJ-2-2017.pdf> (accessed: 07.11.2023).
3. Shayzhanov NS, Zagidullin ShG, Akhmetov AV. Activity Analysis of Hydrogenation Catalysts in the Process of High-Density Jet Fuels Production. *Bashkir Chemical Journal*. 2014;21(2):94–98. URL: <https://cyberleninka.ru/article/n/analiz-aktivnosti-katalizatorov-gidrirovaniya-v-protssesse-polucheniya-vysokoplotnyh-reaktivnyh-topliv/viewer> (accessed: 07.11.2023).
4. Koledina KF, Koledin SN, Karpenko AP, Gubaydullin IM, Vovdenko MK. Multi-Objective Optimization of Chemical Reaction Conditions Based on a Kinetic Model. *Journal of Mathematical Chemistry*. 2019;57(2):484–493. <https://doi.org/10.1007/s10910-018-0960-z>

5. Emmerich M, Deutz A. *Multicriteria Optimization and Decision Making: Master Course*. Leiden: Leiden University Publishing; 2014. 102 p. URL: <https://liacs.leidenuniv.nl/~emmerichmtm/modapage/MCOReaderEmmeirchDeutz2017.pdf> (accessed: 17.11.2023).
6. Deb K, Mohan M, Mishra S. Towards a Quick Computation of Well-Spread Pareto-Optimal Solutions. In book: CM Fonseca, PJ Fleming, E Zitzler, L Thiele, K Deb (eds). *Evolutionary Multi-Criterion Optimization*. Berlin, Heidelberg: Springer; 2003. P. 222–236. https://doi.org/10.1007/3-540-36970-8_16
7. Koledina KF. Multi-Criteria Interval Optimization of Conditions for Complex Chemical Reactions on the Basis of a Kinetic Model. *Mathematical Models and Computer Simulations*. 2022;34(8):97–109. <https://doi.org/10.20948/mm-2022-08-06>
8. Miernik K, Węglińska E, Danek T, Leśniak A. An Application of the NSGA-II Algorithm in Pareto Joint Inversion of 2D Magnetic and Gravity Data. *Geology Geophysics & Environment*. 2021;47(2):59–70. <https://doi.org/10.7494/geol.2021.47.2.59>
9. Martínez S, Perez E, Eguia P, Erkoreka A, Granada E. Model Calibration and Exergoeconomic Optimization with NSGA-II Applied to a Residential Cogeneration. *Applied Thermal Engineering*. 2020;169:114916. <https://doi.org/10.1016/j.applthermaleng.2020.114916>
10. Kamshilova YuA, Semekin ES. Comparative Analysis of Multiobjective Evolutionary Algorithms' SPEA2 and NSGA-II Efficiency. In: *Proc. XVI Int. Sci. Conf. dedicated to the memory of the General Designer of rocket and space systems Academician MF Reshetnev "Reshetnev Readings"*. Part 2. Krasnoyarsk: Siberian State Aerospace University named after academician MF Reshetnev; 2012. P. 484. URL: https://disk.sibsau.ru/website/reshetnevsite/materials/2012_2.pdf (accessed: 17.11.2023).
11. Cîrciu MS, Leon F. Comparative Study of Multiobjective Genetic Algorithms. *Bulletin of the Polytechnic Institute of Iasi*. 2010;56(60):1-13. URL: <https://www.researchgate.net/publication/228845090> (accessed: 02.03.2024).
12. Koledina KF, Gubaidullin IM, Zagidullin ShG, Koledin SN, Sabirov DSh. Kinetic Regularities of Hydrogenation of Polycyclic Aromatic Hydrocarbons on Nickel Catalysts. *Russian Journal of Physical Chemistry A*. 2023;97(10):2104–2110. <https://doi.org/10.1134/s003602442309008x>
13. Zagidullin ShG, Koledina KF. Mathematical Modeling of the Kinetics of Hydration of Polycyclic Aromatic Hydrocarbons. *Bulletin of BSU*. 2021;26(3):664–669. <https://doi.org/10.33184/bulletin-bsu-2021.3.23>
14. Bukhtoyarov SE, Emelichev VA. Stability Aspects of Multicriteria Integer Linear Programming Problems. *Journal of Applied and Industrial Mathematics*. 2019;13:22–29. <https://doi.org/10.1134/S1990478919010034>
15. Tan Liguu, Novikova SV. Application of the Step Learning Method for the Evolutionary Algorithm in Problems of Multi-Criteria Optimization. *Vestnik KGEU*. 2022;14(3):114–124.

About the Authors:

Anastasiya A. Alexandrova, graduate student of the Information Technologies and Applied Mathematics Department, Ufa State Petroleum Technological University (1, Kosmonavtov St., Ufa, 450064, RF), SPIN-code: [4026-5240](#), [ORCID](#), nastena1425@gmail.ru

Sergey N. Koledin, Cand.Sci. (Phys.-Math.), Associate Professor of the Information Technologies and Applied Mathematics Department, Ufa State Petroleum Technological University (1, Kosmonavtov St., Ufa, 450064, RF), SPIN-code: [4243-6265](#), [ORCID](#), koledinsrg@gmail.com

Claimed contributorship:

AA Alexandrova: software development, text preparation, formulation of conclusions.

SN Koledin: academic advising, providing source data, correction of the conclusions, the text revision.

Conflict of interest statement: the authors do not have any conflict of interest.

All authors have read and approved the final version of the manuscript.

Received 15.12.2023

Revised 12.01.2024

Accepted 18.01.2024

Об авторах:

Анастасия Александровна Александрова, магистрант кафедры информационных технологий и прикладной математики Уфимского государственного нефтяного технического университета (450064, РФ, г. Уфа, ул. Космонавтов, 1), SPIN-код: [4026-5240](#), [ORCID](#), nastena1425@gmail.ru

Сергей Николаевич Коледин, кандидат физико-математических наук, доцент кафедры информационных технологий и прикладной математики Уфимского государственного нефтяного технического университета (450064, РФ, г. Уфа, ул. Космонавтов, 1), SPIN-код: [4243-6265](#), [ORCID](#), koledinsrg@gmail.com

Заявленный вклад авторов:

А.А. Александрова — разработка программного обеспечения, подготовка текста, формулировка выводов.

С.Н. Коледин — научное руководство, предоставление исходных данных, корректировка выводов, доработка текста.

Конфликт интересов: авторы заявляют об отсутствии конфликта интересов.

Все авторы прочитали и одобрили окончательный вариант рукописи.

Поступила в редакцию 15.12.2023

Поступила после рецензирования 12.01.2024

Принята к публикации 18.01.2024